

CHAPTER 2

Transmitter and Receiver Systems

| | |
|--|------------|
| Acronyms..... | vii |
| Chapter 2. Transmitter and Receiver Systems..... | 2-1 |
| 2.1 Radio Frequency Standards for Telemetry | 2-1 |
| 2.2 Bands..... | 2-1 |
| 2.2.1 Allocation of the Lower L-Band (1435 to 1535 MHz)..... | 2-2 |
| 2.2.2 Allocation of the Lower S-Band (2200 to 2300 MHz) | 2-2 |
| 2.2.3 Allocation of the Upper S-Band (2310 to 2395 MHz) | 2-3 |
| 2.2.4 Allocation of the Lower C-Band (4400 to 4940 MHz)..... | 2-3 |
| 2.2.5 Allocation of the Middle C-Band (5091 to 5150 MHz) | 2-3 |
| 2.2.6 Allocation of the Upper C-Band (5925 to 6700 MHz)..... | 2-3 |
| 2.3 Telemetry Transmitter Systems | 2-3 |
| 2.3.1 Center Frequency Tolerance | 2-3 |
| 2.3.2 Output Power | 2-4 |
| 2.3.3 Modulation..... | 2-4 |
| 2.3.4 Spurious Emission and Interference Limits..... | 2-13 |
| 2.3.5 Operational Flexibility..... | 2-13 |
| 2.3.6 Modulated Transmitter Bandwidth..... | 2-13 |
| 2.3.7 Valid Center Frequencies Near Telemetry Band Edges | 2-14 |
| 2.4 Telemetry Receiver Systems..... | 2-14 |
| 2.4.1 Spurious Emissions | 2-14 |
| 2.4.2 Frequency Tolerance..... | 2-15 |
| 2.4.3 Receiver Phase Noise..... | 2-15 |
| 2.4.4 Spurious Responses | 2-15 |
| 2.4.5 Operational Flexibility..... | 2-15 |
| 2.4.6 Intermediate Frequency Bandwidths | 2-15 |
| 2.4.7 C-band Downconversion | 2-16 |
| 2.5 Codes for Telemetry Systems | 2-16 |
| 2.5.1 Low-Density Parity-Check Code..... | 2-16 |
| 2.5.2 Space-Time Code..... | 2-17 |
| 2.6 Randomization Methods for Telemetry Systems..... | 2-17 |
| 2.6.1 Introduction..... | 2-17 |
| 2.6.2 Randomizer Types | 2-17 |
| 2.6.3 Randomizer Application | 2-17 |
| 2.7 Data Quality Metrics and Data Quality Encapsulation..... | 2-18 |
| 2.8 Interference Protection Criteria for Aeronautical Mobile Telemetry Systems | 2-18 |
| Appendix 2-A. Frequency Considerations for Telemetry..... | A-1 |

| | | |
|--------|--|------|
| A.1. | Purpose..... | A-1 |
| A.2. | Scope..... | A-1 |
| A.2.a. | Definitions..... | A-1 |
| A.2.b. | Modulation methods | A-1 |
| A.2.c. | Other Notations | A-2 |
| A.3. | Authorization to Use a Telemetry System | A-2 |
| A.3.a. | RF Spectrum Support Certification | A-2 |
| A.3.b. | Frequency Authorization | A-3 |
| A.4. | Frequency Usage Guidance | A-4 |
| A.4.a. | Minimum Frequency Separation..... | A-4 |
| A.4.b. | Geographical Separation..... | A-8 |
| A.4.c. | Multicarrier Operation | A-8 |
| A.4.d. | Transmitter Antenna System Emission Testing..... | A-8 |
| A.5. | Bandwidth | A-8 |
| A.5.a. | Concept | A-9 |
| A.5.b. | Bandwidth Estimation and Measurement | A-10 |
| A.5.c. | Other Bandwidth Measurement Methods | A-12 |
| A.5.d. | Spectral Equations | A-14 |
| A.5.e. | Receiver Bandwidth..... | A-16 |
| A.5.f. | Receiver Noise Bandwidth | A-17 |
| A.5.g. | Symmetry..... | A-17 |
| A.5.h. | FM Transmitters (alternating current-coupled) | A-17 |
| A.6. | Spectral Occupancy Limits | A-17 |
| A.6.a. | Spectral Mask..... | A-17 |
| A.6.b. | Spectral Mask Examples..... | A-19 |
| A.7. | Technical Characteristics of Digital Modulation Methods | A-20 |
| A.8. | FQPSK-B and FQPSK-JR Characteristics..... | A-21 |
| A.9. | SOQPSK-TG Characteristics..... | A-25 |
| A.10. | Advanced Range Telemetry Continuous Phase Modulation Characteristics | A-26 |
| A.11. | PCM/FM | A-27 |
| A.12. | Valid Center Frequencies Near Telemetry Band Edges | A-28 |

Appendix 2.B. Properties of the Differential Encoder Specified in IRIG

Standard 106 for OQPSK Modulations..... B-33

| | | |
|------|---|------|
| B.1. | Introduction..... | B-33 |
| B.2. | The Need For Differential Encoding | B-33 |
| B.3. | A Simple Solution To The Carrier Phase Ambiguity Problem..... | B-35 |
| B.4. | Immunity to Carrier Phase Rotation | B-38 |
| B.5. | Initial Values | B-40 |
| B.6. | Error Propagation..... | B-41 |
| B.7. | Recursive Processing and Code Memory | B-41 |
| B.8. | Frequency Impulse Sequence Mapping for SOQPSK | B-43 |

| | | |
|--|---|------------|
| B.9. | Summary | B-44 |
| B.10. | System-Level Software Reference Implementation of Differential Encoder Defined in IRIG Standard 106 for FQPSK and SOQPSK Modulations..... | B-44 |
| B.10.a. | Introduction..... | B-44 |
| B.10.b. | Matlab Workspace Operation | B-45 |
| B.10.c. | Script For Modules | B-46 |
| Appendix 2-C. Telemetry Transmitter Command and Control Protocol..... | | C-1 |
| C.1. | Introduction..... | C-1 |
| C.2. | Command Line Interface | C-1 |
| C.2.a. | User Command Line Interface..... | C-1 |
| C.2.b. | Optional Programming Interface | C-1 |
| C.3. | Initialization | C-2 |
| C.4. | Basic Command Set..... | C-2 |
| C.4.a. | Basic Command Set Summary | C-2 |
| C.4.b. | Commands: Basic Command Set..... | C-3 |
| C.5. | Extended Command Set..... | C-10 |
| C.5.a. | Extended Command Set Summary | C-10 |
| C.5.b. | Commands: Extended Command Set | C-11 |
| C.6. | Transmitter Communication Example..... | C-14 |
| C.7. | Non-Standard Commands | C-14 |
| C.8. | Physical Layer(s) | C-14 |
| Appendix 2-D. Low-Density Parity-Check Codes for Telemetry Systems..... | | D-1 |
| D.1. | Background | D-1 |
| D.2. | Code Description | D-1 |
| D.3. | Parity Check Matrices..... | D-2 |
| D.4. | Encoding | D-9 |
| D.4.a. | Code Rate =1/2, Information Block Size = 1024, $M = 512$ | D-11 |
| D.4.b. | Code Rate =1/2, Information Block Size = 4096, $M = 2048$ | D-12 |
| D.4.c. | Code Rate =2/3, Information Block Size = 1024, $M = 256$ | D-17 |
| D.4.d. | Code Rate =2/3, Information Block Size = 4096, $M = 1024$ | D-21 |
| D.4.e. | Code Rate =4/5, Information Block Size = 1024, $M = 128$ | D-27 |
| D.4.f. | Code Rate =4/5, Information Block Size = 4096, $M = 512$ | D-34 |
| D.5. | Synchronization | D-41 |
| D.6. | Randomization | D-42 |
| D.7. | Performance | D-43 |
| Appendix 2-E. Space-Time Coding for Telemetry Systems | | E-1 |
| E.1. | Code Description | E-1 |
| E.2. | Modulation..... | E-3 |
| E.3. | Resources | E-4 |

| | |
|--|------------|
| Appendix 2-F. Use of Recommendation ITU-R M.1459 for Protection of AMT Ground Stations from Terrestrial, Airborne, and Satellite Interference | F-1 |
| F.1. Introduction and Summary | F-1 |
| F.2. Practical Application of the Rec M.1459 Protection Criteria | F-1 |
| Appendix 2-G. Standards for Data Quality Metrics and Data Quality Encapsulation | G-1 |
| G.1. Purpose..... | G-1 |
| G.2. Scope..... | G-1 |
| G.3. Data Quality Metric | G-1 |
| G.4. Data Quality Encapsulation Protocol..... | G-2 |
| Appendix 2-I. Citations..... | H-1 |

Table of Figures

| | |
|---|------|
| Figure 2-1. FQPSK-JR Baseband Signal Generator..... | 2-6 |
| Figure 2-2. Basic SOQPSK | 2-8 |
| Figure 2-3. SOQPSK Transmitter..... | 2-10 |
| Figure 2-4. Conceptual CPM Modulator | 2-11 |
| Figure 2-5. Continuous Single-Sideband Phase Noise Power Spectral Density | 2-12 |
| Figure A-1. Spectra of 10-Mbps PCM/FM, ARTM CPM, FQPSK-JR, SOQPSK-TG Signals..... | A-4 |
| Figure A-2. 5 Mbps PCM/FM Signals with 11 MHz Center Frequency Separation | A-6 |
| Figure A-3. 10 Mbps ARTM CPM Signals with 9 MHz Center Frequency Separation..... | A-7 |
| Figure A-4. RNRZ PCM/FM Signal | A-11 |
| Figure A-5. Spectrum Analyzer Calibration of 0-dBc Level | A-12 |
| Figure A-6. Bi ϕ PCM/PM Signal | A-13 |
| Figure A-7. FM/AM Signal and Carson's Rule | A-14 |
| Figure A-8. Typical Receiver RLC IF Filter Response (-3 dB Bandwidth = 1 MHz) | A-16 |
| Figure A-9. RLC and SAW IF Filters | A-16 |
| Figure A-10. Filtered 5-Mbps RNRZ PCM/FM Signal and Spectral Mask..... | A-19 |
| Figure A-11. Unfiltered 5-Mbps RNRZ PCM/FM Signal and Spectral Mask..... | A-19 |
| Figure A-12. Typical 5-Mbps SOQPSK TG Signal and Spectral Mask | A-20 |
| Figure A-13. Typical 5-Mbps ARTM CPM Signal and Spectral Mask..... | A-20 |
| Figure A-14. OQPSK Modulator..... | A-21 |
| Figure A-15. I and Q Constellation | A-22 |
| Figure A-16. FQPSK Wavelet Eye Diagram..... | A-22 |
| Figure A-17. FQPSK-B I & Q Eye Diagrams (at Input to IQ Modulator)..... | A-23 |
| Figure A-18. FQPSK-B Vector Diagram | A-23 |
| Figure A-19. 5 Mbps FQPSK-JR Spectrum with Random Input Data and Small (Blue) and Large (Red) Modulator Errors | A-24 |
| Figure A-20. FQPSK-B Spectrum with All 0's Input and Large Modulator Errors | A-24 |
| Figure A-21. FQPSK-JR BEP vs. E_b/N_0 | A-25 |
| Figure A-22. Measured SOQPSK-TG Phase Trajectory..... | A-25 |

| | | |
|--------------|--|------|
| Figure A-23. | SOQPSK-TG Power Spectrum (5 Mbps) | A-26 |
| Figure A-24. | BEP vs. Eb/N0 Performance of 5 Mbps SOQPSK-TG | A-26 |
| Figure A-25. | Power Spectrum of 5 Mbps ARTM CPM..... | A-27 |
| Figure A-26. | BEP vs. Eb/N0 Performance of 5 Mbps ARTM CPM | A-27 |
| Figure A-27. | Power Spectrum of 5 Mbps PCM/FM Signal | A-28 |
| Figure A-28. | BEP vs. Eb/N0 Performance of 5-Mbps PCM/FM with Multi-Symbol Bit Detector and Three Single-Symbol Receivers/Detectors | A-28 |
| Figure A-29. | Spectral Masks at -25 dBm | A-29 |
| Figure A-30. | Bit Rate vs. Band Edge Back-off..... | A-30 |
| Figure B-1. | Transmission System | B-34 |
| Figure B-2. | OQPSK 106 Symbol-to-Phase Mapping Convention..... | B-34 |
| Figure B-3. | Detection Ambiguity..... | B-35 |
| Figure B-4. | QPSK State Timing..... | B-36 |
| Figure B-5. | OQPSK State Timing..... | B-36 |
| Figure B-6. | SOQPSK Transmitter..... | B-43 |
| Figure B-7. | OQPSK Transmitter (With Precoder)..... | B-44 |
| Figure C-1. | Terminal Window for STC-Enabled Transmitter | C-10 |
| Figure C-2. | Typical Terminal Window | C-14 |
| Figure D-1. | Parity Check Matrix H for (n=2048, k=1024) Rate 1/2..... | D-4 |
| Figure D-2. | Parity Check Matrix H for (n=8192, k=4096) Rate 1/2..... | D-5 |
| Figure D-3. | Parity Check Matrix H for (n=1536, k=1024) Rate 2/3..... | D-6 |
| Figure D-4. | Parity Check Matrix H for (n=6144, k=4096) Rate 2/3..... | D-7 |
| Figure D-5. | Parity Check Matrix H for (n=1280, k=1024) Rate 4/5..... | D-8 |
| Figure D-6. | Parity Check Matrix H for (n=5120, k=4096) Rate 4/5..... | D-9 |
| Figure D-7. | Quasi-Cyclic Encoder Using Feedback Shift Register | D-10 |
| Figure D-8. | ASM/Codeblock Structure..... | D-41 |
| Figure D-9. | Codeblock Randomizer..... | D-42 |
| Figure D-10. | LDPC Detection Performance with 4-state Trellis Demodulator | D-43 |
| Figure D-11. | LDPC Detection Performance with Symbol-by-Symbol Demodulator..... | D-44 |
| Figure E-1. | Symbol-to-Phase Mapping for IRIG-106 Offset QPSK Modulation | E-1 |
| Figure E-2. | Notional Diagram Illustrating the Periodic Insertion of 128 Pilot Bits Every 3200 Alamouti-Encoded Bits | E-3 |
| Figure E-3. | A Notional Block Diagram of the Space-Time Code Transmitter | E-4 |
| Figure F-1. | Excerpt from Article 21 of the International Radio Regulations | F-5 |
| Figure F-2. | Geometry of a Geostationary Link Showing (a) Elevation, (b) Azimuth from a Point T on the Earth..... | F-8 |
| Figure F-3. | Digital Audio Radio Service Downlink Beam Gain Contours | F-9 |
| Figure F-4. | Elevation Angles from Surface of the Earth to the 115.2° West Longitude Orbital Location | F-10 |
| Figure F-5. | FCC Emission Mask for the WCS OOB Band from 2360 – 2390 MHz..... | F-11 |
| Figure F-6. | Simulated OOB Emissions from an LTE Handset | F-13 |
| Figure F-7. | Graphical Representation of the Two-Ray Model | F-14 |
| Figure F-8. | Comparison of Free-Space One-Slope and Two-Ray Propagation Models | F-15 |
| Figure F-9. | Rayleigh Fading of a Signal Transmitted from a Moving Platform | F-17 |
| Figure F-10. | S-band Telemetry Signal Received from an Aircraft in Flight..... | F-17 |

| | | |
|--------------|---|------|
| Figure F-11. | Rayleigh Distribution as Presented in Figure 2 of Rec M.1459 (Jablonski 2004). | F-18 |
| Figure F-12. | EDX Signal Pro Map of Hypothetical Transmitters and Receivers in the Pax River Region. | F-21 |
| Figure F-13. | EDX Signal Pro Path Loss Profile for the TX007 to RX007 Path | F-21 |
| Figure F-14. | Actual Measured Path Loss Data from an NTIA Report (cf. footnote 71) | F-22 |
| Figure F-15. | Composite AMT Pattern from Rec M.1459 | F-26 |
| Figure F-16. | Aggregate Interference as a Function of AMT Antenna Pointing Angle | F-27 |
| Figure F-17. | Statgain Pattern | F-31 |

Table of Tables

| | | |
|-------------|--|------|
| Table 2-1. | Telemetry Frequency Allocations | 2-1 |
| Table 2-3. | FQPSK-B and FQPSK-JR Phase Map..... | 2-7 |
| Table 2-4. | SOQPSK-TG Parameters | 2-10 |
| Table 2-5. | SOQPSK Pre-Coding Table for IRIG-106 Compatibility | 2-10 |
| Table 2-6. | Dibit to Impulse Area Mapping | 2-11 |
| Table 2-7. | Standard Receiver Intermediate Frequency Bandwidths | 2-15 |
| Table 2-8. | Interference Protection Criteria by Band and Angle of Arrival..... | 2-18 |
| Table A-1. | Coefficients for Minimum Frequency Separation Calculation | A-4 |
| Table A-2. | B99% for Various Digital Modulation Methods | A-9 |
| Table A-3. | Characteristics of Various Modulation Methods | A-20 |
| Table A-4. | L-Band Frequency Range (10 W, 5 Mbps)..... | A-29 |
| Table A-5. | Valid Center Frequency, Band Edge Back-Off | A-31 |
| Table B-1. | Constellation Axis Rotations | B-35 |
| Table B-2. | Response to Run of 1s..... | B-38 |
| Table B-3. | SOQPSK Pre-Coding Table for IRIG-106 Compatibility | B-43 |
| Table B-1. | Script “runDEdemo” Output..... | B-45 |
| Table C-1. | Basic Command Set..... | C-2 |
| Table C-2. | Extended Command Set..... | C-10 |
| Table D-1. | Codeblock Length per Information Block Size | D-2 |
| Table D-2. | Submatrix Size per Information Block Size | D-2 |
| Table D-3. | Generator Matrix Sizes | D-10 |
| Table D-4. | First Rows of Circulants in Generator Matrix, $r=1/2$, $k=1024$ | D-11 |
| Table D-5. | First Rows of Circulants in Generator Matrix, $r=1/2$, $k=4096$ | D-13 |
| Table D-6. | First Rows of Circulants in Generator Matrix, $r=2/3$, $k=1024$ | D-17 |
| Table D-7. | First Rows of Circulants in Generator Matrix, $r=2/3$, $k=4096$ | D-21 |
| Table D-8. | First Rows of Circulants in Generator Matrix, $r=4/5$, $k=1024$ | D-27 |
| Table D-9. | First Rows of Circulants in Generator Matrix, $r=4/5$, $k=4096$ | D-34 |
| Table D-10. | ASM Definition | D-41 |
| Table D-11. | Bandwidth Expansion Factor | D-42 |
| Table F-1. | Statgain Formulas | F-31 |
| Table G-1. | BEP Verses DQM | G-1 |

Acronyms

| | |
|-----------------|--|
| μV | microvolt |
| AFTRCC | Aerospace and Flight Test Radio Coordinating Council |
| AM | amplitude modulation |
| AMT | aeronautical mobile telemetry |
| ARTM | Advanced Range Telemetry |
| ASM | attached synchronization marker |
| AWGN | additive white Gaussian noise |
| BPSK | binary phase shift keying |
| BEP | bit error probability |
| BER | bit error rate |
| $\text{Bi}\phi$ | bi-phase |
| BSS | Broadcasting-Satellite Service |
| CPFSK | continuous phase frequency shift keying |
| CPM | continuous phase modulation |
| CCSDS | Consultative Committee for Space Data Systems |
| dB | decibel |
| dBc | decibels relative to the carrier |
| dB _i | decibels isotropic |
| dBm | decibels referenced to one milliwatt |
| dBW | decibels relative to one watt |
| DoD | Department of Defense |
| DQE | data quality encapsulation |
| DQM | data quality metric |
| EESS | Earth Exploration-Satellite Services |
| EIRP | effective isotropic radiated power |
| FCC | Federal Communications Commission |
| FEC | forward error correction |
| FM | frequency modulation |
| FQPSK | Feher's quadrature phase shift keying |
| Hz | hertz |
| IF | intermediate frequency |
| I/N | interference-to-noise ratio |
| IPC | interference protection criteria |
| IRIG | Inter-Range Instrumentation Group |
| ITM | Irregular Terrain Model |
| kHz | kilohertz |
| LDPC | low-density parity-check |
| L-R | Longley-Rice |
| LTE | Long-Term Evolution |
| Mbps | megabits per second |
| MCEB | Military Communications - Electronics Board |
| MHz | megahertz |
| MIL-STD | Military Standard |
| MSK | minimum shift keying |
| NRZ-L | non-return-to-zero-level |

| | |
|--------|--|
| NTIA | National Telecommunications and Information Administration |
| OOBE | out-of-band emission |
| OQPSK | offset quadrature phase shift keying |
| PAPR | peak-to-average-power-ratio |
| PCM | pulse code modulation |
| PFD | power flux density |
| PM | phase modulation |
| PSD | power spectral density |
| QPSK | quadrature phase shift keying |
| RCC | Range Commanders Council |
| RF | radio frequency |
| RLC | resistor-inductor-capacitor |
| RNRZ | randomized non-return-to-zero |
| SAW | surface acoustic wave |
| SDARS | Satellite Digital Audio Radio Service |
| SHF | super-high frequency |
| STC | space-time code |
| SOQPSK | shaped offset quadrature phase shift keying |
| UHF | ultra-high frequency |
| US&P | United States and Possessions |
| VCO | voltage-controlled oscillator |
| VHF | very-high frequency |
| WCS | Wireless Communication Service |

CHAPTER 2

Transmitter and Receiver Systems

2.1 Radio Frequency Standards for Telemetry

These standards provide the criteria to determine equipment and frequency use requirements and are intended to ensure efficient and interference-free use of the radio frequency (RF) spectrum. These standards also provide a common framework for sharing data and providing support for test operations between ranges. The RF spectrum is a limited natural resource; therefore, efficient use of available spectrum is mandatory. In addition, susceptibility to interference must be minimized. Systems not conforming to these standards require justification upon application for frequency allocation, and the use of such systems is highly discouraged. The standards contained herein are derived from the National Telecommunications and Information Administration's (NTIA) Manual of Regulations and Procedures for Federal Radio Frequency Management.¹

2.2 Bands

The bands used for telemetry are described in [Table 2-1](#).

| Table 2-1. Telemetry Frequency Allocations | | | |
|---|-------------------------------|---|-----------------------|
| Frequency Range (MHz) | Unofficial Designation | Comments | Refer to: |
| 1435-1525 | Lower L-band | Telemetry primary service (part of mobile service) in USA | 2.2.1 |
| 1525-1535 | Lower L-band | Mobile satellite service (MSS) primary service, telemetry secondary service in USA | 2.2.1 |
| 2200-2290 | Lower S-band | Telemetry co-primary service in USA | 2.2.2 |
| 2310-2360 | Upper S-band | Wireless Communications Service (WCS) and Broadcasting-Satellite Service (BSS) primary services, telemetry secondary service in USA | 2.2.3 |
| 2360-2395 | Upper S-band | Telemetry primary service in USA | 2.2.3 |
| 4400-4940 | Lower C-band | See Paragraph 2.2.4 | 2.2.4 |
| 5091-5150 | Middle C-band | See Paragraph 2.2.5 | 2.2.5 |
| 5925-6700 | Upper C-band | See Paragraph 2.2.6 | 2.2.6 |

The 1755-1850 MHz band (unofficially called “upper L-band”) can also be used for telemetry at many test ranges, although it is not explicitly listed as a telemetry band in the NTIA Table of Frequency Allocations.² The mobile service is a primary service in the 1755-1850 MHz band and telemetry is a part of the mobile service. Since the 1755-1850 MHz band is not considered a standard telemetry band per this document, potential users must coordinate, in

¹ National Telecommunications and Information Administration. “Manual of Regulations and Procedures for Federal Radio Frequency Management.” September 2015. May be superseded by update. Retrieved 23 March 2017. Available at https://www.ntia.doc.gov/files/ntia/publications/manual_sep_2015.pdf.

² Code of Federal Regulations, Table of Frequency Allocations, title 47, sec. 2.106.

advance, with the individual range(s) and ensure use of this band can be supported at the subject range and that it will meet their technical requirements. While these band designations are common in telemetry parlance, they may have no specific meaning to anyone else. Telemetry assignments are made for testing³ manned and unmanned aircraft, for missiles, space, land, and sea test vehicles, and for rocket sleds and systems carried on such sleds. Telemetry assignments are also made for testing major components of the aforementioned systems.

2.2.1 Allocation of the Lower L-Band (1435 to 1535 MHz)

This band is allocated in the United States and Possessions (US&P) for government and nongovernmental aeronautical telemetry use on a shared basis. The Aerospace and Flight Test Radio Coordinating Council (AFTRCC) coordinates the non-governmental use of this band. The frequencies in this range will be assigned for aeronautical telemetry and associated remote-control operations⁴ for testing of manned or unmanned aircraft, missiles, rocket sleds, and other vehicles or their major components. Authorized usage includes telemetry associated with launching and reentry into the earth's atmosphere as well as any incidental orbiting prior to reentry of manned or unmanned vehicles undergoing flight tests. The following frequencies are shared with flight telemetering mobile stations: 1444.5, 1453.5, 1501.5, 1515.5, 1524.5, and 1525.5 MHz.

2.2.1.1 1435 to 1525 MHz

This frequency range is allocated for the exclusive use of aeronautical telemetry in the United States of America.

2.2.1.2 1525 to 1530 MHz

The 1525 to 1530 MHz band was reallocated at the 1992 World Administrative Radio Conference. The mobile-satellite service is now a primary service in this band. The mobile service, which includes aeronautical telemetry, is now a secondary service in this band.

2.2.1.3 1530 to 1535 MHz

The maritime mobile-satellite service is a primary service in the frequency band from 1530 to 1535 MHz.⁵ The mobile service (including aeronautical telemetry) is a secondary service in this band.

2.2.2 Allocation of the Lower S-Band (2200 to 2300 MHz)

No provision is made in this band for the flight testing of manned aircraft.

2.2.2.1 2200 to 2290 MHz

These frequencies are shared equally by the United States Government's fixed, mobile, space research, space operation, and the Earth Exploration-Satellite Services (EESS), and include telemetry associated with launch vehicles, missiles, upper atmosphere research rockets, and space vehicles regardless of their trajectories.

³ A telemetry system as defined here is not critical to the operational (tactical) function of the system.

⁴ The word used for remote-control operations in this band is *telecommand*.

⁵ Reallocated as of 1 January 1990.

2.2.2.2 2290 to 2300 MHz

Allocations in this range are for the space research service (deep space only) on a shared basis with the fixed and mobile (except aeronautical mobile) services.

2.2.3 Allocation of the Upper S-Band (2310 to 2395 MHz)

This band is allocated to the fixed, mobile, radiolocation, and BSS in the United States of America. Government and nongovernmental telemetry users share this band in a manner similar to that of the L-band. Telemetry assignments are made for flight-testing of manned or unmanned aircraft, missiles, space vehicles, or their major components.

2.2.3.1 2310 to 2360 MHz

These frequencies have been reallocated and were auctioned by the Federal Communications Commission (FCC) in April 1997. The WCS is the primary service in the frequencies 2305-2320 MHz and 2345-2360 MHz. The BSS is the primary service in the 2320-2345 MHz band. In the 2320-2345 MHz band, the mobile and radiolocation services are allocated on a primary basis until a broadcasting-satellite (sound) service has been brought into use in such a manner as to affect or be affected by the mobile and radiolocation services in those service areas

2.2.3.2 2360 to 2395 MHz

The mobile service (including aeronautical telemetry) is a primary service in this band.

2.2.4 Allocation of the Lower C-Band (4400 to 4940 MHz)

Telemetry is an operation that is currently allowed under the mobile service allocation.

2.2.5 Allocation of the Middle C-Band (5091 to 5150 MHz)

The process of incorporating aeronautical telemetry operations into the NTIA Table of Frequency Allocations for this band has been initiated but not yet completed.

2.2.6 Allocation of the Upper C-Band (5925 to 6700 MHz)

This band is not currently allocated as a government band. The process of incorporating federal government use of aeronautical telemetry operations into the NTIA Table of Frequency Allocations for this band has been initiated but not yet completed.

2.3 **Telemetry Transmitter Systems**

Telemetry requirements for air, space, and ground systems are accommodated in the appropriate bands as described in Section [2.2](#).

2.3.1 Center Frequency Tolerance

Unless otherwise dictated by a particular application, the frequency tolerance for a telemetry transmitter shall be $\pm 0.002\%$ of the transmitter's assigned center frequency. Transmitter designs shall control transient frequency errors associated with startup and power interruptions. During the first second after turn-on, the transmitter output frequency shall be within the occupied bandwidth of the modulated signal at any time when the transmitter output power exceeds -25 decibels (dB) referenced to one milliwatt (dBm). Between 1 and 5 seconds after initial turn-on, the transmitter frequency shall remain within twice the specified limits for the assigned radio frequency. After 5 seconds, the standard frequency tolerance is applicable for

any and all operations where the transmitter power output is -25 dBm or greater (or produces a field strength greater than 320 microvolts [μ V]/meter at a distance of 30 meters from the transmitting antenna in any direction). Specific uses may dictate tolerances more stringent than those stated.

2.3.2 Output Power

Emitted power levels shall always be limited to the minimum required for the application. The output power shall not exceed 25 watts⁶. The effective isotropic radiated power (EIRP) shall not exceed 25 watts.

2.3.3 Modulation

The traditional modulation methods for aeronautical telemetry are frequency modulation (FM) and phase modulation (PM). Pulse code modulation (PCM)/FM has been the most popular telemetry modulation since around 1970. The PCM/FM method could also be called filtered continuous phase frequency shift keying (CPFSK). The RF signal is typically generated by filtering the baseband non-return-to-zero-level (NRZ-L) signal and then frequency modulating a voltage-controlled oscillator (VCO). The optimum peak deviation is 0.35 times the bit rate and a good choice for a premodulation filter is a multi-pole linear phase filter with bandwidth equal to 0.7 times the bit rate. Both FM and PM have a variety of desirable features but may not provide the required bandwidth efficiency, especially for higher bit rates. When better bandwidth efficiency is required, the standard methods for digital signal transmission are the Feher's patented quadrature phase shift keying (FQPSK-B and FQPSK-JR), the shaped offset quadrature phase shift keying (SOQPSK-TG), and the Advanced Range Telemetry (ARTM) continuous phase modulation (CPM). Each of these methods offer constant, or nearly constant, envelope characteristics and are compatible with non-linear amplifiers with minimal spectral regrowth and minimal degradation of detection efficiency. The first three methods (FQPSK-B, FQPSK-JR, and SOQPSK-TG) are interoperable and require the use of the differential encoder described in Subsection [2.3.3.1.1](#) below. Additional information on this differential encoder is contained in [0](#). All of these bandwidth-efficient modulation methods require the data to be randomized. Additional characteristics of these modulation methods are discussed in the following paragraphs and in Section [A.7](#).

2.3.3.1 Characteristics of FQPSK-B

The FQPSK-B method is described in the Digcom Inc. publication, "*FQPSK-B, Revision A1, Digcom-Feher Patented Technology Transfer Document, January 15, 1999.*" This document can be obtained under a license from:

Digcom Inc.
44685 Country Club Drive
El Macero, CA 95618
Telephone: 530-753-0738
FAX: 530-753-1788

⁶ An exemption from this EIRP limit will be considered; however, systems with EIRP levels greater than 25 watts will be considered nonstandard systems and will require additional coordination with affected test ranges.

2.3.3.1.1 Differential Encoding

Differential encoding shall be provided for FQPSK-B, FQPSK-JR, and SOQPSK-TG and shall be consistent with the following definitions.

The NRZ-L data bit sequence $\{b_n\}$ is sampled periodically by the transmitter at time instants:

$$t = nT_b \quad n = 0, 1, 2, \dots$$

where T_b is the NRZ-L bit period.

Using the bit index values n as references to the beginning of symbol periods, the differential encoder alternately assembles I-channel and Q-channel symbols to form the following sequences:

$$I_2, I_4, I_6, \dots$$

and

$$Q_3, Q_5, Q_7, \dots$$

according to the following rules:

$$I_{2n} = b_{2n} \oplus \overline{Q_{(2n-1)}} \quad n > 0 \quad (2-1)$$

$$Q_{(2n+1)} = b_{(2n+1)} \oplus I_{2n} \quad n > 0 \quad (2-2)$$

Where \oplus denotes the exclusive-or operator, and the bar above a variable indicates the ‘not’ or inversion operator. Q-channel symbols are offset (delayed) relative to I-channel symbols by one bit period.

2.3.3.1.2 Characteristics of FQPSK-JR

The FQPSK-JR method is a cross-correlated, constant envelope, spectrum-shaped variant of FQPSK. It assumes a quadrature modulator architecture and synchronous digital synthesis of the I and Q-channel modulating signals as outlined in [Figure 2-1](#).

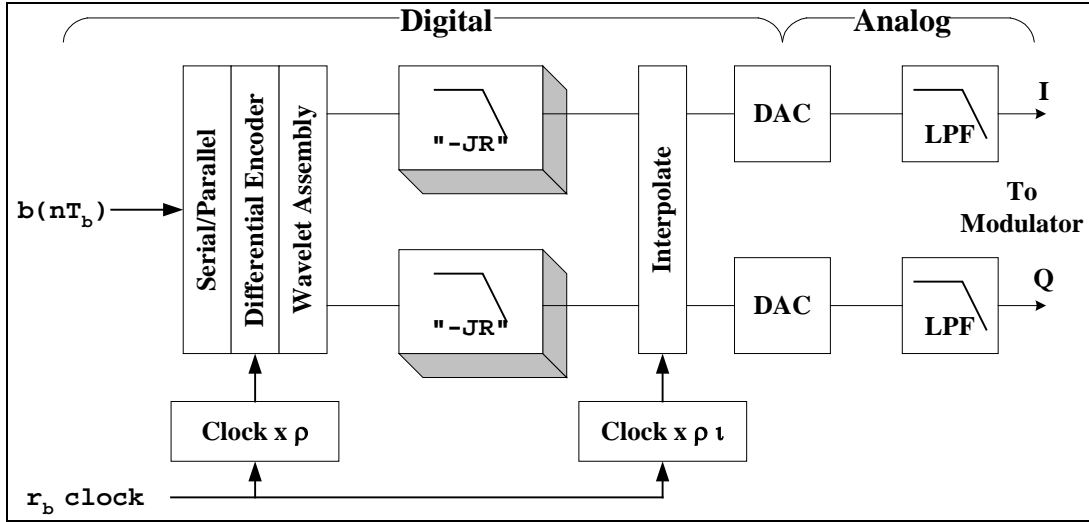


Figure 2-1. FQPSK-JR Baseband Signal Generator

The FQPSK-JR method utilizes the time domain wavelet functions defined in United States Patent 4,567,602⁷ with two exceptions. The transition functions used in the cited patent,

$$G(t) = \begin{cases} \pm \left[1 - K \cos^2\left(\frac{\pi t}{T_s}\right) \right] \\ \pm \left[1 - K \sin^2\left(\frac{\pi t}{T_s}\right) \right] \end{cases} \quad (2-3)$$

$$K = 1 - A = 1 - \frac{\sqrt{2}}{2}$$

are replaced with the following transition functions:

$$G(t) = \begin{cases} \pm \sqrt{1 - A^2 \cos^2\left(\frac{\pi t}{T_s}\right)} \\ \pm \sqrt{1 - A^2 \sin^2\left(\frac{\pi t}{T_s}\right)} \end{cases} \quad (2-4)$$

$$A = \frac{\sqrt{2}}{2}$$

where $T_s = 2/r_b$ is the symbol period.

The digital “JR” spectrum-shaping filter used for each channel is a linear phase, finite impulse response filter. The filter is defined in terms of its impulse response sequence $h(n)$ in

⁷ Feher, Kamilo, and Shuzo Kato. Correlated signal processor. US Patent 4,567,602. Filed 13 June 1983 and issued 28 January 1986.

[Table 2-2](#) and assumes a fixed wavelet sample rate of $\rho = 6$ samples per symbol. The JR_{equiv} column is the aggregate response of the cascaded JR_a and JR_b filters actually used.

| Table 2-2. FQPSK-JR Shaping Filter Definition | | | |
|--|---------------------|----------|----------------------|
| Filter Weight | JR_{equiv} | JR_a | JR_b |
| $h(0)$ | -0.046875 | 2^{-2} | $-(2^{-3} + 2^{-4})$ |
| $h(1)$ | 0.109375 | $h(0)$ | $(2^{-1} + 2^{-3})$ |
| $h(2)$ | 0.265625 | $h(0)$ | $h(1)$ |
| $h(3)$ | $h(2)$ | - | $h(0)$ |
| $h(4)$ | $h(1)$ | - | - |
| $h(5)$ | $h(0)$ | - | - |

Digital interpolation is used to increase sample rate, moving all alias images created by digital-to-analog conversion sufficiently far away from the fundamental signal frequency range so that out-of-channel noise floors can be well-controlled. The FQPSK-JR reference implementations currently utilize 4-stage Cascade-Integrator-Comb interpolators with unity memory lag factor.⁸ Interpolation ratio “ t ” is adjusted as a function of bit rate such that fixed cutoff frequency post-digital-to-analog anti-alias filters can be used to cover the entire range of required data rates.⁹

2.3.3.1.3 Carrier Suppression

The remnant carrier level shall be no greater than -30 dB relative to the carrier (dBc). Additional information of carrier suppression can be seen at Section [A.7](#).

2.3.3.1.4 Quadrature Modulator Phase Map

[Table 2-3](#) lists the mapping from the input to the modulator (after differential encoding and FQPSK-B or FQPSK-JR wavelet assembly) to the carrier phase of the modulator output. The amplitudes in [Table 2-3](#) are $\pm a$, where “ a ” is a normalized amplitude.

| Table 2-3. FQPSK-B and FQPSK-JR Phase Map | | |
|--|-----------|-------------------------|
| I Channel | Q Channel | Resultant Carrier Phase |
| a | a | 45 degrees |
| $-a$ | a | 135 degrees |
| $-a$ | $-a$ | 225 degrees |
| a | $-a$ | 315 degrees |

⁸ Eugene Hogenauer. “An Economical Class of Digital Filters for Decimation and Interpolation” in *IEEE Transactions on Acoustics, Speech, and Signal Processing*, 29, No. 2 (1981): 155-162.

⁹ The FQPSK-JR definition does not include a specific interpolation method and a post-D/A filter design; however, it is known that benchmark performance will be difficult to achieve if the combined effects of interpolation and anti-alias filter produce more than .04 dB excess attenuation at 0.0833 times the input sample rate and more than 1.6 dB of additional attenuation at 0.166 times the sample rate where the input sample rate is referred to the input of the interpolator assuming 6 samples per second.

2.3.3.2 Characteristics of SOQPSK-TG

The SOQPSK method is a family of constant-envelope CPM waveforms.^{10, 11, 12, 13} It is most simply described as a non-linear FM modeled as shown in [Figure 2-2](#).

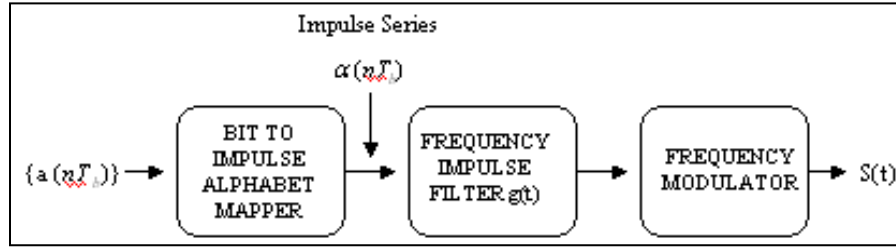


Figure 2-2. Basic SOQPSK

The SOQPSK waveform family is uniquely defined in terms of impulse excitation of a frequency impulse shaping filter function $g(t)$:

$$g(t) = n(t)w(t) \quad (2-5)$$

where

$$\begin{aligned}
 n(t) &\equiv \left[\frac{A \cos \pi \theta_1(t)}{1 - 4\theta_1^2(t)} \right] \left[\frac{\sin \theta_2(t)}{\theta_2(t)} \right] \\
 \theta_1(t) &= \frac{\rho B t}{T_s} \\
 \theta_2(t) &= \frac{\pi B t}{T_s}
 \end{aligned} \quad (2-6)$$

¹⁰ T. J. Hill. "An Enhanced, Constant Envelope, Interoperable Shaped Offset QPSK (SOQPSK) Waveform for Improved Spectral Efficiency." Paper presented during 36th Annual International Telemetry Conference, San Diego, CA. October 23-26, 2000.

¹¹ Younes B., James Brase, Chitra Patel, and John Wesdock. "An Assessment of Shaped Offset QPSK for Use in NASA Space Network and Ground Network Systems" in *Proceedings of the CCSDS RF and Modulation Subpanel 1E Meeting of May 2001 Concerning Bandwidth-Efficient Modulation*. CCSDS B20.0-Y-2. June 2001. Retrieved 4 June 2015. Available at <http://public.ccsds.org/publications/archive/B20x0y2.pdf>.

¹² Mark Geoghegan. "Implementation and Performance Results for Trellis Detection of SOQPSK." Paper presented at the 37th Annual International Telemetry Conference, Las Vegas, NV, October 2001.

¹³ Marvin Simon. "Bandwidth-Efficient Digital Modulation with Application to Deep Space Communications." JPL Publication 00-17. June 2001. Retrieved 3 June 2015. Available at <http://descanso.jpl.nasa.gov/monograph/series3/complete1.pdf>.

$$\begin{aligned}
& 1, \quad \left| \frac{t}{T_s} \right| \leq T_1 \\
& w(t) \equiv \frac{1}{2} \left[1 + \cos \left(\frac{\pi \left(\left| \frac{t}{T_s} \right| - T_1 \right)}{T_2} \right) \right], \quad T_1 < \left| \frac{t}{T_s} \right| \leq T_1 + T_2 \\
& 0, \quad \left| \frac{t}{T_s} \right| > T_1 + T_2
\end{aligned} \tag{2-7}$$

The function $n(t)$ is a modified spectral raised cosine filter of amplitude A , rolloff factor ρ , and an additional time scaling factor B . The function $w(t)$ is a time domain windowing function that limits the duration of $g(t)$. The amplitude scale factor A is chosen such that

$$\int_{-(T_1+T_2)T_s}^{(T_1+T_2)T_s} g(t) dt = \frac{\pi}{2} \tag{2-8}$$

Given a time series binary data sequence

$$\vec{a} = (\dots, a_{-2}, a_{-1}, a_0, a_1, a_2, \dots) \tag{2-9}$$

wherein the bits are represented by normalized antipodal amplitudes $\{+1, -1\}$, the ternary impulse series is formed with the following mapping rule (see also Geoghegan, *Implementation* and Simon, *Bandwidth*), ...

$$\alpha = (-1)^{i+1} \frac{a_{i-1}(a_i - a_{i-2})}{2} \tag{2-10}$$

that will form a data sequence alphabet of three values $\{+1, 0, -1\}$. It is important to note that this modulation definition does not establish an absolute relationship between the digital in-band inter-switch trunk signaling (dibits) of the binary data alphabet and transmitted phase as with conventional quadriphase offset quadrature phase shift keying (OQPSK) implementations. In order to achieve interoperability with coherent FQPSK-B demodulators, some form of precoding must be applied to the data stream prior to, or in conjunction with, conversion to the ternary excitation alphabet. The differential encoder defined in Subsection [2.3.3.1.1](#) fulfills this need; however, to guarantee full interoperability with the other waveform options, the polarity relationship between frequency impulses and resulting frequency or phase change must be controlled. Thus, SOQPSK modulators proposed for this application shall guarantee that an impulse value of (+1) will result in an advancement of the transmitted phase relative to that of the nominal carrier frequency (i.e., the instantaneous frequency is above the nominal carrier).

For purposes of this standard, only one specific variant of SOQPSK and SOQPSK-TG is acceptable. This variant is defined by the parameter values given in [Table 2-4](#).

| Table 2-4. SOQPSK-TG Parameters | | | | |
|--|--------------------------|----------|-------------------------|-------------------------|
| SOQPSK Type | ρ | B | T_1 | T_2 |
| SOQPSK-TG | 0.70 | 1.25 | 1.5 | 0.50 |

As discussed above, interoperability with FQPSK-B equipment requires a particular pre-coding protocol or a functional equivalent thereof. A representative model is shown in [Figure 2-3](#).

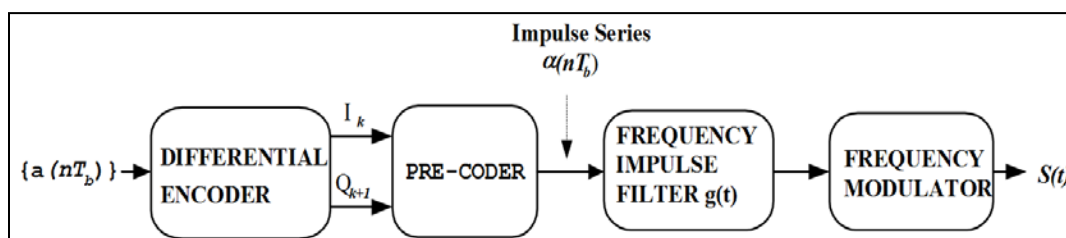


Figure 2-3. SOQPSK Transmitter

The differential encoder block will be implemented in accordance with the definition of Subsection [2.3.3.1.1](#). Given the symbol sequences I_k and Q_k , and the proviso that a normalized impulse sign of +1 will increase frequency, the pre-coder will provide interoperability with the FQPSK signals defined herein if code symbols are mapped to frequency impulses in accordance with [Table 2-5](#) where $\Delta\Phi$ is the phase change.

| Table 2-5. SOQPSK Pre-Coding Table for IRIG-106 Compatibility | | | | | | | | | |
|--|-----------|-----------|--------------|------------|--|-------|-----------|--------------|----------------|
| Map α_k from I_k | | | | | Map α_{k+1} from Q_{k+1} | | | | |
| I_k | Q_{k-1} | I_{k-2} | $\Delta\Phi$ | α_k | Q_{k+1} | I_k | Q_{k-1} | $\Delta\Phi$ | α_{k+1} |
| -1 | X* | -1 | 0 | 0 | -1 | X* | -1 | 0 | 0 |
| +1 | X* | +1 | 0 | 0 | +1 | X* | +1 | 0 | 0 |
| -1 | -1 | +1 | $-\pi/2$ | -1 | -1 | -1 | +1 | $+\pi/2$ | +1 |
| -1 | +1 | +1 | $+\pi/2$ | +1 | -1 | +1 | +1 | $-\pi/2$ | -1 |
| +1 | -1 | -1 | $+\pi/2$ | +1 | +1 | -1 | -1 | $-\pi/2$ | -1 |
| +1 | +1 | -1 | $-\pi/2$ | -1 | +1 | +1 | -1 | $+\pi/2$ | +1 |

* Note: Does not matter if "X" is a +1 or a -1

2.3.3.3 Characteristics of Advanced Range Telemetry Continuous Phase Modulation

The ARTM CPM is a quaternary signaling scheme in which the instantaneous frequency of the modulated signal is a function of the source data stream. The frequency pulses are shaped for spectral containment purposes. The modulation index alternates at the symbol rate between two values to improve the likelihood that the transmitted data is faithfully recovered. Although the following description is in terms of carrier frequency, other representations and generation methods exist that are equivalent. A block diagram of a conceptual ARTM CPM modulator is illustrated in [Figure 2-4](#). Source bits are presented to the modulator and are mapped into impulses that are applied to a filter with an impulse response $g(t)$. The resulting waveform $f(t)$ is proportional to the instantaneous frequency of the desired modulator output. This signal can be used to frequency modulate a carrier to produce an RF signal representation.

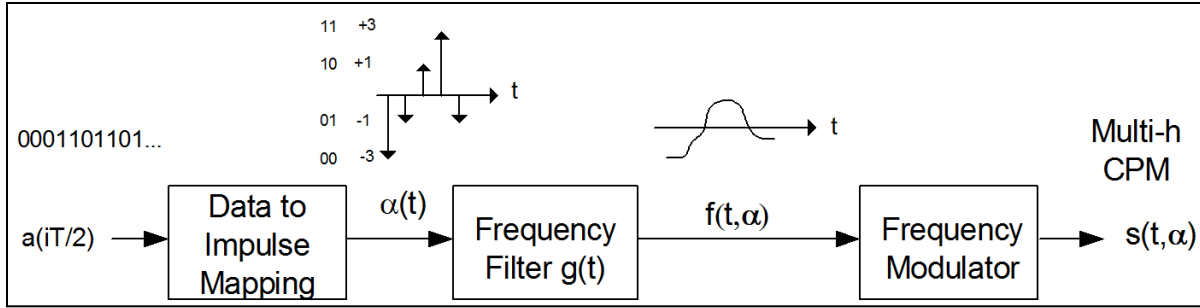


Figure 2-4. Conceptual CPM Modulator

Variables and function definitions in [Figure 2-4](#) are as follows.

- $a(iT/2)$ = i th bit of binary source data, either a 0 or 1.
- The frequency pulse shape for ARTM CPM is a three-symbol-long raised cosine pulse defined by the following equation for $0 \leq t \leq 3T$,

$$g(t) = \frac{1}{6T} \left[1 - \cos\left(\frac{2\pi t}{3T}\right) \right] \quad (2-11)$$

- T = Symbol period equal to $2/(\text{bit rate in bits/second})$.
- $\alpha(iT)$ = i th impulse with area equal to either a +3, +1, -1, or -3 determined by [Table 2-6](#). Note that an impulse is generated for each dibit pair (at the symbol rate).

| Table 2-6. Dibit to Impulse Area Mapping | |
|--|--------------|
| Input Dibit [a(i) a(i+1)] | Impulse Area |
| 1 1 | +3 |
| 1 0 | +1 |
| 0 1 | -1 |
| 0 0 | -3 |

- $f(t, \alpha)$ = frequency filter output equal to the following equation.

$$\pi h_i \sum_{i=-\infty}^{+\infty} \alpha(iT) g(t - iT) \quad (2-12)$$

- h = modulation index; h alternates between h_1 and h_2 where $h_1 = 4/16$, $h_2 = 5/16$.

For more information on the ARTM CPM waveform, please refer to [0](#) and to Geoghegan's paper.¹⁴

2.3.3.4 Data Randomization

The data input to the transmitter shall be randomized using either an encryptor that provides randomization or an Inter-Range Instrumentation Group (IRIG) 15-bit randomizer as

¹⁴ Mark Geoghegan. "Description and Performance Results for the Multi-h CPM Tier II Waveform." Paper presented at the 36th International Telemetry Conference, San Diego, CA, October 2000.

described in [Chapter 6](#) and [Annex A.2](#). The purpose of the randomizer is to prevent degenerative data patterns from degrading data quality.

2.3.3.5 Bit Rate

The bit rate range for FQPSK-B, FQPSK-JR, and SOQPSK-TG shall be between 1 megabit per second (Mbps) and 20 Mbps. The bit rate range for ARTM CPM shall be between 5 Mbps and 20 Mbps.

2.3.3.6 Transmitter Phase Noise

The sum of all discrete spurious spectral components (single-sideband) shall be less than -36 dBc. The continuous single-sideband phase noise power spectral density (PSD) shall be below the curve shown in [Figure 2-5](#). The maximum frequency for the curve is one-fourth of the bit rate. For bit rates greater than 4 Mbps, the phase noise PSD shall be less than -100 dBc/hertz (Hz) between 1 MHz and one-fourth of the bit rate.

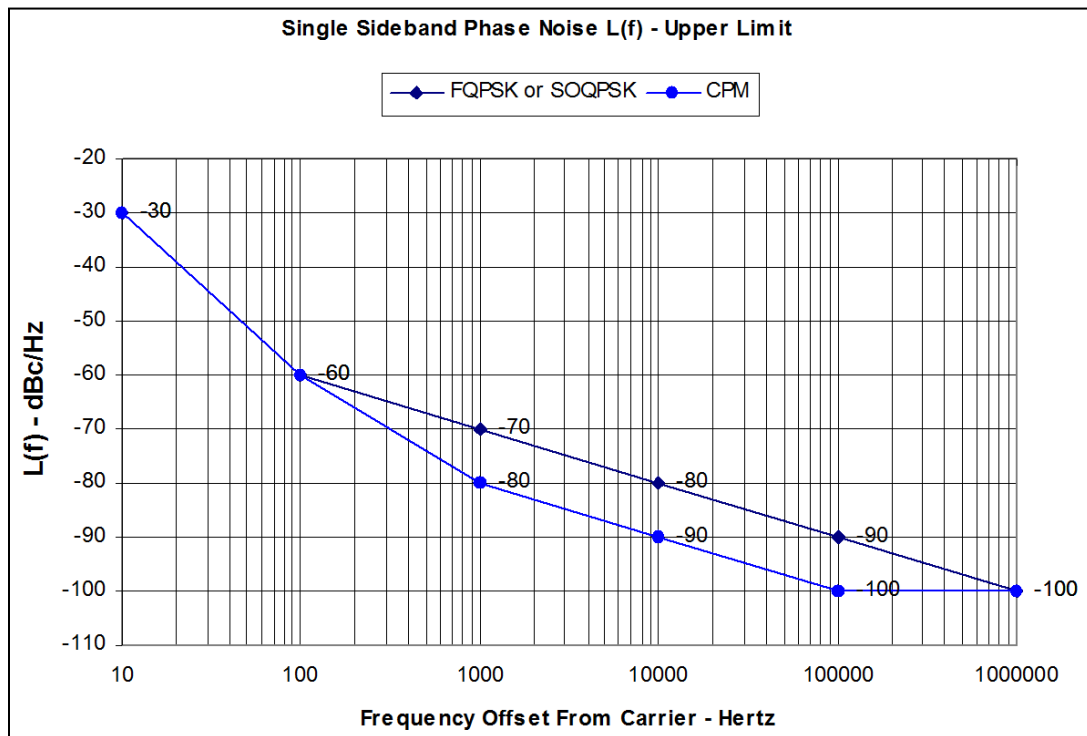


Figure 2-5. Continuous Single-Sideband Phase Noise Power Spectral Density

2.3.3.7 Modulation Polarity

An increasing voltage at the input of an FM transmitter shall cause an increase in output carrier frequency. An increase in voltage at the input of a PM transmitter shall cause an advancement in the phase of the output carrier. An increase in voltage at the input of an amplitude modulation (AM) transmitter shall cause an increase in the output voltage of the output carrier.

2.3.4 Spurious Emission and Interference Limits

Spurious¹⁵ emissions from the transmitter case, through input and power leads, and at the transmitter RF output and antenna-radiated spurious emissions are to be within required limits shown in Military Standard (MIL-STD)-461.¹⁶ Other applicable standards and specifications may be used in place of MIL-STD-461 if necessary.

2.3.4.1 Transmitter-Antenna System Emissions

Emissions from the antenna are of primary importance. For example, a tuned antenna may or may not attenuate spurious frequency products produced by the transmitter, and an antenna or multi-transmitter system may generate spurious outputs when a pure signal is fed to its input. The transmitting pattern of such spurious frequencies is generally different from the pattern at the desired frequency. Spurious outputs in the transmitter output line shall be limited to -25 dBm. Antenna-radiated spurious outputs shall be no greater than $320 \mu\text{V}/\text{meter}$ at 30 meters in any direction.

| | |
|----------------|---|
| WARNING | Spurious levels of -25 dBm may severely degrade performance of sensitive receivers whose antennas are located in close proximity to the telemetry transmitting antenna. Therefore, lower spurious levels may be required in certain frequency ranges, such as near Global Positioning System frequencies. |
|----------------|---|

2.3.4.2 Conducted and Radiated Interference

Interference (and the RF output itself) radiated from the transmitter or fed back into the transmitter power, signal, or control leads could interfere with the normal operation of the transmitter or the antenna system to which the transmitter is connected. All signals conducted by the transmitter's leads (other than the RF output cable) in the range of 150 kilohertz (kHz) to 50 MHz and all radiated fields in the range of 150 kHz to 10 gigahertz (GHz) (or other frequency ranges as specified) must be within the limits of the applicable standards or specifications.

2.3.5 Operational Flexibility

Each transmitter shall be capable of operating at all frequencies within its allocated band without design modification.¹⁷

2.3.6 Modulated Transmitter Bandwidth¹⁸

Telemetry applications covered by this standard shall use 99-percent power bandwidth to define occupied bandwidth and -25 dBm bandwidth as the primary measure of spectral efficiency. The -25 dBm bandwidth is the minimum bandwidth that contains all spectral components that are -25 dBm or larger. A power level of -25 dBm is exactly equivalent to an attenuation of the transmitter power by $55 + 10 \times \log(P)$ dB where P is the transmitter power expressed in watts. The spectra are assumed symmetrical about the transmitter's center

¹⁵ Any unwanted signal or emission is spurious whether or not it is related to the transmitter frequency (harmonic).

¹⁶ Department of Defense. "Requirements for the Control of Electromagnetic Interference Characteristics of Subsystems and Equipment." MIL-STD-461. 11 December 2015. May be superseded by update. Retrieved 23 March 2017. Available at http://quicksearch.dla.mil/qsDocDetails.aspx?ident_number=35789.

¹⁷ The intent is that fixed-frequency transmitters can be used at different frequencies by changing crystals or other components. All applicable performance requirements will be met after component change.

¹⁸ These bandwidths are measured using a spectrum analyzer with the following settings: 30-kHz resolution bandwidth, 300-Hz video bandwidth, and no max hold detector or averaging.

frequency unless specified otherwise. All spectral components larger than $-(55 + 10 \times \log(P))$ dBc at the transmitter output must be within the spectral mask calculated using the following equation:

$$M(f) = K + 90 \log R - 100 \log |f - f_c|; |f - f_c| \geq \frac{R}{m} \quad (2-13)$$

where $M(f)$ = power relative to P (i.e., units of dBc) at frequency f (MHz)

K = -20 for analog signals

= -28 for binary signals

= -61 for FQPSK-B, FQPSK-JR, SOQPSK-TG

= -73 for ARTM CPM

f_c = transmitter center frequency (MHz)

R = bit rate (Mbps) for digital signals or $(\Delta f + f_{\max})$ (MHz) for analog FM signals

m = number of states in modulating signal;

$m = 2$ for binary signals

$m = 4$ for quaternary signals and analog signals

Δf = peak deviation

f_{\max} = maximum modulation frequency

Note that the mask in this standard is different than the masks contained in earlier versions of the Telemetry Standards. Equation [2-13](#) does not apply to spectral components separated from the center frequency by less than R/m . The -25 dBm bandwidth is not required to be narrower than 1 MHz. Binary signals include all modulation signals with two states while quaternary signals include all modulation signals with four states (quadrature phase shift keying [QPSK] and FQPSK-B are two examples of four-state signals). Section [A.6](#) contains additional discussion and examples of this spectral mask.

2.3.7 Valid Center Frequencies Near Telemetry Band Edges

The telemetry bands, as specified, start and stop at discrete frequencies. Telemetry transmitters transmitting PCM/FM or SOQPSK-TG/FQPSK-B/FQPSK-JR or ARTM CPM, even with optimal filtering, do not have discrete start and stop frequencies. In order to determine a valid carrier frequency, the transmitter power, modulation scheme, and data rate must be known. The distance, in frequency, from the point in which the spectral masks, as described in Subsection [2.3.6](#), intersect the absolute value of -25 dBm equals the amount in which the transmitter carrier frequency must be from the band edge frequency. Subsection [A.12](#) contains additional discussion and examples of center frequency determination when operating near telemetry band edges.

2.4 Telemetry Receiver Systems

As a minimum, receiver systems shall have the following characteristics.

2.4.1 Spurious Emissions

The RF energy radiated from the receiver itself or fed back into the power supply, and/or the RF input, output, and control leads in the range from 150 kHz to 10 GHz shall be within the limits specified in MIL-STD-461. The receiver shall be tested in accordance with MIL-STD-461

or RCC Document 118, Volume II.¹⁹ Other applicable standards and specifications may be used in place of MIL-STD-461, if necessary.

2.4.2 Frequency Tolerance

The accuracy of all local oscillators within the receiver shall be such that the conversion accuracy at each stage and overall is within ± 0.001 percent of the indicated tuned frequency under all operating conditions for which the receiver is specified.

2.4.3 Receiver Phase Noise

The sum of all discrete spurious spectral components (single-sideband) shall be less than -39 dBc. The continuous single-sideband phase noise PSD shall be 3 dB below the curve shown in [Figure 2-5](#). The maximum frequency for the curve in [Figure 2-5](#) is one-fourth of the bit rate. For bit rates greater than 4 Mbps, the phase noise PSD shall be less than -103 dBc/Hz between 1 MHz and one-fourth of the bit rate.

2.4.4 Spurious Responses

Rejection of any frequency other than the one to which the receiver is tuned shall be a minimum of 60 dB referenced to the desired signal over the range 150 kHz to 10 GHz.

2.4.5 Operational Flexibility

All ground-based receivers shall be capable of operating over the entire band for which they are designed. External down-converters may be either intended for the entire band or a small portion but capable of retuning anywhere in the band without modification.

2.4.6 Intermediate Frequency Bandwidths

The standard receiver intermediate frequency (IF) bandwidths are shown in [Table 2-7](#). These bandwidths are separate from and should not be confused with post-detection low-pass filtering that receivers provide.²⁰ The ratio of the receiver's -60 dB bandwidth to the -3 dB bandwidth shall be less than 3 for new receiver designs.

| Table 2-7. Standard Receiver Intermediate Frequency Bandwidths | | |
|---|---------|--------|
| 300 kHz | 1.5 MHz | 6 MHz |
| 500 kHz | 2.4 MHz | 10 MHz |
| 750 kHz | 3.3 MHz | 15 MHz |
| 1000 kHz | 4.0 MHz | 20 MHz |

NOTE



1. For data receivers, the IF bandwidth should typically be selected so that 90 to 99 percent of the transmitted spectrum is within the receiver 3 dB bandwidth. In most cases, the optimum IF bandwidth will be narrower than the 99 percent power bandwidth.

¹⁹ Range Commanders Council. *Test Methods for Telemetry Systems and Subsystems Volume 2*. RCC 118-12. May be superseded by update. Retrieved 4 June 2015. Available at http://www.wsmr.army.mil/RCCsite/Documents/118-12_Vol_2-Test_Methods_for_Telemetry_RF_Subsystems/.

²⁰ In most instances, the output low-pass filter should *not* be used to “clean up” the receiver output prior to use with demultiplexing equipment.

| | |
|--|---|
| | <p>2. Bandwidths are expressed at the points where response is 3 dB below the response at the design center frequency, assuming that passband ripple is minimal, which may not be the case. The 3-dB bandwidth is chosen because it closely matches the noise bandwidth of a “brick-wall” filter of the same bandwidth. The “optimum” bandwidth for a specific application may be other than that stated here. Ideal IF filter response is symmetrical about its center frequency; in practice, this may not be the case.</p> <p>3. Not all bandwidths are available on all receivers or at all test ranges. Additional receiver bandwidths may be available at some test ranges, especially if the range has receivers with digital IF filtering</p> |
|--|---|

2.4.7 C-band Downconversion

For telemetry receive systems employing C-band downconversion, the following mapping of C-band RF to C-band IF frequencies is recommended for the lower C and middle C bands. This downconversion scheme utilizes a high-side local oscillator frequency of 5550 MHz to minimize the potential of mixing products interfering with received telemetry signals. Additionally, using a standardized approach fosters interoperability between manufacturers of telemetry antenna systems employing downconversion and manufacturers of telemetry receivers with C-IF tuners.

No recommendation will be made at this point for the downconversion of the upper C band (5925-6700 MHz).

Examples:

$$\text{C-IF Frequency} = (5550 \text{ MHz} - \text{C-RF Frequency})$$

$$1150 \text{ MHz} = (5550 \text{ MHz} - 4400 \text{ MHz})$$

$$610 \text{ MHz} = (5550 \text{ MHz} - 4940 \text{ MHz})$$

$$459 \text{ MHz} = (5550 \text{ MHz} - 5091 \text{ MHz})$$

$$400 \text{ MHz} = (5550 \text{ MHz} - 5150 \text{ MHz})$$

2.5 Codes for Telemetry Systems

2.5.1 Low-Density Parity-Check Code

Forward error correction (FEC) is a way of adding additional information to a transmitted bit stream in order to decrease the required signal-to-noise ratio to the receiver for a given bit error rate (BER). Low-density parity-check (LDPC) code is a block code, meaning that a block of information bits has parity added to them in order to correct for errors in the information bits. The term “low-density” stems from the parity check matrix containing mostly 0’s and relatively few 1’s. This specific LDPC variant comes from the satellite link community and is identical to the Accumulate-Repeat-4-Jagged-Accumulate code described by the Consultative Committee for Space Data Systems (CCSDS) standard 131.1-O-2-S.1,²¹ which describes nine different LDPC codes with different coding rates (rate 1/2, 2/3, 4/5) and information block sizes (1024, 4096, 16384). In the trade between the transmission channel characteristics, bandwidth efficiency,

²¹ Consultative Committee for Space Data Systems. *Low Density Parity Check Codes for Use in Near-Earth and Deep Space Applications*. Standard CCSDS 131.1-O-2-S. September 2007. Rescinded. Retrieved 30 June 2015. Available at <http://public.ccsds.org/publications/archive/131x1o2e2s.pdf>.

coding gain, and block size all three rates and block sizes 1024 and 4096 are considered in this standard. Additional information on this LDPC code is contained in [Appendix 2-D](#).

2.5.2 Space-Time Code

As the name suggests, this code uses space diversity and time diversity to overcome the two-antenna problem, which is characterized by large variances in the antenna gain pattern from a test article caused by transmitting the same telemetry signal time through two transmit antennas. These signals are typically delayed in time and have differing amplitudes. The space-time code (STC) in this standard applies to only SOQPSK-TG modulation. The input bit stream is space-time coded, resulting in two parallel bit streams that then have a pilot sequence added to each at fixed bit intervals (or blocks). These encoded/pilot-added streams are then individually modulated through phase-locked transmitters to a carrier using SOQPSK-TG modulation, power amplified, then connected to a top and bottom antenna. The job of estimating frequency offset, delays, gains, and phase shifts due to the transmission channel then space-time decode the signal is done with the STC receiver. Additional information on the STC is contained in [Appendix 2-E](#).

2.6 **Randomization Methods for Telemetry Systems**

2.6.1 Introduction

The following randomization and de-randomization methods are recommended for wireless serial streaming telemetry data links. The choice of randomization method used should be based on whether or not a self-synchronizing randomizer is required for the application.

2.6.2 Randomizer Types

2.6.2.1 Self-Synchronizing Randomizers

Self-synchronizing randomizers, such as the traditional IRIG randomizer described in [Annex A.2](#), work best when there are no known identifiers in the bit stream to aid in synchronizing the de-randomizer. This type of de-randomizer has the characteristic of creating additional bit errors when a bit error is received at the de-randomizer input. For this randomizer a single bit error at the input will create an additional two bit errors in the output stream. This BER extension will cause a degradation in detection efficiency of the link of approximately 0.5 dB.

2.6.2.2 Non-Self-Synchronizing Randomizers

Non-self-synchronizing randomizers, such as the CCSDS randomizer described in [Appendix 2-D](#), do not create additional bit errors when a bit error is received at the de-randomizer input. Therefore there is no extension of BER; however, these types of randomizers need to be synchronized with the incoming bit stream. This is usually accomplished through the use of pilot bits or synchronization markers in the data stream to aid in synchronization. Performance of this type of randomizer will exceed that of a self-synchronizing randomizer lending itself as a better choice for coded links or links requiring data-aided synchronization.

2.6.3 Randomizer Application

As defined in [Appendix 2-D](#), CCSDS randomization as defined in should be used for coded links such as LDPC links or links exhibiting a block structure with synchronization markers.

Traditional IRIG randomization as defined in [Annex A.2](#) should be used for non-encrypted links that are absent of synchronization markers or do not contain markers of any type. Encrypted telemetry links do not require randomization.

2.7 Data Quality Metrics and Data Quality Encapsulation

A reliable metric for estimating data quality can be very useful when controlling telemetry data processing equipment, such as Best Source Selectors, that require an understanding of received data quality in order to operate effectively. To accomplish this, a standardized method for estimating bit error probability (BEP) is needed. In addition to the metric, a standardized method for transporting the metric with the associated data is required. [Appendix 2-G](#) provides a standard for a Data Quality Metric (DQM), determined in the telemetry receiver demodulator, and a standard for Data Quality Encapsulation (DQE) allowing for transport of the received telemetry data and associated DQM.

2.8 Interference Protection Criteria for Aeronautical Mobile Telemetry Systems

Aeronautical mobile telemetry (AMT) ground stations use very high gain directional antenna systems that are sensitive to interference from other RF communication systems. Without appropriate interference protection, these systems could be severely impacted or even rendered useless for mission support. To prevent this from happening, appropriate interference protection criteria (IPC) are needed.

[Table 2-8](#) lists the acceptable power flux density (PFD) levels for interference in each telemetry band. These levels are based on the well-established and accepted IPC contained in International Telecommunications Union Radio Service (ITU-R) Recommendation M.1459²² (Rec M.1459). These IPCs provide AMT protection for aggregate interference from satellites and terrestrial emitters as a function of the angle of arrival α of the interfering signal(s) at or above the horizon derived using the methodology given in Annex A of Rec M.1459.

| Table 2-8. Interference Protection Criteria by Band and Angle of Arrival | | |
|---|--------------------------------|--|
| L band, from 1435 – 1535 MHz | | |
| –181.0 | dB(W/m ²) in 4 kHz | for $0 \leq \alpha \leq 4^\circ$ |
| $-193.0 + 20 \log \alpha$ | dB(W/m ²) in 4 kHz | for $4 < \alpha \leq 20^\circ$ |
| $-213.3 + 35.6 \log \alpha$ | dB(W/m ²) in 4 kHz | for $20 < \alpha \leq 60^\circ$ |
| –150.0 | dB(W/m ²) in 4 kHz | for $60 < \alpha \leq 90^\circ$ |
| Upper L band, from 1755 – 1855 MHz | | |
| –181.0 | dB(W/m ²) in 4 kHz | for $0^\circ \leq \alpha \leq 3^\circ$ |
| $-190.878 + 21.948 \log \alpha$ | dB(W/m ²) in 4 kHz | for $3^\circ < \alpha \leq 15^\circ$ |
| $-185.722 + 18.286 \log \alpha$ | dB(W/m ²) in 4 kHz | for $15^\circ < \alpha \leq 60^\circ$ |
| –153.7 | dB(W/m ²) in 4 kHz | for $60^\circ < \alpha \leq 90^\circ$ |
| Lower S band, from 2200 – 2290 MHz | | |
| –180.0 | dB(W/m ²) in 4 kHz | for $0^\circ \leq \alpha \leq 2^\circ$ |

²² International Telecommunication Union. “Protection criteria for telemetry systems in the aeronautical mobile service...” ITU-R Recommendation M.1459. May 2000. May be superseded by update. Available at <https://www.itu.int/rec/R-REC-M.1459-0-200005-I/en>.

| Table 2-8. Interference Protection Criteria by Band and Angle of Arrival | | |
|---|--------------------------------|---|
| $-186.613 + 21.206 \log \alpha$ | dB(W/m ²) in 4 kHz | for $2^\circ < \alpha \leq 15^\circ$ |
| -161 | dB(W/m ²) in 4 kHz | for $15^\circ < \alpha \leq 90^\circ$ |
| Upper S band, from 2310 – 2390 MHz | | |
| -180.0 | dB(W/m ²) in 4 kHz | for $0^\circ \leq \alpha \leq 2^\circ$ |
| $-187.5 + 23.66 \log \alpha$ | dB(W/m ²) in 4 kHz | for $2^\circ < \alpha \leq 11.5^\circ$ |
| -162 | dB(W/m ²) in 4 kHz | for $11.5^\circ < \alpha \leq 90^\circ$ |
| Lower C band, from 4400 – 4940 MHz | | |
| -178.0 | dB(W/m ²) in 4 kHz | for $0^\circ \leq \alpha \leq 1^\circ$ |
| $-180.333 + 2.333 \alpha$ | dB(W/m ²) in 4 kHz | for $1^\circ < \alpha \leq 4^\circ$ |
| -171.0 | dB(W/m ²) in 4 kHz | for $4^\circ < \alpha \leq 90^\circ$ |
| Middle C band, from 5091 – 5150 MHz | | |
| -178.0 | dB(W/m ²) in 4 kHz | for $0^\circ \leq \alpha \leq 1^\circ$ |
| $-180.0 + 2.0 \alpha$ | dB(W/m ²) in 4 kHz | for $1^\circ < \alpha \leq 3^\circ$ |
| -174.0 | dB(W/m ²) in 4 kHz | for $3^\circ < \alpha \leq 90^\circ$ |
| Upper C band, from 5925 – 6700 MHz | | |
| -178.0 | dB(W/m ²) in 4 kHz | for $0^\circ \leq \alpha \leq 1^\circ$ |
| $-181.6 + 3.6 \alpha$ | dB(W/m ²) in 4 kHz | for $1^\circ < \alpha \leq 2^\circ$ |
| -174.4 | dB(W/m ²) in 4 kHz | for $2^\circ < \alpha \leq 90^\circ$ |

[Appendix 2-F](#) provides additional explanation and example calculations to aid in understand the application of these IPCs for different interference scenarios.

This page intentionally left blank.

APPENDIX 2-A

Frequency Considerations for Telemetry

A.1. Purpose

This appendix was prepared with the cooperation and assistance of the Range Commanders Council (RCC) Frequency Management Group. This appendix provides guidance to telemetry users for the most effective use of the telemetry bands. Coordination with the frequency managers of the applicable test ranges and operating areas is recommended before a specific frequency band is selected for a given application. Government users should coordinate with the appropriate Area Frequency Coordinator and commercial users should coordinate with the AFTRCC. A list of the points of contact can be found in the NTIA manual (NTIA 2015).

A.2. Scope

This appendix is to be used as a guide by users of telemetry frequencies at Department of Defense (DoD)-related test ranges and contractor facilities. The goal of frequency management is to encourage maximal use and minimal interference among telemetry users and between telemetry users and other users of the electromagnetic spectrum.

A.2.a. Definitions

The following terminology is used in this appendix.

Allocation (of a Frequency Band). Entry of a frequency band into the Table of Frequency Allocations²³ for use by one or more radio communication services or the radio astronomy service under specified conditions.

Assignment (of a Radio Frequency or Radio Frequency Channel). Authorization given by an administration for a radio station to use an RF or RF channel under specified conditions.

Authorization. Permission to use an RF or RF channel under specified conditions.

Certification. The Military Communications - Electronics Board's (MCEB) process of verifying that a proposed system complies with the appropriate rules, regulations, and technical standards.

J/F 12 Number. The identification number assigned to a system by the MCEB after the Application for Equipment Frequency Allocation (DD Form 1494) is approved; for example, J/F 12/6309 (sometimes called the J-12 number).

Resolution Bandwidth. The -3 dB bandwidth of the measurement device.

A.2.b. Modulation methods

A.2.b(1) Traditional Modulation Methods

The traditional modulation methods for aeronautical telemetry are FM and PM. The PCM/FM method has been the most popular telemetry modulation since around 1970. The

²³ The definitions of the radio services that can be operated within certain frequency bands contained in the radio regulations as agreed to by the member nations of the International Telecommunications Union. This table is maintained in the United States by the Federal Communications Commission and the NTIA.

PCM/FM method could also be called filtered CPFSK. The RF signal is typically generated by filtering the baseband NRZ-L signal and then frequency modulating a VCO. The optimum peak deviation is 0.35 times the bit rate and a good choice for a premodulation filter is a multi-pole linear phase filter with bandwidth equal to 0.7 times the bit rate. Both FM and PM have a variety of desirable features but may not provide the required bandwidth efficiency, especially for higher bit rates.

A.2.b(2) Improved Bandwidth Efficiency

When better bandwidth efficiency is required, the standard methods for digital signal transmission are the FQPSK-B and FQPSK-JR, the SOQPSK-TG, and the ARTM CPM. Each of these methods offers constant, or nearly constant, envelope characteristics and is compatible with nonlinear amplifiers with minimal spectral regrowth and minimal degradation of detection efficiency. The first three methods (FQPSK-B, FQPSK-JR, and SOQPSK-TG) are interoperable and require the use of the differential encoder described in Subsection [2.3.3.1.1](#). Additional information on this differential encoder is contained in [0](#). All of these bandwidth-efficient modulation methods require the data to be randomized.

A.2.c. Other Notations

The following notations are used in this appendix. Other references may define these terms slightly differently.

- a. **B99%** - Bandwidth containing 99% of the total power.
- b. **B-25dBm** - Bandwidth containing all components larger than -25 dBm.
- c. **B-60dBc** - Bandwidth containing all components larger than the power level that is 60 dB below the unmodulated carrier power.
- d. **dBc** - Decibels relative to the power level of the unmodulated carrier.
- e. **f_c** - Assigned center frequency.

A.3. Authorization to Use a Telemetry System

All RF emitting devices must have approval to operate in the US&P via a frequency assignment unless granted an exemption by the national authority. The NTIA is the President's designated national authority and spectrum manager. The NTIA manages and controls the use of RF spectrum by federal agencies in US&P territory. Obtaining a frequency assignment involves the two-step process of obtaining an RF spectrum support certification of major RF systems design, followed by an operational frequency assignment to the RF system user. These steps are discussed below.

A.3.a. RF Spectrum Support Certification

All major RF systems used by federal agencies must be submitted to the NTIA, via the Interdepartment Radio Advisory Committee, for system review and spectrum support certification prior to committing funds for acquisition/procurement. During the system review process, compliance with applicable RF standards, RF allocation tables, rules, and regulations is checked. For DoD agencies and for support of DoD contracts, this is accomplished via the submission of a DD Form 1494 to the MCEB. Noncompliance with standards, the tables, rules, or regulations can result in denial of support, limited support, or support on an unprotected non-

priority basis. All RF users must obtain frequency assignments for any RF system (even if not considered major). This assignment is accomplished by submission of frequency use proposals through the appropriate frequency management offices. Frequency assignments may not be granted for major systems that have not obtained spectrum support certification.

A.3.a(1) Frequency Allocation

As stated before, telemetry systems must normally operate within the frequency bands designated for their use in the Table of Frequency Allocations. With sufficient justification, use of other bands may at times be permitted, but the certification process is much more difficult, and the outcome is uncertain. Even if certification is granted on a noninterference basis to other users, the frequency manager is often unable to grant assignments because of local users who will get interference.

a. *Telemetry Bands*

Air and space-to-ground telemetering is allocated in the ultra-high frequency (UHF) bands 1435 to 1535, 2200 to 2290, and 2310 to 2390 MHz (commonly known as the lower L-band, the lower S-band, and the upper S-band) and in the super-high frequency (SHF) bands 4400 to 4940 and 5091 to 5150 MHz (commonly known as lower C-band and middle C-band). Other mobile bands, such as 1755-1850 MHz, can also be used at many test ranges. Since these other bands are not considered a standard telemetry band per this document, potential users must coordinate, in advance, with the individual range(s) and ensure use of this band can be supported at the subject range(s) and that their technical requirements will be met.

b. *Very High Frequency Telemetry*

The very-high frequency (VHF) band, 216-265 MHz, was used for telemetry operations in the past. Telemetry bands were moved to the UHF bands as of 1 January 1970 to prevent interference to critical government land mobile and military tactical communications. Telemetry operation in this band is strongly discouraged and is considered only on an exceptional case-by-case basis.

A.3.a(2) Technical Standards

The MCEB and the NTIA review proposed telemetry systems for compliance with applicable technical standards. For the UHF and SHF telemetry bands, the current revisions of the following standards are considered applicable:

- a. RCC Document IRIG 106, Telemetry Standards;
- b. MIL-STD-461;
- c. NTIA Manual of Regulations and Procedures for Federal Radio Frequency Management.

Applications for certification are also thoroughly checked in many other ways, including necessary and occupied bandwidths, modulation characteristics, reasonableness of output power, correlation between output power and amplifier type, and antenna type and characteristics. The associated receiver normally must be specified or referenced. The characteristics of the receiver are also verified.

A.3.b. Frequency Authorization

Spectrum certification of a telemetry system verifies that the system meets the technical requirements for successful operation in the electromagnetic environment; however, a user is not permitted to radiate with the telemetry system before requesting and receiving a specific

frequency assignment. The assignment process considers when, where, and how the user plans to radiate. Use of the assignments is tightly scheduled by and among the individual ranges to make the most efficient use of the limited telemetry RF spectrum and to ensure that one user does not interfere with other users.

A.4. Frequency Usage Guidance

Frequency usage is controlled by scheduling in the areas where the tests will be conducted. [Figure A-1](#) displays the four modulation methods addressed in this section. The following recommendations are based on good engineering practice for such usage and it is assumed that the occupied bandwidth fits within the telemetry band in all cases.

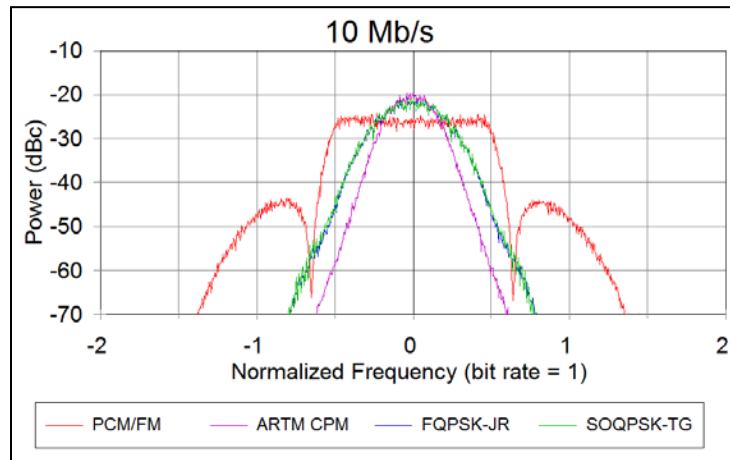


Figure A-1. Spectra of 10-Mbps PCM/FM, ARTM CPM, FQPSK-JR, SOQPSK-TG Signals

A.4.a. Minimum Frequency Separation

The minimum required frequency separation can be calculated using the formula:

$$\Delta F_0 = a_s * R_s + a_i * R_i \quad (A-1)$$

where ΔF_0 = the minimum required center frequency separation in MHz;
 R_s = bit rate of desired signal in Mbps;
 R_i = bit rate of interfering signal in Mbps;
 a_s is determined by the desired signal type and receiving equipment ([Table A-1](#)).

| Table A-1. Coefficients for Minimum Frequency Separation Calculation | | |
|--|---|-------|
| Modulation Type | a_s | a_i |
| NRZ PCM/FM | 1.0* for receivers with resistor-inductor-capacitor (RLC) final IF filters 0.7 for receivers with surface acoustic wave (SAW) or digital IF filters 0.5 with multi-symbol detectors (or equivalent devices) | 1.2 |
| FQPSK-B, FQPSK-JR, SOQPSK-TG | 0.45 | 0.65 |

| | | |
|--|------|-----|
| ARTM CPM | 0.35 | 0.5 |
| *The minimum frequency separation for typical receivers with RLC final IF filters and NRZ-L PCM/FM signals is the larger of 1.5 times the actual IF –3 dB bandwidth and the value calculated using the equation above. | | |

The minimum spacing needs to be calculated for signal 1 as the desired signal and signal 2 as the interferer and vice versa. Note that the values for a_i match the –57 dBc points for the four modulation methods shown in [Figure A-1](#) quite closely. It is not surprising that the required frequency spacing from the interferer is directly related to the power spectrum of the interfering signal. The values for a_s are a function of the effective detection filter bandwidths and the co-channel interference resistance of the desired signal modulation method and detector. The values for a_s and a_i are slightly conservative for most cases and assume the receiver being used does not have spurious responses that cause additional interference. This section was completely rewritten from previous editions of the Telemetry Standards because addition of new modulation methods and new receiving equipment rendered the old method obsolete. The values of a_s and a_i were determined empirically from the results of extensive adjacent channel interference testing. The main assumptions are as follows.

- The NRZ PCM/FM signals are assumed to be premodulation filtered with a multi-pole filter with –3 dB point of 0.7 times the bit rate and the peak deviation is assumed to be approximately 0.35 times the bit rate.
- The receiver IF filter is assumed to be no wider than 1.5 times the bit rate and provides at least 6 dB of attenuation of the interfering signal.
- The interfering signal is assumed to be no more than 20 dB stronger than the desired signal.
- The receiver is assumed to be operating in linear mode; no significant intermodulation products or spurious responses are present.

Examples are shown below.

5-Mbps PCM/FM and 0.8-Mbps PCM/FM using a receiver with 6-MHz IF bandwidth for the 5-Mbps signal (this receiver has RLC IF filters)

$$1.0*5 + 1.2*0.8 = 5.96 \text{ MHz} \qquad 1.0*0.8 + 1.2*5 = 6.8 \text{ MHz} \qquad 1.5*6 = 9.0 \text{ MHz}$$

The largest value is 9 MHz and the frequencies are assigned in 1-MHz steps, so the minimum spacing is 9 MHz.

5-Mbps PCM/FM and 5-Mbps PCM/FM using a receiver with 6-MHz IF bandwidth for the 5-Mbps signals (these receivers have RLC IF filters; see [Figure A-2](#))

$$1.0*5 + 1.2*5 = 11 \text{ MHz} \qquad 1.5*6 = 9.0 \text{ MHz}$$

The larger value is 11 MHz and the frequencies are assigned in 1-MHz steps, so the minimum spacing is 11 MHz.

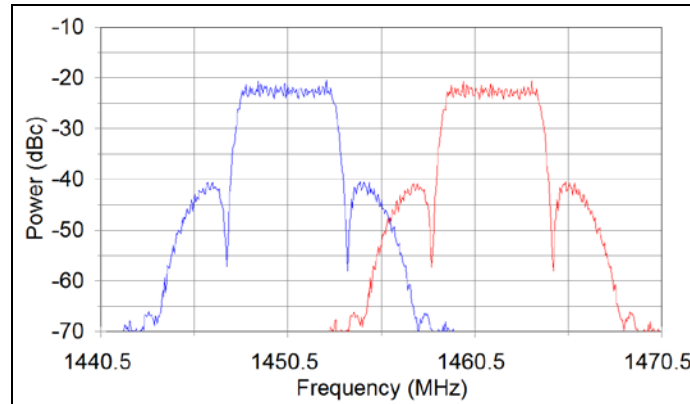


Figure A-2. 5 Mbps PCM/FM Signals with 11 MHz Center Frequency Separation

5-Mbps PCM/FM and 5-Mbps PCM/FM using a receiver with 6-MHz IF bandwidth for the 5-Mbps signal (this receiver has RLC IF filters but a multi-symbol detector is used)

$$0.5*5 + 1.2*5 = 8.5 \text{ MHz}$$

The frequencies are assigned in 1-MHz steps, so the minimum spacing is 9 MHz.

5-Mbps PCM/FM and 5-Mbps SOQPSK-TG using a receiver with 6-MHz IF bandwidth for the 5-Mbps signals (this receiver has RLC IF filters but a multi-symbol detector is used)

$$0.5*5 + 0.65*5 = 5.75 \text{ MHz} \quad 0.45*5 + 1.2*5 = 8.25 \text{ MHz}$$

The largest value is 8.25 MHz and the frequencies are assigned in 1-MHz steps, so the minimum spacing is 9 MHz.

5-Mbps FQPSK-B and 5-Mbps ARTM CPM using a receiver with 6-MHz IF bandwidth for the 5-Mbps signals

$$0.45*5 + 0.5*5 = 4.75 \text{ MHz} \quad 0.35*5 + 0.7*5 = 5.25 \text{ MHz}$$

The largest value is 5.25 MHz and the frequencies are assigned in 1-MHz steps, so the minimum spacing is 6 MHz.

10-Mbps ARTM CPM and 10-Mbps ARTM CPM (see [Figure A-3](#))

$$0.35*10 + 0.5*10 = 8.5 \text{ MHz}$$

The frequencies are assigned in 1-MHz steps, so the minimum spacing is 9 MHz.

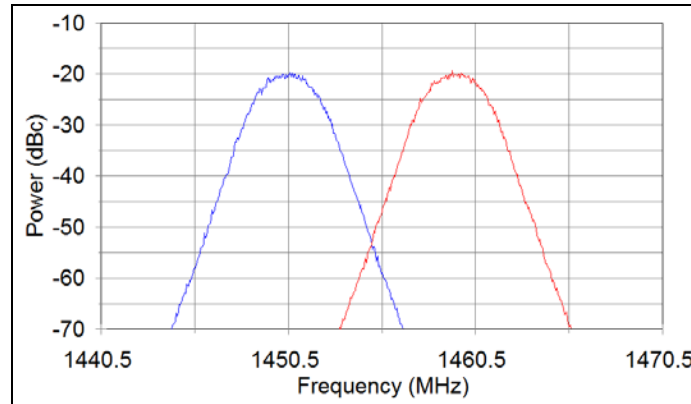


Figure A-3. 10 Mbps ARTM CPM Signals with 9 MHz Center Frequency Separation

In some cases it may be desirable to set aside a bandwidth for each signal independent of other signals. If one uses a bandwidth factor of $2 \cdot a_i$ for each signal, then one gets a separation of $\Delta F_0 = a_i \cdot R_s + a_i \cdot R_i$ and one gets a more conservative (wider) separation than one would using $\Delta F_0 = a_s \cdot R_s + a_i \cdot R_i$ because the value of a_i is bigger than the value of a_s for all of these modulation methods. One problem with this approach is that it does not include receiver or detector characteristics and therefore the calculated frequency separations are often different from those calculated using the formula in Subsection [A.4.a](#).

Examples of frequency separation are shown below.

5-Mbps PCM/FM and 0.8-Mbps PCM/FM using a receiver with 6-MHz IF bandwidth for the 5-Mbps signal (this receiver has RLC IF filters)

$$1.2 \cdot 5 + 1.2 \cdot 0.8 = 6.96 \text{ MHz}$$

The frequencies are assigned in 1-MHz steps, so the minimum spacing is 7 MHz.

5-Mbps PCM/FM and 5-Mbps PCM/FM using a receiver with 6-MHz IF bandwidth for the 5-Mbps signals (these receivers have RLC IF filters)

$$1.2 \cdot 5 + 1.2 \cdot 5 = 12 \text{ MHz}$$

The frequencies are assigned in 1-MHz steps, so the minimum spacing is 12 MHz.

5-Mbps PCM/FM and 5-Mbps PCM/FM using a receiver with 6-MHz IF bandwidth for the 5-Mbps signal (this receiver has RLC IF filters but a multi-symbol detector is used)

$$1.2 \cdot 5 + 1.2 \cdot 5 = 12 \text{ MHz}$$

The frequencies are assigned in 1-MHz steps, so the minimum spacing is 12 MHz.

5-Mbps PCM/FM and 5-Mbps SOQPSK-TG using a receiver with 6-MHz IF bandwidth for the 5-Mbps signals (this receiver has RLC IF filters but a multi-symbol detector is used)

$$1.2 \cdot 5 + 0.65 \cdot 5 = 9.25 \text{ MHz}$$

The frequencies are assigned in 1-MHz steps, so the minimum spacing is 10 MHz.

5-Mbps FQPSK-B and 5-Mbps ARTM CPM using a receiver with 6-MHz IF bandwidth for the 5-Mbps signals

$$0.7*5 + 0.5*5 = 6 \text{ MHz}$$

The frequencies are assigned in 1-MHz steps, so the minimum spacing is 6 MHz.

10-Mbps ARTM CPM and 10-Mbps ARTM CPM

$$0.5*10 + 0.5*10 = 10 \text{ MHz}$$

The frequencies are assigned in 1-MHz steps, so the minimum spacing is 10 MHz.

A.4.b. Geographical Separation

Geographical separation can be used to further reduce the probability of interference from adjacent signals.

A.4.c. Multicarrier Operation

If two transmitters are operated simultaneously and sent or received through the same antenna system, interference due to intermodulation is likely at $(2f_1 - f_2)$ and $(2f_2 - f_1)$. Between three transmitters, the two-frequency possibilities exist, but intermodulation products may exist as well at $(f_1 + f_2 - f_3)$, $(f_1 + f_3 - f_2)$, and $(f_2 + f_3 - f_1)$, where f_1 , f_2 , and f_3 represent the output frequencies of the transmitters. Intermodulation products can arise from nonlinearities in the transmitter output circuitry that cause mixing products between a transmitter output signal and the fundamental signal coming from nearby transmitters. Intermodulation products also can arise from nonlinearities in the antenna systems. The generation of intermodulation products is inevitable, but the effects are generally of concern only when such products exceed -25 dBm. The general rule for avoiding third-order intermodulation interference is that in any group of transmitter frequencies, the separation between any pair of frequencies should not be equal to the separation between any other pair of frequencies. Because individual signals have sidebands, it should be noted that intermodulation products have sidebands spectrally wider than the sidebands of the individual signals that caused them.

A.4.d. Transmitter Antenna System Emission Testing

Radiated tests will be made in lieu of transmitter output tests only when the transmitter is inaccessible. Radiated tests may still be required if the antenna is intended to be part of the filtering of spurious products from the transmitter or is suspected of generating spurious products by itself or in interaction with the transmitter and feed lines. These tests should be made with normal modulation.

A.5. Bandwidth

The definitions of bandwidth in this section are universally applicable. The limits shown here are applicable for telemetry operations in the telemetry bands specified in [Chapter 2](#). For the purposes of telemetry signal spectral occupancy, the bandwidths used are B99% and

B-25dBm. A power level of -25 dBm is exactly equivalent to an attenuation of the transmitter power by $55 + 10 \times \log(P)$ dB where P is the transmitter power expressed in watts. How bandwidth is actually measured and what the limits are, expressed in terms of that measuring system, are detailed in the following paragraphs.

A.5.a. Concept

The term “bandwidth” has an exact meaning in situations where an AM, double-sideband, or single-sideband signal is produced with a band-limited modulating signal. In systems employing FM or PM, or any modulation system where the modulating signal is not band limited, bandwidth is infinite with energy extending toward zero and infinite frequency falling off from the peak value in some exponential fashion. In this more general case, bandwidth is defined as the band of frequencies in which most of the signal’s energy is contained. The definition of “most” is imprecise. The following terms are applied to bandwidth.

A.5.a(1) Authorized Bandwidth

For purposes of this document, the authorized bandwidth is the necessary bandwidth required for transmission and reception of intelligence and does not include allowance for transmitter drift or Doppler shift.

A.5.a(2) Occupied Bandwidth

The width of a frequency band such that below the lower and above the upper frequency limits, the mean powers emitted are each equal to a specified percentage of the total mean power of a given emission. Unless otherwise specified by the ITU for the appropriate class of emission, the specified percentage shall be 0.5%. In this document occupied bandwidth and B99% are interchangeable.

A.5.a(3) Necessary Bandwidth for a Given Class of Emission

For a given class of emission, the width of the frequency band that is just sufficient to ensure the transmission of information at the rate and with the quality required under specified conditions. Note: the term “under specified conditions” does not include signal bandwidth required when operating with adjacent channel signals (i.e., potential interferers).

a. *The NTIA Manual*

This manual states that “All reasonable effort shall be made in equipment design and operation by Government agencies to maintain the occupied bandwidth of the emission of any authorized transmission as closely to the necessary bandwidth as is reasonably practicable.”

b. *Necessary Bandwidth (DD Form 1494)*

The necessary bandwidth is part of the emission designator on the DD Form 1494. For telemetry purposes, the necessary bandwidth can be calculated using the equations shown in [Table A-2](#). Equations for these and other modulation methods are contained in Annex J of the NTIA Manual.

| Table A-2. B99% for Various Digital Modulation Methods | |
|---|-------------|
| Description | B99% |
| NRZ PCM/FM, premod filter BW=0.7R, $\Delta f=0.35R$ | 1.16 R |
| NRZ PCM/FM, no premod filter, $\Delta f=0.25R$ | 1.18 R |
| NRZ PCM/FM, no premod filter, $\Delta f=0.35R$ | 1.78 R |

| | |
|---|--------|
| NRZ PCM/FM, no premod filter, $\Delta f=0.40R$ | 1.93 R |
| NRZ PCM/FM, premod filter BW=0.7R, $\Delta f=0.40R$ | 1.57 R |
| Minimum shift keying (MSK), no filter | 1.18 R |
| FQPSK-B, FQPSK-JR or SOQPSK-TG | 0.78 R |
| ARTM CPM | 0.56 R |

Filtered NRZ PCM/FM. $B_n = 1.16 \times \text{bit rate}$ with $h=0.7$ and premodulation filter bandwidth = 0.7 times bit rate. Example: PCM/FM modulation used to send 5 Mbps using FM with 2 signaling states and 1.75 MHz peak deviation; bit rate= 5×10^6 ; necessary bandwidth (B_n) = 5.8 MHz.

Constant envelope OQPSK; FQPSK-B, FQPSK-JR, or SOQPSK-TG. $B_n = 0.78 \times \text{bit rate}$. Example: SOPQSK-TG modulation used to send 5 Mbps using 4 signaling states; bit rate= 5×10^6 ; $B_n = 3.9$ MHz.

ARTM CPM. $B_n = 0.56 \times \text{bit rate}$ with $h=4/16$ and $5/16$ on alternating symbols; digital modulation used to send 5 Mbps using FM with 4 signaling states and with alternating modulation index each symbol; bit rate= 5×10^6 ; $B_n = 2.8$ MHz.

A.5.a(4) Received (or Receiver) Bandwidth

The received bandwidth is usually the -3 dB bandwidth of the receiver IF section.

A.5.b. Bandwidth Estimation and Measurement

Various methods are used to estimate or measure the bandwidth of a signal that is not band limited. The bandwidth measurements are performed using a spectrum analyzer (or equivalent device) with the following settings: 30-kHz resolution bandwidth, 300-Hz video bandwidth, and no max hold detector or averaging. These settings are different than those in earlier versions of the Telemetry Standards. The settings were changed to get more consistent results across a variety of bit rates, modulation methods, and spectrum analyzers. The most common measurement and estimation methods are described in the following paragraphs.

A.5.b(1) B99%

This bandwidth contains 99% of the total power. Typically, B99% is measured using a spectrum analyzer or estimated using equations for the modulation type and bit rate used. If the two points that define the edges of the band are not symmetrical about the assigned center frequency, their actual frequencies and difference should be noted. The B99% edges of randomized NRZ (RNRZ) PCM/FM signals are shown in [Figure A-4](#). [Table A-2](#) presents B99% for several digital modulation methods as a function of the bit rate (R).

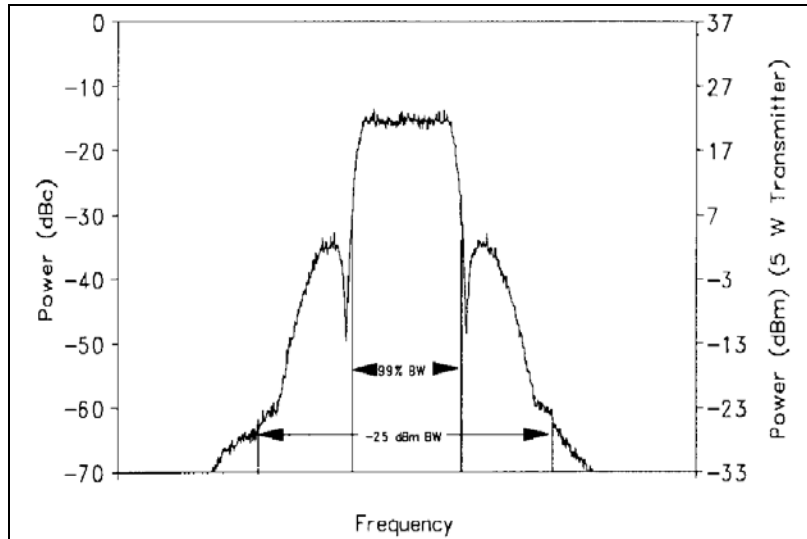


Figure A-4. RNRZ PCM/FM Signal

A.5.b(2) B-25dBm

B-25dBm is the bandwidth containing all components larger than -25 dBm. A power level of -25 dBm is exactly equivalent to an attenuation of the transmitter power by $55 + 10 \times \log(P)$ dB where P is the transmitter power expressed in watts. B-25dBm limits are shown in [Figure A-4](#). B-25dBm is primarily a function of the modulation method, transmitter power, and bit rate. The transmitter design and construction techniques also strongly influence B-25dBm. With a bit rate of 5 Mbps and a transmitter power of 5 watts, the B-25dBm of an NRZ PCM/FM system with near optimum parameter settings is about 13.3 MHz, while B-25dBm of an equivalent FQPSK-B system is about 7.5 MHz, and B-25dBm of an equivalent ARTM CPM system is about 5.8 MHz.

A.5.b(3) Scheduled Bandwidth

This bandwidth should be used by organizations responsible for either requesting or scheduling bandwidth required for telemetry signals. These signals are either packed tightly within existing telemetry bands, operating without adjacent signals, or are scheduled near telemetry band edges. Scheduled bandwidth should be calculated for these three cases in the following manner.

- If the telemetry signal will be operating in the absence of adjacent signals, use the B99% (occupied bandwidth) calculations in [Table A-2](#) to determine scheduled bandwidth.
- If the telemetry signal will be operating in the presence of adjacent telemetry signals, use the minimum frequency separation calculations in [Table A-1](#) to determine scheduled bandwidth.
- If the telemetry signal will be operating near a telemetry band edge, use the calculations in [Section A.12](#) to determine proper spacing from the band edge.

A.5.c. Other Bandwidth Measurement Methods

The methods discussed above are the standard methods for measuring the bandwidth of telemetry signals. The following methods are also sometimes used to measure or to estimate the bandwidth of telemetry signals.

a. *Below Unmodulated Carrier*

This method measures the power spectrum with respect to the unmodulated carrier power. To calibrate the measured spectrum on a spectrum analyzer, the unmodulated carrier power must be known. This power level is the 0-dB reference (commonly set to the top of the display). In AM systems, the carrier power never changes; in FM and PM systems, the carrier power is a function of the modulating signal. Therefore, a method to estimate the unmodulated carrier power is required if the modulation cannot be turned off. For most practical angle modulated systems, the total carrier power at the spectrum analyzer input can be found by setting the spectrum analyzer's resolution and video bandwidths to their widest settings, setting the analyzer output to max hold, and allowing the analyzer to make several sweeps (see [Figure A-3](#)). The maximum value of this trace will be a good approximation of the unmodulated carrier level. [Figure A-5](#) shows the spectrum of a 5-Mbps RNRZ PCM/FM signal measured using the standard spectrum analyzer settings discussed previously and the spectrum measured using 3-MHz resolution, video bandwidths, and max hold.

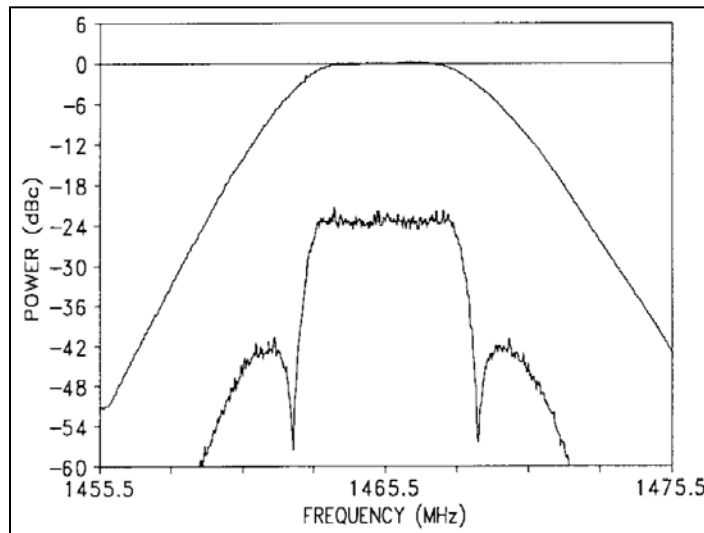


Figure A-5. Spectrum Analyzer Calibration of 0-dBc Level

The peak of the spectrum measured with the latter conditions is very close to 0-dBc and can be used to estimate the unmodulated carrier power (0-dBc) in the presence of FM or PM. In practice, the 0-dBc calibration would be performed first, and the display settings would then be adjusted to use the peak of the curve as the reference level (0-dBc level) to calibrate the spectrum measured using the standard spectrum analyzer settings. With the spectrum analyzer set for a specific resolution bandwidth, video bandwidth, and detector type, the bandwidth is taken as the distance between the two points outside of which the spectrum is thereafter some number (say, 60 dB) below the unmodulated carrier power determined above. B-60dBc for the 5-Mbps signal shown in [Figure A-5](#) is approximately 13 MHz.

B-60dBc of an RNRZ PCM/FM signal with a peak deviation of $0.35R$, a four-pole premodulation filter with -3 dB corner at $0.7R$, and a bit rate greater than or equal to 1 Mbps can be approximated by the following equation:

$$B - 60dBc = [2.78 - 0.3 * \log_{10}(R)] * R \quad (A-2)$$

where B is in MHz;
 R is in Mbps.

Thus B-60dBc of a 5-Mbps RNRZ signal under these conditions would be approximately 12.85 MHz. B-60dBc will be greater if peak deviation is increased or the number of filter poles is decreased.

b. Below Peak

This method is not recommended for measuring the bandwidth of telemetry signals. The modulated peak method, the least accurate measurement method, measures between points where the spectrum is thereafter XX dB below the level of the highest point on the modulated spectrum. [Figure A-6](#) shows the RF spectrum of a 400-kbps bi-phase (Bi ϕ)-level PCM/PM signal with a peak deviation of 75° and a pre-modulation filter bandwidth of 800 kHz.

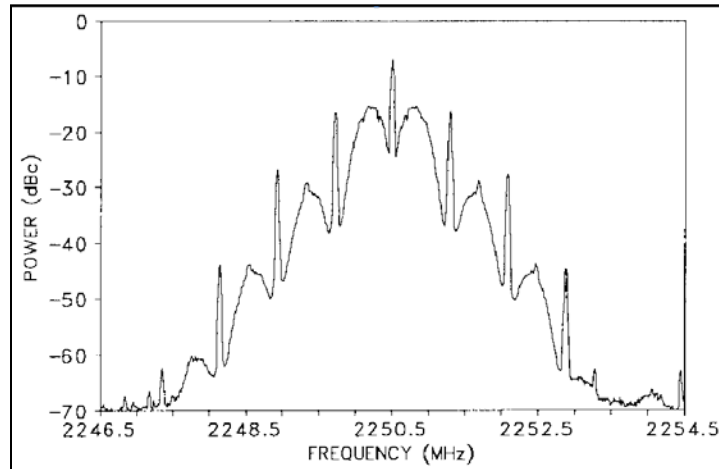


Figure A-6. Bi ϕ PCM/PM Signal

The largest peak has a power level of -7 dBc. In comparison, the largest peak in [Figure A-5](#) had a power level of -22 dBc. This 15-dB difference would skew a bandwidth comparison that used the peak level in the measured spectrum as a common reference point. In the absence of an unmodulated carrier to use for calibration, the below-peak measurement is often (erroneously) used and described as a below-unmodulated-carrier measurement. Using max hold exacerbates this effect still further. In all instances the bandwidth is overstated, but the amount varies.

c. Carson's Rule

Carson's Rule is a method to estimate the bandwidth of an FM subcarrier system. Carson's Rule states the following:

$$B = 2(\Delta f + f_{\max}) \quad (A-3)$$

where B is the bandwidth;
 Δf is the peak deviation of the carrier frequency;
 f_{\max} is the highest frequency in the modulating signal.

Figure A-7 shows the spectrum that results when a 12-channel constant bandwidth multiplex with 6-dB/octave pre-emphasis frequency modulates an FM transmitter. B99% and the bandwidth calculated using Carson's Rule are also shown. Carson's Rule will estimate a value greater than B99% if little of the carrier deviation is due to high-frequency energy in the modulating signal.

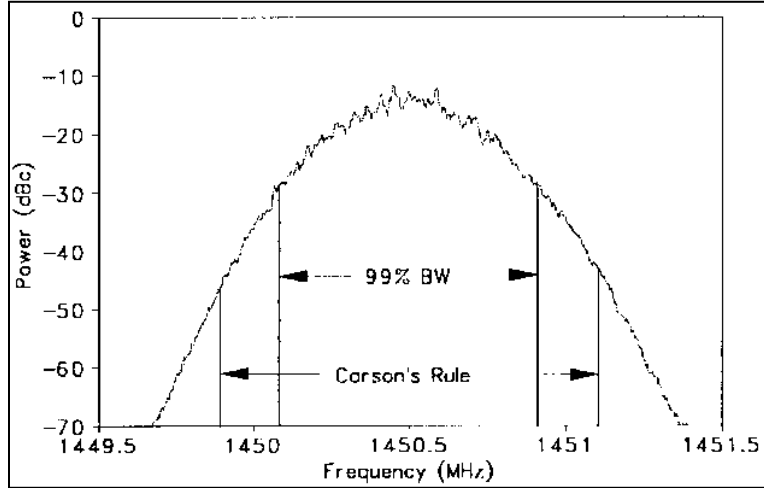


Figure A-7. FM/AM Signal and Carson's Rule

A.5.d. Spectral Equations

The following equations can be used to calculate the RF spectra for several digital modulation methods with unfiltered waveforms.^{24, 25, 26} These equations can be modified to include the effects of filtering.^{27, 28}

RNRZ PCM/FM (valid when $D \neq \text{integer}$, $D = 0.5$ gives MSK spectrum)

$$S(f) = \frac{4 B_{SA}}{R} \left(\frac{D}{\pi(D^2 - X^2)} \right)^2 \frac{(\cos \pi D - \cos \pi X)^2}{1 - 2 \cos \pi D \cos \pi X + \cos^2 \pi D}, \quad \cos \pi D < Q \quad (\text{A-4})$$

²⁴ I. Korn. Digital Communications, New York, Van Nostrand, 1985.

²⁵ M. G. Pelchat. "The Autocorrelation Function and Power Spectrum of PCM/FM with Random Binary Modulating Waveforms," IEEE Transactions, Vol. SET-10, No. 1, pp. 39-44, March 1964.

²⁶ W. M. Tey and T. Tjhung. "Characteristics of Manchester-Coded FSK," IEEE Transactions on Communications, Vol. COM-27, pp. 209-216, January 1979.

²⁷ Watt, A. D., V. J. Zurick, and R. M. Coon. "Reduction of Adjacent-Channel Interference Components from Frequency-Shift-Keyed Carriers," IRE Transactions on Communication Systems, Vol. CS-6, pp. 39-47, December 1958.

²⁸ E. L. Law. "RF Spectral Characteristics of Random PCM/FM and PSK Signals," International Telemetry Conference Proceedings, pp. 71-80, 1991.

RNRZ PSK

$$S(f) = \frac{B_{SA}}{R} \frac{\sin^2\left(\frac{\pi X}{2}\right)}{\left(\frac{\pi X}{2}\right)^2} \quad (\text{A-5})$$

RNRZ QPSK and OQPSK

$$S(f) = \frac{2B_{SA}}{R} \frac{\sin^2(\pi X)}{(\pi X)^2} \quad (\text{A-6})$$

Random Biφ PCM/FM

$$S(f) = \frac{B_{SA}}{4R} \left(\frac{\pi D}{2} \frac{\sin\left(\frac{\pi(X-D)}{4}\right)}{\frac{\pi(X-D)}{4}} \frac{\sin\left(\frac{\pi(X+D)}{4}\right)}{\frac{\pi(X+D)}{4}} \right)^2 + \left(\frac{D \sin\left(\frac{\pi D}{2}\right)}{\frac{\pi(X^2 - D^2)}{2}} \right)^2 \delta\{(f - f_c) - nR\} \quad (\text{A-7})$$

Random Biφ PCM/PM

$$S(f) = \frac{B_{SA} \sin^2(\beta)}{R} \frac{\sin^4\left(\frac{\pi X}{4}\right)}{\left(\frac{\pi X}{4}\right)^2} + \cos^2(\beta) \delta(f - f_c), \quad \beta \leq \frac{\pi}{2} \quad (\text{A-8})$$

- where
- S(f) = power spectrum (dBc) at frequency f
 - B_{SA} = spectrum analyzer resolution bandwidth*
 - R = bit rate
 - D = 2Δf/R
 - X = 2(f-f_c)/R
 - Δf = peak deviation
 - β = peak phase deviation in radians
 - f_c = carrier frequency
 - δ = Dirac delta function
 - N = 0, ±1, ±2, ...
 - Q = quantity related to narrow band spectral peaking when D ≈ 1, 2, 3, ...
 - Q ≈ 0.99 for B_{SA} = 0.003 R, Q ≈ 0.9 for B_{SA} = 0.03 R

*The spectrum analyzer resolution bandwidth term was added to the original equations.

A.5.e. Receiver Bandwidth

Receiver predetection bandwidth is typically defined as the points where the response to the carrier before demodulation is -3 dB from the center frequency response. The carrier bandwidth response of the receiver is, or is intended to be, symmetrical about the carrier in most instances. [Figure A-8](#) shows the response of a typical older-generation telemetry receiver with RLC IF filters and a 1-MHz IF bandwidth selected. Outside the stated bandwidth, the response usually falls fairly rapidly, often 20 dB or more below the passband response at 1.5 to 2 times the passband response.

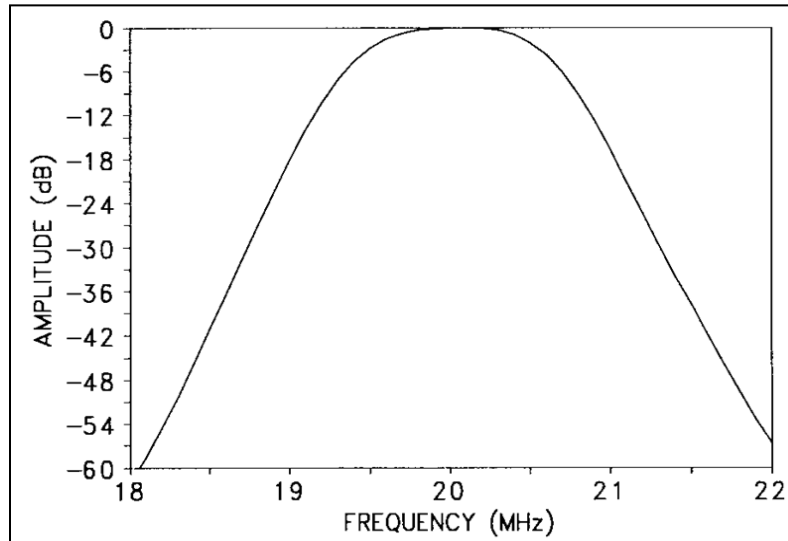


Figure A-8. Typical Receiver RLC IF Filter Response (-3 dB Bandwidth = 1 MHz)

[Figure A-9](#) shows an overlay of an RLC IF filter and a SAW filter. Note that the SAW filter rolls off much more rapidly than the RLC filter. The rapid falloff outside the passband helps reduce interference from nearby channels and has minimal effect on data.

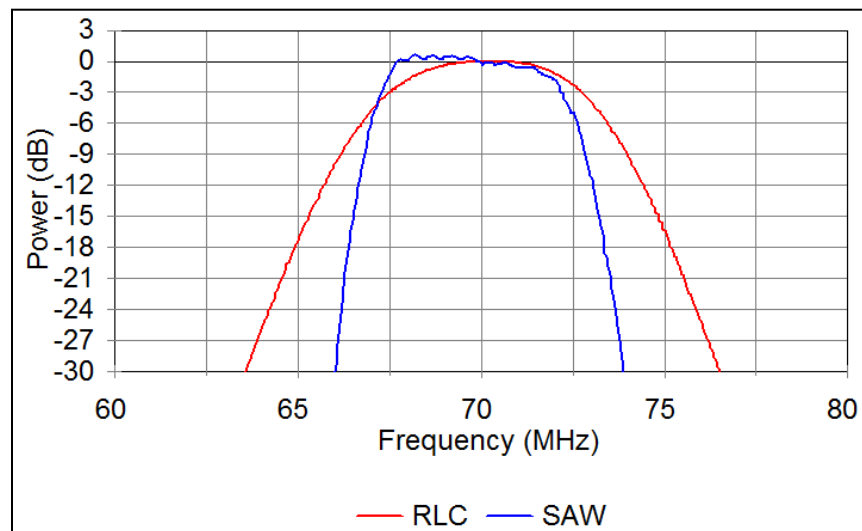


Figure A-9. RLC and SAW IF Filters

A.5.f. Receiver Noise Bandwidth

For the purpose of calculating noise in the receiver, the bandwidth must be integrated over the actual shape of the IF, which, in general, is not a square-sided function. Typically, the value used for noise power calculations is the -3 dB bandwidth of the receiver.

A.5.g. Symmetry

Many modulation methods produce a spectrum that is asymmetrical with respect to the carrier frequency. Exceptions include FM/FM systems, RNRZ PCM/FM systems, and randomized FQPSK, SOQPSK-TG, and ARTM CPM systems. The most extreme case of asymmetry is due to single-sideband transmission, which places the carrier frequency at one edge of the occupied spectrum. If the spectrum is not symmetrical about the band center, the bandwidth and the extent of asymmetry must be noted for frequency management purposes.

A.5.h. FM Transmitters (alternating current-coupled)

Alternating current-coupled FM transmitters should not be used to transmit NRZ signals unless the signals to be transmitted are randomized. This is because changes in the ratio of 1s to 0s will increase the occupied bandwidth and may degrade the BER. When alternating current-coupled transmitters are used with RNRZ signals, it is recommended that the lower -3 dB frequency response of the transmitter be no greater than the bit rate divided by 4000. For example, if a randomized 1-Mbps NRZ signal is being transmitted, the lower -3 dB frequency response of the transmitter should be no larger than 250 Hz.

A.6. Spectral Occupancy Limits

Telemetry applications covered by this standard shall use B99% to define occupied bandwidth and B-25dBm as the primary measure of spectral efficiency. The spectra are assumed symmetrical about the center frequency unless otherwise specified. The primary reason for controlling the spectral occupancy is to control adjacent channel interference, thereby allowing more users to be packed into a given amount of frequency spectrum. The adjacent channel interference is determined by the spectra of the signals and the filter characteristics of the receiver.

A.6.a. Spectral Mask

One common method of describing the spectral occupancy limits is a spectral mask. The aeronautical telemetry spectral mask is described below. Note that the mask in this standard is different than the masks contained in the earlier versions of the Telemetry Standards. All spectral components larger than $-[55 + 10 \times \log(P)]$ dBc (i.e., larger than -25 dBm) at the transmitter output must be within the spectral mask calculated using the following equation:

$$M(f) = K + 90 \log R - 100 \log |f - f_c|; \quad |f - f_c| \geq \frac{R}{m} \quad (\text{A-9})$$

where $M(f)$ = power (dBc) at frequency f (MHz)
 $K = -20$ for analog signals
 $K = -28$ for binary signals

$K = -61$ for FQPSK-B, FQPSK-JR, SOQPSK-TG

$K = -73$ for ARTM CPM

f_c = transmitter center frequency (MHz)

R = bit rate (Mbps) for digital signals or $(\Delta f + f_{\max})(\text{MHz})$ for analog FM signals

M = number of states in modulating signal ($m = 2$ for binary signals, $m = 4$ for quaternary signals and analog signals)

Δf = peak deviation

f_{\max} = maximum modulation frequency

These bandwidths are measured using a spectrum analyzer with settings of 30-kHz resolution bandwidth, 300-Hz video bandwidth, and no max hold detector or averaging. Note that these settings are different than those listed in previous editions of the Telemetry Standards. The changes were made to get more consistent results with various bit rates and spectrum analyzers. The spectra measured with these settings give slightly larger power levels than with the previous settings; this is why the value of K was changed from -63 to -61 for FQPSK and SOQPSK signals. The power levels near center frequency should be approximately $J - 10\log(R)$ dBc where $J = -10$ for ARTM CPM, -12 for FQPSK and SOQPSK-TG, and -15.5 for PCM/FM signals. For a bit rate of 5 Mbps, the level is approximately -17 dBc for ARTM CPM, -19 dBc for FQPSK, and -22.5 dBc for PCM/FM. If the power levels near center frequency are not within 3 dB of these values, then a measurement problem exists and the carrier power level (0 dBc) and spectrum analyzer settings should be verified.

B-25dBm is not required to be narrower than 1 MHz. The first term K in equation A-9 accounts for bandwidth differences between modulation methods. Equation A-9 can be rewritten as $M(f) = K - 10\log R - 100\log|(f - f_c)/R|$. When equation A-9 is written this way, the $10\log R$ term accounts for the increased spectral spreading and decreased power per unit bandwidth as the modulation rate increases. The last term forces the spectral mask to roll off at 30 dB/octave (100 dB/decade). Any error detection or error correction bits, which are added to the data stream, are counted as bits for the purposes of this spectral mask. The spectral masks are based on the power spectra of random real-world transmitter signals. For instance, the binary signal spectral mask is based on the power spectrum of a binary NRZ PCM/FM signal with peak deviation equal to 0.35 times the bit rate and a multipole premodulation filter with a -3 dB frequency equal to 0.7 times the bit rate (see [Figure A-4](#)). This peak deviation minimizes the BER with an optimum receiver bandwidth while also providing a compact RF spectrum. The premodulation filter attenuates the RF sidebands while only degrading the BER by the equivalent of a few tenths of a dB of RF power. Further decreasing of the premodulation filter bandwidth will only result in a slightly narrower RF spectrum, but the BER will increase dramatically. Increasing the premodulation filter bandwidth will result in a wider RF spectrum, and the BER will only be decreased slightly. The recommended premodulation filter for NRZ PCM/FM signals is a multipole linear phase filter with a -3 dB frequency equal to 0.7 times the bit rate. The unfiltered NRZ PCM/FM signal rolls off at 12 dB/octave so at least a three-pole filter (filters with four or more poles are recommended) is required to achieve the 30 dB/octave slope of the spectral mask. The spectral mask includes the effects of reasonable component variations (unit-to-unit and temperature).

A.6.b. Spectral Mask Examples

[Figure A-10](#) and [Figure A-11](#) show the binary spectral mask of equation A-9 and the RF spectra of 5-Mbps RNRZ PCM/FM signals. The RF spectra were measured using a spectrum analyzer with 30-kHz resolution bandwidth, 300-Hz video bandwidth, and no max hold detector. The span of the frequency axis is 20 MHz. The transmitter power was 5 watts, and the peak deviation was 1750 kHz. The modulation signal for [Figure A-10](#) was filtered with a 4-pole linear-phase filter with -3 dB frequency of 3500 kHz. All spectral components in [Figure A-10](#) were contained within the spectral mask. The minimum value of the spectral mask was -62 dBc (equivalent to -25 dBm). The peak modulated signal power levels were about 22.5 dB below the unmodulated carrier level (-22.5 dBc). [Figure A-11](#) shows the same signal with no premodulation filtering. The signal was not contained within the spectral mask when a premodulation filter was not used.

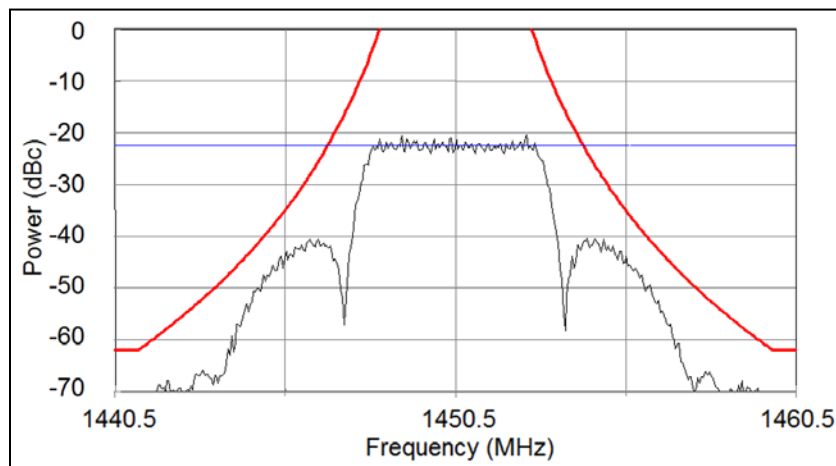


Figure A-10. Filtered 5-Mbps RNRZ PCM/FM Signal and Spectral Mask

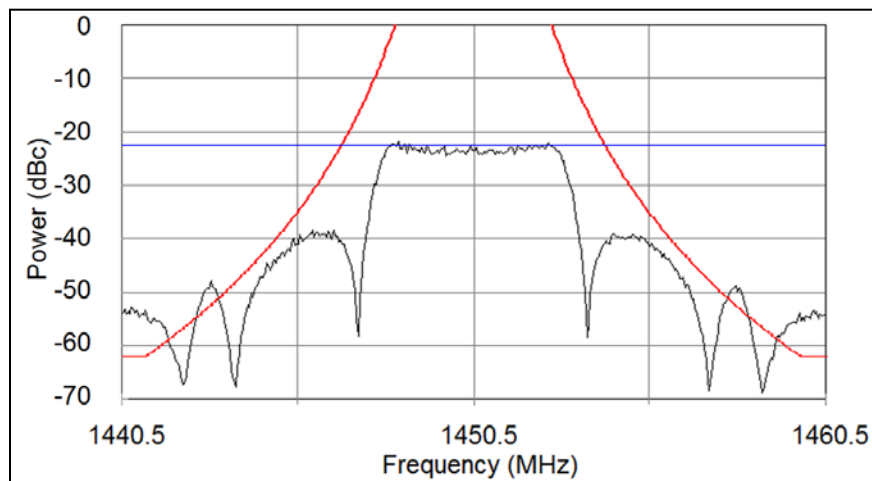


Figure A-11. Unfiltered 5-Mbps RNRZ PCM/FM Signal and Spectral Mask

[Figure A-12](#) shows the FQPSK/SOQPSK mask of equation A-9 and the RF spectrum of a 5-Mbps SOQPSK-TG signal. The transmitter power was assumed to be 5 watts in this example.

The peak value of the SOQPSK-TG signal was about -19 dBc. [Figure A-13](#) shows a typical 5-Mbps ARTM CPM signal and its spectral mask. The peak value of the ARTM CPM signal was about -17 dBc.

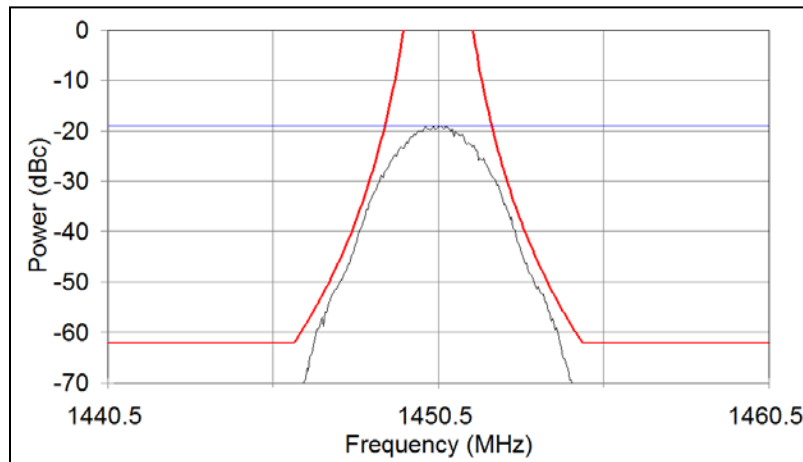


Figure A-12. Typical 5-Mbps SOQPSK TG Signal and Spectral Mask

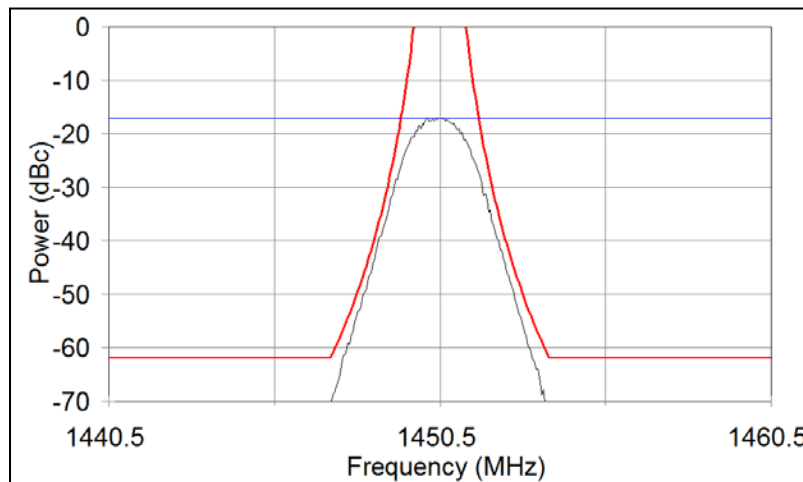


Figure A-13. Typical 5-Mbps ARTM CPM Signal and Spectral Mask

A.7. Technical Characteristics of Digital Modulation Methods

[Table A-3](#) provides a summary of some of the technical characteristics of the modulation methods discussed in this summary.

| Table A-3. Characteristics of Various Modulation Methods | | | | |
|---|-------------------------------------|------------------------------------|------------------------------|---------------|
| Characteristic | PCM/FM with single symbol detection | PCM/FM with multi-symbol detection | FQPSK-B, FQPSK-JR, SOQPSK-TG | ARTM CPM |
| Occupied Bandwidth | 1.16 bit rate | 1.16 bit rate | 0.78 bit rate | 0.56 bit rate |
| Sensitivity (E_b/N_0 for $BEP=1e-5$) | 11.8-15+ dB | 9.5 dB | 11.8-12.2 dB | 12.5 dB |

| | | | | |
|--|--------------------|----------|----------------------|------------------------|
| Synchronization time | 100 to 10,000 bits | 250 bits | 5,000 to 30,000 bits | 30,000 to 150,000 bits |
| Synchronization threshold level (E_b/N_0) | 3 to 4 dB | 2 dB | 4.5 to 5 dB | 8.5 dB |
| Phase noise susceptibility* | 2 | 1 | 3 | 4 |
| Co-channel interference susceptibility* | 2 | 1 | 3 | 4 |
| * 1=Best, 2=Second Best, 3=Third Best, 4=Worst | | | | |

A.8. FQPSK-B and FQPSK-JR Characteristics

Modulations of FQPSK-B and FQPSK-JR are a variation of OQPSK, which is described in most communications textbooks. A generic OQPSK (or quadrature or I & Q) modulator is shown in [Figure A-14](#). In general, the odd bits are applied to one channel (say Q), and the even bits are applied to the I channel.

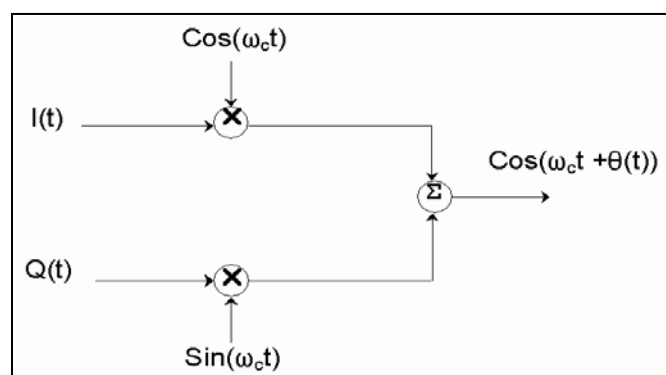


Figure A-14. OQPSK Modulator

If the values of I and Q are ± 1 , we get the diagram shown in [Figure A-15](#). For example, if $I=1$ and $Q=1$ then the phase angle is 45 degrees $\{(I,Q) = (1, 1)\}$. A constant envelope modulation method, such as MSK, would follow the circle indicated by the small dots in [Figure A-15](#) to go between the large dots. In general, band-limited QPSK and OQPSK signals are not constant envelope and would not follow the path indicated by the small dots but rather would have a significant amount of amplitude variation; however, FQPSK-B and FQPSK-JR are nearly constant envelope and essentially follow the path indicated by the small dots in [Figure A-15](#).

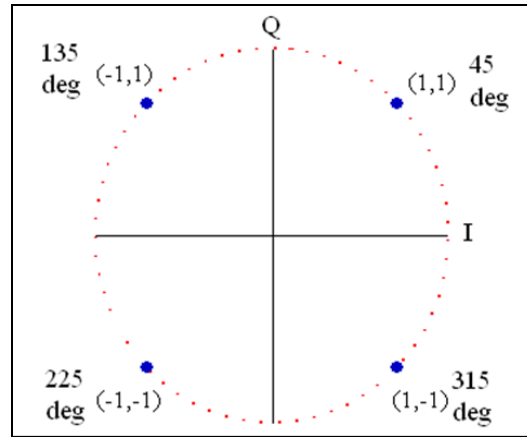


Figure A-15. I and Q Constellation

The typical implementation of FQPSK-B or FQPSK-JR involves the application of data and a bit rate clock to the baseband processor of the quadrature modulator. The data are differentially encoded and converted to I and Q signals as described in [Chapter 2](#). The I and Q channels are then cross-correlated, and specialized wavelets are assembled that minimize the instantaneous variation of $(I^2(t) + Q^2(t))$. The FQPSK-B baseband wavelets are illustrated in [Figure A-16](#).

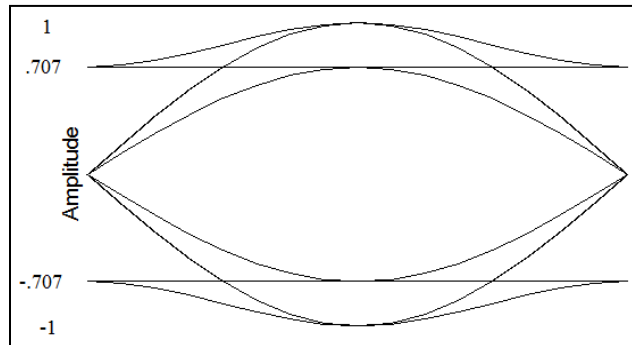


Figure A-16. FQPSK Wavelet Eye Diagram

The appropriate wavelet is assembled based on the current and immediate past states of I and Q, where Q is delayed by one-half symbol (one bit) with respect to I as shown in [Figure A-17](#).

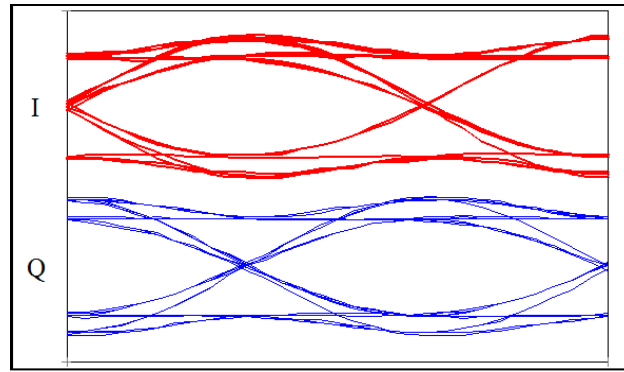


Figure A-17. FQPSK-B I & Q Eye Diagrams (at Input to IQ Modulator)

A common method at looking at I-Q modulation signals is the use of a vector diagram. One method of generating a vector diagram is to use an oscilloscope that has an XY mode. The vector diagram is generated by applying the I signal to the X input and the Q signal to the Y input. A sample vector diagram of FQPSK-B at the input terminals of an I-Q modulator is illustrated in [Figure A-18](#). Note that the vector diagram values are always within a few percent of being on a circle. Any amplitude variations may cause spectral spreading at the output of a nonlinear amplifier.

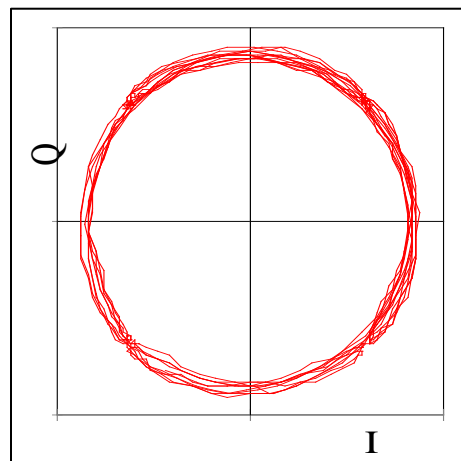


Figure A-18. FQPSK-B Vector Diagram

[Figure A-19](#) illustrates a nearly ideal FQPSK-JR spectrum (blue trace) and an FQPSK-JR spectrum with moderately large modulator errors (red trace). These spectra were measured at the output of a fully saturated RF nonlinear amplifier with a random pattern of 1s and 0s applied to the input. The bit rate for [Figure A-19](#) was 5 Mbps. The peak of the spectrum was approximately -19 dBc. B99% of FQPSK-B is typically about 0.78 times the bit rate. Note that with a properly randomized data sequence and proper transmitter design, FQPSK-B does not have significant sidebands (blue trace).

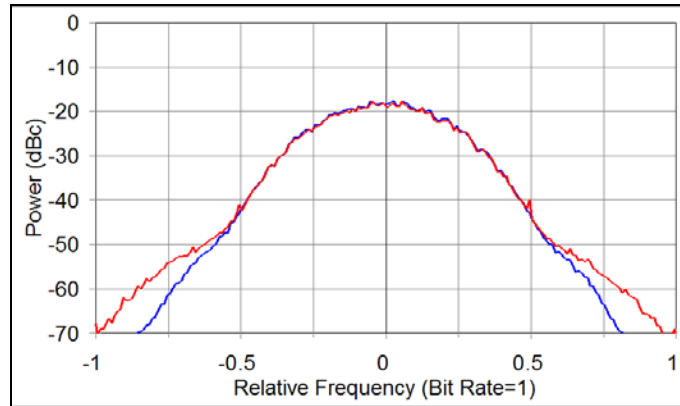


Figure A-19. 5 Mbps FQPSK-JR Spectrum with Random Input Data and Small (Blue) and Large (Red) Modulator Errors

[Figure A-20](#) illustrates an FQPSK-B transmitter output with all 0s as the input signal. With an all 0s input, the differential encoder, cross-correlator, and wavelet selector provide unity amplitude sine and cosine waves with a frequency equal to 0.25 times the bit rate to the I and Q modulator inputs. The resulting signal (from an ideal modulator) would be a single frequency component offset from the carrier frequency by exactly +0.25 times the bit rate. The amplitude of this component would be equal to 0 dBc. If modulator errors exist (they always will), additional frequencies will appear in the spectrum as shown in [Figure A-20](#). The spectral line at a normalized frequency of 0 (carrier frequency) is referred to as the remnant carrier. This component is largely caused by direct current imbalances in the I and Q signals. The remnant carrier power in [Figure A-20](#) is approximately -31 dBc. Well-designed FQPSK-B transmitters will have a remnant carrier level less than -30 dBc. The spectral component offset, 0.25 times the bit rate below the carrier frequency, is the other sideband. This component is largely caused by unequal amplitudes in I and Q and by a lack of quadrature between I and Q. The power in this component should be limited to -30 dBc or less for good system performance.

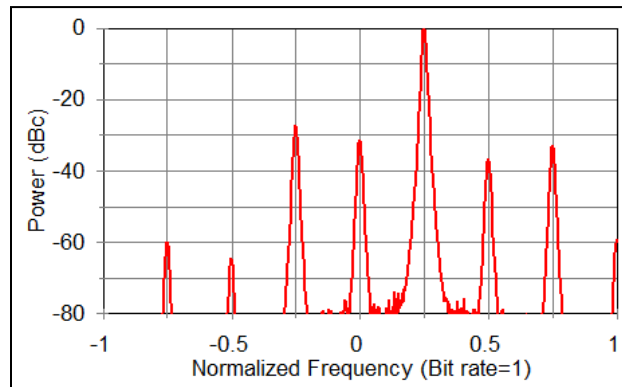


Figure A-20. FQPSK-B Spectrum with All 0's Input and Large Modulator Errors

[Figure A-21](#) shows the measured BEP versus signal energy per bit/noise power per Hz (E_b/N_0) of two FQPSK-JR modulator/demodulator combinations including nonlinear amplification and differential encoding/decoding in an additive white Gaussian noise (AWGN) environment with no fading. Other combinations of equipment may have different performance.

Phase noise levels higher than those recommended in [Chapter 2](#) can significantly degrade the BEP performance. Computer simulations have shown that a BEP of 10^{-5} may be achievable with an E_b/N_0 of slightly greater than 11 dB (with differential encoding/decoding). The purpose of the differential encoder/decoder is to resolve the phase detection ambiguities that are inherent in QPSK, OQPSK, and FQPSK modulation methods. The differential encoder/decoder used in this standard will cause one isolated symbol error to appear as two bits in error at the demodulator output; however, many aeronautical telemetry channels are dominated by fairly long burst error events, and the effect of the differential encoder/decoder will often be masked by the error events.

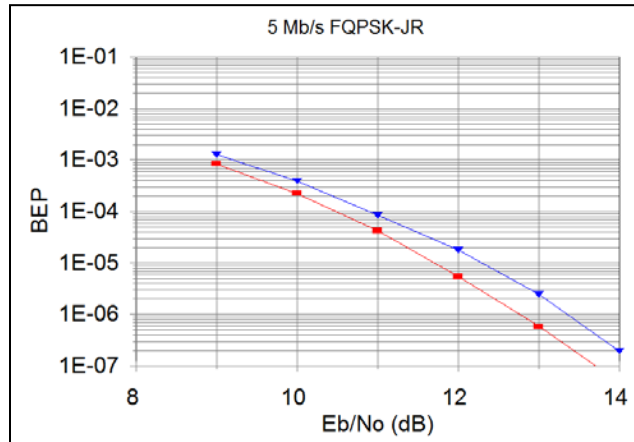


Figure A-21. FQPSK-JR BEP vs. E_b/N_0

A.9. SOQPSK-TG Characteristics

The SOQPSK is a family of constant envelope CPM waveforms defined by Hill.²⁹ The details of SOQPSK-TG are described in Subsection [2.3.3.2](#). The SOQPSK-TG signal amplitude is constant and the phase trajectory is determined by the coefficients in [Table 2-4](#). Therefore, SOQPSK-TG can be implemented using a precision phase or frequency modulator with proper control of the phase trajectory. [Figure A-22](#) illustrates the measured phase trajectory of an SOQPSK-TG signal. The vertical lines correspond approximately to the “bit” decision times.

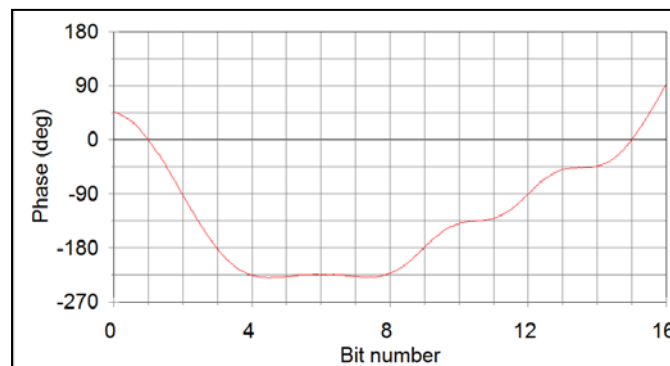


Figure A-22. Measured SOQPSK-TG Phase Trajectory

²⁹ Hill, “An Enhanced, Constant Envelope, Interoperable Shaped Offset QPSK.”

The power spectrum of a random 5-Mbps SOQPSK-TG signal is shown in [Figure A-23](#). B-60dBc of this 5-Mbps signal was about 7.34 MHz. Note that the maximum power level is about -19 dBc.

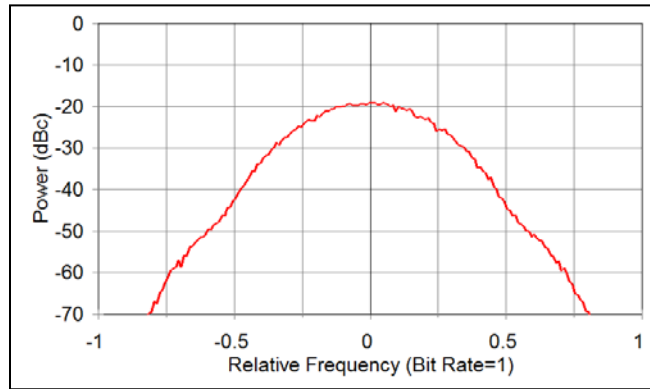


Figure A-23. SOQPSK-TG Power Spectrum (5 Mbps)

[Figure A-24](#) shows the measured BEP versus signal energy per bit/noise power per Hz (E_b/N_0) of two SOQPSK-TG modulator/demodulator combinations including nonlinear amplification and differential encoding/decoding in an AWGN environment with no fading. Other combinations of equipment may have different performance. Phase noise levels higher than those recommended in [Chapter 2](#) can significantly degrade the BEP performance.

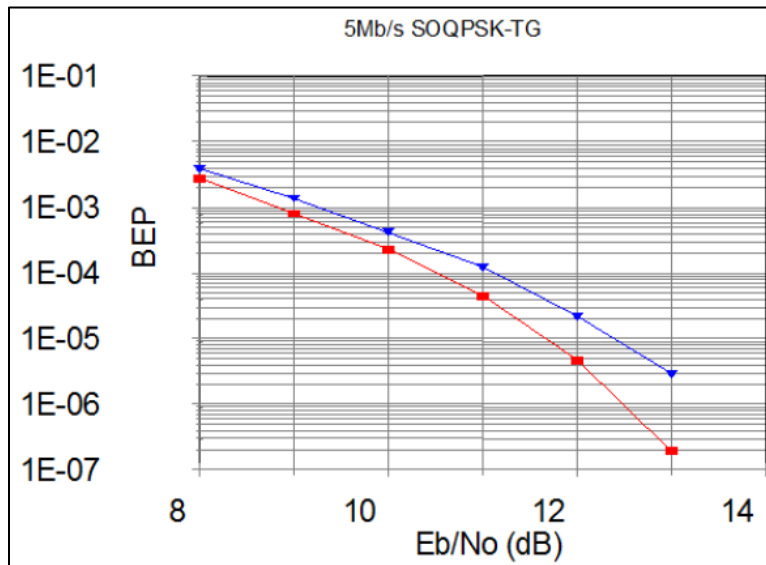


Figure A-24. BEP vs. E_b/N_0 Performance of 5 Mbps SOQPSK-TG

A.10. Advanced Range Telemetry Continuous Phase Modulation Characteristics

The ARTM CPM is a quaternary signaling scheme in which the instantaneous frequency of the modulated signal is a function of the source data stream. The frequency pulses are shaped for spectral containment purposes. As defined for this standard, the modulation index alternates at the symbol rate between $h=4/16$ and $h=5/16$. The purpose of alternating between two modulation indices is to maximize the minimum distance between data symbols, which results in

minimizing the BEP. These particular modulation indices were selected as a good tradeoff between spectral efficiency and data-detection ability. [Figure A-25](#) shows the power spectrum of a 5-Mbps ARTM CPM signal and [Figure A-26](#) shows the measured BEP versus E_b/N_0 . The maximum power level was about -19 dBc. B-60dBc of this 5-Mbps signal was about 5.54 MHz. Note that the power spectrum of ARTM CPM is about 25% narrower than that of SOQPSK-TG but the BEP performance is worse. The ARTM CPM is also more susceptible to phase noise than SOQPSK-TG.

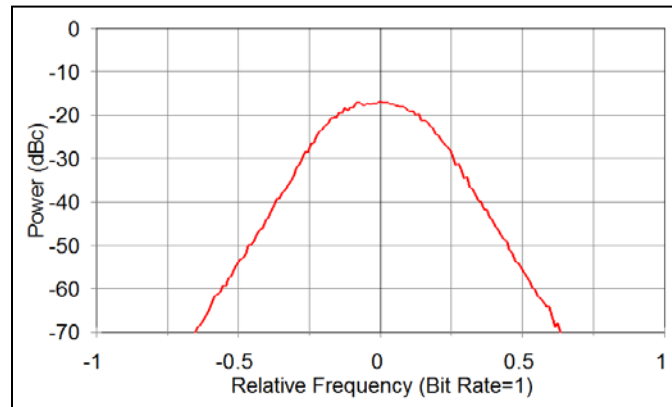


Figure A-25. Power Spectrum of 5 Mbps ARTM CPM

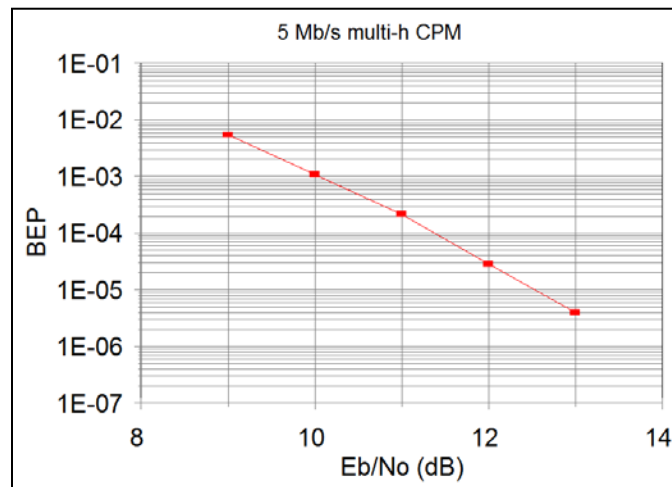


Figure A-26. BEP vs. E_b/N_0 Performance of 5 Mbps ARTM CPM

A.11. PCM/FM

The most popular telemetry modulation since 1970 is PCM/ FM, also known as CPFSK. The RF signal is typically generated by filtering the baseband NRZ-L signal and then frequency modulating a VCO. The optimum peak deviation is 0.35 times the bit rate ($h=0.7$) and a good choice for a premodulation filter is a multi-pole linear phase filter with bandwidth equal to 0.7 times the bit rate. [Figure A-27](#) shows the power spectrum of a pseudo-random 5-Mbps PCM/FM signal with peak deviation of 1.75 MHz and a 3.5-MHz linear phase low-pass filter. Note that the spectrum is nearly flat from a frequency equal to -0.5 times the bit rate to a frequency equal to $+0.5$ times the bit rate. The power level near the center frequency is about -22.5 dBc for a bit rate of 5 Mbps and the standard spectrum analyzer settings.

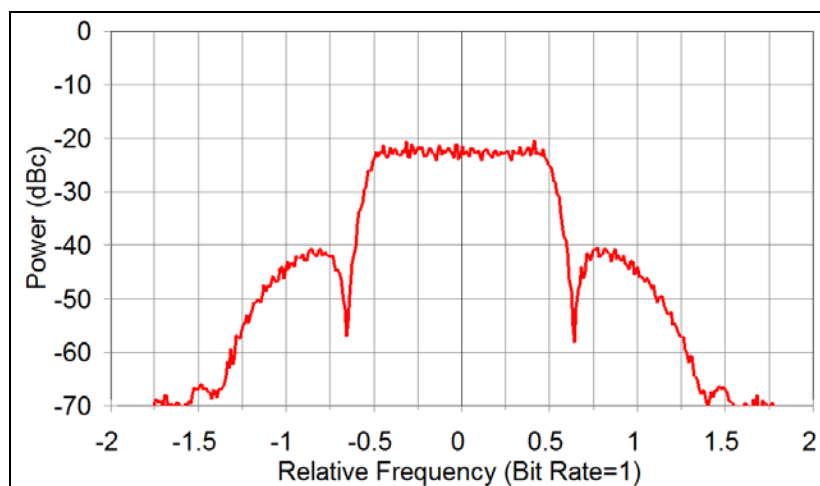
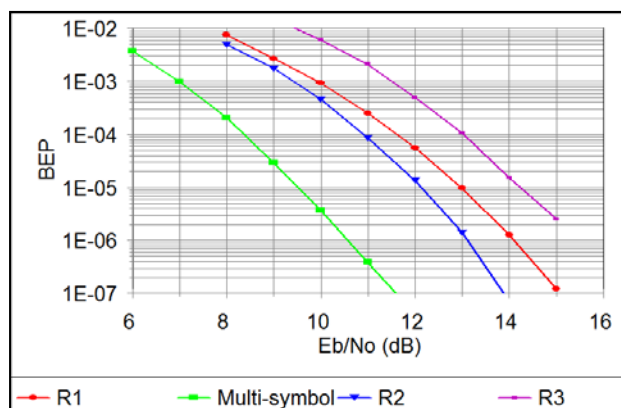


Figure A-27. Power Spectrum of 5 Mbps PCM/FM Signal

[Figure A-28](#) shows the BEP versus E_b/N_0 performance of 5-Mbps PCM/FM with a multi-symbol bit detector and with three different receivers/detectors. Note that an E_b/N_0 of about 9.5 dB is required to achieve a BEP of about 10^{-5} with the multi-symbol detector^{30, 31} while an E_b/N_0 of about 12 to 14 dB is typically required to achieve a BEP of about 10^{-5} with typical FM demodulators and single-symbol detectors. The PCM/FM modulation method is fairly insensitive to phase noise.

Figure A-28. BEP vs. E_b/N_0 Performance of 5-Mbps PCM/FM with Multi-Symbol Bit Detector and Three Single-Symbol Receivers/Detectors

A.12. Valid Center Frequencies Near Telemetry Band Edges

The telemetry bands and associated frequency ranges identified in [Table 2-1](#) identify the frequency limits for each band. Telemetry transmitters cannot be centered at the band edges due to obvious out-of-band emissions (OOBE). Bit rate to the transmitter and modulation scheme drive the amount of separation required between the center frequency and the band edge. To

³⁰ Osborne, W. P. and M. B. Luntz. "Coherent and Noncoherent Detection of CPFSK," IEEE Transactions on Communications, August 1974.

³¹ Mark Geoghegan. "Improving the Detection Efficiency of Conventional PCM/FM Telemetry by using a Multi-Symbol Demodulator", Proceedings of the 2000 International Telemetry Conference, Volume XXXVI, 675-682, San Diego CA, October 2000.

determine the amount of back-off required, the distance from the center of the spectral masks for each modulation scheme (see Subsection 2.3.6) to the intersection of the mask and the absolute limit of -25 dBm must be calculated. To illustrate this, see [Figure A-29](#). Using these calculations will assure that outside the specified telemetry bands no part of the modulated spectrum is over the absolute limit of -25 dBm.

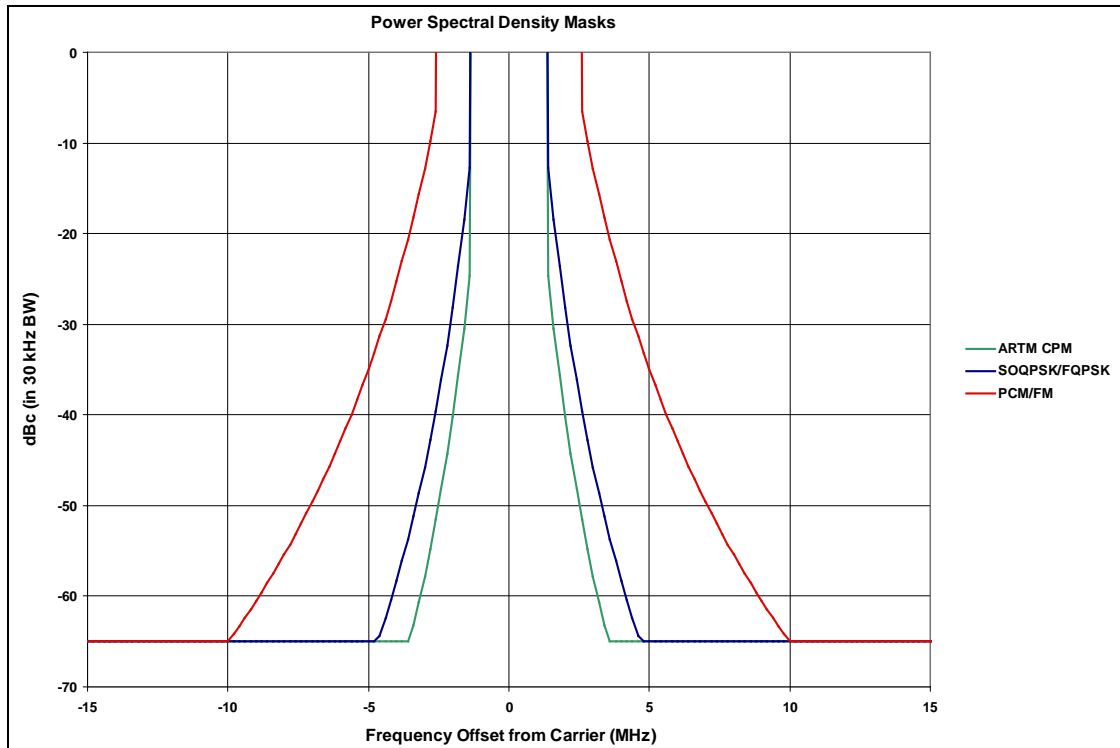


Figure A-29. Spectral Masks at -25 dBm

The mask is calculated for all the modulation schemes at a bit rate of 5 Mbps with transmitter output power assumed to be 10 W. This transmitter operating with PCM/FM as its modulation scheme requires a back-off from band edge of 9.98 MHz; since channelization in these bands is limited to 0.5-MHz steps, this value is rounded up to 10 MHz. This same transmitter operating with SOQPSK/FQPSK will require 4.67 MHz, rounded up to 5 MHz, of back-off from band edge. Likewise, for ARTM-CPM the back-off is 3.54 MHz or 4 Mbps when rounded up. To further this example, if this was an L-band transmitter, viable carrier frequencies would be as specified in [Table A-4](#).

| Table A-4. L-Band Frequency Range (10 W, 5 Mbps) | |
|---|-------------------------------|
| Modulation Type | Viable L-Band Frequency Range |
| PCM/FM | 1445-1515 MHz |
| SOQPSK/FQPSK | 1440-1520 MHz |
| ARTM CPM | 1439-1521 MHz |

For a given modulation scheme and transmitter output power, as the bit rate increases, the amount of back-off from the band edge also increases. [Figure A-30](#) illustrates this point.

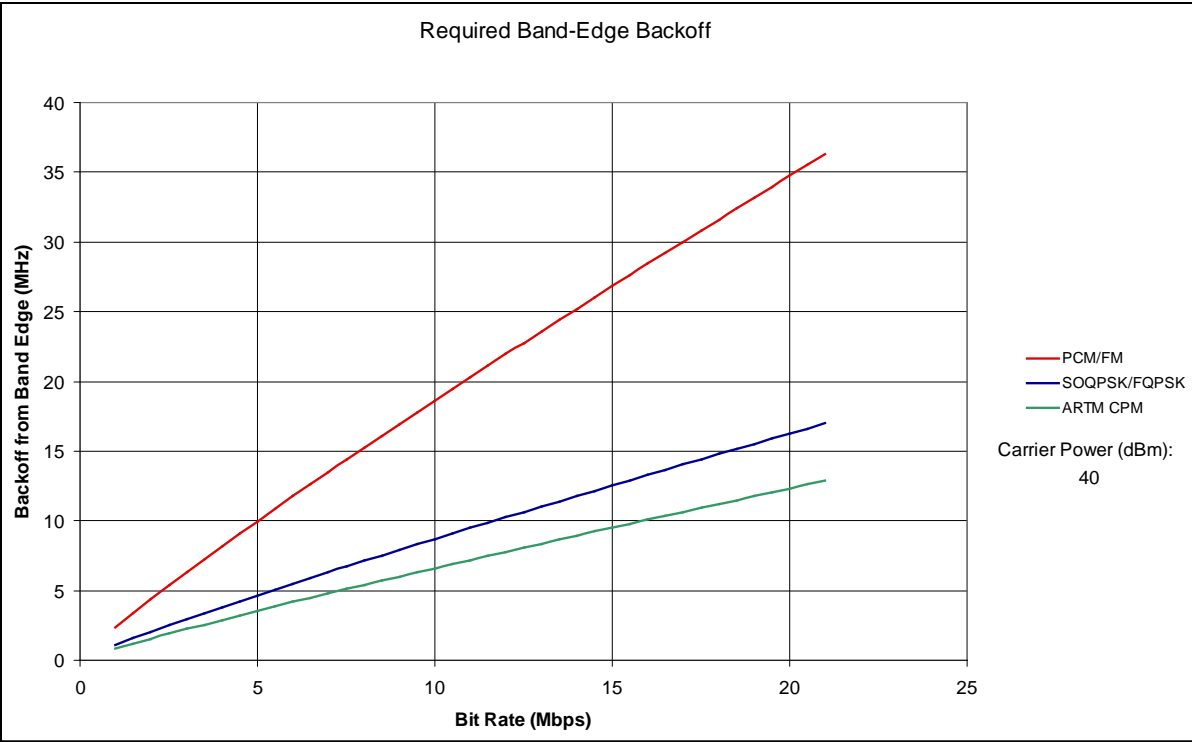


Figure A-30. Bit Rate vs. Band Edge Back-off

NOTE



For ease in making calculations, an Excel spreadsheet application can be used. [Table A-5](#) provides an example of a 10-watt transmitter operating at 1 Mbps in L-band and S-band using the formulas in the spreadsheet. The Excel file that created [Table A-5](#) can be downloaded [here](#) and used for interactive calculations.

The input values for transmitter output power and bit rate are in the cells highlighted in yellow. The amount of back-off will be displayed in the cells highlighted in light blue. Additionally, each telemetry band is displayed with the useable carrier frequency range for each modulation scheme given in blue.

Table A-5. Valid Center Frequency, Band Edge Back-Off

| | | | | | |
|---|---|----------|--------------|----------|-----------------|
| Carrier Power or EIRP (dBm): | | 40 | Input Number | | |
| Mask floor (at this nominal TX power): | | −65 | dBc | | |
| Bit Rate (Mbps): | | 1.00 | 1.00 | 1.00 | Input Number |
| | | PCM/FM | SOQPSK/FQPSK | ARTM CPM | |
| | K = | −28 | −61 | −73 | |
| | m = | 2 | 4 | 4 | |
| | Bit Rate (bps) | 1.00E+06 | 1.00E+06 | 1.00E+06 | |
| | Mask hits floor at offset of (MHz) | 2.34 | 1.10 | 0.83 | |
| Band-edge backoff (MHz, rounded to nearest 0.5 MHz) | | 2.5 | 1.5 | 1 | Result |
| L- Band | Band Edge, Lower (MHz) | 1435 | | | |
| | Band Edge, Upper (MHz) | 1525 | | | |
| | Lower center freq. at this bit rate (MHz) | 1437.5 | 1436.5 | 1436.0 | |
| | Upper center freq. at this bit rate (MHz) | 1522.5 | 1523.5 | 1524.0 | |
| L- Band | Band Edge, Lower (MHz) | 1755 | | | |
| | Band Edge, Upper (MHz) | 1850 | | | |
| | Lower center freq. at this bit rate (MHz) | 1757.5 | 1756.5 | 1756.0 | |
| | Upper center freq. at this bit rate (MHz) | 1847.5 | 1848.5 | 1849.0 | |
| S- Band | Band Edge, Lower (MHz) | 2200 | | | |
| | Band Edge, Upper (MHz) | 2290 | | | |
| | Lower center freq. at this bit rate (MHz) | 2202.5 | 2201.5 | 2201.0 | |
| | Upper center freq. at this bit rate (MHz) | 2287.5 | 2288.5 | 2289.0 | |
| S- Band | Band Edge, Lower (MHz) | 2360 | | | |
| | Band Edge, Upper (MHz) | 2395 | | | |
| | Lower center freq. at this bit rate (MHz) | 2362.5 | 2361.5 | 2361.0 | |
| | Upper center freq. at this bit rate (MHz) | 2392.5 | 2393.5 | 2394.0 | |

This page intentionally left blank.

APPENDIX 2-B

Properties of the Differential Encoder Specified in IRIG Standard 106 for OQPSK Modulations

B.1. Introduction

This appendix summarizes a study of the differential encoder originally adopted by the US DoD ARTM project and the RCC and incorporated into the IRIG 106 for FQPSK-B modulation. The study, performed by Mr. Robert Jefferis of the TYBRIN Corporation, was prompted by inquiries from industry representatives who were concerned that this particular differential code was not associated with commercial telecommunication standards and the fact that manufacturers had experienced confusion over correct implementation. The study results shown in this appendix prove the code to be robust, reliable, and applicable to SOQPSK-TG as well as FQPSK-B and FQPSK-JR.³²

This appendix is organized along the following structure. Section [B.2](#) describes the need for differential encoding. Section [B.3](#) explains the IRIG-106 differential code for OQPSK. Section [B.4](#) demonstrates differential code's invariance with respect to constellation rotation. Section [B.5](#) shows the differential decoder to be self-synchronizing. Section [B.6](#) reviews the differential decoder's error propagation characteristics. Section [B.7](#) analyzes a recursive implementation of the differential code. Section [B.8](#) describes use of this code with frequency modulator-based SOQPSK transmitters. A description of the implementation of the entire coding and decoding process can be seen at [B.10](#) to this appendix.

B.2. The Need For Differential Encoding

Practical carrier recovery techniques like Costas loops and squaring loops exhibit a troublesome M-fold carrier phase ambiguity. The following paragraphs provide a description of ambiguity problems and how to overcome them.

[Figure B-1](#) shows a simplified quadriphase transmission system that is one of the methods recommended for transparent point-to-point transport of a serial binary data stream. Transparent means that only revenue-bearing data is transmitted. There is no in-line channel coding nor is special bit pattern insertion allowed. The assumption is made for an NRZ-L data stream containing the bit sequence $b(nT_b)$ transmitted at rate $r_b = 1/T_b$ bits per second. For QPSK and OQPSK modulations, the bit stream is divided into subsets e containing even-numbered bits and o containing odd numbered bits. The transmission rate associated with the split symbol streams is $r_s = r_b/2$ symbols per second. Symbol values are converted to code symbols by the differential encoder described in Section [B.3](#). A baseband waveform generator converts the digital symbol time series into continuous time signals suitable for driving the vector modulator as prescribed for the particular modulation in use. Thus, each subset modulates one of two orthogonal subcarriers, the in-phase (I) channel, and the quadrature (Q) channel. The modulator combines these subcarriers, creating a phase-modulated RF signal $S(t)$. On the receive side, demodulation separates the subcarriers, translates them back to baseband, and

³² FQPSK-JR is an FQPSK variant developed by Mr. Robert Jefferis, TYBRIN Corporation, and Mr. Rich Formeister, RF Networks, Inc.

constructs replicas of the code symbol series $E'(nT_s)$ and $O'(nT_s)$. Decoding reverses the encoding process and a multiplexer recreates a replica of the bit stream $b'(nT_b)$.

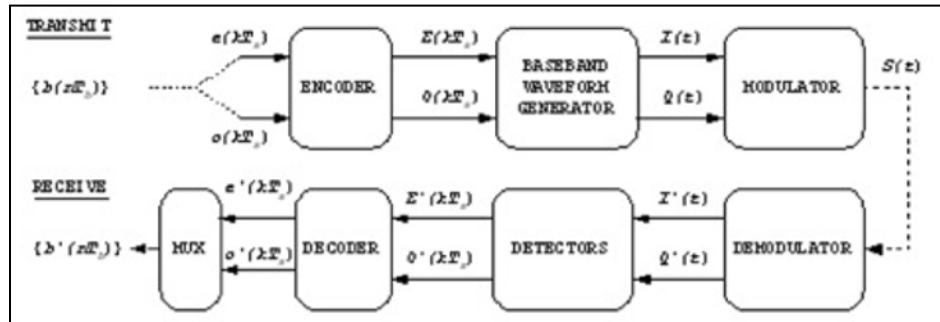


Figure B-1. Transmission System

Most QPSK and OQPSK systems employ coherent demodulation. [Figure B-2](#) is a simplified diagram of commonly used modulation and demodulation structures. Note the optional single-bit delay shown in the odd symbol path. This creates the significant difference between QPSK and OQPSK, the delay being inserted to create OQPSK.³³ Practical carrier recovery techniques like Costas loops and squaring loops exhibit a troublesome M-fold phase ambiguity ($M=4$ for QPSK and OQPSK).³⁴ Each time the demodulator carrier synchronizer phase locks to the modulator local oscillator its absolute phase relationship to the local oscillator contains the offset term β , which can take on values of $0, \pm \pi/2$, or π radians.³⁵

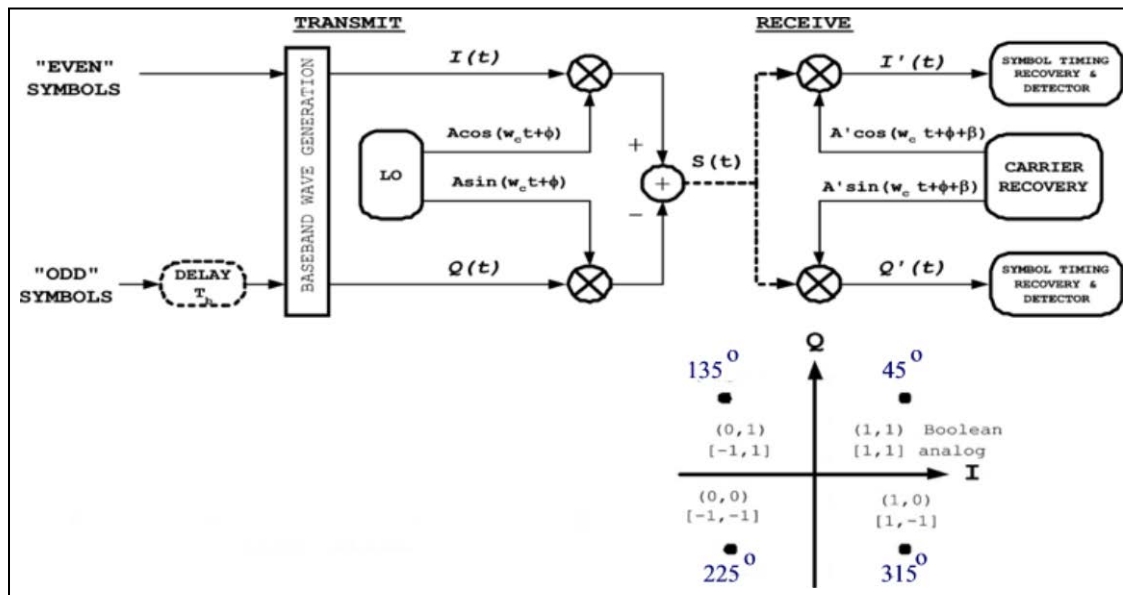


Figure B-2. OQPSK 106 Symbol-to-Phase Mapping Convention

³³ The delay can be inserted into either channel. The IRIG-106 convention and most published literature regarding FQPSK and SQPSK indicate the delay in the odd (or Q) channel.

³⁴ Proakis, J. G. and M. Salehi. *Digital Communications*. 5th Edition. Boston: McGraw-Hill, 2008.

³⁵ The initial offset angle ϕ is generally unknown and uncontrolled; it is tracked by the carrier recovery circuitry and the symbol timing circuits automatically ignore.

The symbol detectors have insufficient information to determine which phase offset exists. They always interpret demodulator output with the assumption that $\beta=0$. The resulting constellation axis rotations and their impact on demodulator output are shown at [Figure B-3](#) and [Table B-1](#). The 180° rotation is symmetric. The Axis (subcarrier) assignment is unchanged but the sense (polarity) of both axes gets reversed. The 90° and 270° rotations are asymmetric. Axis assignment is swapped and one axis polarity is reversed in each case.

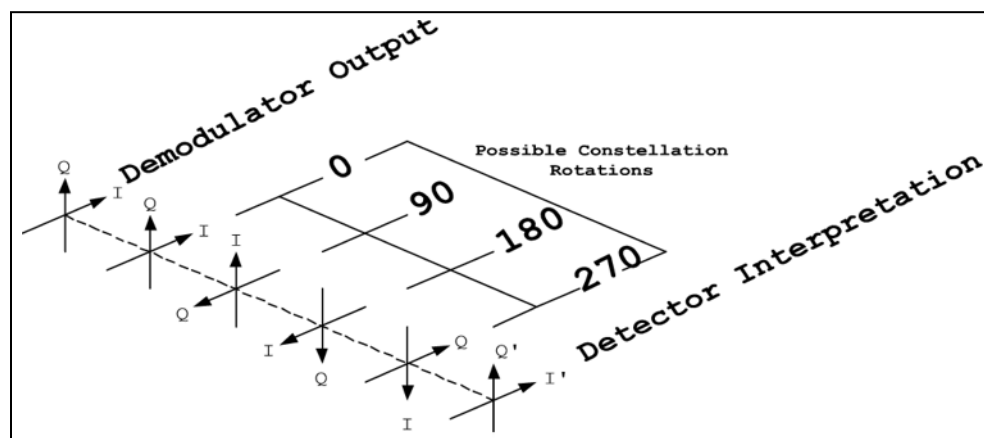


Figure B-3. Detection Ambiguity

| Table B-1. Constellation Axis Rotations | | |
|---|-------|-------|
| Rotation | $+I'$ | $+Q'$ |
| 0 | I | Q |
| $\pi/2$ | $-Q$ | I |
| π | $-I$ | $-Q$ |
| $3\pi/2$ | Q | $-I$ |

B.3. A Simple Solution To The Carrier Phase Ambiguity Problem

Differential encoding has been used to work around the carrier ambiguity for many years. For phase modulations, source data is coded such that phase differences rather than absolute phase coordinates become the information-bearing attribute of the signal. The QPSK and OQPSK modulations use I and Q independently, with each channel transporting one symbol stream. Starting with the first binary digit, bit 0, even-numbered bits form the sequence $\{e_k\}$ and odd-numbered bits form the sequence $\{o_{k+1}\}$ where the counting index is changed from the bit index n to the symbol pair index

$$k = 2n \quad k \in \{0, 2, 4, 6, \dots\} \quad (\text{B-1})$$

[Figure B-4](#) illustrates how QPSK modulators process bits in pairs (dibits), mapping and asserting time coincident symbol phase coordinates (I_k, Q_k).³⁶ Phase state changes commence and end on symbol interval timing boundaries, each state taking on one of four possible values at detector decision instants; however, the case of interest is shown in [Figure B-5](#).

³⁶ Rectangular I and Q baseband waveforms are used only for illustration.

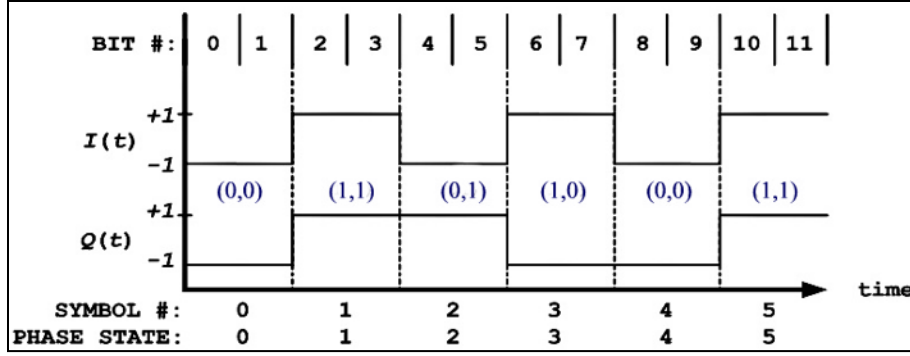


Figure B-4. QPSK State Timing

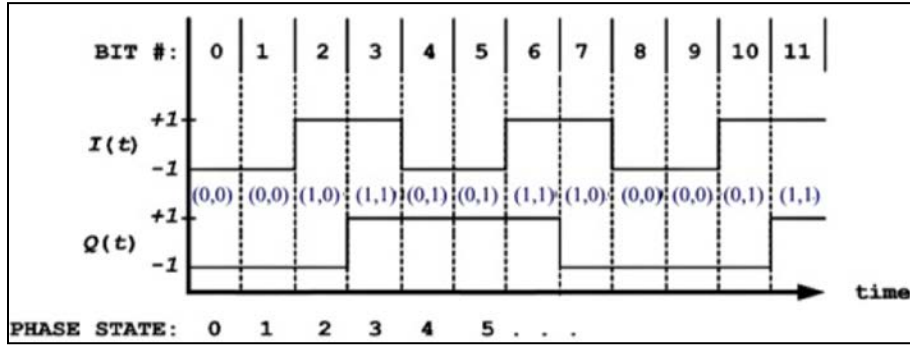


Figure B-5. OQPSK State Timing

The Q channel half-symbol delay causes OQPSK phase trajectories to evolve on a half-symbol (bit) rate basis. For the particular cases of FQPSK and SOQPSK-TG, carrier phase either remains unchanged or changes by $\pm\pi/4$ or $\pm\pi/2$ radians over the pending bit interval.

The OQPSK inter-channel delay might at first seem a difficult complication because it creates additional ambiguity; in other words, the receiver must resolve relative inter-channel delay; however, as shown below, this is not a problem.

The differential encoding rule adopted in IRIG-106 for OQPSK appears in Feher³⁷ and is therein attributed to Clewer³⁸ and Weber.³⁹ Bit by bit, the code symbol sets $\{E_k\}$ and $\{O_{k+1}\}$ are formed with the Boolean expressions:

$$E_k \equiv e_k \oplus \overline{O}_{k-1} \quad (\text{B-2a})$$

(B-2)

$$O_{(k+1)} \equiv o_{k+1} \oplus E_k \quad (\text{B-2b})$$

³⁷ Kamilo Feher. *Digital Communications: Satellite/Earth Station Engineering*. Englewood Cliffs: Prentice-Hall, 1983, pp. 168-170.

³⁸ R. Clewer. "Report on the Status of Development of the High Speed Digital Satellite modem", RML-009-79-24, Spar Aerospace Limited, St. Anne de Bellevue, P.Q., Canada, November 1979. Quoted in Kamilo Feher. *Digital Communications: Satellite/Earth Station Engineering*. Englewood Cliffs: Prentice-Hall, 1983.

³⁹ W. J. Weber III. "Differential Encoding for Multiple Amplitude and Phase Shift Keying Systems." In IEEE Transactions on Communications, Vol. COM-26, No. 3, March 1978.

Two bits are coded for each value of k in a two-step process. First, the even symbol E_k is coded with current bit e_k . Then the next bit, o_{k+1} becomes current and the odd symbol O_{k+1} is computed. In each code set the exclusive-or operator is applied to the state defining variables just like binary phase shift keying (BPSK) differential encoding. Unlike BPSK however, the current source bit and the most recent code symbol from the other channel determine adjacent phase transitions. The inverted code symbol in equation B-2a introduces asymmetry in the equations. Its significance will become evident in the next section.

The code symbol sets $\{E\}$ and $\{O\}$ are applied to the I and Q channels of the OQPSK modulator. The initial assignment of $\{E\}$ to either I or Q can be made arbitrarily; however, with this code definition, once the choice is made at the modulator, decoding will fail if channel assignment conventions change anywhere during the transmission or decoding processes. Thus, the assignment convention must extend to the physical modulator and demodulator. The IRIG-106 assigns I to the physical I subcarrier (also known as the “real” or “cosine” subcarrier) and Q is applied to the physical Q subcarrier (also known as the “imaginary” or “sine” subcarrier). In order to stress this assignment convention, IRIG-106 expresses equation B-2 explicitly in terms of the I and Q channel variables:

$$I_k \equiv e_k \oplus \overline{Q}_{(k-1)} \quad (\text{B-3a})$$

(B-3)

$$Q_{(k+1)} \equiv o_{(k+1)} \oplus I_k \quad (\text{B-3b})$$

Decoding is straightforward. When $\beta=0$, $I'=I$, and $Q'=Q$, inspection of the following truth tables reveals simple decoding instructions:

Equation B-3a

Equation B-3b

| I_k | $\overline{Q}_{(k-1)}$ | e_k | $Q_{(k+1)}$ | I_k | $o_{(k+1)}$ | |
|-------|------------------------|-------|-------------|-------|-------------|---------------------------------|
| 0 | 0 | 0 | 0 | 0 | 0 | |
| 0 | 1 | 1 | 1 | 0 | 1 | \Rightarrow decoding equation |
| 1 | 0 | 1 | 0 | 1 | 1 | |
| 1 | 1 | 0 | 1 | 1 | 0 | |

Equation B-3

$$e'_k = I'_k \oplus \overline{Q}'_{k-1} \quad (\text{B-4a})$$

(B-4)

$$o'_{k+1} = Q'_{k+1} \oplus I'_k \quad (\text{B-4b})$$

The equations at B-3 may not convey an intuitive sense of the shift from absolute phase states to phase differences. Extending B-3a backwards in time by substituting B-3b into B-3a results in:

$$I_k = e_k \oplus (\overline{o_{k-1} \oplus I_{k-2}}) = I_{k-2} \oplus (\overline{e_k \oplus o_{k-1}}) \quad (\text{B-5})$$

Similarly, for the next bit interval the results are:

$$Q_{k+1} = o_{k+1} \oplus (e_k \oplus \bar{Q}_{k-1}) = Q_{k-1} \oplus (\overline{o_{k+1} \oplus e_k}) \quad (\text{B-6})$$

This recursive form clearly shows that on a bit-by-bit basis, the current and most recent bits control phase trajectory motion, not absolute phase. Note that B-5 and B-6 do not define the sign of a phase change. Predictable decoder output requires that two additional conventions be established and maintained. Boolean logic polarity conventions used throughout the system must be consistent. The IRIG-106 assumes positive true logic. Finally, sign conventions and channel assignment used within the transmitter (baseband signal generator and modulator) and the receiver (demodulator) must be constrained to produce a consistent code symbol-to-phase mapping convention. The IRIG-106 convention is shown in [Figure B-2](#). For example, if {b} were to consist entirely of logic one values, i.e., a run of 1s, the differential encoding process and mapping convention will produce the phase trajectory shown in [Table B-2](#).

| Table B-2. Response to Run of 1s | | | | | | | |
|---|-------------|----------|----------------------|------------------------|------------------------|--------------------|----------------|
| n | b(n) | k | I_k | Q_{k-1} | Q_{k+1} | Phase (deg) | Phase Δ |
| 0 | 1 | 0 | 0 | 0* | | 225* | |
| 1 | 1 | | | | 1 | 135 | $-\pi/2$ |
| 2 | 1 | 1 | 1 | 1 | | 45 | $-\pi/2$ |
| 3 | 1 | | | | 0 | 315 | $-\pi/2$ |
| 4 | 1 | 2 | 0 | 0 | | 225 | $-\pi/2$ |
| 5 | 1 | | | | 1 | 135 | $-\pi/2$ |
| * denotes assumed initial conditions | | | | | | | |

The trajectory spins clockwise, and the phase is retarded by 90° during each bit interval.⁴⁰ Obviously, any single (unbalanced) sign change and any change to the mapping convention will alter the trajectory.

B.4. Immunity to Carrier Phase Rotation

The equations at B-3 and B-4 are invariant with respect to cardinal constellation rotation as shown in the following.

Proof:

The $\beta=0$ case is decoded correctly by definition according to equations B-5 and B-6. At [Table B-1](#), when $\beta = \pi$ there is no axis swap but the decoder is presented with

$$I'_k = \bar{I}_k$$

$$Q'_{k+1} = \bar{Q}_{k+1}$$

Decoding will progress as follows:

Step 1. Even channel; apply equation B-4a;

⁴⁰ FQPSK-B, FQPSK-JR, and SOQPSK-TG modulations respond to a run of 1s with an S(t) that is ideally, a pure tone at frequency $f_c - r_b/4$ Hz. This is referred as “lower sideband” mode. Similarly, a run of zeroes will produce a constant anti-clockwise trajectory spin and a tone at $f_c + r_b/4$ Hz (“upper sideband” mode).

$$e'_k = I'_k \oplus \overline{Q}'_{k-1} = \bar{I}_k \oplus Q_{k-1} = I_k \oplus \overline{Q}_{k-1} = e_k$$

Step 2. Odd channel; apply equation B-4b;

$$o'_{k+1} = Q'_{k+1} \oplus I'_k = \overline{Q}_{k+1} \oplus \bar{I}_k = Q_{k+1} \oplus I_k = o_{k+1}$$

Thus, symmetric rotation is transparent to the code. When $\beta=\pi/2$ the decoder sees the following.

$$\begin{aligned} I'_k &= \overline{Q}_{k-1} \\ Q'_{k+1} &= I_k \end{aligned}$$

Decoding takes place in the same sequence:

Step 1. Even channel, apply equation B-4a;

$$e'_k = I'_k \oplus \overline{Q}'_{k-1} = \overline{Q}_{k-1} \oplus \bar{I}_k = I_k \oplus Q_{k-1} = o_{k-1}$$

Step 2. Odd channel, apply equation B-4b;

$$o'_{k+1} = Q'_{k+1} \oplus I'_k = I_k \oplus \overline{Q}_{k-1} = e_k$$

In this case the bit sequence is recovered correctly and the code definition coupled with consistent sign conventions automatically compensates for the asymmetric rotation by reversing the application order of B-4a and B-4b. As a result, the output indices are shifted back in time one bit period. Asymmetric rotation causes a one-bit delay in the decoding process. Finally, the same result is seen when $\beta=3\pi/2$:

$$\begin{aligned} I'_k &= Q_{k-1} \\ Q'_{k+1} &= \bar{I}_k \end{aligned}$$

Step 1. Even channel; apply equation B-4a;

$$e'_k = I'_k \oplus \overline{Q}'_{k-1} = Q_{k-1} \oplus I_k = I_k \oplus Q_{k-1} = o_{k-1}$$

Step 2. Odd channel; apply equation B-4b;

$$o'_{k+1} = Q'_{k+1} \oplus I'_k = \bar{I}_k \oplus Q_{k-1} = I_k \oplus \overline{Q}_{k-1} = e_k$$

In all cases the decoder correctly reproduces the original bit sequence. Decoding is instantaneous for symmetric rotations but it is delayed by one bit in 2 out of 4 possible asymmetric rotation startup scenarios.

The need for consistent function assignment now becomes clear. Application of B-4b to a code symbol formed with B-3a produces the complement of the original bit. Likewise, application of B-4a to a symbol coded with B-3b inverts the result.

At this point, the OQPSK inter-channel delay ambiguity mentioned in Section [B.2](#) has not been resolved. The roles of I' and Q' reverse with asymmetric rotations and there is no way to determine when this occurs; however, as long as the code symbol time sequence is preserved

at the decoder and the roles of I' and Q' do not get reversed in terms of the application of B-6a and B-6b, inter-channel delay is transparent to the code with respect to reconstruction of the original data sequence.⁴¹

B.5. Initial Values

Equations B-3 and B-4 do not impose any implementation constraints on initial values when encoding or decoding starts. To confirm this it is assumed that hardware power-up (or initial data presentation) may cause encoding to commence with either channel. It is further assumed that no provisions for specific initial values in encoder and decoder state memories have been made. If coding starts with I (see equation B-3a), the first code symbol will be computed:

$$\|I_0\| = e_0 \oplus \langle \overline{Q}_{-1} \rangle$$

where $\langle . \rangle$ denotes an unknown initial value and double vertical bars denote computed values influenced by initial values. Encoding equations B-3a and B-3b will progress as follows:

$$\|Q_1\| = o_1 \oplus \|I_0\|$$

$$\|I_2\| = e_2 \oplus \|\overline{Q}_1\|$$

The initial values do establish the absolute sense of code symbols for the duration of transmission; but, on both ends of the process, two of three terms in every equation are affected consistently by the initial value, which by symmetry has no effect on the outcome of exclusive-or operations. Obviously, identical results occur if the encoder starts with Q . Independent of starting channel and initial value then, the first and all subsequent adjacent code symbol pairs contain valid state change information.

Initial decoder values can produce errors. Again starting with I , and using equations B-4a and B-4b, decoding will progress as follows:

$$\|e'_0\| = I'_0 \oplus \langle \overline{Q}_{-1} \rangle$$

$$o'_1 = Q'_1 \oplus I'_0$$

It is seen that on the second cycle the initial value of the decoder has been flushed out. At most, one bit will be decoded in error. Similarly, if decoding starts with Q , output will progress:

$$\|o'_1\| = Q'_1 \oplus \langle I'_0 \rangle$$

$$e'_2 = I'_2 \oplus \overline{Q}'_1$$

Again, only the first decoded bit may be incorrect. The conclusion, then, is that initial values can produce at most one decoded bit error; however, there is another source of startup

⁴¹ If for some reason the system application requires that one can determine whether a specific symbol was originally transmitted via I or Q , then this code is not appropriate.

errors that is seen as an initial value problem. Section B.4 showed that odd phase rotations ($\pi/2$ and $3\pi/2$) cause a single bit delay in the decoder. Examining this further, the first symbol index value will be $k = 0$. If the decoder starts with equation B-4a, the first decoded bit will be:

$$e'_0 = I'_0 \oplus \langle \overline{Q}_{-1} \rangle = I_0 \oplus \langle Q_{-1} \rangle = \langle o_{-1} \rangle$$

If the decoder starts with equation B-4b the first result will be:

$$o'_1 = Q'_1 \oplus I'_0 = I_0 \oplus \langle \overline{Q}_{-1} \rangle = \|e_0\|$$

The first case produces the aforementioned delay. The decoder emits an extra bit. The second bit emitted is actually the first bit of the sequence reconstruction and is still subject to the single initial value error probability of startup processing. The latter case does not produce a delay; it only presents the possibility of a first bit decoding error.

B.6. Error Propagation

Differential encoding incurs a bit error penalty because received code symbols influence more than one decoded bit. First consider a single-symbol detection error in current symbol E' that is labeled ε_k . The following sequence of decoding steps shows how the error propagates. Since the E channel was chosen as current, decoding starts with equation B-4a. The single detection error creates two sequential decoding errors. By symmetry we can state that the same result occurs if a single error occurs in O' .

$$\begin{aligned} b'_k &= \varepsilon_k \oplus \overline{Q}_{k-1} = \overline{b}_k \Rightarrow \text{error} \\ b'_{k+1} &= Q_{k+1} \oplus \varepsilon_k = \overline{b}_{k+1} \Rightarrow \text{error} \\ b'_{k+2} &= E'_{k+2} \oplus Q'_{k+1} = b_{k+2} \Rightarrow \text{correct} \end{aligned}$$

Next is the case of two symbol detection errors occurring consecutively on E' and O' , i.e., detectors emit error symbols $E'_k = \varepsilon_k$ and $O'_{k+1} = \varepsilon_{k+1}$. Starting again with equation B-4a yields:

$$\begin{aligned} b'_k &= \varepsilon_k \oplus \overline{Q}_{(k-1)} = \overline{b}_k \Rightarrow \text{error} \\ b'_{(k+1)} &= \varepsilon_{(k+1)} \oplus \varepsilon_k = O'_{(k+1)} \oplus E_k = b_{(k+1)} \Rightarrow \text{correct} \\ b'_{(k+2)} &= E'_{(k+2)} \oplus \varepsilon_{(k+1)} = b_{(k+2)} \Rightarrow \text{error} \\ b'_{(k+3)} &= O'_{(k+3)} \oplus E'_{(k+2)} = b_{(k+3)} \Rightarrow \text{correct} \end{aligned}$$

Two consecutive symbol errors produce two decoding errors but the errors are not adjacent. The conclusion from this is that symbol detection errors influence no more than two decoding cycles, i.e., the maximum error multiplication factor is 2.

B.7. Recursive Processing and Code Memory

Most systems reconstruct the original bit rate clock and $\{b\}$ by merging $\{e'\}$ and $\{o'\}$. For a variety of reasons, designers might be tempted to multiplex $\{I'\}$ and $\{Q'\}$ into a bit rate code symbol sequence $\{B_n\}$ prior to decoding; however, the same considerations that foster

desire for post-multiplex decoding are likely to be accompanied by loss of transmitted code symbol order, i.e., loss of knowledge whether a given code symbol came from I or Q . The question arises as to whether $\{B_n\}$ alone contains enough information for unique decoding. The answer is no, and the proof is shown below.

Proof:

A decoding function can be derived by inspection of equations B-5 and B-6. Equation B-5 can be rearranged as follows:

$$I_k = e_k \oplus o_{k-1} \oplus \bar{I}_{k-2} \quad (\text{B - 7})$$

Similarly, from equation B-6 we can write

$$Q_{k+1} = o_{k+1} \oplus e_k \oplus \bar{Q}_{k-1} \quad (\text{B - 8})$$

Here are two instances of a seemingly identical recursive relationship, i.e., the current code symbol is the difference between the current bit, the previous bit, and the inverse of the most recent code symbol from the current channel. We can consolidate these equations by converting to post-multiplex bit rate indexing, i.e.,

$$B_n = b_n \oplus b_{(n-1)} \oplus \bar{B}_{(n-2)} \quad (\text{B - 9})$$

from which we can immediately write the decoding function

$$b'_n = b'_{(n-1)} \oplus B'_n \oplus \bar{B}'_{(n-2)} \quad (\text{B - 10})$$

On the surface it seems that equation B-10 will work;⁴² however, these relations involve two differences, rather than one, and therefore introduce superfluous initial condition dependence. For brevity, only the pitfalls of B-10 are examined herein, assuming that a non-recursive encoder is used. From startup, decoding will progress as follows.

$$\begin{aligned} \|b'_0\| &= \langle b'_{-1} \rangle \oplus B'_0 \oplus \langle \bar{B}'_{-2} \rangle \\ \|b'_1\| &= \|b'_0\| \oplus B'_1 \oplus \langle \bar{B}'_{-1} \rangle \\ \|b'_2\| &= \|b'_1\| \oplus B'_2 \oplus \bar{B}'_0 \\ \|b'_3\| &= \|b'_2\| \oplus B'_3 \oplus \bar{B}'_1 \end{aligned}$$

.
.
.

As seen, absolute polarity of the first and all subsequent decoded bits is determined by three initial values. Absent appropriate side information for selecting initial values, the post-multiplex decoder offers a 50-50 chance of decoding with correct polarity. The code sequence

⁴² The interested reader is left to confirm that equation C-10 is indeed rotation invariant.

defined by equations at B-3 has a two-symbol memory. Additional symbols do not provide new information regarding the trajectory history. Another way to view this problem is to note that this recursive decoder does not guarantee preservation of symbol order, which is a prerequisite to reliable decoding.

B.8. Frequency Impulse Sequence Mapping for SOQPSK

The SOQPSKs first described by Hill⁴³ and Geoghegan⁴⁴ are defined as special cases of CPM. Since 1998, at least two manufacturers have exploited the fact that modern digital waveform synthesis techniques enable direct implementation of the CPM equations with virtually ideal frequency modulators and filter impulse responses. A generic model of these implementations is in [Figure B-6](#). The I and Q channels, per se, do not exist in this transmitter. At the beginning of each bit interval, impulses from the bit-to-impulse alphabet mapper direct the impulse filter/frequency modulator to advance the carrier phase by 90°, retard it by or 90°, or leave the phase unchanged. This is accomplished with a ternary alphabet of frequency impulses having normalized amplitudes of $\{-1,0,1\}$.⁴⁵ This structure cannot be mapped directly into the constellation convention of a quadriphase implementation because there is no way to control absolute phase. The equations at B-3 can be applied to this non-quadrature architecture via pre-coding. A general treatment SOQPSK pre-coding is contained in Simon.⁴⁶ The pre-coding truth table given in [Table B-3](#) applied to the model in [Figure B-7](#) will yield a phase trajectory history identical to one generated by the quadriphase counterpart of [Figure B-2](#) using the equations at B-3; however, one more constraint is necessary to establish compatibility with the IRIG-106 quadriphase convention. [Table B-3](#) assumes the stipulation that positive sign impulse values will cause the modulator to increase carrier frequency.

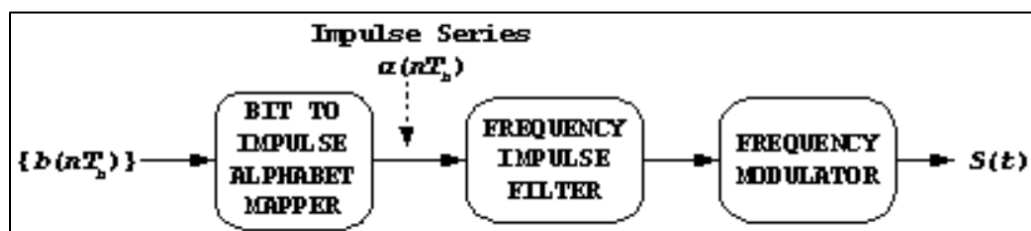


Figure B-6. SOQPSK Transmitter

| Table B-3. SOQPSK Pre-Coding Table for IRIG-106 Compatibility | | | | | | | | | |
|---|-----------|-----------|--------------|------------|-----------------------------------|-------|-----------|--------------|----------------|
| MAP α_k FROM I_k | | | | | MAP α_{k+1} FROM Q_{k+1} | | | | |
| I_k | Q_{k-1} | I_{k-2} | $\Delta\Phi$ | α_k | Q_{k+1} | I_k | Q_{k-1} | $\Delta\Phi$ | α_{k+1} |
| -1 | X* | -1 | 0 | 0 | -1 | X* | -1 | 0 | 0 |
| +1 | X* | +1 | 0 | 0 | +1 | X* | +1 | 0 | 0 |
| -1 | -1 | +1 | $-\pi/2$ | -1 | -1 | -1 | +1 | $+\pi/2$ | +1 |

⁴³ Hill, "An Enhanced, Constant Envelope, Interoperable Shaped Offset QPSK."

⁴⁴ Geoghegan, "Implementation and Performance Results."

⁴⁵ The so-called ternary alphabet is actually 2 binary alphabets $\{-1,0\}$ and $\{0,1\}$, the appropriate one chosen on a bit-by-bit basis according to certain state transition rules.

⁴⁶ Marvin Simon. "Multiple-Bit Differential Detection of Offset Quadriphase Modulations." IPN Progress Report 42-151. 15 November 2002. Jet Propulsion Laboratory, Pasadena, CA. Retrieved 4 June 2015. Available at http://ipnpr.jpl.nasa.gov/progress_report/42-151/151A.pdf.

| | | | | | | | | | |
|--|----|----|----------|----|----|----|----|----------|----|
| -1 | +1 | +1 | $+\pi/2$ | +1 | -1 | +1 | +1 | $-\pi/2$ | -1 |
| +1 | -1 | -1 | $+\pi/2$ | +1 | +1 | -1 | -1 | $-\pi/2$ | -1 |
| +1 | +1 | -1 | $-\pi/2$ | -1 | +1 | +1 | -1 | $+\pi/2$ | +1 |
| * Note: Does not matter if “X” is a +1 or a -1 | | | | | | | | | |

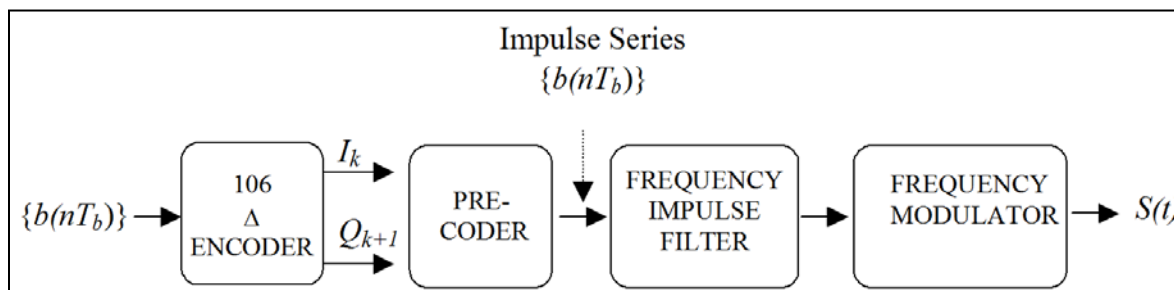


Figure B-7. OQPSK Transmitter (With Precoder)

B.9. Summary

This investigation confirmed that the differential encoder defined in the equations at B-3 is entirely satisfactory for SOQPSK, FQPSK-JR, and FQPSK-B systems where conventional coherent demodulation and single-symbol detection is used. In addition, a method of extending this code to SOQPSK is presented without proof.

Specifically, the following has been shown.

- When accompanied by consistent sign conventions, a consistent symbol-to-phase mapping rule, and preservation of symbol order, the OQPSK differential code defined in B-3 and the decoding rule defined in B-4 is rotation invariant and unambiguously reconstructs the original data bit sequence.
- Decoding is instantaneous.
- Equations B-3 and B-4 do not require attention to initial values.
- At most, two consecutive output bits will be in error after carrier and symbol synchronization is acquired.
- The recursive relations in equations B-9 and B-10 are ambiguous and therefore unreliable.
- The code exhibits a detection error multiplication factor of at most two.

B.10. System-Level Software Reference Implementation of Differential Encoder Defined in IRIG Standard 106 for FQPSK and SOQPSK Modulations

B.10.a. Introduction

The Matlab®™ program listings below provide a Matlab function “Desysdemo” and an execution control script “runDEdemo”. In the context of differential encoding, the function provides a complete system simulation including a differential encoder, an ideal vector modulator, channel phase rotation, demodulation, the functional equivalent of an ideal single-symbol sample and hold detector, and a decoder. The user can create sample data vectors or use the example data provided. In addition, the user can manipulate the initial value vectors to

explore all possible initial value and demodulator phase rotation combinations of the quadriphase implementation model.

By setting the variable “style” to zero, the function will also emulate the pre-coded frequency modulator architecture required for SOQPSKs; however, the initial value of transmitter carrier phase is hard-coded at 45° . This was done to avoid proliferation of initial value options and is thought to be an insignificant omission because it does not affect generality of the phase rotation options.

This material assumes that the user is familiar with Matlab workspace operation. The program relies only on basic Matlab license libraries. No special toolboxes or blocksets are required.

B.10.b. Matlab Workspace Operation

The user should place the script (shown below in Section [B.10.c](#)) in the directory of choice and make that directory current in the workspace. In order to execute the canned example, the user needs to create the variable “example” in the workspace and set its value to 1.

Executing the script “runDEdemo” should produce the output displayed in Table B-1.

| Table B-1. Script “runDEdemo” Output | | | | |
|---|----------------|-----------------|----------------|-----------------|
| results = | | | | |
| Model: Quadriphase Vector Modulator | | | | |
| Demodulator Phase Rotation = 0° | | | | |
| Initial States: | Encoder Memory | Encoder Channel | Decoder Memory | Decoder Channel |
| | (0,0) | 0 | (0,0) | 0 |
| Input Bit | TX Phase | RX Phase | Output Bit | Decoding Error |
| 1 | 225 | 225 | 1 | 0 |
| 1 | 135 | 135 | 1 | 0 |
| 1 | 45 | 45 | 1 | 0 |
| 0 | 45 | 45 | 0 | 0 |
| 0 | 135 | 135 | 0 | 0 |
| 1 | 135 | 135 | 1 | 0 |
| 0 | 135 | 135 | 0 | 0 |
| 1 | 135 | 135 | 1 | 0 |
| 1 | 45 | 45 | 1 | 0 |
| 1 | 315 | 315 | 1 | 0 |
| 0 | 315 | 315 | 0 | 0 |
| 0 | 45 | 45 | 0 | 0 |
| 1 | 45 | 45 | 1 | 0 |
| 0 | 45 | 45 | 0 | 0 |

The first column of the results shown above is a replica of the input data vector. The second column shows the initial value-dependent evolution of transmitted phase. The third column shows the effect of any non-zero phase rotation chosen. The fourth column shows the

decoded output bit stream. The fifth column flags decoding errors with values of 1. Certain combinations of phase rotation and initial values will produce values of 9 in the fourth and fifth columns; results of this nature are associated with cases that delay the output decoding process by one bit.

Variable definitions and implied instructions for manipulating the runtime options can be obtained by using the normal Matlab help command for these specific programs.

B.10.c. Script For Modules

Electronic copies of these programs have been provided to the RCC Telemetry Group. The script for the modules discussed above is shown on the following pages.

```

% Control Script 'runDEdemo', for running system demonstration
% of differential encoder and phase mapping convention
% defined in RCC standard IRIG-106 for FQPSK-B modulation.
% This version extends demonstration options to the pre-coder
% required for implementing SOQPSK with frequency modulators.
%
% Each example run requires input variables in the Matlab workspace:
%
% "example" - a flag to run with user supplied data vector or run
%   the example data set that consists of two repetitions of a
%   a 7-bit pseudo random sequence(0=user, 1=example)
% "data" - optional user supplied binary bit sequence (arbitrary
length)
% "rotation_choice" - pointer to demodulator phase rotation options:
%   1=0, 2= $\pi/2$ , 3= $\pi$ , 4= $3\pi/2$ 
% "initTX" - vector of binary encoder startup values:
%   initTX(1)= 1st of two encoder code symbol memory values(binary,
arbitrary)
%   initTX(2)= 2nd encoder code symbol memory value(binary, arbitrary)
%   initTX(3)= starting channel for encoder(binary, 0=I, 1=Q)
% "initRX" - vector of binary decoding startup values
%   initRX(1)= 1st of two decoder state memory values(binary, arbitrary)
%   initRX(2)= 2nd decoder state memory value(binary, arbitrary)
%   initRX(3)= starting channel for decoder(binary, 0=I, 1=Q)
% "style" - 1=quadrature transmitter architecture (FQPSK)
%   0=frequency modulator transmitter architecture (SOQPSK)
% The example values are:
% data=[1 1 1 0 0 1 0 1 1 1 0 0 1 0]
% rotation_choice=1
% initTX=[0 0 0]
% initRX=[0 0 0]
% style=1

% R.P.Jefferis, TYBRIN Corp., JULY, 2002
% SOQPSK model added 14JUL03
% This version has been tested with Matlab versions:5.2,6.1

% *** Sample Input Setup ***
if example
    data=[1 1 1 0 0 1 0 1 1 1 0 0 1 0];
    rotation_choice=1;
    initTX=[0 0 0];
    initRX=[0 0 0];
    style=1;
end

% *** Run the Reference Implementation ***

[test,delay]=DEsysdemo(data,rotation_choice,initTX,initRX,style);

% *** Prepare Screen Output ***

```

```

ROTATION=[0 90 180 270];
if style
    results=sprintf('Model: Quadriphase Vector Modulator\n')
else
    results=sprintf('Model: Frequency modulator (SOQPSK) model\n')
end
results=[results sprintf('Demodulator Phase Rotation = %3.0f
degrees\n',ROTATION(rotation_choice))];
results=[results sprintf('Initial States: Encoder Encoder Decoder
Decoder\n')];
results=[results sprintf('
Memory Channel Memory
Channel\n')];
results=[results sprintf('-----
----\n')];
results=[results sprintf('
(%d,%d) %d (%d,%d)
%d\n\n',...
    initTX(1:2),initTX(3),initRX(1:2),initRX(3))];
results=[results sprintf(' Input TX RX Output Decoding\n')];
results=[results sprintf(' Bit Phase Phase Bit Error\n')];
results=[results sprintf('-----\n')];
for n=1:length(data)
    results=[results sprintf(' %d %3.0f %3.0f %d
%d\n',...
        test(n,:))];
end
results

% _____END OF CONTROL SCRIPT_____

function [result,delay]=
DEsysdemo(inbits,rotation_choice,initTX,initRX,style)
% Reference simulation for Range Commanders Council standard IRIG 106-
2000
% FQPSK-B differential encoding and phase mapping convention.
%
% Input arguments: see "help" for "runDEdemo" script
% Output arguments:
% "result" - Mx5 matrix,M=number of input bits,columns contain:
% (:,1)input bit,(:,2)TX phase,(:,3)RX phase,(:,4)output
bit,(:,5)status
% "delay" - overall encode/decode process delay in bits

% "TX" prefixes refer to transmitter/encoder variables, "RX" prefixes
% refer to receiver/decoder variables
% Robert P. Jefferis, TYBRIN Corp., July,2002.
% SOQPSK model added 14JUL03
% This version has been tested with Matlab versions: 5.2,6.1
numbits=length(inbits)

% *****
% * Transmitter *
% *****

```

```

% *** differential encoder (also SOQPSK pre-coder)****

% encoder memory initial values:
%[(last I ch. code symbol) (last Q ch. code symbol)]
TXlastSYM=initTX(1:2);
% point encoder to either I or Q starting channel(0=I)
TXpoint=initTX(3);
for n=1:numbits
    switch TXpoint
        case 0
            %TXlastSYM
            % compute "current" I channel code symbol
            TXnewISYM=xor(inbits(n),~TXlastSYM(2));
            TXcodeSYM(n,:)=[TXnewISYM TXlastSYM(2)]; % new phase
coordinates(I,Q)
            TXlastSYM(1)=TXnewISYM; % update encoder memory state
            TXpoint = ~TXpoint; % point to Q channel eq. for next bit
        case 1
            % compute "current" Q channel code symbol
            TXnewQSYM=xor(inbits(n),TXlastSYM(1));
            TXcodeSYM(n,:)=[TXlastSYM(1) TXnewQSYM]; % new phase
coordinates(I,Q)
            TXlastSYM(2)=TXnewQSYM;% update encoder memory state
            TXpoint= ~TXpoint; % point to I channel eq. for next bit
        otherwise
            disp('Invalid Specification of Encoder starting channel');
        end
    end
end

% *** modulate ***

switch style
case 1 % ** Quadriphase vector modulator **

    % RCC IRIG 106 FQPSK-B phase mapping convention: (I,Q)
    for n=1:numbits
        index=floor(2*TXcodeSYM(n,1)+TXcodeSYM(n,2));
        switch index
            case 3 % [1 1]
                TXphase(n)=45; % TX phase angle, degrees
            case 1 % [0 1]
                TXphase(n)=135;
            case 0 % [0 0]
                TXphase(n)=225;
            case 2 % [1 0]
                TXphase(n)=315;
            otherwise, disp('map error')
        end
    end
end
case 0 % ** Frequency modulator w/pre-coder **

```

```

% * pre-coder *
% map code symbol sequence to frequency impulse series, alpha(n)
alpha=zeros(1,numbits);
TXpoint=initTX(3); % in this mode, points to start index
for n=3:numbits
    if TXpoint % Q(k+1) map
        if TXcodeSYM(n,2)==TXcodeSYM(n-2,2)
            elseif xor(TXcodeSYM(n,2),TXcodeSYM(n-1,1))
                alpha(n)=-1;
            else
                alpha(n)=1;
            end
        else % I(k) map
            if TXcodeSYM(n,1)==TXcodeSYM(n-2,1)
                elseif xor(TXcodeSYM(n,1),TXcodeSYM(n-1,2))
                    alpha(n)=1;
                else
                    alpha(n)=-1;
                end
            end
        TXpoint=~TXpoint; % switch to complement function for next bit
    end

    % convert alpha to phase trajectory
    lastTXphase=45; % initial phase of S(t)
    for n=1:numbits
        TXphase(n)=mod(lastTXphase+alpha(n)*90,360);
        lastTXphase=TXphase(n);
    end
otherwise
end

% *****
% * Receiver *
% *****

% *** Demodulator Phase Rotation ***
ROTATE=[0 pi/2 pi 3*pi/2];
rotate=ROTATE(rotation_choice);
for n=1:numbits
    switch rotate
    case 0
        RXphase(n)=TXphase(n);
    case pi/2
        RXphase(n)=mod(TXphase(n)+90,360);
    case pi
        RXphase(n)=mod(TXphase(n)+180,360);
    case 3*pi/2
        RXphase(n)=mod(TXphase(n)+270,360);
    otherwise
    end
end
end

```

```

% *** detector ***
for n=1:numbits
    switch RXphase(n)
    case 45
        RXcodeSYM(n,:)=[1 1];
    case 135
        RXcodeSYM(n,:)=[0 1];
    case 225
        RXcodeSYM(n,:)=[0 0];
    case 315
        RXcodeSYM(n,:)=[1 0];
    otherwise
    end
end

% *** decode and reconstruct data bit sequence ***

% decoder memory initial values:
% [(last decoded I channel bit) (last decoded Q channel bit)]
RXlastSYM=initRX(1:2);
% point decoder channel to either I or Q starting channel (0=I)
RXpoint=initRX(3);
for n=1:numbits
    switch RXpoint
    case 0
        % compute "current" decoded I channel bit
        RXbits(n)=xor(RXcodeSYM(n,1),~RXlastSYM(2));
        RXlastSYM=RXcodeSYM(n,:); % update decoder state
        RXpoint = ~RXpoint; % point to Q channel eq. for next bit
    case 1
        % compute "current" decoded Q channel bit
        RXbits(n)=xor(RXcodeSYM(n,2),RXlastSYM(1));
        RXlastSYM=RXcodeSYM(n,:); % update decoder state
        RXpoint= ~RXpoint; % point to I channel eq. for next bit

    otherwise
    end
end

% _____ END OF TX and RX Processing _____

% *****
% * Assemble Output *
% *****

% identify delay incurred in overall process
offset=xcorr(inbits,RXbits);
offset(1:numbits-1)=[];
[offset,delay]=max(offset(1:min(length(offset),10)));
delay=delay-1;

```

```

% adjust RX output bit vector to compensate for delay,
% inserting values of 9 at beginning of vector to represent
% artifact bits associated with asymmetric rotation cases
checkbits=inbits;
if delay
    newfront=ones(1,delay)*9;
    checkbits=[newfront inbits];
    checkbits(end-delay+1:end)=[];
    RXbits(1:delay)=9;
end
% identify decoding errors in reconstructed bit stream
xmsn_error=checkbits~=RXbits;
xmsn_error(1:delay)=9;
% assemble output matrix
result(:,1)=inbits';
result(:,2)=TXphase';
result(:,3)=RXphase';
result(:,4)=RXbits';
result(:,5)=xmsn_error';

% _____END OF FUNCTION DEsysdemo_____

```

APPENDIX 2-C

Telemetry Transmitter Command and Control Protocol**C.1. Introduction**

This appendix provides standards for commands, queries, and status information when communicating with telemetry transmitters configured with communication ports. The commands are divided into two categories of command sets as follows.

- a. Basic. The basic command set contains the minimum (required) commands for transmitter control, query, and status.
- b. Extended. The extended command set contains optional commands that may or may not be implemented and may be shown as references.

C.2. Command Line Interface**C.2.a. User Command Line Interface**

This interface is the default upon power up of the transmitter. Each command or query is ended by a carriage return <CR>. Information returned from the transmitter will be followed by a carriage return <CR> and the ">" will be displayed to indicate the transmitter is ready to receive commands or queries.

NOTE

With regard to this standard, it is assumed that a carriage return <CR> is followed by a line feed. The transmitter will return the "OK" mnemonic for each command that is accepted. The transmitter will return "ERR" for a command or query that was interpreted as an error. Verification that a query was either accepted or found to be in error will be the response to the query. All commands are case-insensitive. The transmitter will operate in half-duplex mode and will echo typed characters to the command terminal.

In addition to the required user command line interface items, the following list contains options that may or may not be implemented.

- a. Backspacing to correct typed errors.
- b. A character input to recall the last command line. The "^" character followed by a <CR> is recommended.

C.2.b. Optional Programming Interface

If the transmitter is not commanded or queried through a terminal program (human interface), there may be an option to operate in half-duplex mode so that concatenated commands can be sent directly to the transmitter (bulk transmitter set-up). If this option is used, the transmitter will only return a single accepted "OK" response if the entire string was interpreted and accepted. When concatenating commands, the semicolon is used as the delimiter for each command. If this optional programming interface is implemented, the transmitter will identify the semicolon delimiter, recognize the character string as a bulk command, and recognize the start of a new command after each delimiter.

C.3. Initialization

Upon successful communication initialization, the transmitter will provide the controlling terminal with (as a minimum) the manufacturer's name, model number, serial number, and supported IRIG-106 release number. Other information (such as information on firmware and temperature) deemed appropriate by the manufacturer is allowed. This information will be displayed only upon a successful power up and communication initialization of the transmitter. Should an unsuccessful power up occur, based upon criteria of the transmitter manufacturer, the transmitter shall return "ERR" and allow only the RE(RES) command to reset the transmitter (see Subsection [C.4.b\(9\)](#)).

Upon successful communication, after a power up, a communication connection, a command, or a query, the transmitter will send a carriage return followed by a ">" to signify the transmitter is ready to accept commands and queries.

C.4. Basic Command Set

C.4.a. Basic Command Set Summary

The basic command fields use a minimum two characters with the optional capability of using a maximum of four characters. If possible, the longer four-character field should be used to add intuitiveness to the basic command set. The commands in the basic command set are shown in [Table C-1](#).

| Table C-1. Basic Command Set | |
|-------------------------------------|---|
| Command | Function |
| FR(FREQ) | Sets or queries the carrier frequency. |
| MO(MOD) | Sets or queries the modulation mode. |
| RA(RAND) | Sets or queries the setting of data randomization (ON or OFF). |
| RF | Sets or queries the RF output (ON or OFF). |
| QA(QALL) | Queries the status of all basic commands. |
| VE(VERS) | Queries, at a minimum, the manufacturer's name, model number, and serial number of the transmitter. |
| SV(SAVE) | Saves the current set-up of the transmitter to on-board nonvolatile random access memory (RAM). |
| RL(RCLL) | Retrieves a transmitter set-up from on-board nonvolatile RAM. |
| RE(RES) | Resets the transmitter to a known configuration or restarts the internal power-up sequence. |
| DS(DSRC) | Sets or queries the data source (INT or EXT). |
| CS(CLKS) | Sets or queries the clock source (INT or EXT). |
| ID(IDP) | Sets or queries the internal data pattern (one of five possible settings). |
| IC(ICR) | Sets or queries the internal clock rate. |
| TE(TEMP) | Queries the internal temperature (in Celsius). |
| FC(FEC) | Sets or queries FEC. |
| ST(STC) | Sets or queries Space Time Coding. |

C.4.b. Commands: Basic Command Set

C.4.b(1) Carrier Frequency

Carrier frequency is set or queried with the FR(FREQ) mnemonic as described below.

- a. Set Frequency. Use “FR(FREQ) XXXX.X <CR>” where XXXX.X is the commanded frequency in MHz in 0.5-MHz steps. If the command is accepted, an “OK <CR>” is issued as a response.

In the event of an incorrect commanded carrier frequency (for example the commanded frequency is out of the tuning range of the transmitter), the transmitter will default to the currently set carrier frequency before the command was issued. The transmitter will then return “ERR FR(FREQ) XXXX.X <CR>” where XXXX.X is the prior frequency set in the transmitter.

- b. Query Frequency. “FR(FREQ) <CR>” queries the currently set carrier frequency and returns “FR(FREQ) XXXX.X <CR>” where XXXX.X is the current set frequency in MHz.

C.4.b(2) Modulation Mode

Modulation mode is set or queried with the MO(MOD) mnemonic.

- a. Set Modulation Mode. Use “MO(MOD) X <CR>” where X corresponds to the modulation mode. If the command is accepted, an “OK <CR>” is issued as a response.

| Command | Modulation Type |
|-----------|-------------------------------|
| MO(MOD) 0 | PCM/FM |
| MO(MOD) 1 | SOQPSK-TG |
| MO(MOD) 2 | ARTM-CPM |
| MO(MOD) 6 | Modulation off (carrier only) |

In the event of an incorrect commanded modulation mode, the transmitter will default to the previous modulation mode and return “ERR MO(MOD) X <CR>” to indicate the error and the current modulation mode. The “MO(MOD) 6” command turns off the modulation for carrier-only mode. Modulation will return upon a new commanded modulation mode. If the transmitter is in single mode, only single mode commands are valid and the above error response will be sent should an invalid modulation mode command be sent. The same logic applies when the transmitter is in dual mode.

- b. Query Modulation Mode. “MO(MOD) <CR>” queries the currently set modulation mode and returns “MO(MOD) X <CR>” where the integer X is represented in the above table.

C.4.b(3) Data Randomization

Data randomization is set or queried with the RA(RAND) mnemonic. For additional information on randomization, see Subsection [2.3.3.4](#). This command only enables/disables the randomizer specified in [Annex A.2](#), Figure A.2-2.

- a. Set Data Randomization. Use “RA(RAND) X <CR>” where X corresponds to a 1 or 0. If the command is accepted, an “OK <CR>” is issued as a response.

| Command | Randomization |
|------------|---------------|
| RA(RAND) 1 | On |
| RA(RAND) 0 | Off |

NOTE

When FEC is enabled, randomization per Section [D.6](#) should be implemented. If RA(RAND) was enabled prior to enabling FEC, it will be disabled when FEC is enabled. The default state for RA(RAND) will be off when FEC is enabled.

In the event of an incorrect data randomization command, the transmitter will default to its current setting and return “ERR RA(RAND) X <CR>” to indicate the error and the currently set state. If FC(FEC) is enabled, a “RA(RAND) 1” command will return an ERR RA(RAND) 1<CR>.

- b. Query Randomization Mode. “RA(RAND) <CR>” queries the currently set randomization and returns “RA(RAND) X <CR>” where integer X is represented in the above table.

C.4.b(4) RF Output

The RF output is set or queried with the RF mnemonic.

- a. Set RF Output. Use “RF X <CR>” where X corresponds to a 1 or 0. If the command is accepted, an “OK <CR>” is issued as a response.

| Command | RF Output |
|---------|-----------|
| RF 1 | On |
| RF 0 | Off |

In the event of an incorrect RF output command, the transmitter will maintain its current state and return “ERR RF X <CR>” to indicate the error and return the current RF output setting for the transmitter.

- b. Query RF Output. “RF <CR>” queries the currently set RF output and returns “RF X <CR>” where X corresponds to the numbers in the above table.

C.4.b(5) Query All

The “query all” command is executed with the QA(QALL) mnemonic.

- a. Query Transmitter Configuration. The command “QA(QALL) <CR>” requests the current setting of all basic commands. The transmitter response will contain, as a minimum, the following, in this order:

- (1) Carrier Frequency. [FR(FREQ) XXXX.X]<CR>
- (2) Modulation Mode. [MO(MOD) X] <CR>
- (3) Randomization setting. [RA(RAND) X] <CR>
- (4) RF Output setting. [RF X] <CR> OK<CR>
- (5) Data Source. [DS(DSRC) X] <CR>

- (6) Internal Data Pattern [ID(IDP) X] <CR>
- (7) Clock Source [CS(CLKS) X] <CR>
- (8) Internal Clock Rate [IC(ICR) XX.XXX] <CR>
- (9) Internal Temperature [TE(TEMP) XXX] <CR>
- (10) Forward Error Correction [FC(FEC) X] <CR>
- (11) Space Time Coding [ST(STC) X] <CR>

- b. Status of Other Commands. If other commands are implemented in the transmitter beyond the basic set, a complete status should be given for each implemented command.

C.4.b(6) Version

The “version” command is executed with the VE(VERS) <CR> mnemonic.

- a. Query Transmitter Version. “VE(VERS) <CR>” requests the current version of the transmitter. The response will contain (at a minimum) the following information about the transmitter and in this order:
 - (1) Manufacturer Name
 - (2) Model Number
 - (3) Serial Number
- b. Formatting and Delimiting the Fields. It is left up to the transmitter manufacturer to format and delimit the above fields and, if chosen, add additional information to the response.

C.4.b(7) Save

The “save” command is executed with the SV(SAVE) mnemonic.

For “Save Transmitter Set-Up”, “SV(SAVE) X<CR>” saves the current settings of the transmitter to register “X” in nonvolatile memory within the transmitter. If only one location is available, the value of “X” is zero. This document puts no limit to the number of storage registers as this is limited by available nonvolatile memory.

The command “SV(SAVE) <CR>” will save to the default location 0.

In the event of an unsuccessful save command, the transmitter will return ERR SV(SAVE) X<CR> to indicate the error and no save function will be performed.

In order to avoid the situation of fielding a flight test item that has been inadvertently programmed to use internal clock and data sources, the transmitter power up configuration will always have the clock and data source as external. In addition, when saving to register “0” clock and data sources will always be set to external.

C.4.b(8) Recall

The recall command is executed with the RL(RCLL) mnemonic.

For “Recall Transmitter Set-up”, “RL(RCLL) X<CR>” retrieves and restores the transmitter set-up from register “X” in nonvolatile memory within the transmitter. Values of X start at zero. The “0” register location should be used exclusively for the default set-up, which is the memory location that is loaded during power-up.

The command “RL(RCLL) <CR> will recall from the default register location “0”.

In the event of an unsuccessful recall command, the transmitter will return ERR RL(RCLL) X<CR> to indicate the error and no recall function will be performed.

During a recall operation the transmitter will always set the clock and data sources to external (see Subsection [C.4.b\(7\)](#)).

C.4.b(9) Reset

The transmitter can be reset with the RE(RES) mnemonic.

- a. Reset Transmitter. “RE(RES) <CR>” resets the transmitter by reinitializing the transmitter. The transmitter will use the following basic settings as a base configuration.

| Transmitter Setting | Command | Result |
|--------------------------|--------------|--|
| Carrier frequency | [FR(FREQ)] | Lowest valid frequency within the tuning range |
| Modulation mode | [MO(MOD)] | MO(MOD) 0, PCM/FM |
| Differential encoding | [DE X] | DE 0, Differential encoding off |
| Randomization | [RA(RAND) X] | RA(RAND) 0, Randomization off |
| RF output | [RF X] | RF 0, RF output off |
| Data source | [DS(DSRC)] | DS(DSRC) 0 External |
| Clock source | [CS(CSRC)] | CS(CSRC) 0 External |
| Internal Data Pattern | [ID(IDP)] 11 | [ID(IDP)] 11 PN11 ($2^{11}-1$) |
| Internal Clock Rate | [IC(ICR)] | IC(ICR) 05.000 5 MHz |
| Forward Error Correction | [FC(FEC)] | FC(FEC) 0, Forward Error Correction is off |
| Space Time Coding | [ST(STC)] | ST(STC) 1, Space Time Coding is on |

- b. Example Command Use. The Reset command would be used if resetting to a known configuration is required, communication to the transmitter could not be established, if commands were not being recognized, or if some other unknown transmitter state was experienced.

C.4.b(10) Data Source

Data source is set or queried with the DS(DSRC) mnemonic.

- a. Set Data Source. Use “DS(DSRC) X <CR>” where X corresponds to a 1 or 0. If the command is accepted, an “OK <CR>” is issued as a response.

| Command | Source |
|------------|----------|
| DS(DSRC) 0 | External |
| DS(DSRC) 1 | Internal |

In the event of an incorrect data source command, the transmitter will return “ERR DS(DSRC) X <CR>” to indicate the error and return the currently set data source state.

- b. Query Data Source. “DS(DSRC) <CR>” queries the currently set data source and returns “DS(DSRC) X <CR>” where integer X is represented in the above table.
- c. Saving Data Source. See Subsection [C.4.b\(7\)](#) regarding saving the data source setting.

C.4.b(11) Clock Source

The clock source is set or queried with the CS(CLKS) mnemonic.

- a. Set Clock Source. Use “CS(CLKS) X <CR>” where X corresponds to a 1 or 0. If the command is accepted, an “OK <CR>” is issued as a response.

| Command | Source |
|------------|----------|
| CS(CLKS) 0 | External |
| CS(CLKS) 1 | Internal |

In the event of an incorrect command, the transmitter will return “ERR CS(CLKS) X <CR>” to indicate the error and the current clock source setting for the transmitter.

- b. Query Clock Source. “CS(CLKS) <CR>” queries the currently set clock source and returns “CS(CLKS) X <CR>” where integer X is represented in the above table.
- c. Example Command Use. Internal data can be clocked either with an external or internal clock. This command allows the user to clock the known data with an existing external clock or select the internal clock for more flexibility.
- d. Saving Clock Source. See Subsection [C.4.b\(7\)](#) regarding saving the clock source setting.

C.4.b(12) Internal Data Pattern

The internal data pattern is set or queried with the ID(IDP) mnemonic.

- a. Set Internal Data Pattern. Use “ID(IDP) X” where X corresponds to the internal data pattern. If the command is accepted, an “OK <CR>” is issued as a response.
- b. Example Internal Data Patterns. Example patterns are shown below.

| Command | Pattern | |
|--------------|------------|-----------------|
| ID(IDP) 9 | 2^9-1 | (511 bits) |
| ID(IDP) 11 | $2^{11}-1$ | (2047 bits) |
| ID(IDP) 15 | $2^{15}-1$ | (32767 bits) |
| ID(IDP) 20 | $2^{20}-1$ | (1048575 bits) |
| ID(IDP) 23 | $2^{23}-1$ | (8388607 bits) |
| ID(IDP) 0000 | 0x0000 | Fixed repeating |
| ID(IDP) FFFF | 0xFFFF | Fixed repeating |
| ID(IDP) AAAA | 0101010 | Fixed repeating |
| ID(IDP) XXXX | 0xFFFF | Fixed repeating |

The minimum supported patterns shall be PN11, PN15, and AAAA. Selection of which additional patterns to implement is left up to the manufacturer. If an error occurs, the transmitter will return “ERR ID(IDP) X <CR>” to indicate the error and return the current data source setting for the transmitter.

- c. Query Internal Data Pattern. “ID(IDP) <CR>” queries the currently set internal data pattern and returns “ID(IDP) X <CR>” where integer X is represented in the above table.

- d. Example Command Use. This feature can be used for system characterization and troubleshooting. A known bit pattern can be used to test and characterize telemetry systems end-to-end or isolate baseband signal problems to the transmitter.

C.4.b(13) Internal Clock Rate

The internal clock rate is set or queried with the IC(ICR) mnemonic.

- a. Set Internal Clock Rate. Use “IC(ICR) XX.XXX <CR>” where XX.XXX corresponds to the clock frequency in MHz and is used to clock the selected internal data pattern. See Subsection [C.4.b\(12\)](#). Actual range for the clock frequency is left to the manufacturer but should correspond to the specified useable input clock frequency range. Resolution should be ± 1 kHz. Accuracy for the internal clock is left to the manufacturer but should correspond to internal values for the transmitter. If the command is accepted, an “OK <CR>” is issued as a response.

In the event of an incorrect command, the transmitter will identify the error, default to its current state, and return “ERR IC(ICR) XX.XXX <CR>” where “XX.XXX” indicates the current clock source for the transmitter.

- b. Query Internal Clock Rate. “IC(ICR) <CR>” queries the currently set internal clock rate and returns “IC(ICR) XX.XXX” where XX.XXX is the current set internal clock rate in MHz.

C.4.b(14) Internal Temperature

Internal temperature is only a query with the TE(TEMP) mnemonic.

Using TE(TEMP) will query the current internal temperature of the transmitter and returns “TE(TEMP) XXX” where XXX is the temperature in Celsius.

C.4.b(15) Forward Error Correction

When used, FEC is set or queried with the FC(FEC) mnemonic. If FEC per [Appendix 2-D](#) is implemented in the transmitter, this command will enable, disable, or query the current setting.

- a. Set Forward Error Correction. Use “FC(FEC) X <CR>” where X corresponds to the table below. If X=1, then the command structure is “FC(FEC) 1 xxxx yy <CR>” where xxxx corresponds to the block size and yy corresponds to the code rate. If the command is accepted, an “OK <CR>” is issued as a response. When FC(FEC) is enabled, randomization in the transmitter [RA(RAND)] shall be disabled.

| Command | Source | Block Size | Code Rate |
|-------------------|---|--------------|--|
| FC(FEC) 0 | Disable | | |
| FC(FEC) 1 xxxx yy | Enable/Block Size/Code Rate | 1024 or 4096 | 12 selects 1/2 23 selects 2/3 45 selects 4/5 |
| FC(FEC) X | Future Error Correction Code Capability | | |

In the event of an incorrect FEC command, the transmitter will return “ERR FC(FEC) X <CR>” to indicate the error and return the current FEC setting for the transmitter.

- b. Query Forward Error Correction Setting. “FC(FEC) <CR>“ queries the currently set FEC condition and returns “FC(FEC) 0<CR>“, when FEC is disabled and returns “FC(FEC) 1 xxxx yy” when FEC is enabled.
- c. Refer to [Appendix 2-D](#) for additional details on FEC and the associated randomization used.

C.4.b(16) Space Time Coding

An STC-enabled transmitter is two independent transmitters when STC is disabled. The command prompt indicates which transmitter is communicating over the serial port. When STC is enabled modulation will be SOQPSK-TG per [Appendix 2-E](#).

- a. Set Space Time Coding. Use “ST(STC) X <CR>“ where X corresponds to a 1 or 0. If the command is accepted, an “OK <CR>“ is issued as a response.

| Command | Space Time Coding | Prompt |
|-----------|-------------------|--------------|
| ST(STC) 0 | Disable | RF1> or RF2> |
| ST(STC) 1 | Enable | > |

- b. Query Space Time Coding. “ST(STC) <CR>“ returns “ST(STC) X<CR>“ where integer X is represented in the table above. “STC 0” is associated with a command prompt of RF1> or RF2>.
- c. Independent Commanding. The following command structure allows independent commanding when STC is disabled.
 - Upon issuing an “ST(STC) 0 <CR>“ command, the command prompt changes from “>“ to “RF1>“, indicating communication with the transmitter associated with RF port 1 (Xmtr1). The default command prompt is “RF1>“.
 - To change to the other transmitter, issue the command “RF2” and the command prompt changes to “RF2>“, indicating communication with the transmitter associated with RF port 2 (Xmtr2).
 - Commands apply to both transmitters independently.
 - Issuing “ST(STC) 1 <CR>“ returns the “>“ prompt indicating STC mode is enabled and commands apply as they would to a single transmitter. At the “>” prompt independent control of each transmitter is not available.
- d. Example Command Use. The examples in [Figure C-1](#) illustrate the use of several commands to configure transmitter parameters.

| | |
|---------------|--|
| > | transmitter is ready to receive commands or queries |
| >ST | Queries STC mode |
| >ST 1 | Responds STC is enabled |
| > | transmitter is ready to receive commands or queries |
| >ST 0 | Disables STC |
| RF1> | Responds RF1 is ready to receive commands or queries |
| RF1>MO 0 | Sets RF1 modulation mode to PCM/FM |
| RF1>ST 1 | Enables STC |
| > | transmitter is ready to receive commands or queries |
| >MO | Queries modulation mode |
| >MO 1 | Responds modulation mode is SOQPSK |
| > | transmitter is ready to receive commands or queries |
| >ST 0 | Disables STC |
| RF1> | RF1 is ready to receive commands or queries |
| RF1>FR 4450.5 | Sets RF1 frequency to 4450.5 MHz |
| RF1>DS 0 | Sets RF1 data source to External |
| RF1>CS 0 | Sets RF1 clock source to External |
| RF1>RF2 | Selects RF2 to receive commands or queries |
| RF2> | RF1 is ready to receive commands or queries |
| RF2>MO 0 | Sets RF2 to PCM/FM modulation mode |
| RF2>FR 4460.5 | Sets RF2 frequency to 4460.5 MHz |
| RF2>DS 0 | Sets RF2 data source to External |
| RF2>CS 0 | Sets RF2 clock source to External |
| RF2>MO 2 | Sets RF2 modulation mode to ARTM-CPM |
| RF2>ST 1 | Enables STC |
| > | transmitter is ready to receive commands or queries |

Figure C-1. Terminal Window for STC-Enabled Transmitter

C.5. Extended Command Set

C.5.a. Extended Command Set Summary

Although the extended command set does not include all possible commands, its use provides a standard way of implementing known features of transmitters. This standard will be updated at appropriate intervals should new capabilities arise. Commands in the extended command set are shown in [Table C-2](#).

| Table C-2. Extended Command Set | |
|---------------------------------|---|
| Command | Function |
| DP(DPOL) | Sets or queries data polarity (NORM or INV) |
| RP(RPWR) | Sets or queries the output RF power (HI or LO) |
| SP(SLP) | Low-power consumption mode, sleep mode |
| VP() | Variable RF power command |
| CP() | Sets or queries the input clock phase |
| DE() | Sets or queries differential encoding (ON or OFF) |
| RZ() | Sets or queries RF power on/off pin polarity |

C.5.b. Commands: Extended Command Set**C.5.b(1) Data Polarity**

Data polarity is set or queried with the DP(DPOL) mnemonic.

- a. Set Data Polarity. Use “DP(DPOL) X <CR>” where X corresponds to a 1 or 0. Actual data polarity, when referenced to the input clock, does not need to be known; this command either inverts the incoming data or does not. If the command is accepted, an “OK <CR>” is issued as a response.

| Command | Polarity |
|------------|----------|
| DP(DPOL) 0 | Normal |
| DP(DPOL) 1 | Inverted |

In the event of an incorrect data polarity command, the transmitter will maintain its current setting and return “ERR DP(DPOL) X <CR>” to indicate the error and return the current data polarity setting for the transmitter.

- b. Query Data Polarity. “DP(DPOL) <CR>” queries the current data polarity and returns “DP(DPOL) X <CR>” where integer X is represented in the above table.

C.5.b(2) RF Power (High/Low)

High output power or low output power is set or queried with the RP(RPWR) mnemonic.

- a. Set RF Output Power. Use “RP(RPWR) X <CR>” where X corresponds to a 1 or a 0. If the command is accepted, an “OK <CR>” is issued as a response.

| Command | Output RF Power Level |
|------------|-----------------------|
| RP(RPWR) 0 | Low |
| RP(RPWR) 1 | High |

- b. Query RF Output Power Level. “RP(RPWR) <CR>” queries the currently set output RF power level and returns “RP(RPWR) X <CR>” where integer X is represented in the above table.

In the event of an incorrect RF power command, the transmitter will return “ERR RP(RPWR) X <CR>” to indicate the error and return the current RF power setting for the transmitter.

- c. Example use. The low setting could be used for lab testing or ground checks when transmitter and receiver antennas are co-located. The high power setting is for normal, over-the-air telemetry transmission.

C.5.b(3) Low Power Consumption, Sleep Mode

The transmitter can be placed into a mode of low input power consumption with the SP(SLP) mnemonic.

- a. Set Low Power Mode. Use “SP(SLP) X” where X corresponds to a 1 or 0 as shown in the following table. If the command is accepted, an “OK <CR>” is issued as a response.

| Command | Source |
|-----------|---------------------|
| SP(SLP) 0 | Full Operation Mode |
| SP(SLP) 1 | Sleep Mode |

Sleep mode powers down all nonessential circuitry within the transmitter to reduce input power consumption. Note, in order to return from sleep mode, the transmitter must monitor and recognize the SP(SLP) 0 command. In the event of an incorrect command, the transmitter will return “ERR SP(SLP) X <CR>” to indicate the error and the current power mode setting for the transmitter.

- b. Query Power Mode. “SP(SLP) <CR>” queries the power mode setting and returns “SP(SLP) X <CR>” where integer X is represented in the above table.

C.5.b(4) Variable Power Mode

The transmitter can support user-selectable output power levels using the VP XX<CR> mnemonic.

- a. Set Variable Power Level. Use “VP XX<CR>” or “VP X<CR>” to set a range of RF output power levels available in discrete predefined steps. If the command is accepted, an “OK<CR>” is issued as a response. In the event of an incorrect command, the transmitter will return “ERR VP XX<CR>” to indicate the error and the current variable power level for the transmitter.
- b. Query Variable Power Level. “VP<CR>” queries the power mode setting and returns “VP XX<CR>” where integer XX is represented in the table below.
- c. Look Up Table. The actual value of output power that corresponds to “XX” is undefined. Each manufacturer will provide an equation or lookup table that defines the output power as a function of “XX”.

| Command | RF Power Level |
|------------------|---------------------------------|
| VP XX | Full Power (equivalent to RP 1) |
| VP (XX – 1) | Less than full power |
| VP 1 (or VPP 01) | More than low power |
| VP 0 (or VPP 00) | Low Power (equivalent to RP 0) |

- d. Variable Power in STC Transmitters. For transmitters with STC capability, the VP command applies to both transmitters. When STC is disabled, output power for each transmitter can be independently controlled with the VP command.

C.5.b(5) Input Clock Phase

The transmitter can support user-selectable input clock phasing using the CP X<CR> mnemonic.

- a. Set Input Clock Phase. Use “CP X<CR>” where X corresponds to a 1, 0, or A. If the command is accepted, an “OK<CR>” is issued as a response. In the event of an incorrect input clock phase command, the transmitter will return “ERR CP X<CR>” to indicate the error and return the current input clock phase setting for the transmitter.

- b. Query Input Clock Phase. “CP<CR>” queries the input clock phase setting and returns “CP X<CR>” where the value of X is represented in the table below.

| Command | Input Clock Phase | Data Transitions |
|---------|-------------------|--|
| CP 0 | 0° | Rising Edge of Clock |
| CP 1 | 180° | Falling Edge of Clock |
| CP A | 0° or 180° | Edge with greatest margin with respect to data transitions |

C.5.b(6) Differential Encoding

Differential encoding is set or queried with the DE mnemonic. For additional information, refer to Subsection [2.3.3.1.1](#) and [0](#). This command is only applicable when modulation mode is set to SOQPSK-TG (MO 1).

- a. Set Differential Encoding. Use “DE X <CR>” where X corresponds to a 1 or 0. If the command is accepted, an “OK <CR>” is issued as a response.

| Command | Differential Encoding |
|---------|-----------------------|
| DE 1 | On |
| DE 0 | Off |

In the event of an incorrect differential encoding command, the transmitter will return “ERR DE X<CR>” to indicate the error and return the current differential encoding setting.

- b. Query Differential Encoding. “DE <CR>” queries the currently set differential encoding status and returns “DE X <CR>” where integer X is represented in the above table.
- c. Default. When switching modulation modes the differential encoding shall be switched appropriately. For example, when switching from SOQPSK-TG to PCM/FM, the differential encoding will be set to off.
- d. Manual Control. For the PCM/FM and ARTM-CPM modulation modes, differential encoding will always be disabled (off). For SOQPSK-TG modulation mode, differential encoding will be enabled upon selection of that mode; however, the user can exercise manual control of differential encoding when using SOQPSK-TG modulation. Additionally if either FEC or STC are enabled, differential encoding will be disabled.

C.5.b(7) RF Power On/Off Pin Polarity

The RF power on/off pin polarity is set or queried with the RZ mnemonic. This command sets the polarity of the pin, either a low or high level, to enable RF power output.

- a. Set RF Power On/Off Pin Polarity.

| Command | RF Power |
|-----------|---------------------|
| RZ(RFZ) 1 | On when pin is high |
| RZ(RFZ) 0 | On when pin is low |

In the event of an incorrect RF power command, the transmitter will return “ERR RF X<CR> X<CR>” to indicate the error and return the current RF power setting.

- b. Query RF Power On/Off Pin Polarity. “RZ(RFZ) <CR>“ queries the currently set RF power status and returns “RZ(RFZ) X <CR>“.
- c. Default. The transmitter will initialize in the RF power pin polarity on/off “On when pin is high” setting.


C.6. Transmitter Communication Example

A typical terminal window is shown in [Figure C-2](#) for clarity. Transmitter communication initialization is assumed.

```
>FR 1435.5
>OK
>FR
>FR 1435.5
>MO 0
>OK
>DE 1
>ERR DE 0
>MO 7
>ERR MOD 0
>RGDW
>ERR
>TE
>TE 085
>QA
>FR 1435.5
>MO 0
>DE 0
>RA 1
>RF 1
>
```

Figure C-2. Typical Terminal Window

C.7. Non-Standard Commands

| | |
|---|--|
|  NOTE | <p>This paragraph is reserved for transmitter commands that fall outside of the commands and command structure discussed above. Additions to this section will be made as non-standard commands are derived and found applicable to this standard.</p> |
|---|--|

C.8. Physical Layer(s)

The above command sets are independent of the physical layer over which the commands are transferred. The command set should be implemented in such a way that it can be translated over any physical layer interfacing with the transmitter.

Should a three-wire serial interface be chosen, it should be compatible with EIA232 (<http://www.eia.org/>). The intent of this standard is not to force complete EIA-232 compliance; rather, the intent is to establish a serial communication interface with the transmitter so that any terminal program, such as Windows® HyperTerminal or Linux Minicom, can be used to communicate with the transmitter. A transmit-and-receive line will be supplied with an associated ground return; the choice of connector pin-out is left up to the manufacturer. The serial interface will operate at one of the common transfer rates. Typical baud rates are 300, 600,

1200, 2400, 4800, 9600, 19200, 38400, 57600, and 115200 baud. The default shall be 9600 baud. Should operation at another baud rate be desired, a command must be implemented to accommodate this capability. The command shall have the form BD(BAUD) as described below.

- a. Baud Rate. Serial communication baud rate shall be set or queried with the BD(BAUD) mnemonic.
- b. Set Baud Rate. Use “BD(BAUD) X <CR>” where X corresponds to a number (0-9) in the following table. If the command is accepted, an “OK” <CR>” is issued as a response.

| Command | Rate |
|------------|--------|
| BD(BAUD) 0 | 300 |
| BD(BAUD) 1 | 600 |
| BD(BAUD) 2 | 1200 |
| BD(BAUD) 3 | 2400 |
| BD(BAUD) 4 | 4800 |
| BD(BAUD) 5 | 9600 |
| BD(BAUD) 6 | 19200 |
| BD(BAUD) 7 | 38400 |
| BD(BAUD) 8 | 57600 |
| BD(BAUD) 9 | 115200 |

- c. Query Baud Rate. “BD(BAUD) <CR>” queries the set baud rate of the transmitter and returns “BD(BAUD) X <CR>” where integer X is represented in the above table.

In the event of an incorrect baud rate command, the transmitter will return “ERR BD(BAUD) X<CR>” to indicate the error and return the current baud rate setting for the transmitter.

Communication should be compatible with a terminal set-up consisting of one of the above baud rates with 8 data bits, 1 stop bit, 1 start bit, and no parity. ASCII characters will be transmitted and received. No hardware or software handshaking should be implemented and connector pin-out is left to the manufacturer.

This page intentionally left blank.

APPENDIX 2-D

Low-Density Parity-Check Codes for Telemetry Systems**D.1. Background**

The LDPC codes presented are intended to decrease error probabilities in a primarily noisy transmission channel for use in the AMT test environment.

The LDPC code is a linear block code. This type of code maps a block of k information bits together with a codeword (or codeblock) of n bits. Think of a linear block code as a chunk of input bits mapped through a coder to a longer chunk of output bits. This is sometimes called an $n-k$ code. When k bits are mapped to a length n codeblock there are 2^k codewords; however, there are 2^n possible codewords composed of n bits. The idea with error correction codes is to pick the 2^k codewords of the 2^n total possible codewords that are far enough apart (in terms of Hamming distance) to guarantee you are able to correct a certain number of errors.

This particular version of LDPC code is systematic, meaning the transmitted codeblock contains duplications of the bits of the original information. It is also a quasi-cyclic linear block code, meaning the construction of these codes involves juxtaposing smaller cyclic submatrices (circulants) to form a larger parity matrix, all through linear operations.

This code, like all other FEC schemes, requires an encoder on the transmission side and a decoder on the receiving side of the telemetry link. The codes offer much higher decoding speeds via highly parallelized decoder structures. This FEC code can only be coupled with SOQPSK-TG/FQPSK-B/FQPSK-JR modulation. The LDPC code itself does not guarantee sufficient bit transitions to keep receiver symbol synchronizers in lock so a randomizer, defined in this appendix, is required when implementing this FEC code.

Since LDPC is a block code, the start of a codeblock(s) must be identified in order for the decoder to function properly. This identifier, known as the attached synchronization marker (ASM), provides this marker and also aids in detection at very low values of E_b/N_0 . Differential encoding/decoding normally associated with SOQPSK-TG/FQPSK-B/FQPSK-JR modulation is NOT required and should be disabled. Phase ambiguities will have to be resolved using the ASM.

D.2. Code Description

The LDPC code is a linear block code with options for $\{n,k\}$, where n is the length of the codeblock and k is the length of the information block. An LDPC code can be entirely defined by its parity check matrix, **H**. The $k \times n$ generator matrix that is used to encode a linear block code can be derived from the parity check matrix through linear operations.

Code rates, r , chosen for this AMT application are 1/2, 2/3, and 4/5. Information block sizes (k) are 1024 and 4096 bits. Given the code rate and information block sizes, codeword block sizes are calculated using $n = k/r$. See [Table D-1](#).

| Table D-1. Codeblock Length per Information Block Size | | | |
|---|-----------------------|----------|----------|
| Information Block Length, k | Codeblock Length, n | | |
| | Rate 1/2 | Rate 2/3 | Rate 4/5 |
| 1024 | 2048 | 1536 | 1280 |
| 4096 | 8192 | 6144 | 5120 |

The $k \times n$ generator matrix \mathbf{G} shall be used to encode a linear block code. The matrix \mathbf{G} can be derived from the parity check matrix \mathbf{H} .

For each $\{n, k\}$ in [Table D-1](#) a parity check matrix \mathbf{H} is constructed from size $M \times M$ submatrices per [Table D-2](#).

| Table D-2. Submatrix Size per Information Block Size | | | |
|---|--------------------|----------|----------|
| Information Block Length, k | Submatrix size M | | |
| | Rate 1/2 | Rate 2/3 | Rate 4/5 |
| 1024 | 512 | 256 | 128 |
| 4096 | 2048 | 1024 | 512 |

D.3. Parity Check Matrices

Given the $\{n, k\}$ in [Table D-1](#), there are six parity check matrices that need to be constructed. Section 3.3 in CCSDS standard 131.1-0-2 (CCSDS September 2007) describes how each parity check matrix is constructed and is repeated here for clarity.

The \mathbf{H} matrices for each code rate are specified below. \mathbf{I}_M is the $M \times M$ identity matrix (main diagonal is 1's, all other entries are 0) and $\mathbf{0}_M$ is the zero matrix.

Parity Check Matrices

$$H_{1/2} = \begin{bmatrix} 0_M & 0_M & I_M & 0_M & I_M \oplus \Pi_1 \\ I_M & I_M & 0_M & I_M & \Pi_2 \oplus \Pi_3 \oplus \Pi_4 \\ I_M & \Pi_5 \oplus \Pi_6 & 0_M & \Pi_7 \oplus \Pi_8 & I_M \end{bmatrix}$$

$$H_{2/3} = \begin{bmatrix} 0_M & 0_M & 0_M & 0_M & I_M & 0_M & I_M \oplus \Pi_1 \\ \Pi_9 \oplus \Pi_{10} \oplus \Pi_{11} & I_M & I_M & I_M & 0_M & I_M & \Pi_2 \oplus \Pi_3 \oplus \Pi_4 \\ I_M & \Pi_{12} \oplus \Pi_{13} \oplus \Pi_{14} & I_M & \Pi_5 \oplus \Pi_6 & 0_M & \Pi_7 \oplus \Pi_8 & I_M \end{bmatrix}$$

$$H_{4/5} = \left[\begin{array}{cccccc} 0_M & 0_M & 0_M & 0_M & 0_M & 0_M \\ \Pi_{21} \oplus \Pi_{22} \oplus \Pi_{23} & I_M & \Pi_{15} \oplus \Pi_{16} \oplus \Pi_{17} & I_M & \Pi_9 \oplus \Pi_{10} \oplus \Pi_{11} & I_M \\ I_M & \Pi_{24} \oplus \Pi_{25} \oplus \Pi_{26} & I_M & \Pi_{18} \oplus \Pi_{19} \oplus \Pi_{20} & I_M & \Pi_{12} \oplus \Pi_{13} \oplus \Pi_{14} \end{array} \right] H_{1/2}$$

Permutation matrix Π_k has non-zero entries in row i and column entries are defined by $\pi_k(i)$ for $i \in \{0, \dots, M-1\}$

$$\pi_k(i) = \frac{M}{4} ((\theta_k + \lfloor 4i / M \rfloor) \bmod 4) + (\phi_k(\lfloor 4i / M \rfloor) + i) \bmod \frac{M}{4}$$

where θ_k and $\phi_k(j)$ are defined in the following tables for the submatrix sizes defined in [Table D-2](#) for each code rate and information block size.

Code Rate = 1/2, Information Block Size = 1024, $M = 512$

| k | Θ_k | $\phi_k(0,M)$ | $\phi_k(1,M)$ | $\phi_k(2,M)$ | $\phi_k(3,M)$ |
|-----|------------|---------------|---------------|---------------|---------------|
| 1 | 3 | 16 | 0 | 0 | 0 |
| 2 | 0 | 103 | 53 | 8 | 35 |
| 3 | 1 | 105 | 74 | 119 | 97 |
| 4 | 2 | 0 | 45 | 89 | 112 |
| 5 | 2 | 50 | 47 | 31 | 64 |
| 6 | 3 | 29 | 0 | 122 | 93 |
| 7 | 0 | 115 | 59 | 1 | 99 |
| 8 | 1 | 30 | 102 | 69 | 94 |

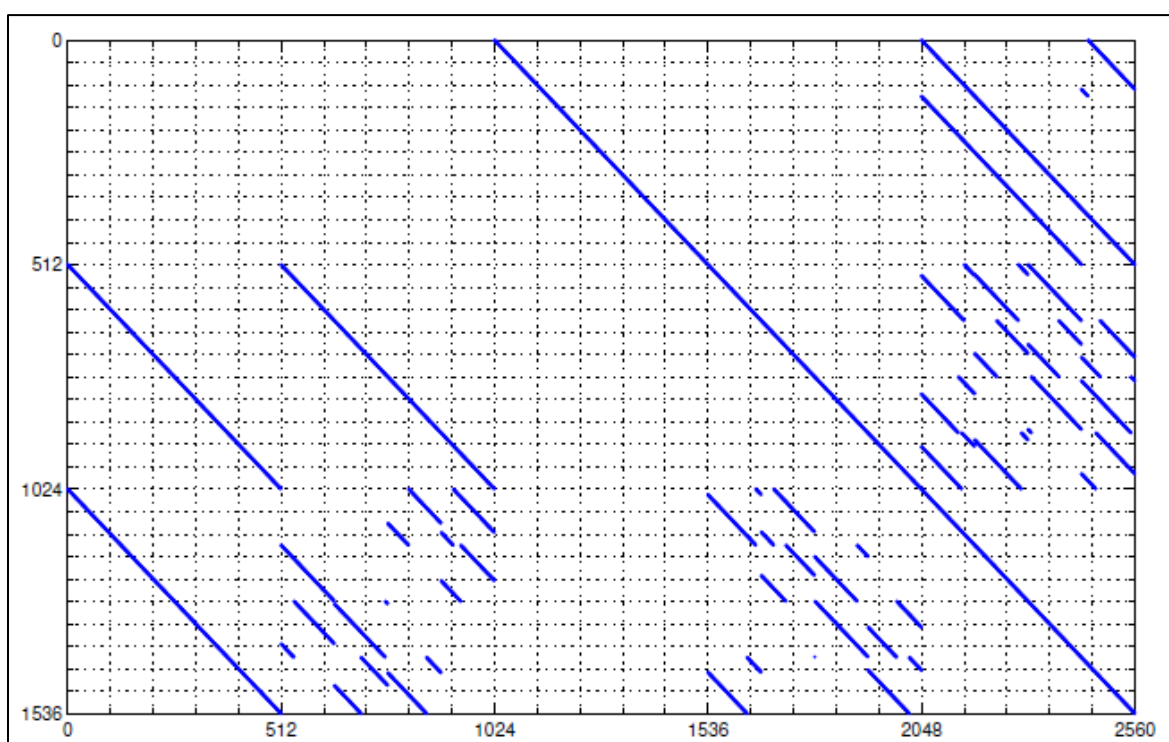


Figure D-1. Parity Check Matrix H for (n=2048, k=1024) Rate 1/2

| k | Θ_k | $\phi_k(0,M)$ | $\phi_k(1,M)$ | $\phi_k(2,M)$ | $\phi_k(3,M)$ |
|-----|------------|---------------|---------------|---------------|---------------|
| 1 | 3 | 108 | 0 | 0 | 0 |
| 2 | 0 | 126 | 375 | 219 | 312 |
| 3 | 1 | 238 | 436 | 16 | 503 |
| 4 | 2 | 481 | 350 | 263 | 388 |
| 5 | 2 | 96 | 260 | 415 | 48 |
| 6 | 3 | 28 | 84 | 403 | 7 |
| 7 | 0 | 59 | 318 | 184 | 185 |
| 8 | 1 | 225 | 382 | 279 | 328 |

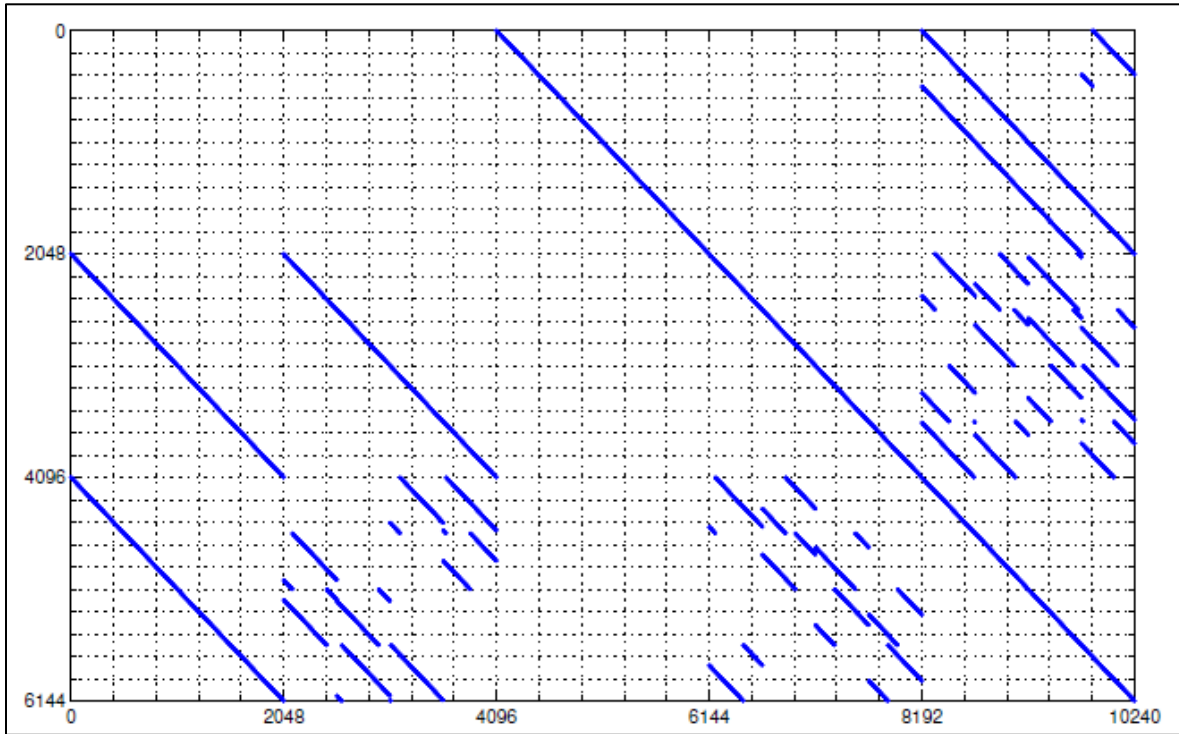


Figure D-2. Parity Check Matrix H for (n=8192, k=4096) Rate 1/2

| k | Θ_k | $\phi_k(0,M)$ | $\phi_k(1,M)$ | $\phi_k(2,M)$ | $\phi_k(3,M)$ |
|-----|------------|---------------|---------------|---------------|---------------|
| 1 | 3 | 59 | 0 | 0 | 0 |
| 2 | 0 | 18 | 32 | 46 | 44 |
| 3 | 1 | 52 | 21 | 45 | 51 |
| 4 | 2 | 23 | 36 | 27 | 12 |
| 5 | 2 | 11 | 30 | 48 | 15 |
| 6 | 3 | 7 | 29 | 37 | 12 |
| 7 | 0 | 22 | 44 | 41 | 4 |
| 8 | 1 | 25 | 29 | 13 | 7 |
| 9 | 0 | 27 | 39 | 9 | 2 |
| 10 | 1 | 30 | 14 | 49 | 30 |
| 11 | 2 | 43 | 22 | 36 | 53 |
| 12 | 0 | 14 | 15 | 10 | 23 |
| 13 | 2 | 46 | 48 | 11 | 29 |
| 14 | 3 | 62 | 55 | 18 | 37 |

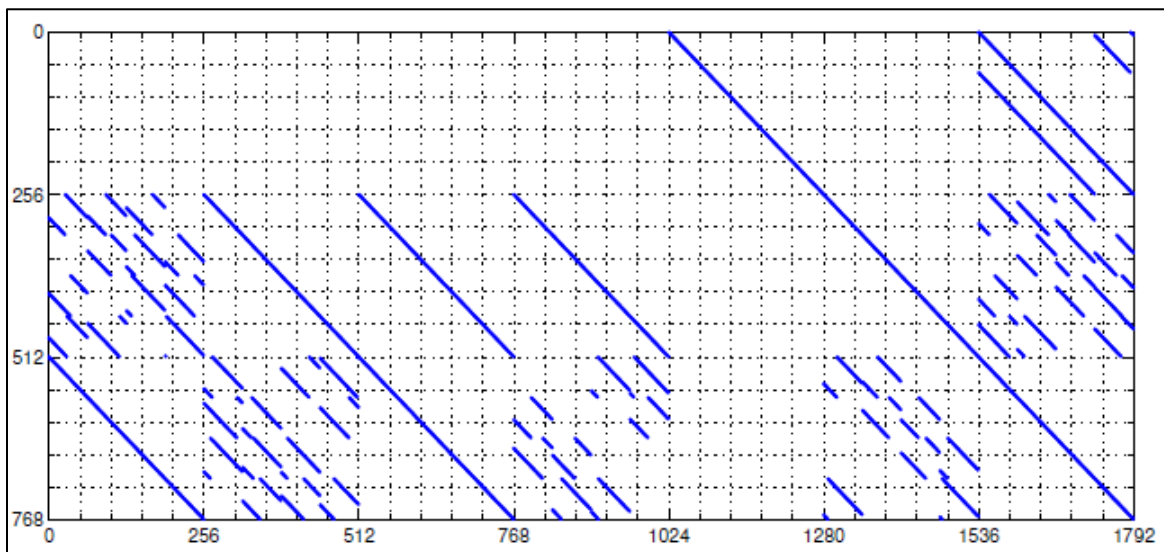


Figure D-3. Parity Check Matrix H for (n=1536, k=1024) Rate 2/3

Code Rate = 2/3, Information Block Size = 4096, $M = 1024$

| k | Θ_k | $\phi_k(0,M)$ | $\phi_k(1,M)$ | $\phi_k(2,M)$ | $\phi_k(3,M)$ |
|-----|------------|---------------|---------------|---------------|---------------|
| 1 | 3 | 160 | 0 | 0 | 0 |
| 2 | 0 | 241 | 182 | 35 | 162 |
| 3 | 1 | 185 | 249 | 167 | 7 |
| 4 | 2 | 251 | 65 | 214 | 31 |
| 5 | 2 | 209 | 70 | 84 | 164 |
| 6 | 3 | 103 | 141 | 206 | 11 |
| 7 | 0 | 90 | 237 | 122 | 237 |
| 8 | 1 | 184 | 77 | 67 | 125 |
| 9 | 0 | 248 | 55 | 147 | 133 |
| 10 | 1 | 12 | 12 | 54 | 99 |
| 11 | 2 | 111 | 227 | 23 | 105 |
| 12 | 0 | 66 | 42 | 93 | 17 |
| 13 | 2 | 173 | 52 | 20 | 97 |
| 14 | 3 | 42 | 243 | 197 | 91 |

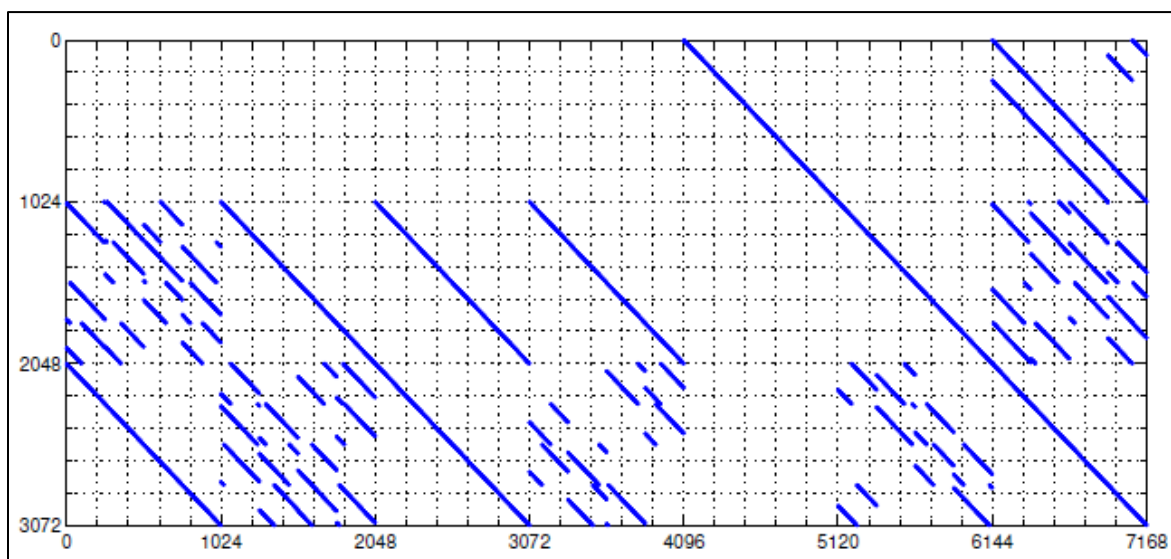


Figure D-4. Parity Check Matrix H for (n=6144, k=4096) Rate 2/3

Code Rate =4/5, Information Block Size = 1024, $M = 128$

| k | Θ_k | $\phi_k(0,M)$ | $\phi_k(1,M)$ | $\phi_k(2,M)$ | $\phi_k(3,M)$ |
|-----|------------|---------------|---------------|---------------|---------------|
| 1 | 3 | 1 | 0 | 0 | 0 |
| 2 | 0 | 22 | 27 | 12 | 13 |
| 3 | 1 | 0 | 30 | 30 | 19 |
| 4 | 2 | 26 | 28 | 18 | 14 |
| 5 | 2 | 0 | 7 | 10 | 15 |
| 6 | 3 | 10 | 1 | 16 | 20 |
| 7 | 0 | 5 | 8 | 13 | 17 |
| 8 | 1 | 18 | 20 | 9 | 4 |
| 9 | 0 | 3 | 26 | 7 | 4 |
| 10 | 1 | 22 | 24 | 15 | 11 |
| 11 | 2 | 3 | 4 | 16 | 17 |
| 12 | 0 | 8 | 12 | 18 | 20 |
| 13 | 2 | 25 | 23 | 4 | 8 |
| 14 | 3 | 25 | 15 | 23 | 22 |
| 15 | 0 | 2 | 15 | 5 | 19 |
| 16 | 1 | 27 | 22 | 3 | 15 |
| 17 | 2 | 7 | 31 | 29 | 5 |
| 18 | 0 | 7 | 3 | 11 | 21 |
| 19 | 1 | 15 | 29 | 4 | 17 |
| 20 | 2 | 10 | 21 | 8 | 9 |
| 21 | 0 | 4 | 2 | 2 | 20 |
| 22 | 1 | 19 | 5 | 11 | 18 |
| 23 | 2 | 7 | 11 | 11 | 31 |
| 24 | 1 | 9 | 26 | 3 | 13 |
| 25 | 2 | 26 | 9 | 15 | 2 |
| 26 | 3 | 17 | 17 | 13 | 18 |

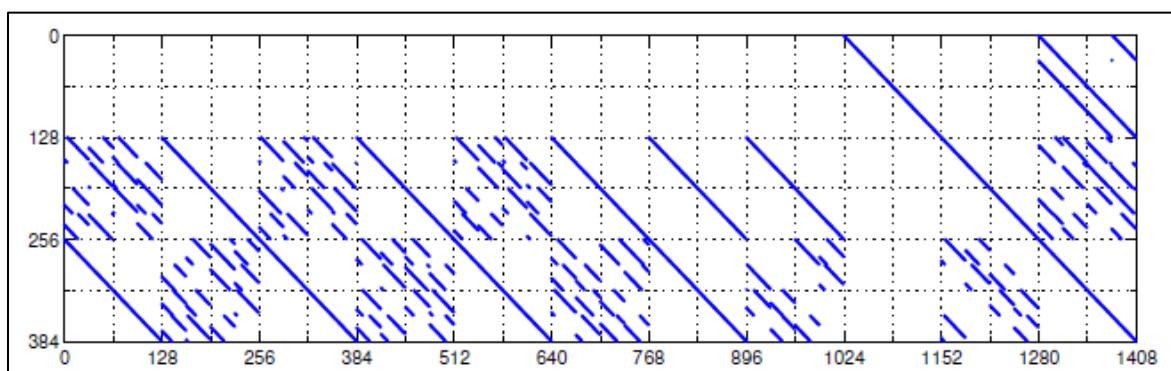


Figure D-5. Parity Check Matrix H for (n=1280, k=1024) Rate 4/5

Code Rate =4/5, Information Block Size = 4096, $M = 512$

| k | Θ_k | $\phi_k(0,M)$ | $\phi_k(1,M)$ | $\phi_k(2,M)$ | $\phi_k(3,M)$ |
|-----|------------|---------------|---------------|---------------|---------------|
| 1 | 3 | 16 | 0 | 0 | 0 |
| 2 | 0 | 103 | 53 | 8 | 35 |
| 3 | 1 | 105 | 74 | 119 | 97 |
| 4 | 2 | 0 | 45 | 89 | 112 |
| 5 | 2 | 50 | 47 | 31 | 64 |
| 6 | 3 | 29 | 0 | 122 | 93 |
| 7 | 0 | 115 | 59 | 1 | 99 |
| 8 | 1 | 30 | 102 | 69 | 94 |
| 9 | 0 | 92 | 25 | 92 | 103 |
| 10 | 1 | 78 | 3 | 47 | 91 |
| 11 | 2 | 70 | 88 | 11 | 3 |
| 12 | 0 | 66 | 65 | 31 | 6 |
| 13 | 2 | 39 | 62 | 19 | 39 |
| 14 | 3 | 84 | 68 | 66 | 113 |
| 15 | 0 | 79 | 91 | 49 | 92 |
| 16 | 1 | 70 | 70 | 81 | 119 |
| 17 | 2 | 29 | 115 | 96 | 74 |
| 18 | 0 | 32 | 31 | 38 | 73 |
| 19 | 1 | 45 | 121 | 83 | 116 |
| 20 | 2 | 113 | 45 | 42 | 31 |
| 21 | 0 | 86 | 56 | 58 | 127 |
| 22 | 1 | 1 | 54 | 24 | 98 |
| 23 | 2 | 42 | 108 | 25 | 23 |
| 24 | 1 | 118 | 14 | 92 | 38 |
| 25 | 2 | 33 | 30 | 38 | 18 |
| 26 | 3 | 126 | 116 | 120 | 62 |

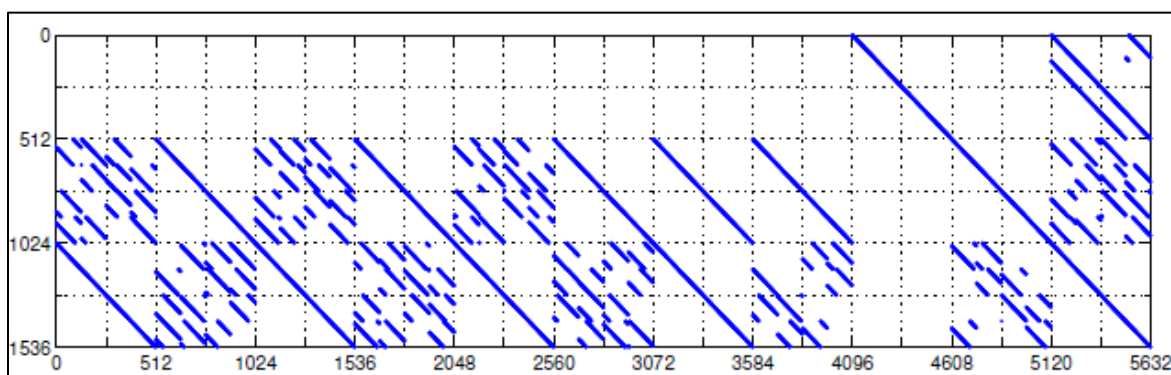


Figure D-6. Parity Check Matrix H for (n=5120, k=4096) Rate 4/5

D.4. Encoding

The recommended method for producing codeblocks consistent with the parity check matrices is to perform matrix multiplication (modulo-2) by block-circulant generator matrices. This family of codes supports rates $K/(K+2)$, where $K=2$ for a rate 1/2 code, $K=4$ for rate 2/3, and

$K=8$ for rate 4/5. Generator matrices, \mathbf{G} , have size $MK \times M(K+3)$ if punctured columns are described in the encoding. (Note: If punctured columns are omitted, as in this case, \mathbf{G} will have a size equal to $MK \times M(K+2)$). [Table D-3](#) lists the size of \mathbf{G} for each information block size and code rate.

| Table D-3. Generator Matrix Sizes | | | |
|--|--|--------------------|--------------------|
| Information Block Length, k | Generator Matrix (\mathbf{G}) Size | | |
| | Rate 1/2 | Rate 2/3 | Rate 4/5 |
| 1024 | 1024×2048 | 1024×1536 | 1024×1280 |
| 4096 | 4096×8192 | 4096×6144 | 4096×5120 |

These generator matrices may be constructed as follows.

1. Let \mathbf{P} be the $3M \times 3M$ submatrix of \mathbf{H} consisting of the last $3M$ columns. Let \mathbf{Q} be the $3M \times MK$ submatrix of \mathbf{H} consisting of the first MK columns.
2. Compute $\mathbf{W}=(\mathbf{P}-\mathbf{1Q})\mathbf{T}$, where the arithmetic is performed modulo-2.
3. Construct the generator matrix $\mathbf{G}=[\mathbf{IMK} \ \mathbf{W}]$ where \mathbf{IMK} is the $MK \times MK$ identity matrix, and \mathbf{W} is a dense matrix of circulants of size $MK \times M(N-K)$. The dimension of \mathbf{W} is $MK \times 2M$.

Because the LDPC code is systematic and the generator matrix \mathbf{G} is block-circulant, an efficient bit-serial encoder can be implemented as shown in [Figure D-7](#). Initially, the binary pattern for the first row of circulants is placed in the shift registers, and the accumulator is set to the length $2M$ zero vector. The contents of the shift registers are added (modulo-2) to the accumulator if the first message bit is a 1, and the shift registers are cyclicly shifted right one place. This is repeated for each subsequent message bit until $m=M/4$ cyclic shifts have been performed. The shift registers are then loaded with binary patterns for the next row of circulants, and the process continues in this manner until all message bits have been encoded.

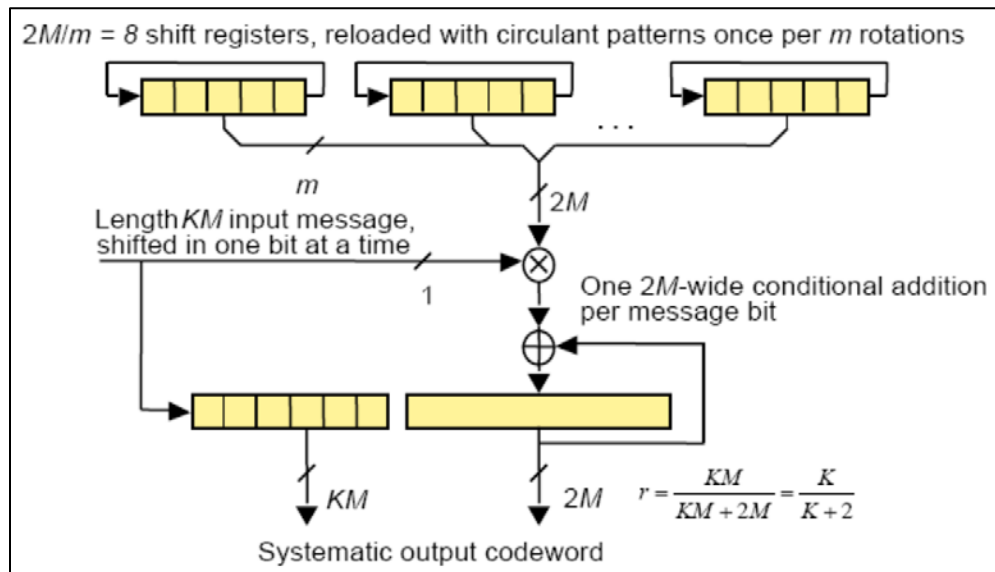


Figure D-7. Quasi-Cyclic Encoder Using Feedback Shift Register

Computing the generator matrix **G** involves inverting a large binary matrix, a computationally demanding task. For convenience, **G** for each information block size and code rate is tabulated here in a compact form.

D.4.a. Code Rate = 1/2, Information Block Size = 1024, $M = 512$

The first 1024 columns of **G** form a 1024×1024 identity matrix and the remaining 1024 columns of **G** form a block matrix composed of 16 rows and 8 columns of circulant matrices, each of size 128×128 . The first row of each circulant is given in hexadecimal format in [Table D-4](#) according to its location in **G**. Subsequent rows of each circulant can be computed by applying the corresponding number of right circular shifts to the first row.

| Table D-4. First Rows of Circulants in Generator Matrix, $r=1/2$, $k=1024$ | |
|---|----------------------------------|
| Row 1 | |
| Columns 1025-1152 | CFA794F49FA5A0D88BB31D8FCA7EA8BB |
| Columns 1153-1280 | A7AE7EE8A68580E3E922F9E13359B284 |
| Columns 1281-1408 | 91F72AE8F2D6BF7830A1F83B3CDBD463 |
| Columns 1409-1536 | CE95C0EC1F609370D7E791C870229C1E |
| Columns 1537-1664 | 71EF3FDF60E2878478934DB285DEC9DC |
| Columns 1665-1792 | 0E95C103008B6BCDD2DAF85CAE732210 |
| Columns 1793-1920 | 8326EE83C1FBA56FDD15B2DDB31FE7F2 |
| Columns 1921-2048 | 3BA0BB43F83C67BDA1F6AEE46AEF4E62 |
| Row 129 | |
| Columns 1025-1152 | 565083780CA89ACAA70CCFB4A888AE35 |
| Columns 1153-1280 | 1210FAD0EC9602CC8C96B0A86D3996A3 |
| Columns 1281-1408 | C0B07FDDA73454C25295F72BD5004E80 |
| Columns 1409-1536 | ACCF973FC30261C990525AA0CBA006BD |
| Columns 1537-1664 | 9F079F09A405F7F87AD98429096F2A7E |
| Columns 1665-1792 | EB8C9B13B84C06E42843A47689A9C528 |
| Columns 1793-1920 | DAAA1A175F598DCFDBAD426CA43AD479 |
| Columns 1921-2048 | 1BA78326E75F38EB6ED09A45303A6425 |
| Row 257 | |
| Columns 1025-1152 | 48F42033B7B9A05149DC839C90291E98 |
| Columns 1153-1280 | 9B2CEBE50A7C2C264FC6E7D674063589 |
| Columns 1281-1408 | F5B6DEAEBF72106BA9E6676564C17134 |
| Columns 1409-1536 | 6D5954558D23519150AAF88D7008E634 |
| Columns 1537-1664 | 1FA962FBAB864A5F867C9D6CF4E087AA |
| Columns 1665-1792 | 5D7AA674BA4B1D8CD7AE9186F1D3B23B |
| Columns 1793-1920 | 047F112791EE97B63FB7B58FF3B94E95 |
| Columns 1921-2048 | 93BE39A6365C66B877AD316965A72F5B |
| Row 385 | |
| Columns 1025-1152 | 1B58F88E49C00DC6B35855BFF228A088 |
| Columns 1153-1280 | 5C8ED47B61EEC66B5004FB6E65CBECF3 |
| Columns 1281-1408 | 77789998FE80925E0237F570E04C5F5B |
| Columns 1409-1536 | ED677661EB7FC3825AB5D5D968C0808C |

| | |
|-------------------|----------------------------------|
| Columns 1537-1664 | 2BDB828B19593F41671B8D0D41DF136C |
| Columns 1665-1792 | CB47553C9B3F0EA016CC1554C35E6A7D |
| Columns 1793-1920 | 97587FEA91D2098E126EA73CC78658A6 |
| Columns 1921-2048 | ADE19711208186CA95C7417A15690C45 |
| Row 513 | |
| Columns 1025-1152 | BE9C169D889339D9654C976A85CFD9F7 |
| Columns 1153-1280 | 47C4148E3B4712DAA3BAD1AD71873D3A |
| Columns 1281-1408 | 1CD630C342C5EBB9183ADE9BEF294E8E |
| Columns 1409-1536 | 7014C077A5F96F75BE566C866964D01C |
| Columns 1537-1664 | E72AC43A35AD216672EBB3259B77F9BB |
| Columns 1665-1792 | 18DA8B09194FA1F0E876A080C9D6A39F |
| Columns 1793-1920 | 809B168A3D88E8E93D995CE5232C2DC2 |
| Columns 1921-2048 | C7CFA44A363F628A668D46C398CAF96F |
| Row 641 | |
| Columns 1025-1152 | D57DBB24AE27ACA1716F8EA1B8AA1086 |
| Columns 1153-1280 | 7B7796F4A86F1FD54C7576AD01C68953 |
| Columns 1281-1408 | E75BE799024482368F069658F7AAAFB0 |
| Columns 1409-1536 | 975F3AF795E78D255871C71B4F4B77F6 |
| Columns 1537-1664 | 65CD9C359BB2A82D5353E007166BDD41 |
| Columns 1665-1792 | 2C5447314DB027B10B130071AD0398D1 |
| Columns 1793-1920 | DE19BC7A6BBCF6A0FF021AABF12920A5 |
| Columns 1921-2048 | 58BAED484AF89E29D4DBC170CEF1D369 |
| Row 769 | |
| Columns 1025-1152 | 4C330B2D11E15B5CB3815E09605338A6 |
| Columns 1153-1280 | 75E3D1A3541E0E284F6556D68D3C8A9E |
| Columns 1281-1408 | E5BB3B297DB62CD2907F09996967A0F4 |
| Columns 1409-1536 | FF33AEEE2C8A4A52FCCF5C39D355C39C |
| Columns 1537-1664 | 5FE5F09ABA6BCCE02A73401E5F87EAC2 |
| Columns 1665-1792 | D75702F4F57670DFA70B1C002F523EEA |
| Columns 1793-1920 | 6CE1CE2E05D420CB867EC0166B8E53A9 |
| Columns 1921-2048 | 9DF9801A1C33058DD116A0AE7278BBB9 |
| Row 897 | |
| Columns 1025-1152 | 4CF0B0C792DD8FDB3ECEAE6F2B7F663D |
| Columns 1153-1280 | 106A1C296E47C14C1498B045D57DEFB5 |
| Columns 1281-1408 | 968F6D8C790263C353CF307EF90C1F21 |
| Columns 1409-1536 | 66E6B632F6614E58267EF096C37718A3 |
| Columns 1537-1664 | 3D46E5D10E993EB6DF81518F885EDA1B |
| Columns 1665-1792 | 6FF518FD48BB8E9DDBED4AC0F4F5EB89 |
| Columns 1793-1920 | BCC64D21A65DB379ABE2E4DC21F109FF |
| Columns 1921-2048 | 2EC0CE7B5D40973D13ECF713B01C6F10 |

D.4.b. Code Rate = 1/2, Information Block Size = 4096, $M = 2048$

The first 4096 columns of \mathbf{G} form a 4096×4096 identity matrix and the remaining 8192 columns of \mathbf{G} form a block matrix composed of 16 rows and 8 columns of circulant matrices,

each of size 512×512 . The first row of each circulant is given in hexadecimal format in [Table D-5](#) according to its location in **G**. Subsequent rows of each circulant can be computed by applying the corresponding number of right circular shifts to the first row.

| Table D-5. First Rows of Circulants in Generator Matrix, $r=1/2$, $k=4096$ | |
|---|--|
| Row 1 | |
| Columns 4097- 4608 | 616DB583006DB99954780CD6DFC9908772D8260D390B1D462A8F62DE8809 216194BE0531EE408AEAF27F50F3AD71865AC7910EEF8824A858CA7B13F C843DAFB1 |
| Columns 4609- 5120 | BA3E0B010860D09066A8632E2B273DABDF90C26FCDD989C2831874EA7F BA23D940A294111C1B0C1CF62F56A376B94CF64FA594B987B19226E52570 4D7F2BC66E |
| Columns 5121- 5632 | 226C671C22A59AC062490596EB1536C9F66AE799C2489FAD2C131E29ED64 A25CB0ADC88D04C5EC8FECD7F78B3825E626858CFAA0DE77772CE8822C 7AA39628A0 |
| Columns 5633- 6144 | 123B1C426E2A93366D067D26DE51362EA0BA916EBD1229521B1B044459B3 25785F3F3E24199B2460151E4CAA9FD26A5DC46BE0D6DA907EFAF38F413 642F702F5 |
| Columns 6145- 6656 | 324AFD5D62F4CC251FF5C0FD95DE0FAB061F0C92CA5BC97F976118AD84 E0663A3BF1B4F07D1CCCC2DF9E09D506B073DED87CC0653C944FC7D438 223C0DF3EB67 |
| Columns 6657- 7168 | E62AE13F8D4000D616E814045495F6E969C473B059386F5DDBCC25F4002E B132D73A98414D85346F55DEBFF875F7CB9D2466A412D180E0A1ADA18D 281376A671 |
| Columns 7169- 7680 | 8EB0FB6BB7B9AD2A2132010511077F6BD424B6F5B578C11D0076B781930F 755EBB72C41ED17519476C257C31C3159BF31FADA2755F1B8A23B22D6A4 28AA290E2 |
| Columns 7681- 8192 | 54CC73C7599AB67C6807C4286BECF8423F3216EF04E1B6DE61349DDB23E 3A0EB0EF70C5BE1AD91D31B0BB532C1098DC619BF80F3853EEA357091C 05D95170A7E |
| Row 513 | |
| Columns 4097- 4608 | 5E6381A718C0A817F8101ECDCDBF825E732E4356CEC42C222DBC476BD70 4837C382B7FBF282B739EDC22B5EEA2909F0EB3ACB9E41FE2AC791130A3 6A9CBFC1D9 |
| Columns 4609- 5120 | D4F8DE28FA77F37E4A6B5A82A58CE917CA74C8397E9DB8EDCB2BF65DB 91954457707FE876DFF812D4B99466DF479A00114F27E702249DB3E9311301 E9CE98703 |
| Columns 5121- 5632 | 74FEAD0013FD861D67D7CE69D3635ECC6266E862D08B63077B45D3098306 EA74159DAEA2263E58705EA5ABE58B7FD41862B9EC1D0F1BD47CD6CB4 2739C24F7FE |
| Columns 5633- 6144 | 7ACFF6D64C8E8F94BEABE280CFDCFCFB26AC7330073C25E0313DCB75E 6C5261F15D82AFA665F73A4B4DA4E5D1648EAB051EDEB9857C13C2F019 FCBBA4F9DF2E1 |
| Columns 6145- 6656 | 9CEFF1147D792C14AA2E211C3B9B94B2C9F24F49B0B1ED6E200C88D743F 5AC1EE283C3A0AC79B9F1F496BDE74A2AA591ACF2F526FB24413A58B49 5F91905F596 |

| | |
|--------------------------|---|
| Columns 6657- 7168 | D8F1469BCA9CC5041C50F1FB479CF2680503AD85BA2C0C6D01D2D739F3 129315E49A9F57236D9585CC0B8A9B4BFE9ADCD97BED9006C33976ACC0 0468693D56FA |
| Columns 7169- 7680 | 1EE66371B0EA6C4E1E172C2C5D76806CB7376B8CDEAD96B14A1EC2B656 298B9425EA2F0671082D70AA23C267D1F215C59239AEB40186DF0AB28462 5DC6BAF45E |
| Columns 7681- 8192 | FBFBEB26BED98BB3B697764A6F82C94039CBF14CB538A7D87801ACBD3A4 44A858BB74F0A4707592EE6B7DC6D21B8F6B4A184B567C8AA4CD825EBF 7F1EDCE015A5 |
| Row 1025 | |
| Columns 4097- 4608 | 25453670647D23C5E445A705953F3BF4A5AF02E7BC46C969C8141D8782F17 1C9CFF7EBB20945DE5D363AD36D3BD5A0BA081C079CDD04B6E5968187 C8A665344A |
| Columns 4609- 5120 | 23E9B1897A6FDF427B5E910AA8D71F9CC6351474BC4563C20FD38953295D 3BA15E7D1010503B7BA1C148251DB8A88AC64E6AF8C1CC056E4EEF1C92 7FEC40C35D |
| Columns 5121- 5632 | 57140969483D9E33429FAFD177D031A43B727CF832C8DFFE8D8960CB55BE 4BE27B69CC26F2FB731B53250D6F8EE7DFDA98812B9AAE9C02AE2FEDE A598D6B6E2F |
| Columns 5633- 6144 | 22B6CCA50541BD9F5D48565E551B310E10A0DFCB8035A5EC86EB9CD8C8 11CDCBCCCEC3732EF93EE8C9418E25CA5744E07C45F9B161E277BCECE3 88B9B84AAEC4 |
| Columns 6145- 6656 | DA37FE277C72CB5CB1BE92AD373867403E46B3535159687ADC79C39DEF7 005C1F11F1CBD5F8877DA66AAC156EF27BB893F5F1132336D52E8AEB60E ACF9BEB3CF |
| Columns 6657- 7168 | D204D92DFA496DAF564272E3FEC51CE53C8F2DF6ACB191E60E14CDEA28 FD5ED0EBE09672ED11A3F6466FE3A967A4EC8390303059AE00DD83102A9 F33B2943E4E |
| Columns 7169- 7680 | 6E56928E7FEE3333A36FF3EE7598744CF7C298FEF3EACC7CCC0F36DCBA6 D87BDD441081163A65E27C958AF79C33A98B81814015E77F82EF5120FBDA B540893B4 |
| Columns 7681- 8192 | 7BEB68CC37F23835C91F5D36D6BA6F0A5E68FEBB6E6A2F247EB5CF57684 D0770249460788DFDC4A1218652BF881B4BB06308EF86484E7070AACC72D 3977CF5D0 |
| Row 1537 | |
| Columns 4097- 4608 | 6230DEF1ACD4425F7B155A2A285CB2A32CB9D46DA09B28167826E77AEB D85F0C416595E136184841451F5B3E1F17D02C3DB32C2AF50091D6376406D 8CB78A9E3 |
| Columns 4609- 5120 | D3B19911ACC450679EAE25B0F290FF372300F1A4BC91A43CB79DB270133 D41DC4970F1420E71C0F816EF938C3C17F0FCBB6E920ED853EAF6D2DC67 92BF87098A |
| Columns 5121- 5632 | B94C2E5DDE78C974AD6F423CD5ACA01EC9420AAF3FE83BEC31D47AAC D3D62FA2476C38595BD66639368181E75B44BAA7ADBC2B42E1D82D7A59 312BB9A16F7D35 |

| | |
|--------------------------|--|
| Columns 5633- 6144 | 0B13B44D828071E69DD90DCD9B713A05FD8C21AA5E6E6D8DA49A5C3B3 4F98A4E5E822513F0DA200235C65BFCA1DC2CE4AB21D146B778F6806680 B8AC75285760 |
| Columns 6145- 6656 | FEF66B861AA67C768A76D585DFADC8EB6556AD841DEA9F44ACB42B601 6142B6B69F1833474FADEB0400CE4D9F3BD62AD96E57F3E93DD229180F2 D4B5E77D098F |
| Columns 6657- 7168 | EEBE2DFA4D4D86ECB07EEE9565FB589855E1F53BA1B9784A8D195A0E37 21551270089C535216636FBEB4D9E50A9EAC3DCB27891A7005A2AD87427 E6B8326F6B3 |
| Columns 7169- 7680 | CA225C7B2A9EABFFDDBBC130B5342917848B029917BA98FFD6EF238900 6A6B417F678C61458EF625C96C0D3D07945ABB9836CF80823EB6244D86D1 14CC5DC2B1 |
| Columns 7681- 8192 | 94F5D55C398B16A71497C4CF102C2F1035C19D5DFC8A301B8DE33D41D90 9C15A3093B09E7489CE6AA14B331B70E76637FE6DDFFFA6DC4C510371C B0D2A6EA3DA |
| Row 2049 | |
| Columns 4097- 4608 | AC5F866DD75CD4C2D5959AC37DE4E1E870313A5B2902F234CD939FE39F3 1FEBF8B46DAC906E3EBA9C3A74DE46E7A9140D3716667BB1EC22A87D5F 8D048BDC5BA |
| Columns 4609- 5120 | 57B6024327CDDFF3296BE6508C48045B71FA519156F8C125F4E3B7356576F 32C63BC588908C4E8B3F9F2D12A9E8F35B6FCF296C17FD8E8D076406FA11 D16175F |
| Columns 5121- 5632 | CC45AE82D672979E8A0A359B2328C79AE61F87EBE04DAC93430305486597 32000CE627417B3F8CFD4A992E7F2B680216AF773385B9337E1743D43FD96 5282CF5 |
| Columns 5633- 6144 | AE71B0CAFEB4DA3E0B95F1341667C519FB9F89D7CEC711E57485F04A965 CDC832CBEC0BE1B2A3E23B5EAF4C5DAD8767E054B2225A60B88BE1DB6 A35E0BAEB237 |
| Columns 6145- 6656 | A206BC721B252D52EA1F8E311203DFF0AE8D65BD1986055701A3C7FEB2D DEDD2D57C3BBA6A2BC56A9157677D7B48AD2907927176F6B22E8A92F6E 9863C9E16D9 |
| Columns 6657- 7168 | 11B6209E06EFE6ACBBBA2214EF5AEAB9D76645476B2C16B8D14E1AE3F3 A85188835922B914D3F32FE05B7987A2516B3D3C8983AE176DFD04349A45 359B422E1E |
| Columns 7169- 7680 | 01CC2266F2B68A4323F8931D7AA37B1CBD70DC2FEE91592327207AA6121 795150A0DC918704A1A293778FE75A99FDCE77E820D0905EF7AC72A682F2 487A6E0FE |
| Columns 7681- 8192 | 03F42D94FDE1C13F958DF61112DB4A27A8A8EF35087FD089729F0864C270 6CCB2B6CBD91A9A7B7B31E08EA3570A6E1BED495FC84FACD829F3234B 1D1DC574B67 |
| Row 2561 | |
| Columns 4097- 4608 | 900AA496432959141795C615CBAEA98002440A0D447EF990435E452CC6902 03BDEBCBA3EEFC7A7CE71EB54B1728AEA9EDE70A7E6A1A8AE8616870 9A899738CCB |

| | |
|--------------------------|--|
| Columns 4609- 5120 | C5B7A094AEBEA8EC95A414A8DE5D3DBE6745CB0D330B78435AC2BB666 6BB2D43A19EAD3B3D9536D0BB92DB949570981C22805E7DEA452FA649C 84EDC4324A7FB |
| Columns 5121- 5632 | E6A9CAF4EE48400720B8F84CAC3A42483B7E571846E2A5F77A983EE31117 9CEC2D99878FF5AA06ACA0CBBA63B36985E0970761E7F837650BC46C9A 2EB1AEFA95 |
| Columns 5633- 6144 | AC4D8AA5C970BB55FDF3408356C9EB2683B6FEE593736B66B49C055BD65 03EEF3C7CADD15C9B86DCA626E1ABF4B971D04C0A9A5AEF8305C3D0E4 CC02C32FA91E |
| Columns 6145- 6656 | D8949EF8FEADF7DA39D395B52D2779A0B305C4FD10C33A434878967D932 1B4835C035CA5802C37F6DC1E39AC30337253114176BBB26576317C72E954 8F179A5A |
| Columns 6657- 7168 | A200FC35B6A0934D57543A60F6114B7B0D78D8DD8932538E545D806A1D9 E47390F092501F4A470CF7B1F9144D0A8F1B0C3D607930A75E5A150233DC EEDB4C10B |
| Columns 7169- 7680 | 217C8EB38D4D2A0EF12557321D504ECA670B41E496441FDE341F0232101D 4E3F4158FF6F4EAECC073AA811DD450F528BC6095868B7BF953926056BD4 09E5FE36 |
| Columns 7681- 8192 | B82831B150B80A736D6CF7B16660ADCD5E1F4DB96E36E33DCC2F1506C7 B8B0F2A4EC362FB0CF7B8B3B08D6CD1AF7440729D4C3C02627AD8733A0 C94B2EBAF526 |
| Row 3073 | |
| Columns 4097- 4608 | FDB4463E6F8FBAF565B1C3320F5704A87309E529842378ECB733784F1CBD 85F4F87FB0525C7C4D307061F74DE2FB3BDFBC77E04EAB75A64FFE51203 AB925E807 |
| Columns 4609- 5120 | 1D1101A16A2C41DBDCA94C128560BEFDA4ECA6F22B44C6E5085A23F841 06E4FD870FAA789E03FC37086E67B69FC8EB6421AA57FBA27866DFF712D 5FEDA21FC51 |
| Columns 5121- 5632 | 76EE3CB2C4A8629C20FC646A7ADF2A4BE73DCEF53FC926067EB9964996 BCEE403C5642CD2F8084E0C14D3627FAD9F0180DADF07331246C007F3AF 95CC9B451CC |
| Columns 5633- 6144 | 3638887EB493F5EE3361F07E00F115BC04AF404BE6BA3467322B37A8E6AB F47710D56C3BC751892CFD12F29CC4319D0562005562D05261D39FDF528A 11E65BBE |
| Columns 6145- 6656 | A0BF07C52E9A9ED7AC3F0FB9196A450E162009509F20BEE74FCC6316BC4 824D93CBAC25E470A7468A629EB520E980DE31F8C8873F4ED21B57AAEB F43A5754359 |
| Columns 6657- 7168 | CD089ABE548975678C2123223CF3F345AE0CECF0A3726BFBB130E34169A 874B6C4CDEFC0A05D7DA1EE475E5407F1535399086700874C13000E2EE21 DF3EEFB65 |
| Columns 7169- 7680 | 4BEF6F2B4137DC6EF197D514E904B8F31BAD6C846D6BD7D7480F4818C3C 57B4C7F53F168E48020273702071EE48EC53422C71C90AA0262982B82BB6F F3100D8A |

| | |
|--------------------------|--|
| Columns 7681- 8192 | EB3E8F033DA73FA82B3B93E50C60E5936A07D3218946588D0EFB39E1A55 C0FB9DBA87DA50C4697EE2ED72B004301019E595B92A2F55F7F1B37C203 0B79057F52 |
| Row 3585 | |
| Columns 4097- 4608 | 59CA13359E16B10A7F8778BBAF5D45E32C643B524022FE777A8F557C1414 1D638E84BC4DBB1CE5866CD0B89C1CC5C6F7BF7E25D2B4FC28A16E67C F8BFAC4F4BD |
| Columns 4609- 5120 | A612F30067700487B6584B1AD578659FC2B7443228B2B7B443882DABBF55 739CB9660F530631A2CFDCBE94D21692CAC01DA9EB5048FFF17BC4FB59 57E8C9DF1F |
| Columns 5121- 5632 | 29E0573D85359FB7924AABBD DCD26F5740FFA6824FCFCBD53BF1DFB5 87E0667641DD3F82962F5E6EA26461279B0F69479645462983DBBBCC544D A90255121EA |
| Columns 5633- 6144 | A97C7B71923F0382DF60C9E34D84CAC289B578899EBCF924F4304B80581C 9887B1198F074143DCC4324D7DF301466AC97903E688DD2E9186EDD2D90 C34202AA3 |
| Columns 6145- 6656 | 90815D489B715FF604788F335322DF5C8856FD85F753785A96F4B2561990F4 58C69D3F99A8ED1BE99C3F5A14B19B37AC729B3F35ABF52006E814B5971 45FA3FD |
| Columns 6657- 7168 | 86A5A2038BB67CF8225BCCF7A587E0D09B47D26BC4DB017F6A77B6DEC5 AF5B117E399D8A336358D4AABE9C8E7EAAF6447638F2DC66EF65C100D0 6EE202013042 |
| Columns 7169- 7680 | AD845A43D23E66FBA72D9D56457D66C7E44D98ED1E5F1D063A5D010439 30E9C2EDED8BA9DEE5F9DFF91CD887F097B9A2DF0099E278C253E0A549 C7A2D81078C6 |
| Columns 7681- 8192 | 680566EA7A1E724A99B5D7099AED278A3065BBC64BED441154DCD346D3 8C9771648D55656B16CF012D0C6EC8F616D3B758089A8147D731AE077D55 7204256F93 |

D.4.c. Code Rate = 2/3, Information Block Size = 1024, $M = 256$

The first 1024 columns of \mathbf{G} form a 1024×1024 identity matrix and the remaining 512 columns of \mathbf{G} form a block matrix composed of 16 rows and 8 columns of circulant matrices, each of size 64×64 . The first row of each circulant is given in hexadecimal format in [Table D-6](#) according to its location in \mathbf{G} . Subsequent rows of each circulant can be computed by applying the corresponding number of right circular shifts to the first row.

| Table D-6. First Rows of Circulants in Generator Matrix, $r=2/3$, $k=1024$ | |
|---|------------------|
| Row 1 | |
| Columns 1025-1088 | 51236781781D416A |
| Columns 1089-1152 | B0C8419FA21559A8 |
| Columns 1153-1216 | 5F14E1E4D88726F1 |
| Columns 1217-1280 | 762F6ED6CF32F06D |
| Columns 1281-1344 | 8ABFD971E17A0BE9 |
| Columns 1345-1408 | A5D147741B698D14 |

| | |
|-------------------|------------------|
| Columns 1409-1472 | 2A58AB30E2BC32D3 |
| Columns 1473-1536 | 9F251FBC5DB8C768 |
| Row 65 | |
| Columns 1025-1088 | D73C205BBEB231CB |
| Columns 1089-1152 | CAB5EFF5B2C76C71 |
| Columns 1153-1216 | FA70FAD48828355F |
| Columns 1217-1280 | 68C6138FA5524A61 |
| Columns 1281-1344 | BB20031D7AA8FE69 |
| Columns 1345-1408 | 432ADE446F49CE27 |
| Columns 1409-1472 | 5E5DB9CCCEBD1326 |
| Columns 1473-1536 | E8782B1B01F2ABA2 |
| Row 129 | |
| Columns 1025-1088 | 4748E9513B41147A |
| Columns 1089-1152 | 17B1FBB78B4F914C |
| Columns 1153-1216 | 281F5680BA56DE50 |
| Columns 1217-1280 | 74B0FB0817E33E2B |
| Columns 1281-1344 | DD166CFB774B5959 |
| Columns 1345-1408 | AC7FDCEA4FECB5BE |
| Columns 1409-1472 | ED747C81B540D66A |
| Columns 1473-1536 | B2A6A2039A87967F |
| Row 193 | |
| Columns 1025-1088 | 4780DCB2DC5CBFAE |
| Columns 1089-1152 | 55BC8FF84EC89440 |
| Columns 1153-1216 | E5D411223F09979F |
| Columns 1217-1280 | DDDE9D940A15A801 |
| Columns 1281-1344 | 194064639D254969 |
| Columns 1345-1408 | 1BE32DDC829B0032 |
| Columns 1409-1472 | 1326515A22EE88A2 |
| Columns 1473-1536 | 0EC664DD2D701891 |
| Row 257 | |
| Columns 1025-1088 | 69748DFE6372F2EF |
| Columns 1089-1152 | 15F3B0D400ACD68A |
| Columns 1153-1216 | CF4144CE1FE2581C |
| Columns 1217-1280 | 79B1A55BA59E54AE |
| Columns 1281-1344 | 65A2B47EEBAB0CF3 |
| Columns 1345-1408 | 24DD87572CB0F71D |
| Columns 1409-1472 | F24ABF15590F4DA6 |
| Columns 1473-1536 | 9C3BAE51969C6502 |
| Row 321 | |
| Columns 1025-1088 | D3A714B60B22789B |
| Columns 1089-1152 | 3DF5504D80F54C5A |
| Columns 1153-1216 | 9D75CF1465031211 |
| Columns 1217-1280 | 09834A0C9F659C99 |
| Columns 1281-1344 | B9241BDF76EB3788 |

| | |
|-------------------|-------------------|
| Columns 1345-1408 | 6F927251C86DECF1 |
| Columns 1409-1472 | 390BE9F5BBB93D05 |
| Columns 1473-1536 | C6F435BFA1FF96B6 |
| Row 385 | |
| Columns 1025-1088 | 222461B658DC3E91 |
| Columns 1089-1152 | B01DF2A2EAD2DAA6 |
| Columns 1153-1216 | 5572EE6278F6F63A |
| Columns 1217-1280 | 17B63CB2FDA3B97F |
| Columns 1281-1344 | B233BB259F3D83F7 |
| Columns 1345-1408 | F64760C774989384 |
| Columns 1409-1472 | 46F57E03F55B1C0B |
| Columns 1473-1536 | 5AC8A6CEA05466C1 |
| Row 449 | |
| Columns 1025-1088 | AE8825521F85CA31 |
| Columns 1089-1152 | 37BEED74B5303407 |
| Columns 1153-1216 | 751FC9A15FCEE486 |
| Columns 1217-1280 | 93F0F69BD04E72A4 |
| Columns 1281-1344 | C0EBFA3F49DF4DBB |
| Columns 1345-1408 | 03E52D815DC99A1D |
| Columns 1409-1472 | 98FE8BF01BB2CD6D |
| Columns 1473-1536 | 009C5290D81A18F6 |
| Row 513 | |
| Columns 1025-1088 | 4FFBAD88545CAA95 |
| Columns 1089-1152 | 0C74659FA4828CA3 |
| Columns 1153-1216 | 60CE56E32DA28B2E |
| Columns 1217-1280 | 299D4BF82FE54B81 |
| Columns 1281-1344 | 51047BE3B3AE4F4B |
| Columns 1345-1408 | F3AC9578B9477A4C |
| Columns 1409-1472 | 3730F81F92767E11 |
| Columns 1473-1536 | 04E84EC3A3AD1F19 |
| Row 577 | |
| Columns 1025-1088 | 2D0E0CAB8EDD2185 |
| Columns 1089-1152 | CEFBEB8F2F538522A |
| Columns 1153-1216 | 92DAEDC22C441893 |
| Columns 1217-1280 | BCB999157B35619D |
| Columns 1281-1344 | 069951BFB90A08E1 |
| Columns 1345-1408 | 54C7E270CBA1656E |
| Columns 1409-1472 | 7FB8B806B6A06FB3 |
| Columns 1473-1536 | 7224943B1C3A5723 |
| Row 641 | |
| Columns 1025-1088 | 1BAA14752EFCEBC0 |
| Columns 1089-1152 | CFF0894975557623 |
| Columns 1153-1216 | FA95908DC3F34D48 |
| Columns 1217-1280 | FECA650999A26E91 |

| | |
|-------------------|------------------|
| Columns 1281-1344 | 245433EBBE9CDA13 |
| Columns 1345-1408 | 5771EAF9B02D8FC |
| Columns 1409-1472 | BCEBCA573D3775C8 |
| Columns 1473-1536 | 1E46F2B951D0EAAB |
| Row 705 | |
| Columns 1025-1088 | 32942F7F4743DDF4 |
| Columns 1089-1152 | 8FA2F60AD62095EF |
| Columns 1153-1216 | 80E4A736B5E1A3A3 |
| Columns 1217-1280 | 0119062872DAEDF4 |
| Columns 1281-1344 | E78006958CD99F95 |
| Columns 1345-1408 | D20625057C99C7A3 |
| Columns 1409-1472 | B569736DE2167610 |
| Columns 1473-1536 | 0E1C6183ADF09FD0 |
| Row 769 | |
| Columns 1025-1088 | E5C492DBB48B319A |
| Columns 1089-1152 | E2D83ADEFEBBDEFE |
| Columns 1153-1216 | AA944EEA53C77DB3 |
| Columns 1217-1280 | 0FAA85D9C13B1F73 |
| Columns 1281-1344 | 8ACED57F3BE4E807 |
| Columns 1345-1408 | 33CB72627624F426 |
| Columns 1409-1472 | A0C6E669B5C74980 |
| Columns 1473-1536 | ABBAEFEA2D3B69AA |
| Row 833 | |
| Columns 1025-1088 | F8366DDAE56A6DDC |
| Columns 1089-1152 | FDED5582F4EA6525 |
| Columns 1153-1216 | 4C9628278ED17036 |
| Columns 1217-1280 | 6E711B6D20A67966 |
| Columns 1281-1344 | 3B28BDF004C21B93 |
| Columns 1345-1408 | 1BC37B730FFC1786 |
| Columns 1409-1472 | 5D20C81D345FE4B9 |
| Columns 1473-1536 | 1D14A5663D369A93 |
| Row 897 | |
| Columns 1025-1088 | 5EBD4BD39B2217D0 |
| Columns 1089-1152 | 56833BE1CDDBA6BC |
| Columns 1153-1216 | B288169B4E3BB726 |
| Columns 1217-1280 | C2ED28FBFC395D1F |
| Columns 1281-1344 | 035B30C68F9A6B6F |
| Columns 1345-1408 | 539836A6E56A7B16 |
| Columns 1409-1472 | CEB1525C6ADB65A5 |
| Columns 1473-1536 | 5F71754AA458B11A |
| Row 961 | |
| Columns 1025-1088 | 0DB9D180B21C0B13 |
| Columns 1089-1152 | 417D86C59DF33E49 |
| Columns 1153-1216 | 183A8F6C44DAFA24 |

| | |
|-------------------|------------------|
| Columns 1217-1280 | 4E224C180C1F0B45 |
| Columns 1281-1344 | C93CD9CA23658555 |
| Columns 1345-1408 | 7DDEC5E9451AD519 |
| Columns 1409-1472 | B122C72A6177EE99 |
| Columns 1473-1536 | 1290B4C6B007D973 |

D.4.d. Code Rate = 2/3, Information Block Size = 4096, $M = 1024$

The first 4096 columns of **G** form a 4096×4096 identity matrix and the remaining 2048 columns of **G** form a block matrix composed of 16 rows and 8 columns of circulant matrices, each of size 256×256 . The first row of each circulant is given in hexadecimal format in [Table D-7](#) according to its location in **G**. Subsequent rows of each circulant can be computed by applying the corresponding number of right circular shifts to the first row.

| Table D-7. First Rows of Circulants in Generator Matrix, $r=2/3$, $k=4096$ | |
|---|--|
| Row 1 | |
| Columns 4097-4352 | 80924F648C014F2C73889C8B87D0491FA9FA060D2902D7ACC8B679CF61EEB5D9 |
| Columns 4353-4608 | 6BB9E90F5C157AA1BF03EF756245D9179063F2CD999EF1E7F7925B3FB7AC7B2D |
| Columns 4609-4864 | 6CD39516B201F491E2BDCA4E34542B5AF3703B3C8EE753FBE998E87323F0B228 |
| Columns 4865-5120 | D1F551B2D7E7822F201E24066584D63CAA00E8DB909EB41C4157EBA0F5C76A50 |
| Columns 5121-5376 | F7C5731746C6DAC260A345189009C0B23372F1E9E0C5A079D00B09158E164B22 |
| Columns 5377-5632 | 33D5F8A268041CAB66317898CD0024E3106EED5C2171B3F6276B8EA59AA981E0 |
| Columns 5633-5888 | 010BFF3F52A49ED9A6FA7F151FCC72B2AF3BD932065043F7447B4D0FC4A2B93B |
| Columns 5889-6144 | F8D345E6D2B0008D1B363BFE296B55AF38E3E16EC5856A122E4931CB3F2424B1 |
| Row 257 | |
| Columns 4097-4352 | A099B776C642FF1D84B0DB797098E17E75FE9BB5CF7FA8739711A89660DAF24D |
| Columns 4353-4608 | 3CA8DE5500F68DB449BFF74251B24E4691EAF386C81014C91AC700298E095F0B |
| Columns 4609-4864 | 12CEE8B5F6B93C11AD628CB6CB81F76BE095C2C994A8BDDB4E2C48C942B4D481 |
| Columns 4865-5120: | 1F7E191B30E8FFD6D4A7E9BEF81BBB0AE6608F647B1AED9CCA7FEC5498C03F0F |
| Columns 5121-5376: | 1132E816BDFA0C3450C3993911E10EB1097CD7A1F32C54C8B009654E56B25A2D |
| Columns 5377-5632: | 5FD58EEAED460CEFC18E2FBAD2954467E32118F01D05456DEA2926A1E761DF76 |

| | |
|-----------------------|---|
| Columns 5633-5888: | 4C6C7BF3A2245C1B4630775DC59EA74A14EBCD8B5D72E343BC6F7FEA 452F2CC2 |
| Columns 5889-6144: | C09CE802B35EBF46D1F3069957DF1D152377F45ADF614CC0F5DAB8FCF 394CCD0 |
| Row 513 | |
| Columns 4097-4352 | FEFBA8CE169FD3775B2280EF3BD870FDDDF7CB95F2943D0EEA84529FF0 D1B1C19 |
| Columns 4353-4608 | 0CA5DB06A87541C81BEF913D5145F20EFAD861F673B32028B4713377C0 56CE97 |
| Columns 4609-4864 | CA3F213365EE380F7E90466945BDE9F44087C8C73A7CC5F9DE71B7683D 018D86 |
| Columns 4865-5120 | A6CDFD8D8117748A4B41C3F5A66765495711EDC02F9581F3E7C2E0FD90 04B03B |
| Columns 5121-5376 | 77D0EF5DE2ACACA2A4371A5B111B877D0EDDF83C3341A5AA51261FA 4B5A0D7EA |
| Columns 5377-5632 | 7C563512A6B73B3B43F8D1D113D751D6B2CABBC350FF0F8C29361DCE5 EB87C8F |
| Columns 5633-5888 | F6DFA5C672C2517931371ACB6462A596D41419CD4F0F84EFF98DCBBE6 10AE03E |
| Columns 5889-6144 | 05FF840FB320DD5C3FB4FE4A5858510914A5161B2AD3C3E7FD02358505 190F0F |
| Row 769 | |
| Columns 4097-4352 | 5B6D534EDE13068A2459CB07007121B0F07B08B8227047C1A629DCA5A4 E30D28 |
| Columns 4353-4608 | 5D00E72E5B6AD57A9F0F9E0608702BDE8BDBFA371C06D96BFE0E60377 5A875CB |
| Columns 4609-4864 | 692EB7DA76BD0D4AFE92FCB5B5184BAA3EEE37900144CA03B7A22EA DE2F061FF |
| Columns 4865-5120 | B3CDE2464AF1212979A99380340974A9F85478E5A2E8B907E74EEFA4CB 7625E5 |
| Columns 5121-5376 | 41AF736E0AA1416EA676E43CF5DFF372CFFC30D6C0A58A333268136A30 20033F |
| Columns 5377-5632 | F50111382FEBA594C255896AB59C06638406956F19B67F80A3A7276060D4 E7F6 |
| Columns 5633-5888 | DCB75287BE9A2620A1F594570B269097A51A32548BAA6DD9B429B8AAF 992C8C0 |
| Columns 5889-6144 | 6210A36B63DE9C732339DC1AFA94CAB475574A6D1C4D0C17F148B8AD 12816B47 |
| Row 1025 | |
| Columns 4097-4352 | E24D7C17BCC46297EDC41AA9B5C9D93689843027C6A78449F8D151E1F4 2BE98F |
| Columns 4353-4608 | 4544BD9E6975DDD4BC9B3EFAD50AFC582CAE269677B130FED2C39D5E BDEE56B8 |
| Columns 4609-4864 | 6A13BB53C03B0C8A4E0D1697322A1A3055054229A69B6CCB7E1FB0B88 5B90CD2 |

| | |
|----------------------|--|
| Columns 4865-5120 | BE5C66B252E5C51D7D9E9E25922566C18F0234F2A330041AEC6A4F2729 A2A30B |
| Columns 5121-5376 | 1E04A65CF0BA05C62B15FEF9967ECD975EC43C035DE4EE6422237F5683 4AC746 |
| Columns 5377-5632 | 4FD0C1AF8A61F56686326F93EF63E2C114D55726A5F74BFD99AE7713DF 2DE6CF |
| Columns 5633-5888 | A9CC4B50995A682C6F6F12C80929FF208C72007D6A253FD36DE363E8EB F2B614 |
| Columns 5889-6144 | 95F6F59DA4CE4BA4D6D4D371A2484F16EFA33CD34F71B81702F0E99C0 31B089D |
| Row 1281 | |
| Columns 4097-4352 | E16A7B75AB838252D1840EF2935AA1CCA5C8470F98202BABA93EEACE 43EE56E1 |
| Columns 4353-4608 | B2D767F35B0F34FCE855B53B6B8DB8DD08BCF47684E904FA47965D7210 7897D1 |
| Columns 4609-4864 | 3D38403A0D2696A767679C6F9CC37537A93A125CE7041EC4F39AD74525 97ED13 |
| Columns 4865-5120 | A0CCD841B7CA93DB6F7039B929A820F55A95AA3786C96E0434DA46A08 4653B1A |
| Columns 5121-5376 | 08A907831A27892D0DD5B6C9FCB5229C0C03663794A4E94E3FB22E4068 ED0EE8 |
| Columns 5377-5632 | 53BCBD15AA8DEC3451CEF53541B04056E4DCA0393836E9B6DFCF9B01 E901D933 |
| Columns 5633-5888 | BD160166307B70BE5618C6E0B4ADEBA46F65C69080D4C3FAADF1AA22 911C2C69 |
| Columns 5889-6144 | 42FB1575074655ABD1EFF5784CBE7FA0B110981C8A0BDF01C650189C2D C9FC74 |
| Row 1537 | |
| Columns 4097-4352 | B403563011DDE16F92630CF312B3F7F495E74B3B582DFB9401F509A35BD 2528C |
| Columns 4353-4608 | A81600F6437FBD00FCF0E4AD41DE3598434EE3903CD1A17CF618E8E2A4 7EBC4C |
| Columns 4609-4864 | A1D7816AE33BA46E3A9D5B3CBDACF93D538802ED0FCCEFF193DB9D6 B79C7E508 |
| Columns 4865-5120 | 54B42DDFAA7DE9B5299F4C1B5DA05487562D20349282F7061E3159E4EA B09D03 |
| Columns 5121-5376 | E15D45F2D1694FF3FF1AA1FC1E58E3FBD6875B71B982AD57AC96CD3B7 BE8ACC6 |
| Columns 5377-5632 | 90CADDAD41374E4BCA29AAB22CAD61989158C474E0725B4C4C5442D6 A12D94D8 |
| Columns 5633-5888 | 2827752CE49CB9C385AD35C1291109892EF85A7A6C043BD8E3BA4AC3D 5146FB7 |
| Columns 5889-6144 | 87002794AC4020B7D229EAE70E01E72F1772B0DA401ABE2C2D487EF607 24DC83 |

| Row 1793 | |
|-------------------|---|
| Columns 4097-4352 | 413A0F58974C76AB4C17AB24F37CB1055FC1827A1DDB0456CCAA7F9477CA64FC |
| Columns 4353-4608 | 904E1D9338D0795C6844F79ED8B26A9D306F66975CE704A925E72EC95509188B |
| Columns 4609-4864 | 2B5EC3212ADF35954F1CDA9CB6CCC28E422F23AF81659F6E4AFDD03E FB8AD730 |
| Columns 4865-5120 | 84D1CCA3B5036F031EEDE0F1121E6F62D232DFB74A0582EB3303D1E98810A6C9 |
| Columns 5121-5376 | 221F0EFC A2C81259B57F8E6943D0CD36088A64DA7FE2E6E7E0F63EAF873B8A79 |
| Columns 5377-5632 | 57E9B39245C6173088B024F34ED7B64F8784413FF95E476474FECDAE7BD62E5A |
| Columns 5633-5888 | 807A807832F6AC83BC7CA7F754BBC7DE72CCC85425068F50ED52419643561832 |
| Columns 5889-6144 | 1B9CF54C055FB01B40740A0D469855292AE8A0C58756BDD3C6DABE268551FD5F |
| Row 2049 | |
| Columns 4097-4352 | DD8CE660B7403DC8672EA620E65301B0865A23FE568C173669EE1D7F7A1BD748 |
| Columns 4353-4608 | 3CCFAC84AB188D906D70525D092C3E2B46C6675C1CF4B30AB346022E43DA20B8 |
| Columns 4609-4864 | A01DC1159652EA260B411971B0E3D0393C1E75AB0EA462E1D07D0847EFA9CFBA |
| Columns 4865-5120 | 4153E6B4F4687D434414BAA200FA38CE46B28D3B4055C633AAD0ED2FACD6B415 |
| Columns 5121-5376 | 5234FA7B72F478A193EC14698C611F3CB70BF72C15E0DCE9CC048A526AC1F46A |
| Columns 5377-5632 | 969C10820390DF8D90AD0138202A32182398B70405520538D08C1F799FBC0755 |
| Columns 5633-5888 | 53D8304A8B5213FF88DD1620B1A5125AF1CC9A07F95C61C5C6C625F64FFCDBE6 |
| Columns 5889-6144 | ED1E06EC959FF323FD3E8AF3553D90BD529D699B08B873F164F59B1CD522AC0F |
| Row 2305 | |
| Columns 4097-4352 | A5C8A02849509DECECFADD4C89C03A78E1564A548D89DECD90DDBCAC7964E9F0 |
| Columns 4353-4608 | 545B207877BBAFB5DED6AEAD3967CA72272E128C97B06868FD3BB85996640432 |
| Columns 4609-4864 | 2995ED49B525D47CE868EFD6FDBB0BB6975DC82C8580D00ABCB9FFC6F532A0CB |
| Columns 4865-5120 | 9F0B1EC3BC16C2E7C94F5149D03677AD039452180B24DA434F5BBAA0BCEE64ED |
| Columns 5121-5376 | 910009CE6C11178F5BC794754EBA72003E9A53CDA988B33CE2D0A0965DAACA23 |

| | |
|----------------------|---|
| Columns 5377-5632 | BF8A7AE5330F4813AE7F8E4F25666EAB3F0351BD34ABBFA8874D88D5F C4E9385 |
| Columns 5633-5888 | 45A0C20F7DFD392872ABDCB19E4F6F097044266B9EA6F0B318A5011D0E 51E735 |
| Columns 5889-6144 | EE58F5FC44AE859564B64F3D173C58FAE938AFB934CBB97245F7B1A1D DD4C559 |
| Row 2561 | |
| Columns 4097-4352 | C7DF1E821B249BE35E6CAB842F3DFCD0141E428141C28BDCF54B09853 29F6E2A |
| Columns 4353-4608 | D8C083075232BDEADEA797B6C9E15606A72B8B48502B1C044BA89A8D BC54EB6E |
| Columns 4609-4864 | 718EF66E726EA72E631B9B22E193F012F3FB2D112468B0DB89F0C3C8A14 3E9B1 |
| Columns 4865-5120 | 7D6BE8EA6A522A10F46EC5A56E3F572586884547536AFFAD0C82A42D88 AAA64B |
| Columns 5121-5376 | 0B740E17EEF10A800DE1916C291C1535845114313E908D313B58018EB77 DED61 |
| Columns 5377-5632 | 9A5F7429731308EFAB68D1725D8F9501234F9035869415A62262095D77A9 613A |
| Columns 5633-5888 | 9BDCBC26ABDE4672BE5F130E1089BE8BF5CA0ED3FCD9F28B75CC07E9 822AA2EF |
| Columns 5889-6144 | 6AC735D6621C86CEA203E9E1FC993207EDC164396C7C8FF227F92979A3 13914D |
| Row 2817 | |
| Columns 4097-4352 | 8E1D4E308C03F66D73D76A715F859BEDBC8D709D4BEFC1558D74B4986 0A90ABA |
| Columns 4353-4608 | B67C75041BFB3A61BBBB73DE2B3D7BB5CB254F10257495E3185C71C35 59D9CD0 |
| Columns 4609-4864 | ACB7A163EB1E088624F946909B29B2C7373C5CF4F6B1F3A75DC49B1574 B3AAB8 |
| Columns 4865-5120 | 327C55142CE3D1382EA917A7C6730E01BA6BA43767D53E84FFB7D61D6 EAD24AD |
| Columns 5121-5376 | CFAAC26024A1D642C795400B8646533A435A4FE899704FAFAE2BF452B D9AF093 |
| Columns 5377-5632 | 53759538B5F4A8614F1AB4840CFC1EFD8CAFCB067C991FDF2658ABA23 F8B0B93 |
| Columns 5633-5888 | 6B3A35CDECD26C58B9F1318AF46F13767758FC0F74B7DD050A9B1A1C7 F98B930 |
| Columns 5889-6144 | 4B4C20D040F3A8C746453ECE10C0A1F4F74BDDDB1A8FCFE1DE2C19148 A5E88F1C |
| Row 3073 | |
| Columns 4097-4352 | A98B4DE68DDB2434893BEF8F2CF8DB584CEE8F0E39D30CD4C87017E7E E6886F8 |
| Columns 4353-4608 | 23024E83F777D7DF0D7E46A8B5F9B1331D0BC2F79BF5559C3241D5BDC7 E7A665 |

| | |
|----------------------|--|
| Columns 4609-4864 | 9E1DD50373C16CC97A5E390921B471EF5B39731CCC2CBDD08876080680F9D974 |
| Columns 4865-5120 | 9DF22EE3AB758F85FD490012FCFF20B3329A5648D25859036C0586C65F46236C |
| Columns 5121-5376 | B009BA2650ABAF45653D61D2BFA255DE767D0B25AC7736E8E5200D21EE3E28F |
| Columns 5377-5632 | FD96F63D0A22CD574ED61899ECDEB4BEB333F994AC7791FF89EC600B857D4DDD |
| Columns 5633-5888 | C2773C7DCE36709F70180CFFAE22AD44A4A20211224F8ECFB336A54A681A1F59 |
| Columns 5889-6144 | 5C00C419C78A79ADA49562EFB784ECE44BAF45C1E75BD84DE7C1C69100F8B93A |
| Row 3329 | |
| Columns 4097-4352 | DAB0C7C65F0D096351BF8A0EE9CEF5F7756A9A47B4EE80420DEFA16B0E74CF18 |
| Columns 4353-4608 | 0FAB86E762595261852E38F9D797D4F796DA18169AFAC99E8235D4DD6C2BB887 |
| Columns 4609-4864 | 15D0F65E9ADB2C67A887E5D8EF4E1080AC968F4C0D673CA7A74759A7F1B4E383 |
| Columns 4865-5120 | 1B5641CE5FADE005EB947BE5E20E7DDAF6372655825B3516F2EC5B36D687895F |
| Columns 5121-5376 | 2C0BB35E3C3EDA32C19BFF6F3A2397A8E25C646059359D90A1372FCAEE250A43 |
| Columns 5377-5632 | 8AABBF162C4499F2FECFA27F8D7582FB607B88D04F4A6100A3D2F8A88A2E5E80 |
| Columns 5633-5888 | D9C26C2A023943BC62F3C18658A0F5C64130BFF0D74BBB85EBFFFE197C94C6EC |
| Columns 5889-6144 | 0AED385393F69FA9F7E69DDC061B85E4E77D0BE2013061E94A0DB8AC2995096F |
| Row 3585 | |
| Columns 4097-4352 | 775369B59AA940DA96B47429C339536B51ECC59C60BAD762FA275A6A8F90885A |
| Columns 4353-4608 | 922A84AE2B06B4003C0A7BE22FB211365376C3FBFC03EB0DEA264F6769B57EE2 |
| Columns 4609-4864 | E518ED3DD8553DC8815E57F23DADC1A3E99030AA02A3529604EE4BD66D770F8E |
| Columns 4865-5120 | 8AB3C94077F85772647897A76CFE4EC56FCAA7A28968065CC73BDD88ADA4D60C |
| Columns 5121-5376 | 9430F05CFEF8ACBBA73038463A9AD3BDE5BA4E94FDA81C6C51AB3C69201906E1 |
| Columns 5377-5632 | 2613EFCF235670383ED865C6161C8A8958DC09289EA03658376277BE6E4E62AA |
| Columns 5633-5888 | 3C90B273B9870A069FE0F5164AA8F837B9905EEE7D3AEB794BA2F4CAA4F1EB01 |

| | |
|----------------------|--|
| Columns 5889-6144 | 01C2973BD37D564B7D21243A206BD8A7B435428BA8DD3DB7045541BCC E000F5F |
| Row 3841 | |
| Columns 4097-4352 | CEA89305914BEB1BE84B59A4A18CC1AEB5CC96326ADC69F3B4957198 C60BB6E7 |
| Columns 4353-4608 | DB38C42E2947EFC39D2BBFA07C18C320A22C7B9C6CBFB72E6909BDC1 31B2E15E |
| Columns 4609-4864 | ABECA69DD1395554C852ED7EE6817A6152B39B42F6D7D56B781D1803B 8307C79 |
| Columns 4865-5120 | 386FFC16B79E309255E7D5933870D116DE3828C68348493D8E288C8A3FB F741F |
| Columns 5121-5376 | 0936252D32CDEC49ACFE91F2BA885044E0A9ADFEA526F53641F97B8666 8C5972 |
| Columns 5377-5632 | F9D8560A97AFA4282DBCC4250B75A871276434FFA80959F04D3400D819 37617D |
| Columns 5633-5888 | 799C3EDF3F1345908B306D8372A740E96707761FCCA9B861402134AE948 8387F |
| Columns 5889-6144 | F2DA86FE2BAA7E675DFDED45499AF1B40AE292B1DE6B7A7D4799C3B 88177704D |

D.4.e. Code Rate =4/5, Information Block Size = 1024, $M = 128$

The first 1024 columns of **G** form a 1024×1024 identity matrix and the remaining 256 columns of **G** form a block matrix composed of 32 rows and 8 columns of circulant matrices, each of size 32×32 . The first row of each circulant is given in hexadecimal format in [Table D-8](#) according to its location in **G**. Subsequent rows of each circulant can be computed by applying the corresponding number of right circular shifts to the first row.

| Table D-8. First Rows of Circulants in Generator Matrix, $r=4/5$, $k=1024$ | |
|---|----------|
| Row 1 | |
| Columns 1025-1056 | 678ECB51 |
| Columns 1057-1088 | FE821D5C |
| Columns 1089-1120 | FA5F424B |
| Columns 1121-1152 | F55927AA |
| Columns 1153-1184 | 3E826913 |
| Columns 1185-1216 | 32E04B0C |
| Columns 1217-1248 | 4F88862B |
| Columns 1249-1280 | 803432EF |
| Row 33 | |
| Columns 1025-1056 | 42B27625 |
| Columns 1057-1088 | 9F8DA1E1 |
| Columns 1089-1120 | F8472D1B |
| Columns 1121-1152 | D943D394 |
| Columns 1153-1184 | 29261575 |

| | |
|-------------------|----------|
| Columns 1185-1216 | BA434C68 |
| Columns 1217-1248 | 18EF349A |
| Columns 1249-1280 | 27CA1CC4 |
| Row 65 | |
| Columns 1025-1056 | EC900397 |
| Columns 1057-1088 | 64A4A063 |
| Columns 1089-1120 | 9BCEC4A6 |
| Columns 1121-1152 | D05BA70F |
| Columns 1153-1184 | E7155BE1 |
| Columns 1185-1216 | 7FF09CC1 |
| Columns 1217-1248 | 6E2E2059 |
| Columns 1249-1280 | 7F1567E5 |
| Row 97 | |
| Columns 1025-1056 | 5616101C |
| Columns 1057-1088 | EA060E2B |
| Columns 1089-1120 | B673068B |
| Columns 1121-1152 | 923BDF8B |
| Columns 1153-1184 | B9B9343D |
| Columns 1185-1216 | 049C63A8 |
| Columns 1217-1248 | 333E9CFE |
| Columns 1249-1280 | 809B362D |
| Row 129 | |
| Columns 1025-1056 | 9D41634C |
| Columns 1057-1088 | 404E17DA |
| Columns 1089-1120 | 3B4161F2 |
| Columns 1121-1152 | 5235992E |
| Columns 1153-1184 | EA4B4B8B |
| Columns 1185-1216 | 4690BCE1 |
| Columns 1217-1248 | F9DA36A1 |
| Columns 1249-1280 | 16439BB1 |
| Row 161 | |
| Columns 1025-1056 | 5D7254B5 |
| Columns 1057-1088 | 15B4978B |
| Columns 1089-1120 | 00D05224 |
| Columns 1121-1152 | 107BD904 |
| Columns 1153-1184 | C85D7E58 |
| Columns 1185-1216 | 0451F1A5 |
| Columns 1217-1248 | EE9D1897 |
| Columns 1249-1280 | 913DA6F9 |
| Row 193 | |
| Columns 1025-1056 | 42819F61 |
| Columns 1057-1088 | 343773CA |
| Columns 1089-1120 | 11A6492A |
| Columns 1121-1152 | 4832F43F |

| | |
|-------------------|----------|
| Columns 1153-1184 | 849C11ED |
| Columns 1185-1216 | F0FE864F |
| Columns 1217-1248 | CC270400 |
| Columns 1249-1280 | 9726D66E |
| Row 225 | |
| Columns 1025-1056 | 89EE2A44 |
| Columns 1057-1088 | 685C1F67 |
| Columns 1089-1120 | 1DF6E416 |
| Columns 1121-1152 | 507BF2EF |
| Columns 1153-1184 | 8759C2FB |
| Columns 1185-1216 | 52162ABF |
| Columns 1217-1248 | 2B61D3FB |
| Columns 1249-1280 | 988708C4 |
| Row 257 | |
| Columns 1025-1056 | 4A8FEA09 |
| Columns 1057-1088 | 53452354 |
| Columns 1089-1120 | A33E2E73 |
| Columns 1121-1152 | 271E8211 |
| Columns 1153-1184 | 16DF62E5 |
| Columns 1185-1216 | 03DF81F4 |
| Columns 1217-1248 | 8848BD0F |
| Columns 1249-1280 | F95DF357 |
| Row 289 | |
| Columns 1025-1056 | 9BE0A7B3 |
| Columns 1057-1088 | 617256EB |
| Columns 1089-1120 | 9A4D0BB4 |
| Columns 1121-1152 | FE3A3A19 |
| Columns 1153-1184 | FAA63D9E |
| Columns 1185-1216 | 65328918 |
| Columns 1217-1248 | D699BA35 |
| Columns 1249-1280 | 4CDE6FE0 |
| Row 321 | |
| Columns 1025-1056 | 848B1FE5 |
| Columns 1057-1088 | 0AB58A6F |
| Columns 1089-1120 | 341707F1 |
| Columns 1121-1152 | EF36474B |
| Columns 1153-1184 | F623A7A5 |
| Columns 1185-1216 | A35EC9BA |
| Columns 1217-1248 | 24909B6E |
| Columns 1249-1280 | 64A7A898 |
| Row 353 | |
| Columns 1025-1056 | BDDF3BAE |
| Columns 1057-1088 | 7202FA26 |
| Columns 1089-1120 | 86F90C57 |

| | |
|-------------------|----------|
| Columns 1121-1152 | A0399F20 |
| Columns 1153-1184 | 972B9A31 |
| Columns 1185-1216 | 87B245AE |
| Columns 1217-1248 | E0C5A338 |
| Columns 1249-1280 | 4959AAD9 |
| Row 385 | |
| Columns 1025-1056 | CF726C27 |
| Columns 1057-1088 | 7B38429A |
| Columns 1089-1120 | BA37C244 |
| Columns 1121-1152 | EE7717DB |
| Columns 1153-1184 | E45C99CA |
| Columns 1185-1216 | 7E3E013B |
| Columns 1217-1248 | 7B800CA4 |
| Columns 1249-1280 | 6527F2E7 |
| Row 417 | |
| Columns 1025-1056 | 75C63782 |
| Columns 1057-1088 | 1CC40137 |
| Columns 1089-1120 | 51E69F16 |
| Columns 1121-1152 | 414B155F |
| Columns 1153-1184 | DF1964DE |
| Columns 1185-1216 | F13C71F7 |
| Columns 1217-1248 | 6E9E8044 |
| Columns 1249-1280 | 6C5CEC86 |
| Row 449 | |
| Columns 1025-1056 | 6F2A6DF8 |
| Columns 1057-1088 | 9FF2BF82 |
| Columns 1089-1120 | D3625355 |
| Columns 1121-1152 | 24466981 |
| Columns 1153-1184 | D5F14AC1 |
| Columns 1185-1216 | E1C24AEA |
| Columns 1217-1248 | A8850D83 |
| Columns 1249-1280 | 7A3C5120 |
| Row 481 | |
| Columns 1025-1056 | BAABADC3 |
| Columns 1057-1088 | 1ECF066D |
| Columns 1089-1120 | 76538348 |
| Columns 1121-1152 | FC5D4D54 |
| Columns 1153-1184 | 43AD46CF |
| Columns 1185-1216 | 3342012C |
| Columns 1217-1248 | 63EBE2DC |
| Columns 1249-1280 | D832EF8E |
| Row 513 | |
| Columns 1025-1056 | E6EC82F1 |
| Columns 1057-1088 | 4AAFE782 |

| | |
|-------------------|----------|
| Columns 1089-1120 | 14D89E38 |
| Columns 1121-1152 | 23C83402 |
| Columns 1153-1184 | 8B48D6BF |
| Columns 1185-1216 | C823B89A |
| Columns 1217-1248 | 68A35626 |
| Columns 1249-1280 | E89FE121 |
| Row 545 | |
| Columns 1025-1056 | 4BBAA331 |
| Columns 1057-1088 | 20EC16C9 |
| Columns 1089-1120 | 6ADABE06 |
| Columns 1121-1152 | D803DA6D |
| Columns 1153-1184 | FCC89D41 |
| Columns 1185-1216 | E57B10E8 |
| Columns 1217-1248 | CC3FF014 |
| Columns 1249-1280 | 4DB74206 |
| Row 577 | |
| Columns 1025-1056 | 503FD586 |
| Columns 1057-1088 | 52F68B91 |
| Columns 1089-1120 | 97D69DF3 |
| Columns 1121-1152 | 129C764E |
| Columns 1153-1184 | 8B2143F7 |
| Columns 1185-1216 | A36EF3BA |
| Columns 1217-1248 | 7C27896C |
| Columns 1249-1280 | 560F67B5 |
| Row 609 | |
| Columns 1025-1056 | D70390E6 |
| Columns 1057-1088 | 98B337EA |
| Columns 1089-1120 | 89568363 |
| Columns 1121-1152 | 2A1681DF |
| Columns 1153-1184 | 4B4E928C |
| Columns 1185-1216 | 41EC3D9C |
| Columns 1217-1248 | DFD92EB2 |
| Columns 1249-1280 | A5D5C85C |
| Row 641 | |
| Columns 1025-1056 | 2A5088BD |
| Columns 1057-1088 | 76CB6810 |
| Columns 1089-1120 | CB693D21 |
| Columns 1121-1152 | C0E9EFD5 |
| Columns 1153-1184 | F992506E |
| Columns 1185-1216 | 299CE082 |
| Columns 1217-1248 | 901155A6 |
| Columns 1249-1280 | 0B93AA16 |
| Row 673 | |
| Columns 1025-1056 | 18FEFECE |

| | |
|-------------------|----------|
| Columns 1057-1088 | B0063536 |
| Columns 1089-1120 | 95487089 |
| Columns 1121-1152 | 4BB31BB9 |
| Columns 1153-1184 | 66F3FD97 |
| Columns 1185-1216 | E32B58A0 |
| Columns 1217-1248 | 2A39427A |
| Columns 1249-1280 | 5CD8DE9F |
| Row 705 | |
| Columns 1025-1056 | 1A8F8616 |
| Columns 1057-1088 | C5F7D2B2 |
| Columns 1089-1120 | 5AD2BC4E |
| Columns 1121-1152 | BF1E86DB |
| Columns 1153-1184 | ACF7BFFA |
| Columns 1185-1216 | F3589597 |
| Columns 1217-1248 | A777654C |
| Columns 1249-1280 | 12DD1364 |
| Row 737 | |
| Columns 1025-1056 | FFC03A59 |
| Columns 1057-1088 | DC450527 |
| Columns 1089-1120 | 33B4C871 |
| Columns 1121-1152 | BAA2EA33 |
| Columns 1153-1184 | 93A751A6 |
| Columns 1185-1216 | F9D72E4D |
| Columns 1217-1248 | 69B50C7F |
| Columns 1249-1280 | F74151F9 |
| Row 769 | |
| Columns 1025-1056 | 7BE8519D |
| Columns 1057-1088 | AF6FFAFA |
| Columns 1089-1120 | 268DBA73 |
| Columns 1121-1152 | A356128C |
| Columns 1153-1184 | 0418BE2C |
| Columns 1185-1216 | 1A43465A |
| Columns 1217-1248 | 60C6DF65 |
| Columns 1249-1280 | 0E2438A0 |
| Row 801 | |
| Columns 1025-1056 | EC25DC05 |
| Columns 1057-1088 | 66AEE4A8 |
| Columns 1089-1120 | A72A030A |
| Columns 1121-1152 | B11FB610 |
| Columns 1153-1184 | DD74DAF7 |
| Columns 1185-1216 | 62F6D565 |
| Columns 1217-1248 | 554EAEB7 |
| Columns 1249-1280 | 15F7AE6C |

| Row 833 | |
|-------------------|----------|
| Columns 1025-1056 | 5147F90A |
| Columns 1057-1088 | FF0EEC01 |
| Columns 1089-1120 | 12A9966C |
| Columns 1121-1152 | 871705B1 |
| Columns 1153-1184 | E935FF30 |
| Columns 1185-1216 | 46E32957 |
| Columns 1217-1248 | 546D69FC |
| Columns 1249-1280 | B8A1BD06 |
| Row 865 | |
| Columns 1025-1056 | 6A80EA6F |
| Columns 1057-1088 | 71A29506 |
| Columns 1089-1120 | EF78AACF |
| Columns 1121-1152 | 8D52B5ED |
| Columns 1153-1184 | 9F0A4966 |
| Columns 1185-1216 | 61B3B68E |
| Columns 1217-1248 | 4B17AF96 |
| Columns 1249-1280 | 5B282C2E |
| Row 897 | |
| Columns 1025-1056 | 75582272 |
| Columns 1057-1088 | 16E54299 |
| Columns 1089-1120 | 7D070B9C |
| Columns 1121-1152 | AB130157 |
| Columns 1153-1184 | 76C619D2 |
| Columns 1185-1216 | 5500E2D5 |
| Columns 1217-1248 | 1F980459 |
| Columns 1249-1280 | 5D9C7F83 |
| Row 929 | |
| Columns 1025-1056 | 6A0DDA1D |
| Columns 1057-1088 | F6E8B610 |
| Columns 1089-1120 | 25D0E0A1 |
| Columns 1121-1152 | 242749E0 |
| Columns 1153-1184 | FEDA4A06 |
| Columns 1185-1216 | 072D69D6 |
| Columns 1217-1248 | 03C7DA79 |
| Columns 1249-1280 | 51AA3355 |
| Row 961 | |
| Columns 1025-1056 | 6E9FEFF0 |
| Columns 1057-1088 | 0797CBF1 |
| Columns 1089-1120 | E936C824 |
| Columns 1121-1152 | C9C1EAF5 |
| Columns 1153-1184 | D4607E46 |
| Columns 1185-1216 | 88ED7B0E |
| Columns 1217-1248 | 92E160AD |

| | |
|-------------------|----------|
| Columns 1249-1280 | 731140AD |
| Row 993 | |
| Columns 1025-1056 | 32FEFCAF |
| Columns 1057-1088 | 70863B75 |
| Columns 1089-1120 | 3846F110 |
| Columns 1121-1152 | C4E23DFF |
| Columns 1153-1184 | 79D3F753 |
| Columns 1185-1216 | 064648FA |
| Columns 1217-1248 | 830452F5 |
| Columns 1249-1280 | B9ED8445 |

D.4.f. Code Rate =4/5, Information Block Size = 4096, $M = 512$

The first 4096 columns of **G** form a 4096×4096 identity matrix and the remaining 1024 columns of **G** form a block matrix composed of 32 rows and 8 columns of circulant matrices, each of size 128×128 . The first row of each circulant is given in hexadecimal format in [Table D-9](#) according to its location in **G**. Subsequent rows of each circulant can be computed by applying the corresponding number of right circular shifts to the first row.

| Table D-9. First Rows of Circulants in Generator Matrix, $r=4/5$, $k=4096$ | |
|---|----------------------------------|
| Row 1 | |
| Columns 4097-4224 | 473BC533A12C3596F642673D0DBF1142 |
| Columns 4225-4352 | 079A3868E1A6F556F0DF3DCA4493AE54 |
| Columns 4353-4480 | AE4C50F12AEF6EEDEA9BB30605F4A24C |
| Columns 4481-4608 | B0B2B4B9035331ABF53DE4752E7EDABF |
| Columns 4609-4736 | E7E08EF3E22EE7EFE645E9E59507A206 |
| Columns 4737-4864 | 52E4A2C06270B2D1A418134BC0D58678 |
| Columns 4865-4992 | 0A84E53303F4092DB47056AD3C0847AD |
| Columns 4993-5120 | 2DEF73813B17101E79A3A58A7E91C4E2 |
| Row 129 | |
| Columns 4097-4224 | 667AA815610234DBA0FFA951CABB8BA7 |
| Columns 4225-4352 | A3271642E4BCDD24F8D89BD783317ABB |
| Columns 4353-4480 | CC64FA95F06AE45C7E38935D78BF5F80 |
| Columns 4481-4608 | 510CE9ABC6156F008B317C79E0122B09 |
| Columns 4609-4736 | 3CB09E20016A5F93E207C144E889F3B9 |
| Columns 4737-4864 | AE6185E4345C5971E03AD499EF850D33 |
| Columns 4865-4992 | FA8B392CE78B5712290CB2F518F3E0CC |
| Columns 4993-5120 | 429C39F0915EB60CA0545B6AB2967149 |
| Row 257 | |
| Columns 4097-4224 | FE9FF6C26898CB926F9BCD129AA52083 |
| Columns 4225-4352 | 3FC159DB58B64D39CB27847434F177E2 |
| Columns 4353-4480 | E040D71365D96A1D54FD20051D3A50E7 |
| Columns 4481-4608 | E8AC736B6D2BB5468FBF68DDF5789C2F |
| Columns 4609-4736 | 4954E4153CFF0F52F8F8F5B243A03E2B |

| | |
|-------------------|-----------------------------------|
| Columns 4737-4864 | 99A1DDD23204D103E323158E0FEE7673 |
| Columns 4865-4992 | 43C2A07046BA1B4307BA6CEC7D740CFE |
| Columns 4993-5120 | CB4E113F94C6CAA4652EFD867B43D199 |
| Row 385 | |
| Columns 4097-4224 | 081E779BF01F34C97337A3ABC8698644 |
| Columns 4225-4352 | 9C9E794155E27547283C1AB2706A388D |
| Columns 4353-4480 | FB9DFD194731EC2AE99EA6B641B309A2 |
| Columns 4481-4608 | 258D45A1BBEAFFC787E61289A54A2473 |
| Columns 4609-4736 | FDF3E96C7679E979911C4BE65A333250 |
| Columns 4737-4864 | 178259F846AA95577C2EC448EE709423 |
| Columns 4865-4992 | A61BE7CCED0342965CA234AF02914916 |
| Columns 4993-5120 | E045B3C585714F272D40C8085AE5E8F4 |
| Row 513 | |
| Columns 4097-4224 | 7FB352B26E544BDC18D76B323C3CE1BB |
| Columns 4225-4352 | 8421967EE08A6F719B675F06F13FF05B |
| Columns 4353-4480 | 672C29DC5B80E18E2F4C42D0F6D5D6D4 |
| Columns 4481-4608 | 7DE072F73A8015862A275B2CEA2FFC1C |
| Columns 4609-4736 | 284B87ABA22362D98952442BBDFBF4A3 |
| Columns 4737-4864 | 2B798BCD5D8C0B02BBE5DE4A96569F99 |
| Columns 4865-4992 | 409E72F4138595F8B3C14074BD8E33E0 |
| Columns 4993-5120 | 3B07838358BBAE631C8258D6B07D2E1C |
| Row 641 | |
| Columns 4097-4224 | 403149A1C88E4D4893FE719B2638B7FF |
| Columns 4225-4352 | 9886F3E90FC018699F3B39183F2219DC |
| Columns 4353-4480 | F5B0D3AA451225867913FF8FF979BBE0 |
| Columns 4481-4608 | 795DFCBCC98210C028FD21380EBDDABF |
| Columns 4609-4736 | 0BBE0D91FA504DC4DC8848AEA001577F |
| Columns 4737-4864 | 51653E755F6CB4F75ACE347EC899304D |
| Columns 4865-4992 | 1D0EE239D8A6C2E2EA13D4CFB3394FCA |
| Columns 4993-5120 | BF707E3ACD882B91FDDDD44A7EA0D1F3D |
| Row 769 | |
| Columns 4097-4224 | 14EB386A5A4524983682993353F8D76E |
| Columns 4225-4352 | F9850534D2FB4F19F787897435C5EB0F |
| Columns 4353-4480 | B680840F8D34A0995BA0A94E309A9194 |
| Columns 4481-4608 | 6C66CAA0567BFFD609B6484BCD477702 |
| Columns 4609-4736 | B62A4053A6916719693D50608EC1D717 |
| Columns 4737-4864 | 23C38E6F64963EE836ADC6BBF39F4CD1 |
| Columns 4865-4992 | A40947C16AEAD43F621457BDB766A157 |
| Columns 4993-5120 | DD6118ACF503356D0B3479828C296016 |
| Row 897 | |
| Columns 4097-4224 | AAB1061EC9FA6BA21E81D7E22D3A7ED2 |
| Columns 4225-4352 | F902B6C336258F5B6B54628AC96116DE |
| Columns 4353-4480 | 5968E3167BB1E221714B0F4B3B9D7E0A |
| Columns 4481-4608 | F12374361559D0F0E0C7FCC959B1A9D8 |

| | |
|-------------------|-----------------------------------|
| Columns 4609-4736 | C103B779B3A769AA8D955160E4B9F9B7 |
| Columns 4737-4864 | 231B28E0B7490C8EB883F29AF6CC4F12 |
| Columns 4865-4992 | A7D1FA32F82AAF128FBC6AC53532AB89 |
| Columns 4993-5120 | 17AC06392CDAC681817D2F5475016296 |
| Row 1025 | |
| Columns 4097-4224 | 434D8612F27169A49ED244393B87DB5E |
| Columns 4225-4352 | B66D806A5A9ADF46D83C7DCFDB4B72CA |
| Columns 4353-4480 | A78E0C64307885C6E67C870BD21EC431 |
| Columns 4481-4608 | 11B79B0BB0B977D9792535C16AA7D982 |
| Columns 4609-4736 | B597FD60982B8C42D019390EFA14B3D5 |
| Columns 4737-4864 | C57FF5CFA1C438AC576782A5B48B78AA |
| Columns 4865-4992 | AE278E95DA048F720B7DB5FB6488287B |
| Columns 4993-5120 | 893C7E7E8DCB6E5ED5DB819D8901B32C |
| Row 1153 | |
| Columns 4097-4224 | B7BA8906FC3AEADE22254872ECA99117 |
| Columns 4225-4352 | 74F39404FA2779F4C55D649E5A6AA628 |
| Columns 4353-4480 | 4A1F8910EBF76F2F4E3EF686266CEBB8 |
| Columns 4481-4608 | 8363A57CF1377C68419BEFE6C848FEDA |
| Columns 4609-4736 | 8F141154BFA88D31446EF367ED965F98 |
| Columns 4737-4864 | 1242B3F840426E98010B84A957090390 |
| Columns 4865-4992 | 9CE9E0B619E61C4A481F1DD44360BCAC |
| Columns 4993-5120 | 0938AE511B2B47A42F5F59FBF547D991 |
| Row 1281 | |
| Columns 4097-4224 | 85B68FFC07A32A495D9A708FAECD2C41 |
| Columns 4225-4352 | 69CFDFFD21D6B2CF3F91CF5820823B83 |
| Columns 4353-4480 | 7D62406050908C82C21CF32B862166F2 |
| Columns 4481-4608 | 82AF2DF8E6CADB5D043FBF863ACE6599 |
| Columns 4609-4736 | 700097EE5FDDDD825468C544985C983CE |
| Columns 4737-4864 | 69EE0178288A8E1A12009EBF2E4382DE |
| Columns 4865-4992 | 2B8D59DE631991AE1B67C70786B43BE2 |
| Columns 4993-5120 | 860FC3354C9FE4253EBF307D1C643E22 |
| Row 1409 | |
| Columns 4097-4224 | 905330D76B16340120BB399A08061CBE |
| Columns 4225-4352 | 9D5765CE993D7092A8150DE46D6CA810 |
| Columns 4353-4480 | E03534D4DA2B66A0BF2AEF3B833E18DF |
| Columns 4481-4608 | 6C1C0D9EAB1E26FD2481F6BB6AB674C6 |
| Columns 4609-4736 | D98BD8D3FC0E0557352CF52EEA654A92 |
| Columns 4737-4864 | 0DF8D4B0FD41AD3EE547119C2446F840 |
| Columns 4865-4992 | 4C1F458D1E2F4B70D9023F0DFC06EFE9 |
| Columns 4993-5120 | 24349C5D9DE2B048DC74D3E888043526 |
| Row 1537 | |
| Columns 4097-4224 | E864E5EE002EB3B4C31A8D3B3E22D2C6 |
| Columns 4225-4352 | B3C4136542237F8E3C75AA228AB1B2F5 |
| Columns 4353-4480 | 43DF20DF407EAC80CAF22FDDADD586C9 |

| | |
|-------------------|----------------------------------|
| Columns 4481-4608 | 9414219FF80742652531AC5CC0E52866 |
| Columns 4609-4736 | 1A68E6BC5CA7FCA386396D0F56A2E7A3 |
| Columns 4737-4864 | D9EC25B8DEA08EDB6A9E6CFFEC7B15C1 |
| Columns 4865-4992 | CD48176480B2E0FED349142BE9888043 |
| Columns 4993-5120 | 9A70BAD89B53A4461301DF6C1763EB67 |
| Row 1665 | |
| Columns 4097-4224 | 5C9B0F852875D4B06EFA7FF418710592 |
| Columns 4225-4352 | 6F7C0712083341F6A97F398A275243DC |
| Columns 4353-4480 | 3D046D9B0B0B6AB3FEB99F72A70BAF35 |
| Columns 4481-4608 | 50F7B484C2530BEF63537B68EBDCF01C |
| Columns 4609-4736 | 672E8B1DD956431036302F8557CBB4E0 |
| Columns 4737-4864 | C9CAD206AB0AD88C655E0F52C70AEEA1 |
| Columns 4865-4992 | FF7EC97F9439C9D4CD71487F10065DE0 |
| Columns 4993-5120 | 532339617D706AEFA50A23B90B57978C |
| Row 1793 | |
| Columns 4097-4224 | B7E0C9A5F3EF66B9ABA49150144FCBEF |
| Columns 4225-4352 | 2C9E63DC18BE8ADDA0FD7E7E8F7FC5FE |
| Columns 4353-4480 | 5C55C60E14C3D7AC4D00D9F6C827E1EC |
| Columns 4481-4608 | 4E40D57E1740089DB1248707D195C038 |
| Columns 4609-4736 | 4500AD976DD321E6133113D244711330 |
| Columns 4737-4864 | 0260379D0A20D10A899019157631007D |
| Columns 4865-4992 | 4DF741A808694A9956E493B4668B67FD |
| Columns 4993-5120 | F89442CABAA2262C398171D62E938504 |
| Row 1921 | |
| Columns 4097-4224 | CCF8A4E13D655D5591DC40D2C6607CEF |
| Columns 4225-4352 | 353E539A020B0C608F843A855BA9B7AE |
| Columns 4353-4480 | CD31CCCB9388FECDEBEE1CCF42943E77 |
| Columns 4481-4608 | 9CA39E64D8AC9E23F15A0CB4C73ACB80 |
| Columns 4609-4736 | 3BF0F0DA9576923D95089979081ACA77 |
| Columns 4737-4864 | 359B090725B62278F00D0222CAD4C0FF |
| Columns 4865-4992 | 4ABA29056D55C5AAD990AA10A9A1A9B2 |
| Columns 4993-5120 | 27A09750826682C157BD7CD2178FDC96 |
| Row 2049 | |
| Columns 4097-4224 | AFC3076AF8AFB82B45FE8F2628F489F1 |
| Columns 4225-4352 | 2CFA95663A96A30FB3831F756D9E666A |
| Columns 4353-4480 | 011EE24F6C5EE283C3EE09A1D5FAF1B9 |
| Columns 4481-4608 | 7B49CB7B94EDEB207221A9436E1FFDF5 |
| Columns 4609-4736 | 5D36302EEBDD74AD27158F4D9DF0FA6E |
| Columns 4737-4864 | 497015959B333E79885FBE22B9B72707 |
| Columns 4865-4992 | E330EEAD520B31BAD1A5DC55EF54193A |
| Columns 4993-5120 | D6C112F89677E27A26F1DC62E08DF49C |
| Row 2177 | |
| Columns 4097-4224 | 2DF5B0291E619A18D802502086037C46 |
| Columns 4225-4352 | 730D20AE9364A6AD090B789D8AA6C6CC |

| | |
|-------------------|-----------------------------------|
| Columns 4353-4480 | EA476A585503E90BCAAD943DD30E1BCC |
| Columns 4481-4608 | 1D5C236ED01E9E5C8E94E96FA7252ABF |
| Columns 4609-4736 | 3EB2DB84FB4837EA5153CA825D11F86B |
| Columns 4737-4864 | 574E63C92DD0E75AD8DDFF2B37CC97C9 |
| Columns 4865-4992 | 5E83299E60C44293BF0824C62EB7980C |
| Columns 4993-5120 | 5678B852002834EB2D630EAC536FFB78 |
| Row 2305 | |
| Columns 4097-4224 | 9A41F048C1C68187734BFB916EC3BFAF |
| Columns 4225-4352 | 4B23BDA1162B30CB7AEA9F03BEB CF597 |
| Columns 4353-4480 | C65460BFAF9C8913608F9888E738F4A1 |
| Columns 4481-4608 | 017AEE470FCA60F9711E9BE5EB98E7C9 |
| Columns 4609-4736 | 4EE8869A59EDF8BDD52C5B5388B35249 |
| Columns 4737-4864 | 8EB0D25B439273CA6545E82E69D8677C |
| Columns 4865-4992 | 5B23991A53041EA4B276405C156A9DE5 |
| Columns 4993-5120 | A90889BC74530A5F87CCF024E591E18F |
| Row 2433 | |
| Columns 4097-4224 | 22735E1E720A8B3C29A80F3696D6F157 |
| Columns 4225-4352 | F68ED2F2389D5D2CDC59D706495D815F |
| Columns 4353-4480 | D0EE25B73218D5717572387BFA03A7C2 |
| Columns 4481-4608 | A0717B27763FE223BDA3EB0DAFB EF276 |
| Columns 4609-4736 | 9DBB8235D11298BEE28B39772ED91A35 |
| Columns 4737-4864 | 92DE6FED2F6766E01DBA188153DEA205 |
| Columns 4865-4992 | 48930E9A21873E62863CA15D6DB058D9 |
| Columns 4993-5120 | 61A29088FE3983D0E1699EF0AAFA5FD1 |
| Row 2561 | |
| Columns 4097-4224 | A73005690098889382252873E627D6FB |
| Columns 4225-4352 | 7862DE8A3D0F1A9387963F38A82E4703 |
| Columns 4353-4480 | 78BAB9252EE72FB0C798C7C684B6E789 |
| Columns 4481-4608 | B7480D9712BFA72D122F243674AD887F |
| Columns 4609-4736 | EC1851EB80A37133B68F0F709DB32E05 |
| Columns 4737-4864 | A809CB3638414FD6E156821BDAC256E0 |
| Columns 4865-4992 | B75342B6CFF7ED428521AB48A4C55D66 |
| Columns 4993-5120 | C9AB047D79A484289C820E8FADD87251 |
| Row 2689 | |
| Columns 4097-4224 | A69C02525644F41D03197EF26112D606 |
| Columns 4225-4352 | 3DF71AD0410035AE1AE7B0AB310B6967 |
| Columns 4353-4480 | C4F82E31B4D9B491EF8E4992FDBA61B0 |
| Columns 4481-4608 | B6B367CDE8DE0CAE22875F641288E733 |
| Columns 4609-4736 | 5C142A9C7C2E259BD38D66117E9E861C |
| Columns 4737-4864 | D27BF85E8EEE1920B57D0C62B512E2D6 |
| Columns 4865-4992 | 68B4500340B7B92EDD05A44D36AC1651 |
| Columns 4993-5120 | 4E77C4ABE92FE174B5D9F79070685288 |
| Row 2817 | |
| Columns 4097-4224 | A22B2A6C9A75D7A6EEA5A0DF8A4950E2 |

| | |
|-------------------|-----------------------------------|
| Columns 4225-4352 | 24C4830123FAE1EB6EB0AC9C2D8C508E |
| Columns 4353-4480 | 1BB99D6785EBCCDD9CD6A50CF53CCA00 |
| Columns 4481-4608 | 0624E36FD0817F2E198340098E60DFBF |
| Columns 4609-4736 | A4EB92DD48085594C6F755C563F35020 |
| Columns 4737-4864 | 04BDFF9A2309C6E673CE08D94A45BBC4 |
| Columns 4865-4992 | 8B8EC43906C28869AD4E41FB147A7696 |
| Columns 4993-5120 | 8AB66E9B68FA00BEF90D3E078D0C6FFC |
| Row 2945 | |
| Columns 4097-4224 | 89A79E9CF0BE90A3D86305B6491A49B9 |
| Columns 4225-4352 | 222A27A68236765AB32D41B1E0616C83 |
| Columns 4353-4480 | 99931668E57EB6378C8F4ED1C27BEDD3 |
| Columns 4481-4608 | 35166846D0C673B9A8D2184C1901433A |
| Columns 4609-4736 | 4D768A5E0109B5CBC198869334D81C43 |
| Columns 4737-4864 | 2C6A48CC47FD21F9608107FF80FE37AA |
| Columns 4865-4992 | 4DD3A7395630BE4B64F776C5FC6B2C31 |
| Columns 4993-5120 | 4DC16B1E2B2A7F6E0E9FDAE3B60F8FAA |
| Row 3073 | |
| Columns 4097-4224 | CFA794F49FA5A0D88BB31D8FCA7EA8BB |
| Columns 4225-4352 | A7AE7EE8A68580E3E922F9E13359B284 |
| Columns 4353-4480 | 91F72AE8F2D6BF7830A1F83B3CDBD463 |
| Columns 4481-4608 | CE95C0EC1F609370D7E791C870229C1E |
| Columns 4609-4736 | 71EF3FDF60E2878478934DB285DEC9DC |
| Columns 4737-4864 | 0E95C103008B6BCDD2DAF85CAE732210 |
| Columns 4865-4992 | 8326EE83C1FBA56FDD15B2DDB31FE7F2 |
| Columns 4993-5120 | 3BA0BB43F83C67BDA1F6AEE46AEF4E62 |
| Row 3201 | |
| Columns 4097-4224 | 565083780CA89ACAA70CCFB4A888AE35 |
| Columns 4225-4352 | 1210FAD0EC9602CC8C96B0A86D3996A3 |
| Columns 4353-4480 | C0B07FDDA73454C25295F72BD5004E80 |
| Columns 4481-4608 | ACCF973FC30261C990525AA0CBA006BD |
| Columns 4609-4736 | 9F079F09A405F7F87AD98429096F2A7E |
| Columns 4737-4864 | EB8C9B13B84C06E42843A47689A9C528 |
| Columns 4865-4992 | DAAA1A175F598DCFDDBAD426CA43AD479 |
| Columns 4993-5120 | 1BA78326E75F38EB6ED09A45303A6425 |
| Row 3329 | |
| Columns 4097-4224 | 48F42033B7B9A05149DC839C90291E98 |
| Columns 4225-4352 | 9B2CEBE50A7C2C264FC6E7D674063589 |
| Columns 4353-4480 | F5B6DEAEBF72106BA9E6676564C17134 |
| Columns 4481-4608 | 6D5954558D23519150AAF88D7008E634 |
| Columns 4609-4736 | 1FA962FBAB864A5F867C9D6CF4E087AA |
| Columns 4737-4864 | 5D7AA674BA4B1D8CD7AE9186F1D3B23B |
| Columns 4865-4992 | 047F112791EE97B63FB7B58FF3B94E95 |
| Columns 4993-5120 | 93BE39A6365C66B877AD316965A72F5B |

| | |
|-------------------|----------------------------------|
| Row 3457 | |
| Columns 4097-4224 | 1B58F88E49C00DC6B35855BFF228A088 |
| Columns 4225-4352 | 5C8ED47B61EEC66B5004FB6E65CBECF3 |
| Columns 4353-4480 | 77789998FE80925E0237F570E04C5F5B |
| Columns 4481-4608 | ED677661EB7FC3825AB5D5D968C0808C |
| Columns 4609-4736 | 2BDB828B19593F41671B8D0D41DF136C |
| Columns 4737-4864 | CB47553C9B3F0EA016CC1554C35E6A7D |
| Columns 4865-4992 | 97587FEA91D2098E126EA73CC78658A6 |
| Columns 4993-5120 | ADE19711208186CA95C7417A15690C45 |
| Row 3585 | |
| Columns 4097-4224 | BE9C169D889339D9654C976A85CFD9F7 |
| Columns 4225-4352 | 47C4148E3B4712DAA3BAD1AD71873D3A |
| Columns 4353-4480 | 1CD630C342C5EBB9183ADE9BEF294E8E |
| Columns 4481-4608 | 7014C077A5F96F75BE566C866964D01C |
| Columns 4609-4736 | E72AC43A35AD216672EBB3259B77F9BB |
| Columns 4737-4864 | 18DA8B09194FA1F0E876A080C9D6A39F |
| Columns 4865-4992 | 809B168A3D88E8E93D995CE5232C2DC2 |
| Columns 4993-5120 | C7CFA44A363F628A668D46C398CAF96F |
| Row 3713 | |
| Columns 4097-4224 | D57DBB24AE27ACA1716F8EA1B8AA1086 |
| Columns 4225-4352 | 7B7796F4A86F1FD54C7576AD01C68953 |
| Columns 4353-4480 | E75BE799024482368F069658F7AAAFB0 |
| Columns 4481-4608 | 975F3AF795E78D255871C71B4F4B77F6 |
| Columns 4609-4736 | 65CD9C359BB2A82D5353E007166BDD41 |
| Columns 4737-4864 | 2C5447314DB027B10B130071AD0398D1 |
| Columns 4865-4992 | DE19BC7A6BBCF6A0FF021AABF12920A5 |
| Columns 4993-5120 | 58BAED484AF89E29D4DBC170CEF1D369 |
| Row 3841 | |
| Columns 4097-4224 | 4C330B2D11E15B5CB3815E09605338A6 |
| Columns 4225-4352 | 75E3D1A3541E0E284F6556D68D3C8A9E |
| Columns 4353-4480 | E5BB3B297DB62CD2907F09996967A0F4 |
| Columns 4481-4608 | FF33AEEE2C8A4A52FCCF5C39D355C39C |
| Columns 4609-4736 | 5FE5F09ABA6BCCE02A73401E5F87EAC2 |
| Columns 4737-4864 | D75702F4F57670DFA70B1C002F523EEA |
| Columns 4865-4992 | 6CE1CE2E05D420CB867EC0166B8E53A9 |
| Columns 4993-5120 | 9DF9801A1C33058DD116A0AE7278BBB9 |
| Row 3969 | |
| Columns 4097-4224 | 4CF0B0C792DD8FDB3ECEAE6F2B7F663D |
| Columns 4225-4352 | 106A1C296E47C14C1498B045D57DEFB5 |
| Columns 4353-4480 | 968F6D8C790263C353CF307EF90C1F21 |
| Columns 4481-4608 | 66E6B632F6614E58267EF096C37718A3 |
| Columns 4609-4736 | 3D46E5D10E993EB6DF81518F885EDA1B |
| Columns 4737-4864 | 6FF518FD48BB8E9DDBED4AC0F4F5EB89 |
| Columns 4865-4992 | BCC64D21A65DB379ABE2E4DC21F109FF |

Columns 4993-5120

2EC0CE7B5D40973D13ECF713B01C6F10

D.5. Synchronization

Current receiver/demodulator designs can perform either coherent or non-coherent detection and demodulation. To accomplish symbol/bit synchronization, the transmitted synchronization sequence must contain sufficient transitions to ensure symbol/bit acquisition and tracking. At the same time, the symbol/bit synchronizer loop bandwidth should be designed for optimal phase-noise filtering and symbol tracking performance. Since the use of LDPC code does not guarantee sufficient bit/symbol transitions to acquire or maintain synchronization, it is highly recommended that a pseudo-randomizer be used after LDPC encoding in accordance with Section D.6.

The ASM, depicted in Figure D-8 and Table D-10, is not randomized. Randomization ensures that coded symbols are spectrally near-white, thus allowing each ASM to provide synchronization for a set of randomized codeblocks in a codeblock frame.

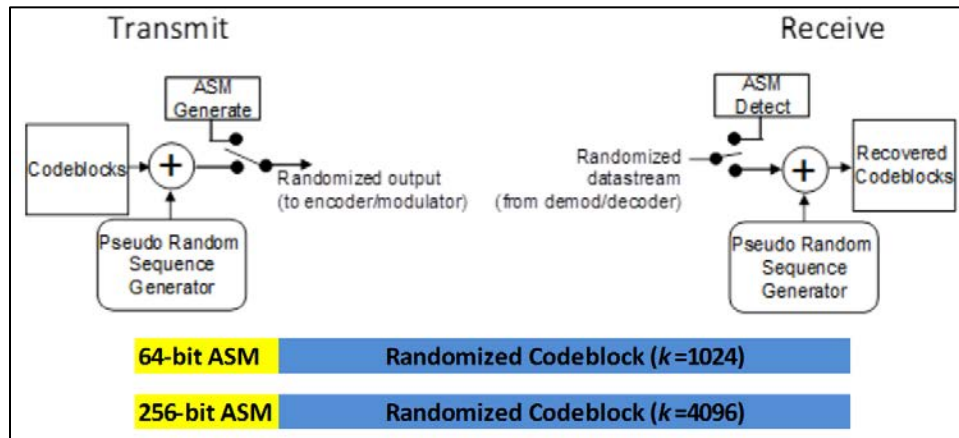


Figure D-8. ASM/Codeblock Structure

| Table D-10. ASM Definition | |
|----------------------------|------------------|
| 64-bit Sequence | Definition (hex) |
| A | FCB88938D8D76A4F |
| \bar{A} | 034776C7272895B0 |

At the transmitter side, the ASM is prepended to each set of randomized codeblocks as the synchronization header. At the receiver side, the ASM is detected and located in the received data stream. Refer to Figure D-8.

Length of the ASM is determined by the information block length (k). For $k=1024$ the ASM length will be 64 bits. For $k=4096$ the ASM will be 256 bits. The ASM is constructed with 64-bit sequences. The 64-bit ASM requires one 64-bit sequence; the 256-bit ASM sequence requires four 64-bit sequences. Let A be one 64-bit sequence and \bar{A} is the inverse of A . The structure of the 64-bit sequence is A ; the structure of the 256-bit ASM is $AA\bar{A}\bar{A}$. Table D-10 defines the two 64-bit sequences.

The resulting randomized codeblock plus ASM is transmitted leftmost bits first, making the first series of bits to be transmitted as FCB8..... or 1111110010111000..... This is true for both 64-bit and 256-bit ASMs.

With the addition of the ASM prepended to the codeblock, over-the-air channel rate is no longer the inverse of the code rate r . [Table D-11](#) shows the exact bandwidth expansion factor for each choice of code rate and information block length.

| Table D-11. Bandwidth Expansion Factor | | | |
|---|----------------------------|----------|----------|
| Information Block Length, k | Bandwidth Expansion Factor | | |
| | Rate 1/2 | Rate 2/3 | Rate 4/5 |
| 1024 | 33/16 | 25/16 | 21/16 |
| 4096 | 33/16 | 25/16 | 21/16 |

As an example, assume an incoming baseband data rate of 5 Mbps. If an information block length of 1024 bits and rate 1/2 are chosen, the new over-the-air channel rate will be:

$$(5 \text{ Mbps}) * (33/16) = 10.3125 \text{ Mbps}$$

D.6. Randomization

At the transmitter/encoder, a set of codeblocks in a codeblock frame shall be randomized by exclusive-ORing the first bit of the first codeblock with the first bit of the pseudo-random sequence until the end of the codeblock. The pseudo-randomizer resets to the initial state of all 1s at the start of each codeblock frame for each ASM period.

The pseudo-random sequence is generated using the following polynomial: $h(x) = x^8 + x^7 + x^5 + x^3 + 1$. It has a maximal length of 255 bits with the first 40 bits of the pseudo-random sequence from the generator as 1111 1111 0100 1000 0000 1110 1100 0000 1001 1010..... The sequence begins at the first bit of a first codeblock in a codeblock frame and repeats after 255 bits, continuing repeatedly until the end of the last codeblock in a codeblock frame. The leftmost bit of the pseudo-random sequence is the first bit to be exclusive-ORed with the first bit of the codeblock. [Figure D-9](#) illustrates the pseudo-randomizer block diagram.

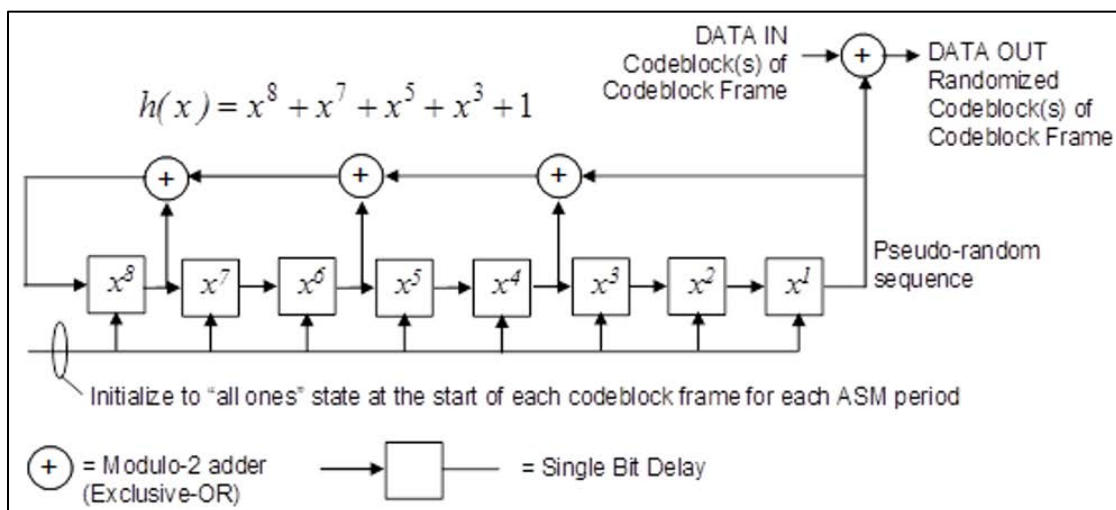


Figure D-9. Codeblock Randomizer

At the receiver, each original codeblock of a codeblock frame is reconstructed using the same pseudo-random sequence. After locating the ASM, the pseudo-random sequence is exclusive-ORed with the received data bits immediately following the ASM. The pseudo-randomizer resets to the initial state of all 1s at the start of each received codeblock frame for each ASM period.

D.7. Performance

The trade that must be made when choosing the information block size and coding rate is one between required coding gain, bandwidth expansion, and fading channel characteristics. Detection performance of the code is tightly coupled to the type of SOQPSK-TG/FQPSK-B/FQPSK-JR demodulator used. Plots of simulated performance for all six combinations of information block size and code rates with two different types of SOQPSK-TG/FQPSK-B/FQPSK-JR demodulators on are shown in [Figure D-10](#) and [Figure D-11](#). Other demodulator configurations are considered in Perrins.⁴⁷

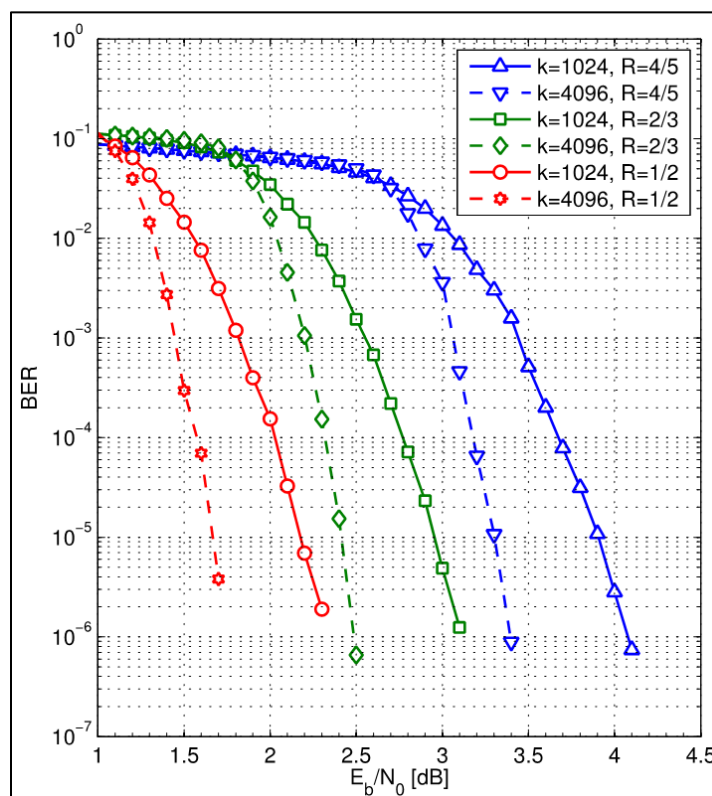


Figure D-10. LDPC Detection Performance with 4-state Trellis Demodulator

⁴⁷ E. Perrins. "FEC Systems for Aeronautical Telemetry". *IEEE Transactions on Aerospace and Electronic Systems*, vol. 49, no. 4, pp. 2340-2352, October 2013.

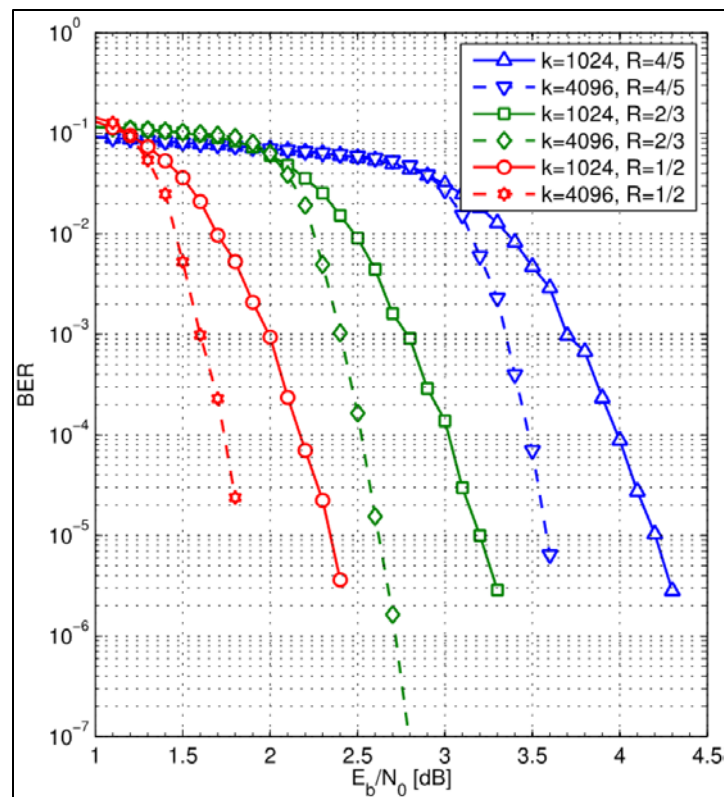


Figure D-11. LDPC Detection Performance with Symbol-by-Symbol Demodulator

APPENDIX 2-E

Space-Time Coding for Telemetry Systems

E.1. Code Description

The STC used in this standard is based on the Alamouti STC⁴⁸ and applied only to SOQPSK-TG or any of its fully interoperable variants. The Alamouti STC may be described in terms of the OQPSK IRIG-106 symbol-to-phase mapping convention illustrated in [Figure E-1](#).

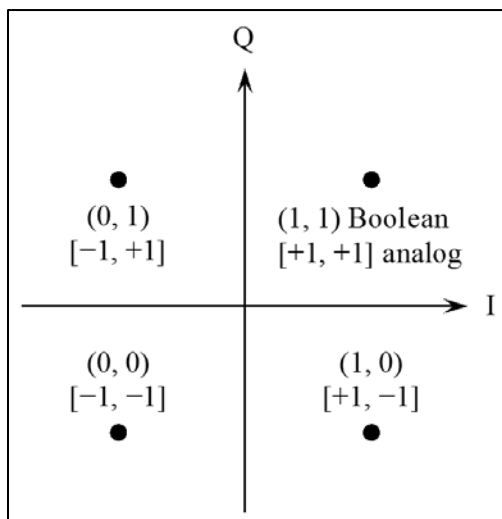


Figure E-1. Symbol-to-Phase Mapping for IRIG-106 Offset QPSK Modulation

The starting point is the normalized analog values corresponding to each of the OQPSK symbols. Let $[a_n, b_n]$ with $a_n = \pm 1$, $b_n = \pm 1$ be the analog value of the n -th symbol. Suppose the bit sequence defines the sequence of symbols

$$[a_0, b_0], [a_1, b_1], [a_2, b_2], [a_3, b_3], \dots, [a_{2k}, b_{2k}], [a_{2k+1}, b_{2k+1}], \dots$$

The Alamouti STC organizes the symbols into blocks of two symbols, starting with the even-indexed blocks as shown. The Alamouti STC assigns the k -th block of symbols

$$[a_{2k}, b_{2k}], [a_{2k+1}, b_{2k+1}]$$

to antenna 0 and antenna 1 over two consecutive symbol times as shown below.

| antenna | symbol time $2k$ | symbol time $2k+1$ |
|---------|------------------------|-------------------------|
| 0 | $[a_{2k}, b_{2k}]$ | $[-a_{2k+1}, b_{2k+1}]$ |
| 1 | $[a_{2k+1}, b_{2k+1}]$ | $[a_{2k}, -b_{2k}]$ |

⁴⁸ S. Alamouti. "A Simple Transmit diversity Technique for Wireless Communications." *IEEE Journal on Selected Areas in Communications*, vol. 16, no. 8, pp. 1451-1458, October 1998.

Using the bit (Boolean) assignments shown in [Figure E-1](#), the Alamouti encoder can be restated in terms of the input bits as follows. Let the sequence of input bits be

$$b_0 \ b_1 \ b_2 \ b_3 \mid b_4 \ b_5 \ b_6 \ b_7 \mid \dots \mid b_{4k} \ b_{4k+1} \ b_{4k+2} \ b_{4k+3} \mid \dots$$

The STC encoder groups the bits into non-overlapping blocks of four bits each as indicated by the vertical lines. The STC encoder produces two bit streams in parallel: \mathbf{b}_0 , which is applied to antenna 0, and \mathbf{b}_1 , which is applied to antenna 1. The relationship between the input bit sequence and these two bit sequences is

$$\begin{aligned}\mathbf{b}_0 &= b_0 b_1 \bar{b}_2 b_3 \mid b_4 b_5 \bar{b}_6 b_7 \mid \dots \mid b_{4k} b_{4k+1} \bar{b}_{4k+2} b_{4k+3} \mid \dots \\ \mathbf{b}_1 &= b_2 b_3 b_0 b_1 \mid b_6 b_7 b_4 b_5 \mid \dots \mid b_{4k+2} b_{4k+3} b_{4k} b_{4k+1} \mid \dots\end{aligned}$$

where \bar{b}_n is the logical complement of bit b_n .

An important point here is the notion of even- and odd-indexed bits. The SOQPSK-TG modulator treats even-indexed and odd-indexed bits slightly differently. Each codeblock must begin with an even-indexed bit.

An example of encoding is as follows. Suppose the input bit sequence is

$$1 \ 0 \ 1 \ 1 \ 0 \ 1 \ 0 \ 0$$

The two STC encoded bit sequences are

$$\begin{aligned}\mathbf{b}_0 &= 1 \ 0 \ 0 \ 1 \ 0 \ 1 \ 1 \ 0 \\ \mathbf{b}_1 &= 1 \ 1 \ 1 \ 1 \ 0 \ 0 \ 0 \ 0\end{aligned}$$

To make provision for the estimation of frequency offset, differential timing, and the channels, a block of known bits, called pilot bits, is periodically inserted into each of the two bit streams. A 128-bit pilot block is inserted every 3200 Alamouti-encoded bits. The pilot bits inserted into the \mathbf{b}_0 bit stream are denoted \mathbf{p}_0 and the pilot bits inserted into the \mathbf{b}_1 bit stream are denoted \mathbf{p}_1 . These pilot bit sequences are

$$\begin{aligned}\mathbf{p}_0 &= 10101000100011011001101011010100 \\ &\quad 11011100010000000100100101000111 \\ &\quad 11100010100100100000001000111011 \\ &\quad 00101011010110011011000100010101\end{aligned}$$

$$\begin{aligned}\mathbf{p}_1 &= 11100011110001110111011101100001 \\ &\quad 11110000011100000011011010111110 \\ &\quad 01111101011011000000111000001111 \\ &\quad 10000110111011101110001111000111\end{aligned}$$

A notional diagram illustrating how \mathbf{p}_0 and \mathbf{p}_1 are periodically inserted into \mathbf{b}_0 and \mathbf{b}_1 , respectively, is illustrated in [Figure E-2](#). Note that the bits comprising \mathbf{b}_0 and \mathbf{b}_1 may change with every occurrence as defined by the input data, but the pilot bits \mathbf{p}_0 and \mathbf{p}_1 do not change with each occurrence.

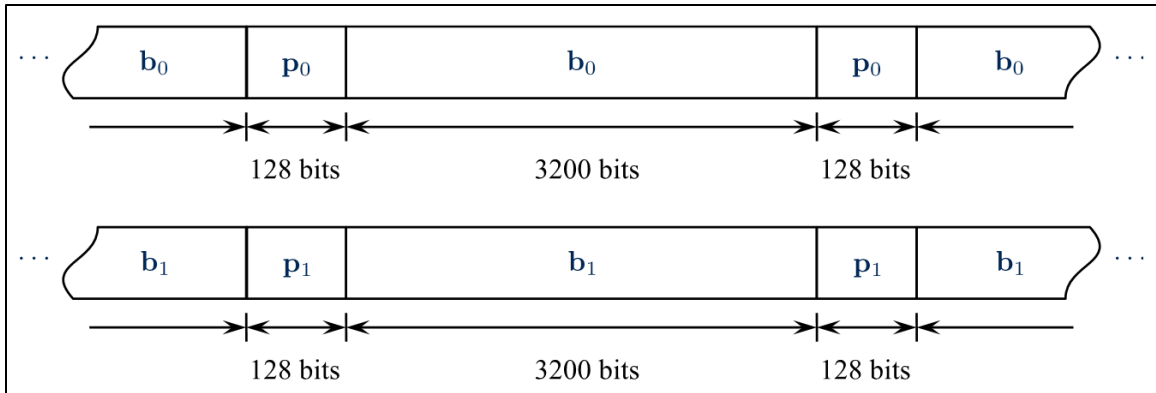


Figure E-2. Notional Diagram Illustrating the Periodic Insertion of 128 Pilot Bits Every 3200 Alamouti-Encoded Bits

E.2. Modulation

The bit sequences described in the previous section are modulated by a pair of SOQPSK-TG modulators (or modulator/transmitters). The modulators should be constructed and used as follows.

- The modulators share a common clock. This common clock is 26/25 times the input clock to accommodate the periodic insertion of 128 pilot bits every 3200 Alamouti-encoded bits.
- The modulators should share a common carrier reference. If this is not possible, the two carrier references should be phase-locked ideally, or frequency-locked at a minimum.
- Randomization, if required, should be applied before the STC encoder.
- Differential encoding should be disabled. The periodically inserted pilot bits are to be used by the demodulator to estimate the magnitudes and phases of the antenna-0-to-receiver channel and the antenna-1-to-receiver channel. There is no need to use differential encoding because data-aided phase estimates do not possess a phase ambiguity.⁴⁹

[Figure E-3](#) is a notional block diagram that shows the relationship between the input data and clock, the bit-level space-time encoder, the periodic pilot bit insertion, and the SOQPSK-TG modulation.

⁴⁹ M. Rice. *Digital Communications: A Discrete-Time Approach*. Pearson/Prentice-Hall. Upper Saddle River, NJ, 2009.

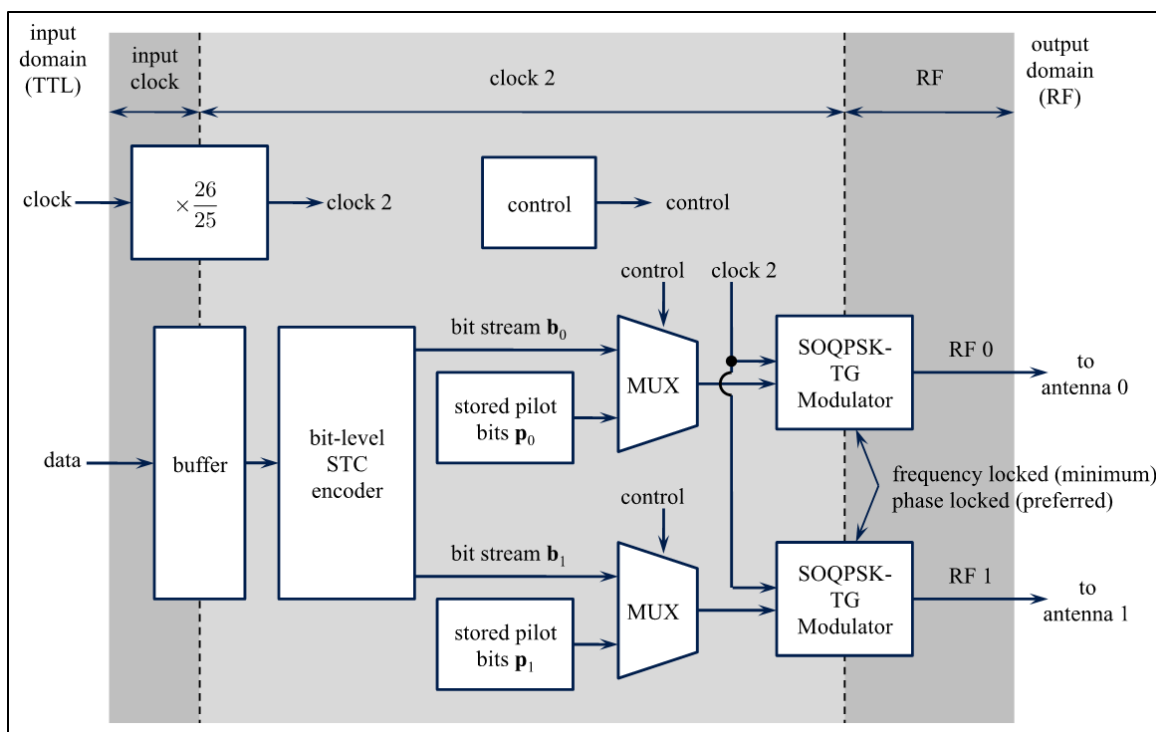


Figure E-3. A Notional Block Diagram of the Space-Time Code Transmitter

E.3. Resources

Jensen, et al.⁵⁰ first described the application of space-time coding to the two-antenna problem. Experimental flights confirmed the effectiveness of the technique.^{51,52,53}

⁵⁰ Jensen, M., M. Rice, and A. Anderson. "Aeronautical Telemetry Using Multiple-Antenna Transmitters." *IEEE Transactions on Aerospace and Electronic Systems*, vol. 43, no. 1, pp. 262-272, January 2007.

⁵¹ M. Rice, "Space-Time Coding for Aeronautical Telemetry: Part 1 – System Description," in *Proceedings of the International Telemetry Conference*, Las Vegas, NV, October 2011.

⁵² Rice, M. and K. Temple, "Space-Time Coding for Aeronautical Telemetry: part II – Experimental Results," in *Proceedings of the International Telemetry Conference*, Las Vegas, NV, October 2011.

⁵³ K. Temple. "Performance Evaluation of Space-Time coding on an Airborne Test Platform." Paper presented at the 50th International Telemetry Conference, San Diego, CA, October 2014

APPENDIX 2-F

Use of Recommendation ITU-R M.1459 for Protection of AMT Ground Stations from Terrestrial, Airborne, and Satellite Interference

F.1. Introduction and Summary

Since it was approved for use by the Radiocommunication Sector of the ITU in 2000, Rec M.1459 has been the international and US standard for defining the interference protection criteria and the use of those criteria for AMT ground stations.

Despite its title, Rec M.1459 pertains to interference not only from satellites, but also from terrestrial sources and has been so applied both domestically and internationally. The methodology presented in Annex A of Rec M.1459 for computing band-specific protection levels also makes it applicable to any frequency band. The protection criteria for lower L and upper S bands given in Rec M.1459 have thus been extended to include protection criteria for upper L, lower S, and lower, middle, and upper C bands. The protection criteria are included in [Chapter 2](#).

The protection criteria provided by Rec M.1459 are in the form of PFD levels defined at the aperture of the affected AMT ground station antenna. Thus, when performing interference analysis, it is not necessary to require information about the specific technical parameters of the affected AMT ground station, such as the actual AMT receive antenna gain, pointing direction, noise figure, or system gain over noise temperature. The only details needed are:

- the geographic location of the AMT ground station antenna;
- the height above ground of the AMT ground station antenna;
- the mid-band value of the wavelength for the frequency band under consideration;
- an accurate terrain data base in/around the AMT receive site (1 arc-second, or 30 meter resolution) for use with propagation models when computing interference from terrestrial sources;
- a composite antenna pattern based on the methodology of Rec M.1459, but adjusted for the average wavelength of the band under consideration, to be used when aggregation from a large number of terrestrial sources is being analyzed.

Section [F.2](#) contains several sample computations that illustrate how this information is used in practice. The examples begin with simple cases involving a small number of satellite and terrestrial interference sources. The scenarios presented increase in size and complexity to include networks comprised of thousands of interference sources (e.g., cellular towers). A variety of models, equations, and computational techniques is demonstrated, underscoring the versatility and comprehensive applicability of the Rec M.1459 protection criteria. A final example provides guidance on how to handle special cases, such as when antennas larger than those anticipated in Rec M.1459, are used.

F.2. Practical Application of the Rec M.1459 Protection Criteria

The examples in this section include, but are not limited to, interference from satellites, terrestrial microwave towers, cellular base stations, portable medical telemetry devices, and smartphones. Both adjacent channel and co-channel interference scenarios are included. Each

example is intended to provide and illustrate one or more building blocks that will sometimes, and perhaps often, be used in end-to-end interference analysis.

The discussions and computations here are based on a combination of publicly available data, standard assumptions regarding typical values of common parameters, and emission limits stipulated in FCC regulations. In some of the scenarios, FCC regulations are used as a source of band-specific emission masks that define the worst-case limits, as a function of frequency, that are permitted for OOB from a particular frequency band or set of bands. Thus, the examples that follow are just that: examples. They are intended to demonstrate computational techniques and analysis. Unless otherwise stated, they should not be interpreted as either assertions or policy statements regarding whether interference does or does not exist in a particular scenario.

Examples 1 - 11 address:

1. Co-channel interference from a planned BSS satellite in geostationary orbit into AMT ground stations operating in the lower L-band between 1435 – 1525 MHz;
2. Co-channel interference from multiple spot-beam communication satellites in geostationary orbit into AMT ground stations operating in a portion of the lower L-band from 1518 – 1525 MHz;
3. Out-of-band interference from a SiriusXM broadcast satellite into an AMT ground station in the upper S-band from 2360 – 2390 MHz;
4. Frequency scaling of interference and interference criteria to different reference bandwidths;
5. Computation of path loss using the two-ray model;
6. Rayleigh fading of the aircraft telemetry signal;
7. Computation of path loss using commercial software that implements the Longley-Rice (L-R)/Irregular Terrain Model (ITM) and P.452 models;
8. Consideration of the antenna patterns of cellular base stations;
9. Aggregation of interference from a network of cellular base stations to one or more AMT ground stations;
10. Considerations for the modeling of interfering systems;
11. Coordination of AMT with 4G Long-Term Evolution (LTE)-A user equipment;
12. Special considerations regarding AMT antennas.

Each of these scenarios was chosen to illustrate a particular point or technique that is independent of Rec M.1459, but which is needed in order for the protection criteria of Rec M.1459 to be properly applied.

At the outset, it should be noted that the curvature of the earth complicates the trigonometry for computing elevation, azimuth, and bearing angles. For example, the elevation angle computed for the path from an AMT ground station to a flight test aircraft 320 km away operating at an altitude of 30,000 feet will be close to zero degrees due to the curvature of the earth.

Using a flat-earth approximation, the angle would be computed to be approximately 4 degrees, thus suggesting incorrectly that interference from terrestrial sources would not be received in the main beam of the AMT ground station.

The equations used in the representative examples below assume a spherical earth, as evidenced by the inclusion of the value for the radius of the earth in km (e.g., 6358 km). The flat-earth approximation is obtained by letting the value of the earth's radius go to infinity.

Use of the correct formulas is particularly important when computing the bearing angle from a cellular tower to an AMT ground station and when coding the table look-up algorithms for choosing appropriate cellular tower sector antenna gain values as functions of pointing angles from the appropriate antenna pattern files.

Example 1. Co-channel interference from a planned BSS satellite in geostationary orbit into AMT ground stations operating in the lower L-band between 1435 – 1525 MHz

Use of Rec M.1459 begins with a simple equation,

$$pfd_{rec} = P_{xmt} G_{xmt} \times (Path_Loss) \times \frac{4\pi}{\lambda^2} \quad (F-1)$$

where PFD is the received PFD in watts per square meter. The quantity $P_{xmt} G_{xmt}$ is the product of the transmit power of the interfering source and the gain of the transmit antenna. Path loss depends on distance, signal blockage due to terrain blockage and/or clutter (e.g., buildings), and wavelength λ . For free-space propagation, however, path loss is given by:

$$path\ loss = \frac{\lambda^2}{(4\pi)^2 r^2} \quad (F-2)$$

Free-space propagation is appropriate for modeling signals from satellites, such as from a geostationary satellite to an AMT ground station antenna. This yields the simple result that:

$$pfd_{rec} = \frac{P_{xmt} G_{xmt}}{4\pi r^2} \quad (F-3)$$

For the sake of completeness, the received power, as measured at the terminals of the receive antenna, requires inclusion of the effective area of the receive antenna. This will be discussed in detail in example 7. It is sufficient to quote the result here:

$$P_{rec} = pfd_{rec} \times A_{eff} = \frac{P_{xmt} G_{xmt} \lambda^2 G_{rec}}{(4\pi)^2 r^2} \quad (F-4)$$

This is the Friis equation, where A_{eff} is the effective area of the receive antenna. For a parabolic dish, A_{eff} is often approximated by $0.5 \times \pi(D/2)^2$, where D is the diameter of the dish. The value for the wavelength of the signal λ is typically the mid-band value where $\lambda=c/f$.

The distance r and elevation angle α from an AMT ground station antenna to a geostationary satellite are determined using either standard textbook equations (included in Example 2), web-based calculators, or from FCC filings, which can be particularly useful because they also include information about the channel bandwidths, signal power, and transmit antenna gain.

The elevation angle α , which does not appear in equations F-1 – F-3, is needed in order to determine the appropriate protection criterion from Rec M.1459. For example, the lower L-band protection criteria from [Table 2-8](#) present these criteria as functions of α .

To apply this to a particular case, a comparison of the PFD contours at ground level of a BSS satellite is compared with the angle-of-arrival dependent protection criteria of Rec M.1459. The contours were made available by the developers of the satellite. The comparison shows

conclusively that the planned deployment of the satellite would cause harmful interference to AMT ground stations in the United States (e.g., -150 decibels relative to one watt [dBW]/m² in 4 kHz, versus the allowed limit of -180 dBW/m² in 4 kHz). As a consequence of this analysis, the satellite was not deployed.

Specifically, the co-channel emissions were so large with respect to the Rec M.1459 protection criteria that it wasn't necessary to perform a detailed, angle-of-arrival-dependent computation of the interference from the satellite.

Example 2. Co-channel interference from multiple spot-beam communication satellites in geostationary orbit into AMT ground stations operating in a portion of the lower L-band from 1518 – 1525 MHz

The 2003 World Radiocommunication Conference coincided with the launch of a new generation of MSS geostationary communication satellites. These satellites, including Inmarsat IV and Thuraya, introduced the use of complex phased-array beam-forming networks with large parabolic reflectors. The resulting spot beams permit the following: the use of portable handsets with omnidirectional antennas for making telephone calls via satellite; and the simultaneous generation of dozens, and even hundreds, of simultaneous beams. Each beam serves a separate user.

In seeking additional spectrum to support the use of these satellites, the mobile satellite community proposed the allocation of the AMT spectrum from 1518 – 1525 MHz for co-channel sharing with the MSS. As with the BSS satellite in example 1, application of Rec M.1459 demonstrated that co-channel sharing was not feasible.

In recognition of this, WRC-2003 modified Table 21-4 of Article 21 of the International Radio Regulations⁵⁴ to include the following PFD fence that protects AMT operations in the continental United States. In other words, the Conference incorporated the protection criteria of Rec M.1459 in the international radio regulations. [Figure F-1](#) is an excerpt of Article 21.16 of these regulations.

⁵⁴ International Telecommunications Union. "Radio Regulations: Articles." 2012. May be superseded by update. Available at <http://search.itu.int/history/HistoryDigitalCollectionDocLibrary/1.41.48.en.101.pdf>.

21.16 § 6 1) The power flux-density at the Earth's surface produced by emissions from a space station, including emissions from a reflecting satellite, for all conditions and for all methods of modulation, shall not exceed the limit given in Table 21-4. The limit relates to the power flux-density which would be obtained under assumed free-space propagation conditions and applies to emissions by a space station of the service indicated where the frequency bands are shared with equal rights with the fixed or mobile service, unless otherwise stated.

TABLE 21-4 (Rev.WRC-12)

| Frequency band | Service* | Limit in dB(W/m ²) for angles of arrival (δ) above the horizontal plane | | | | Reference bandwidth |
|---|---|--|----------------------------------|-----------------------------------|-----------------------------------|---------------------|
| | | 0°-5° | 5°-25° | 25°-90° | | |
| 1 670-1 700 MHz | Earth exploration-satellite Meteorological-satellite | -133 (value based on sharing with meteorological aids service) | | | | 1.5 MHz |
| 1 518-1 525 MHz (Applicable to the territory of the United States in Region 2 between the longitudes 71° W and 125° W) | Mobile-satellite (space-to-Earth) | $0^\circ \leq \delta \leq 4^\circ$ | $4^\circ < \delta \leq 20^\circ$ | $20^\circ < \delta \leq 60^\circ$ | $60^\circ < \delta \leq 90^\circ$ | 4 kHz |
| | | -181.0 | -193.0 + 20 log δ | -213.3 + 35.6 log δ | -150.0 | |

Figure F-1. Excerpt from Article 21 of the International Radio Regulations

Example 3. Out-of-band interference from a SiriusXM broadcast satellite into an AMT ground station in the upper S-band from 2360 – 2390 MHz

This next example provides a computation of OOBE into an AMT ground station from an operational geostationary satellite. This example serves to show an end-to-end computation of the out-of-band signal received at an AMT ground station antenna at Patuxent River (Pax River), Maryland from the SiriusXM satellite denoted as FM-6. This is a Satellite Digital Audio Radio Service (SDARS) broadcast satellite in geostationary orbit above the equator at 115.2 degrees west longitude.⁵⁵ FM-6 broadcasts in a 4.1-MHz portion of the 2320.0 – 2332.5 MHz band.

Note that the SDARS band (2320-2345 MHz) is separated from the 2360 – 2390 MHz AMT band by the 2345 – 2360 MHz WCS band (which is the topic of example 6, below).

Given that the SDARS channel is more than 15 MHz away from the edge of the AMT band at 2360 MHz, co-channel sharing is not relevant; however, the OOBE of the FM-6 satellite remain a concern, due to the high gain (30 – 40 decibels isotropic [dBi] and more) of a typical AMT ground station antenna.

The FCC restricts the OOBE of FM-6, relative to its mean transmitter power level P_{xmt} (and not including the effects of the satellite's antenna gain G_{xmt}) in the FCC Rules, part §25.202(f) (1), (2), and (3).⁵⁶ These are available online, but are restated here:

⁵⁵ The satellite is actually in operation at 116.1° W, but the computations here are performed for its originally intended geostationary orbital slot.

⁵⁶ Code of Federal Regulations, Frequencies, frequency tolerance, and emission limits, title 47, sec. 25.202.

The mean power of emissions shall be attenuated below the mean output power of the transmitter in accordance with the following schedule:

- (1) In any 4 kHz band, the center frequency of which is removed from the assigned frequency by more than 50 percent up to and including 100 percent of the authorized bandwidth: 25 dB;
- (2) In any 4 kHz band, the center frequency of which is removed from the assigned frequency by more than 100 percent up to and including 250 percent of the authorized bandwidth: 35 dB;
- (3) In any 4 kHz band, the center frequency of which is removed from the assigned frequency by more than 250 percent of the authorized bandwidth: An amount equal to 43 dB plus 10 times the logarithm (to the base 10) of the transmitter power in watts.

Since the authorized bandwidth of FM-6 is 4.1 MHz and the AMT band is removed from this frequency by more than 250%, the $43 + 10 \log(P)$ rule applies, where P is the out-of-band transmitter PSD in watts per 4 kHz of bandwidth. Specifically, the value $43 + 10 \log(P)$ is the amount the OOB must be attenuated with respect to the transmitter power P per 4 kHz of bandwidth. With the rule written in this manner, if the transmitter power P is increased, the amount by which the OOB must be attenuated increases by the same amount.

(This is a well-recognized OOB standard, but it is essential to note that the reference bandwidth for the example here is stipulated to be 4 kHz, whereas a reference value of 1 MHz may be more common in FCC rules).

The purpose of the $\log(P)$ term is to set a hard OOB power limit that is independent of the mean in-band transmitter power P . For the purpose of computing interference into AMT operations in 2360 – 2390 MHz using equations F-1-F-3, the interference from FM-6 can be characterized simply by setting the transmitter power P to 0 dBW. Then, the magnitude of the interfering level P_{xmt} is -43 dBW, which is equal to -13 dBm, or $50 \mu\text{W}$ per 4 kHz. This corresponds to an attenuation of the in-band power by 43 dB. Note that if the in-band power is set to 10 dBW, the $43 + 10 \log(P)$ rule requires 53 dB of out-of-band attenuation, and the value of P_{xmt} is unchanged.

With respect to equations F-1 – F-3, to compute the interference from FM-6 into any AMT ground station, it is also necessary to know the following.

- The satellite's transmit antenna gain G_{xmt} in the direction of the affected AMT site (in order to convert the $43 + 10 \log(P)$ value into a radiated power level). This satellite-specific information is usually derived from information provided by the satellite operator or from FCC and/or ITU technical filings. For this example, the information is obtained from an FCC filing, as shown later in this section.
- The angle of arrival of the signal at the AMT site (in order to determine the appropriate value of the protection criteria). This can be obtained from a graph in the same FCC filing or can be computed from equations F-5a and F-5b.
- The distance from the satellite to the ground station (in order to compute the free space path loss). This is computed from equation F-6.

Note that these equations, as written, apply only to geostationary satellites.⁵⁷

$$\alpha_s = \arcsin[\cos(\theta_e)\cos(\phi_{se})] \quad (\text{F-5a})$$

$$\alpha = \arctan\left\{\frac{\sin(\alpha_s) - R_{earth}/R_{satellite}}{\cos(\alpha_s)}\right\} \quad (\text{F-5b})$$

$$r = \sqrt{R_{satellite}^2 - R_{earth}^2 \cos^2(\alpha) - R_{earth} \sin(\alpha)} \quad (\text{F-5c})$$

where α is the elevation angle to the satellite (which is the same as the angle of arrival α of the interference from the satellite), θ_e is the latitude of the AMT ground station, ϕ_{se} is the difference in the longitude values of the earth station and the satellite, and r is the distance from the AMT ground station to the satellite. Note that for geostationary satellites, the orbital radius $R_{satellite}$ is the radius of the earth, 6358 km, added to the height of the satellite above the surface of the earth, 36,000 km. For an angle of arrival of $\alpha = 90^\circ$, equation F-5 yields the value of $r = (R_{satellite} - R_{earth})$.

The geometry described by these equations is shown in [Figure F-2](#), excerpted from the text by Richharia.⁵⁸ The angle η in the figure corresponds to the angle α in equations F-5 and F-6. The elevation cut is a two-dimensional surface for which the trigonometry of the earth's curvature can be solved by inspection. For the sake of completeness, the geometry used for computing the azimuth angle is also shown. Although computation of the azimuth angle is not required here, it is needed for, and discussed in, example 8.

⁵⁷ This is because the declination of the satellite is set to 0 degrees, which causes several of the terms from a more general set of equations to disappear.

⁵⁸ M. Richharia. *Satellite Communications Systems, Second Edition*, New York; London: McGraw-Hill, 1999, page 37.

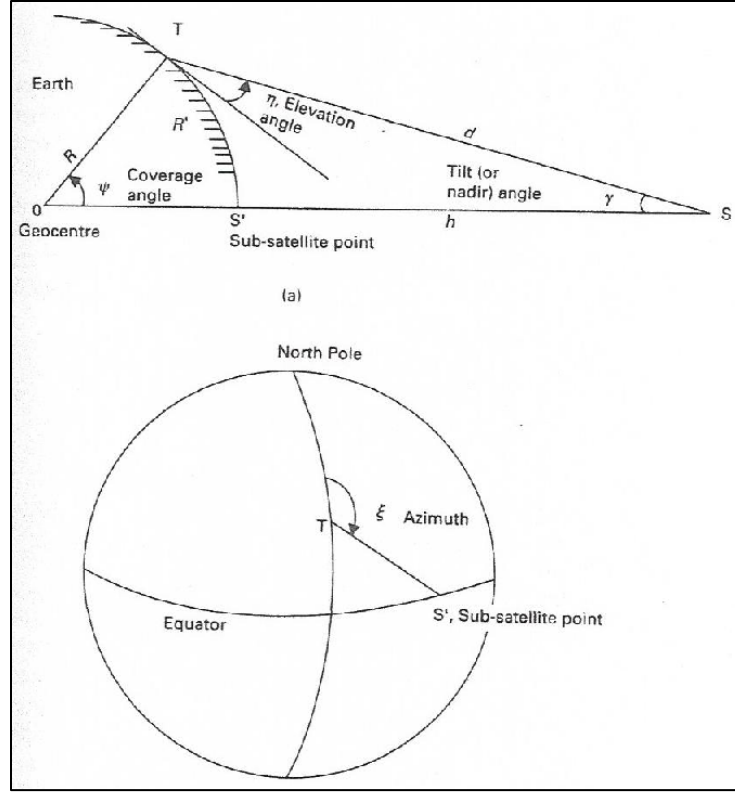


Figure F-2. Geometry of a Geostationary Link Showing (a) Elevation, (b) Azimuth from a Point T on the Earth.

For Pax River, the latitude/longitude is approximately 38°N/76°W. Assuming an earth radius of 6358 km, a satellite orbital radius of 6358 km + 36,000 km, a satellite sub-orbital longitude (also known as Right Ascension) of 115.2°W, an OOB of -43 dBW/4kHz, and the maximum value of the FM-6 antenna gain of 34.7 dBi (from [Figure F-3](#)) yields:

$$\alpha_s = \arcsin[\cos(38^\circ)\cos(115.2^\circ - 76^\circ)] = 37.64^\circ \quad (\text{F-6a})$$

$$\alpha = \arctan\left\{\frac{\sin(\alpha_s) - 6358\text{km}/42358\text{km}}{\cos(\alpha_s)}\right\} = 30.18^\circ \quad (\text{F-6b})$$

$$r = \sqrt{42358^2\text{km}^2 - 6358^2\text{km}^2\cos^2(30.18^\circ)} - 6358\text{km}\sin(30.18^\circ) = 38804\text{km} \quad (\text{F-6c})$$

Contours shown in [Figure F-3](#) are -2, -4, -6, -8, -10, -15, and -20 dB relative to the beam peak of 34.7 dBi.

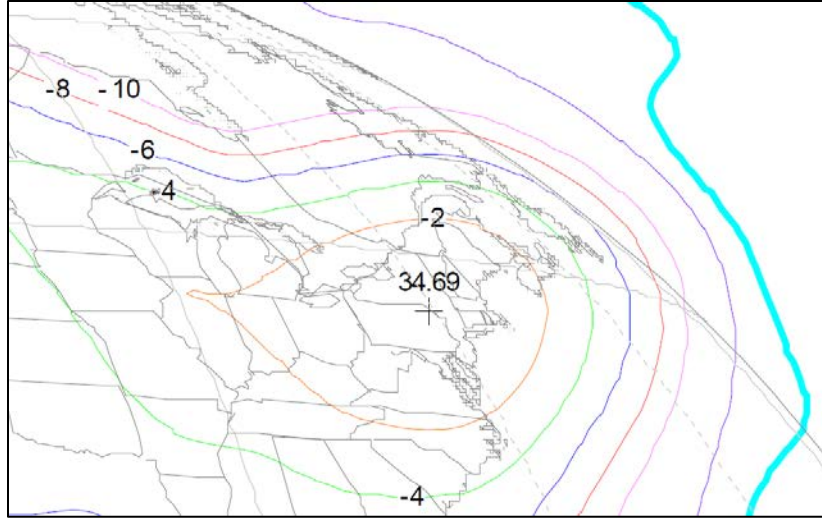


Figure F-3. Digital Audio Radio Service Downlink Beam Gain Contours

Thus, the elevation angle $\alpha = 30.2^\circ$ and the distance r from the ground station to the satellite is 38,804 km. Using the Friis equation, we have a received PFD at the ground station PFD_{rec} of

$$\frac{P_T G_T}{4\pi r^2} = \frac{10^{-4.3} \times 10^{3.47}}{4\pi (38804 \times 10^3)^2} = -171 \text{ dBW/m}^2 \text{ in 4 kHz} \quad (\text{F-7})$$

The upper S-band protection criteria provide three PFD protection values as a function of α , as shown in [Table 2-8](#).

Thus, the relevant Rec M.1459 protection criterion for this example is the value for an interference angle of arrival $>11.5^\circ$, which is -162 dBW/m^2 in 4 kHz.

Since the OOB fall below the maximum level stipulated by Rec M.1459 for this angle of arrival, there is no out-of-band interference from FM-6 to the AMT site at Pax River. Note that the derivation of this result required no information about the size, tower height, or pointing direction of the AMT antenna.

Repeating the computation for other ground stations is straightforward; however, since no analytic expression for the antenna gain of the satellite is available, the appropriate value of the gain of the satellite's downlink antenna must be obtained from [Figure F-3](#). [Figure F-4](#), which shows the angle of arrival of the signal from the satellite, provides a convenient check of the computation of α from equations F-5a and F-5b.

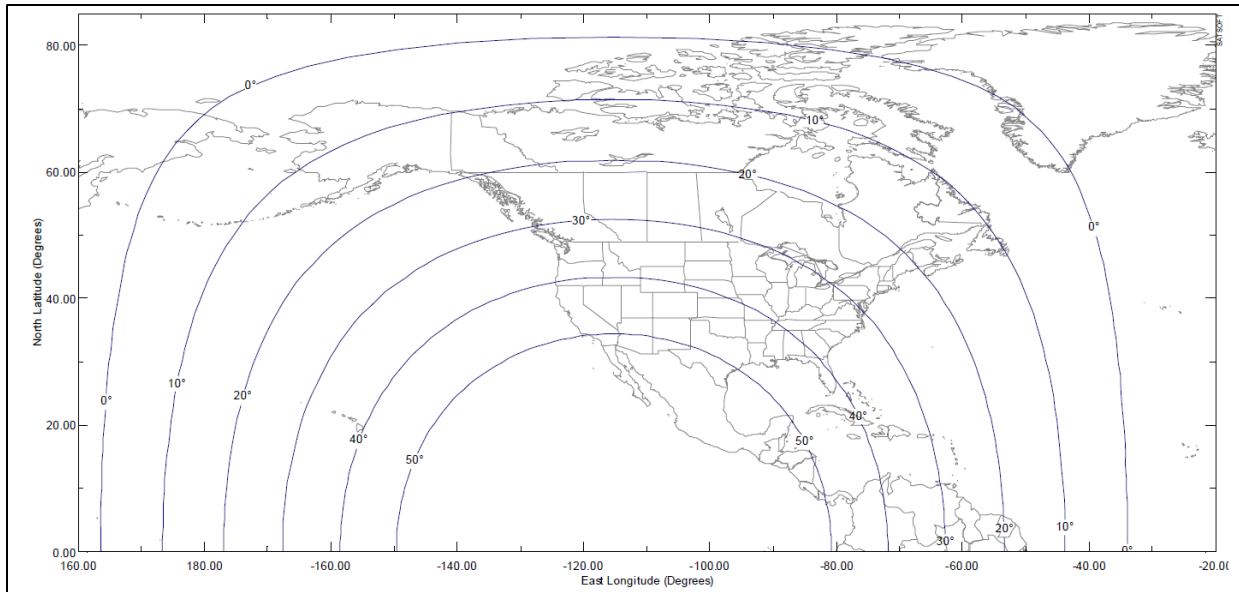


Figure F-4. Elevation Angles from Surface of the Earth to the 115.2° West Longitude Orbital Location

Example 4. Frequency scaling of interference and interference criteria to different reference bandwidths

As mentioned above, the reference bandwidth of 4 kHz for the PFD protection levels in Rec M.1459 is easily scaled to other values. This is done assuming that the required protection level is independent, of which 4 kHz of a typically 1 – 5 MHz AMT channel is affected.

This example must also take into account the reference bandwidths. For example, the permitted interference into a 1-MHz AMT channel is $10^6/4000$ times the appropriate dB(W/m²) in 4 kHz protection level from the list above; however, the spectral density of the interference into, for example, a 5-MHz AMT channel at 1520 – 1525 MHz, may vary across the 5 MHz in question. In addition, the reference bandwidth specified for the protection criterion for a given frequency band may be as large as 27 MHz, which is the case for the EESS band from 1400 – 1427 MHz; however, the interference into the AMT band may be a function of frequency. This is the case for interference from the WCS service in 2345 – 2360 MHz (i.e., the band that separates SiriusXM from the AMT frequencies in the upper S-band from 2360 – 2395 MHz).

In Section 27.53 of its rules (cf. footnote 392 of the FCC’s Order on Reconsideration)⁵⁹, the FCC stipulates that interference into the AMT band at 2360 – 2390 MHz from the WCS band at 2345 – 2360 MHz is to decrease as a function of frequency according to the following emission mask:

Specifically, WCS base and fixed stations’ OOB must be attenuated by a factor of not less than $43 + 10 \log (P)$ dB in the 2360-2362.5 MHz band, $55 + 10 \log (P)$ dB at 2362.5-2365 MHz band, $70 + 10 \log (P)$ dB at 2365-2367.5 MHz band, 72

⁵⁹ Federal Communications Commission. “Amendment of Part 27 of the Commission’s Rules to Govern the Operations of Wireless Communications Services in the 2.3 GHz Band.” WT Docket No. 07-293. In *Order on Reconsideration*. FCC 12-130. 17 October 2012. Available at https://apps.fcc.gov/edocs_public/attachmatch/FCC-12-130A1.pdf.

+ 10 log (P) dB at 2367.5-2370 MHz band, and 75 + 10 log (P) dB above 2370 MHz. WCS mobile and portable devices' OOB E must be attenuated by a factor of not less than 43 + 10 log (P) dB at 2360-2365 MHz, and 70 + 10 log (P) dB above 2365 MHz. *See 2010 WCS R&O*, 25 FCC Rcd at 11766 para. 135, 11785 para. 182; 47 C.F.R. §§ 27.53(a)(1)(iii) and (4)(iii).

[Figure F-5](#) shows the FCC-specified emissions profile in graphical form. The vertical axis represents $xx + 10 \log(P)$ in dB.

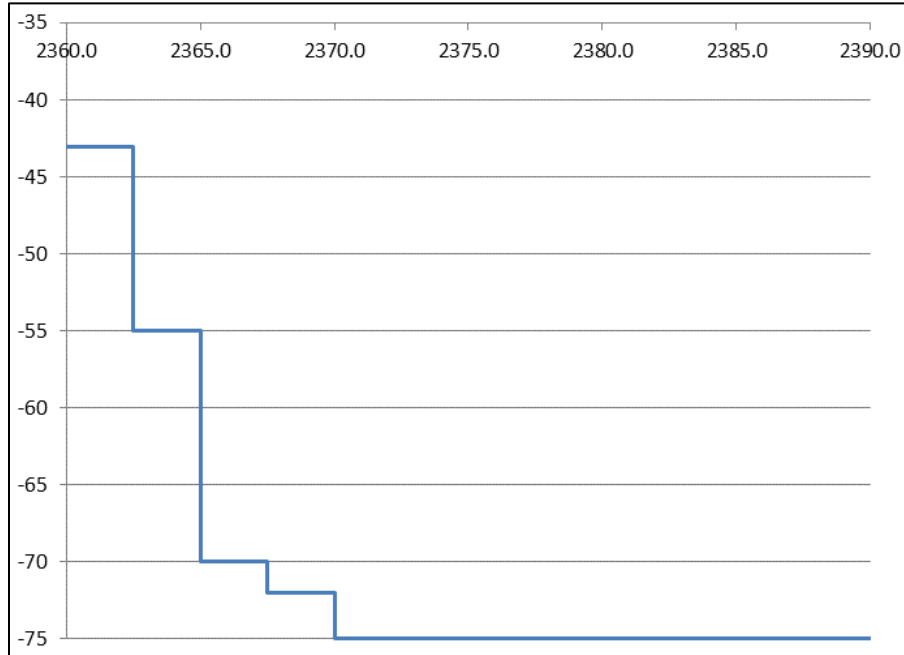


Figure F-5. FCC Emission Mask for the WCS OOB E Band from 2360 – 2390 MHz

The rule above provides the guidance on how to compute the net interference from a WCS transmitter into a 5-MHz AMT band, for example, operating at 2360 – 2365 MHz. The two OOB E levels, -43 dBW and -55 dBW are averaged according to the following equation:

$$\begin{aligned} & \text{OOB E in Watts per 4 kHz averaged across 5 MHz at (2360 – 2365 MHz)} \\ &= G_{WCS\ xmt} \times \frac{4 \times 10^3}{5 \times 10^6} \times \left\{ \left(\frac{2.5}{5} \right) \times 10^{-4.3} + \left(\frac{2.5}{5} \right) \times 10^{-5.5} \right\} \end{aligned} \quad (\text{F-8})$$

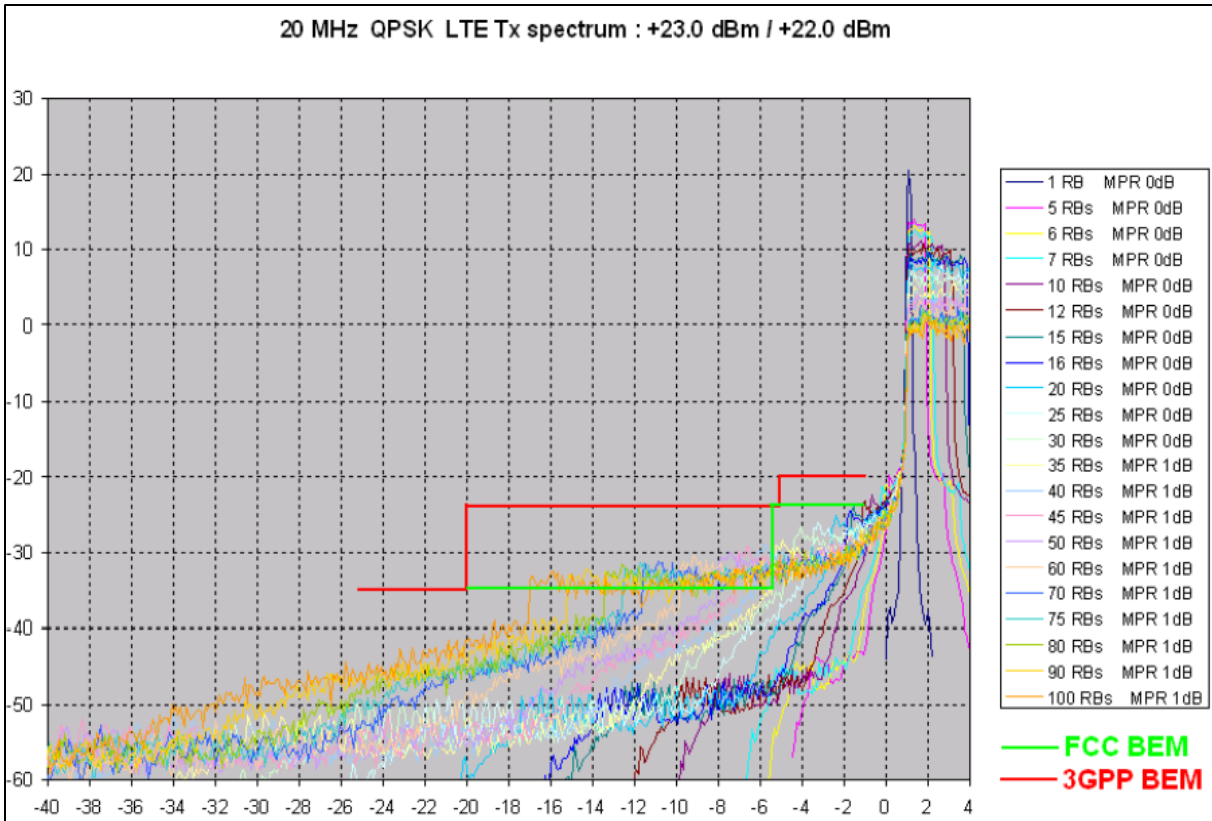
To convert from watts to dBW, the result of equation F-8 is converted to a base ten logarithm and multiplied by 10, as usual.

Note that $G_{WCS\ xmt}$ is the gain of the WCS transmit antenna in the direction of the AMT ground station antenna that is being considered. In equation F-8, the $4E3/5E6$ term re-normalizes the average OOB E level across the 5-MHz-wide AMT channel width to the 4-kHz reference bandwidth of Rec M.1459.

Equation F-8 is the EIRP of the interfering WCS transmitter as measured at the aperture of the WCS transmit antenna. To compute the interference received at the aperture of the AMT ground station antenna, it is necessary to include the path loss by using equation F-1. It is necessary when using equation F-1 to convert the path loss to dB or the EIRP from dBW to watts when using equation F-1. For comparison with the protection levels of Rec M.1459, the result of equation F-1 should be converted to dBW/m² in 4 kHz.

It is important to note that the OOB levels given above represent a “stair-step pattern”, where the OOB in each segment of spectrum (in this case, each 2.5-MHz segment) is constant. Actual OOB measurements, which are typically used for computations when available, decrease from one end of the band segment to the other. In order to average the OOB properly in these conditions, the 2.5-MHz segments are broken up into, for example, 0.1 to 1.0-MHz segments. These are then averaged using the methodology of equation F-8, but with more terms inside the curly brackets. To determine whether the segments are narrow enough, it is sufficient to keep dividing the segments by a factor of 2 and then re-computing the OOB using equation F-8. This is repeated until the end result is constant within the desired resolution of the computation (e.g., 0.1 dB).

[Figure F-6](#) illustrates the difference between the stair-step emissions masks published by the FCC and by an industry group, in this case the Third Generation Partnership Project, or 3GPP consortium. [Figure F-6](#) also shows the simulated in-band and OOB of a 4G LTE-A handset uplink as a function of the number of resource blocks assigned to a particular signal.

Figure F-6. Simulated OOB Emissions from an LTE Handset⁶⁰

It is useful to work the problem of OOB from aircraft AMT transmitters into the EESS spectrum from 1400 – 1427 MHz. Resolution 750⁶¹ stipulates that the net radiated OOB from an AMT transmitter operating in the band 1429 – 1452 MHz (not including the gain of its antenna), when averaged over the entire 27-MHz EESS band,⁶² should not exceed a power level of –28 dBW.

[Chapter 2](#) stipulates that the OOB in any 1 MHz from an AMT transmitter be attenuated by an amount of at least $55 + 10 \log(P)$ dBW. When scaled to a bandwidth of 27 MHz, an additional $10 \log(27 \text{ MHz}/1 \text{ MHz}) = 14.3 \text{ dB}$ must be added to the –55 dBW OOB level. This yields an OOB of –41 dBW per 27 MHz, which is well below the requirement of Resolution 750.

The point here is that when scaling from one reference bandwidth to another, at least some insight into the context of the problem is needed. Simply applying the same rule, by rote, from one scenario to another can lead to errors.

⁶⁰ Wireless Communications Association. “4G Device Out of Band Emissions and Larger Channel Bandwidths,” October 2011. Accessed 21 March 2017. Available at <https://ecfsapi.fcc.gov/file/7021715550.pdf>.

⁶¹ International Telecommunications Union. “Compatibility between the Earth exploration-satellite service (passive) and relevant active services” *Final Acts WRC-15 – World Radiocommunication Conference*. Geneva, 2015. pp. 399-403.

⁶² The wideband radiometric sensors aboard EESS satellites apparently receive signals across the entire 27 MHz of the band at once, with no effort made to determine where in the band a signal originates.

Example 5: Computation of path loss using the two-ray model

For computing interference to an AMT ground station from terrestrial sources, it is necessary to include the effects of terrain, the curvature of the earth, ground reflections, Fresnel zone impingement, etc. All of these effects can be lumped into the value of path loss that is defined by equation F-2.

With the exception of what is known as the two-ray model, consideration of these effects in a path loss computation requires, in addition to antenna height information and the distance between the interferer and victim receiver, an accurate terrain database (i.e., a topographical map of the path between the interference source and the AMT site). Other effects, such as additional path loss caused by buildings and other clutter, can be included as long as the details of such loss are justified by measurements and databases whose accuracy and precision go well beyond the 1 arc-second (30 meter) resolution that is typically used for path loss modeling at this time.

The two-ray model treats the ground as a reflector, and takes into account the interference nulls caused by this reflection that occur at various distances and heights from the transmitting aircraft or interference source. [Figure F-7](#) shows this graphically. When a resulting null coincides in position with the aperture of the AMT receive antenna, a significant signal fade (15 – 30 dB) occurs. Depending on the bandwidth of the signal, the fade can cause attenuation across the entire bandwidth of the signal, or can cause just a portion of the signal bandwidth to suffer a reduction in received signal power.

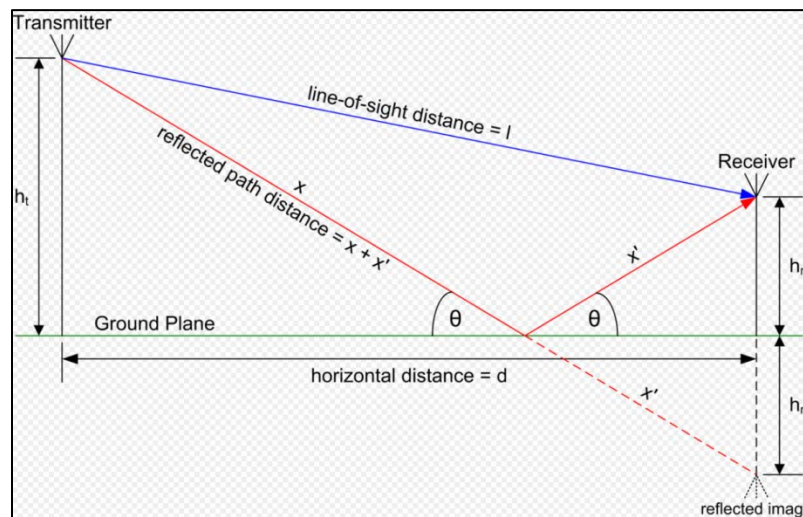


Figure F-7. Graphical Representation of the Two-Ray Model

Reflection can also cause enhancement of the received signal (or interference); however, for a two-ray, as opposed to three-or-more-ray model, this enhancement cannot exceed 3 dB. As noted, the fades can always be considerably larger than 3 dB in their amplitude. In fact, for aircraft, fades can occur not only from ground reflection of the telemetry signal, but from unwanted reflections of the telemetry signal from aircraft structures or from blockage of the direct signal path from the aircraft antenna to the ground station during aircraft maneuvers.

Since an aircraft in flight is constantly moving, telemetry signal fades are strong functions of time. For modeling purposes, this time dependence is characterized by a change in

the availability of the telemetry link. This is a key feature of Rec M.1459, and is the subject of example 6.

For static interferers, such as interference from a cellular tower, fades can be regarded as being constant, and are accounted for in the path loss software.

A graphical representation of path loss versus distance of the two-ray model is shown in [Figure F-8](#).⁶³ Note that the fades are deep and the signal enhancements are shallow. It is important to understand that the graph is for a particular combination of tower heights and signal wavelength.

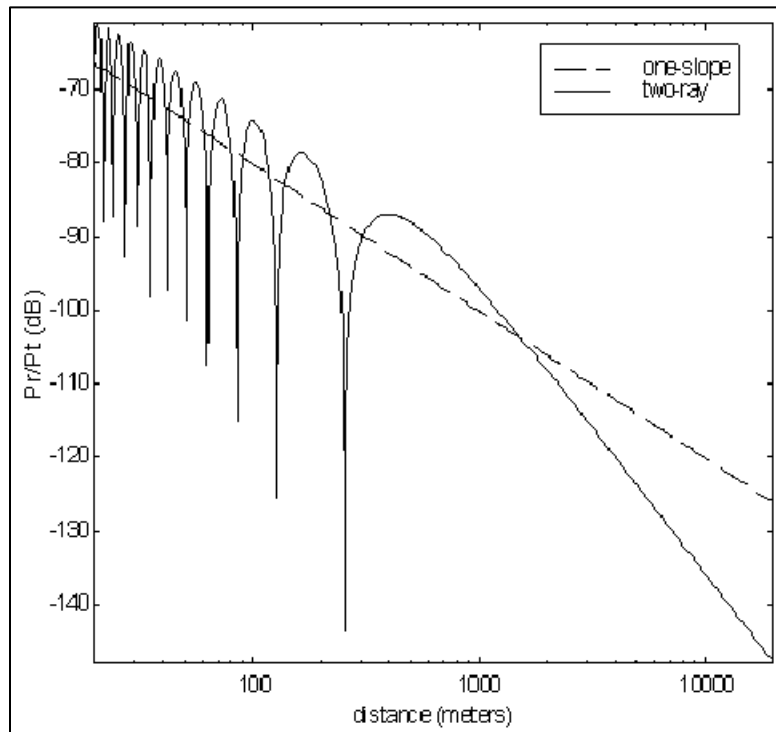


Figure F-8. Comparison of Free-Space One-Slope and Two-Ray Propagation Models

Fades are most prominent near the transmitter. For example, the two-ray model is evident on airport aprons when a telemetry test cart is used to receive TM signals from an aircraft parked several hundred feet away. More importantly, the long-range reduction in signal strength for the two-ray model falls faster than the $1/r^2$ (i.e., 20 dB per decade of frequency) of the free-space single-ray signal. The $1/r^4$ roll-off of the two-ray model is 40 dB per decade.

The equations for computing the two-ray model can be found online, in text books, or from direct computation. If path loss software is available, it is convenient to compute the two-ray results for a particular situation by setting the terrain height to zero and using the default value of ground electrical conductivity provided by the software.

⁶³ Thomas Schwengler. "Wireless & Cellular Communications. Class notes for TLEN-5510 - Fall 2016. Accessed 27 July 2017. Available at <http://morse.colorado.edu/~tlen5510/text/classwebch3.html>.

Although the equations for the two-ray model can be rather daunting, in its simplest form, one uses flat-earth trigonometry to compute the difference in path lengths between the direct and reflected signals. This depends on the horizontal distance d , the altitude of the aircraft h_t , and the height above ground of the AMT receive antenna, h_r . Using trigonometry and assuming that the signal is reflected from the ground and/or sea with a reflection coefficient of magnitude 1, the aircraft altitudes and locations can be computed for which positive and negative signal reinforcement due to multipath occur. When the direct path and the reflected path differ by an even number of signal half-wavelengths $\lambda/2$, signal reinforcement occurs. When they differ by an odd number of half-wavelengths, deep fades occur.

For reflections from a smooth ocean surface, the conductivity of salt water can be used; however, Rec M.1459 anticipates this, and most interference to AMT ground station paths are not over water. Hence, the default value for ground conductivity is typically the correct value to use.

The equation for computing the curve shown in [Figure F-8](#) is given by

$$p_0(t) = \sqrt{(G_t G_r)} \frac{\lambda}{4\pi} \left(\frac{\exp(j2\pi l_0/\lambda)}{l_0} + \Gamma \frac{\exp(j2\pi l'_0/\lambda)}{l'_0} \right) \quad (\text{F-9})$$

Where l_0 and l'_0 are the line-of-sight distances l and $x + x'$ shown in [Figure F-7](#).

With respect to the phrase “direct line of sight”, it is convenient to note that this is computed as

$$D_{LOS} = \sqrt{2h_1 R_{earth} \times 4/3} + \sqrt{2h_2 R_{earth} \times 4/3} \quad (\text{F-10})$$

where h_1 and h_2 are the heights of the transmit and receive antennas, R_{earth} is the nominal radius of the earth of 6358 km, and the factor of $4/3$ accounts for atmospheric refraction.

Example 6. Rayleigh fading of the aircraft telemetry signal

There is a generalization of the two-ray model that adds the effects of reflections of the telemetry signal from aircraft structures and/or blockage of the telemetry signal by these same structures during aircraft maneuvers. This is Rayleigh scattering that plays an important role in the technical details of Rec M.1459. The resulting Rayleigh distribution can be used to predict the percentage of time that the link margin of any air-to-ground telemetry link will fall below the threshold value needed for the link to be viable. This is illustrated by [Figure F-9](#), [Figure F-10](#), and [Figure F-11](#).

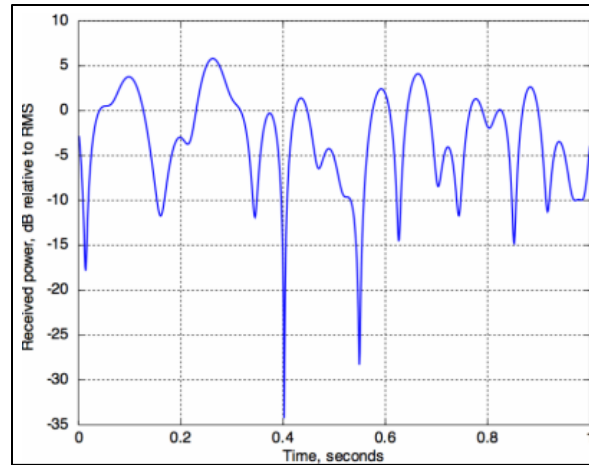


Figure F-9. Rayleigh Fading of a Signal Transmitted from a Moving Platform⁶⁴



Figure F-10. S-band Telemetry Signal Received from an Aircraft in Flight⁶⁵

⁶⁴ Wikipedia. "Rayleigh fading." Retrieved 27 July 2017. Available at https://en.wikipedia.org/wiki/Rayleigh_fading

⁶⁵ D.G. Jablonski. "Demonstration Of Closed Loop Steering of Antenna Patterns For Mitigating Antenna-To-Antenna Interference In Two-Antenna Telemetry Installations On Military Aircraft," Instrumentation Test Technical Symposium, New Orleans, LA, 25 August 2004.

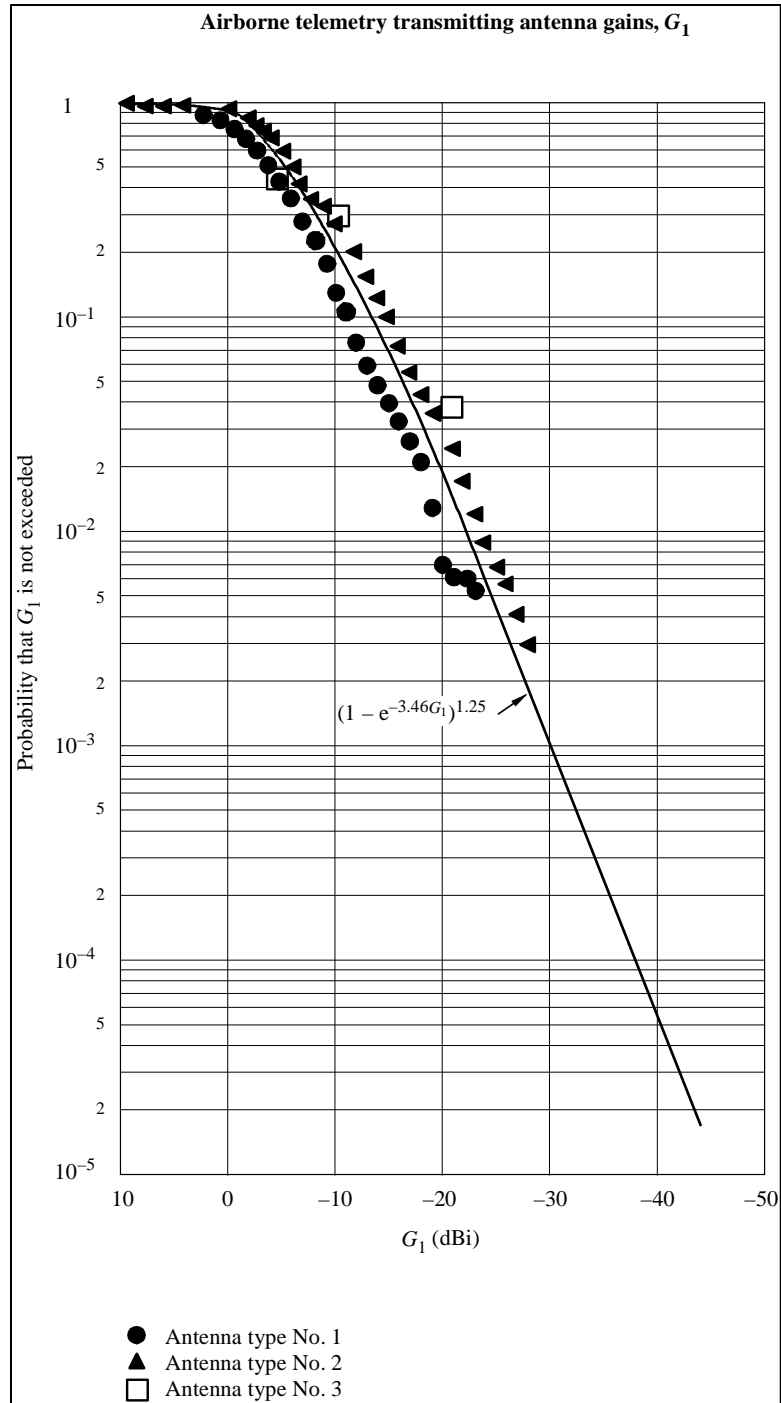


Figure F-11. Rayleigh Distribution as Presented in Figure 2 of Rec M.1459 (Jablonski 2004).

[Figure F-9](#) is a one-second time slice of the strength of a Rayleigh-faded signal as received from a moving transmitter. [Figure F-10](#) is the measured signal strength of a Rayleigh-faded aircraft telemetry signal as a function of time as received at an AMT ground station.

[Figure F-11](#) relates the depth of a fade to a numerical value of the probability as a percentage of time that such a fade will occur. The mathematical expression given in the figure

is an essential component of the computations of the Rec M.1459 protection criteria. Specifically, the Rayleigh distribution provides the connection between interference and link availability. This is an extension of less-sophisticated link budgets that consider only the effect of interference on BER, without considering whether the interference will cause the link to fail completely.

Note that the Rayleigh distribution presented above is typically used in AMT link budget computations by including the fade in the instantaneous value of the gain G_{xmt} of the aircraft telemetry transmit antenna, as opposed to including it as a component of the path loss. This keeps the consideration of fading due to aircraft geometry and motion independent of the consideration of terrain effects (described below), for which Rayleigh scattering is typically not relevant.

Rec M.1459 requires a threshold signal-to-noise value of $(C/N)_T$ of 15 dB. For the AMT system values specified in Rec M.1459, the AMT channel bandwidth is 3 MHz and the system noise temperature is 250 Kelvin. The required AMT telemetry signal receive power is

$$C = kTB \times 10^{1.5} = 1.38 \times \frac{10^{-23} \text{ Joule}}{\text{Kelvin}} \times 250 \text{ Kelvin} \times (3 \times 10^6 \text{ Hz}) = 3.27 \times 10^{-13} \text{ Watts} = -124.85 \text{ dBW}. \quad (\text{F-11a})$$

The corresponding expression for the Friis equation for an aircraft antenna transmit gain of -25 dB and including the effective area of $\lambda^2 G_{rec}/4\pi$ of the AMT ground station receive antenna with $P_T = 3\text{W}$, $G_{rec} = 41.2 \text{ dB}$, $r = 320 \text{ km}$, and $\lambda = 0.2 \text{ meter}$ (per Rec M.1459) is

$$\frac{P_T G_T \lambda^2 G_{rec}}{(4\pi r)^2} = \frac{3 \times 10^{-2.5} \times (.2)^2 \times 10^{4.12}}{(4\pi)^2 \times (320 \times 10^3)^2} = 3.09 \times 10^{-13} \text{ Watts} = -125.10 \text{ dBW} \quad (\text{F-11b})$$

Example 7: Computation of path loss using commercial software that implements the L-R/ITM and P.452 models

Since the two-ray model is seldom adequate for predicting path loss over terrain, a wide assortment of models that include the effects of terrain has been developed. These are based on different combinations of assumptions regarding reflection, refraction, diffraction, signal blockage, Fresnel zone impingement, etc., and are available with terrain databases already included. These include several, such as Terrain-Integrated Rough-Earth Model, L-R, ITM, and Free-space plus reflection and multiple diffraction.

Another category of models is contained in ITU-R recommendations that are similar in structure to Rec M.1459. Three of the most important models are:

- P.452-16: Prediction procedure for the evaluation of interference between stations on the surface of the Earth at frequencies above about 0.1 GHz;⁶⁶

⁶⁶ International Telecommunication Union. "Prediction procedure for the evaluation of interference between stations on the surface of the Earth at frequencies above about 0.1 GHz." ITU-R Recommendation P.452-16. July 2015. May be superseded by update. Retrieved 30 March 2017. Available at <https://www.itu.int/rec/R-REC-P.452/en>.

- P.1546: Method for point-to-area predictions for terrestrial services in the frequency range 30 MHz to 3 000 MHz;⁶⁷
- P.528: Propagation curves for aeronautical mobile and radionavigation services using the VHF, UHF, and SHF bands.⁶⁸

As this example only makes use of the L-R/ITM and P.452 models, information regarding the other two models is excluded from this document. The P.452 model can be regarded as the internationally approved version of the ITM, which is an outgrowth of the L-R model. The ITM and L-R models were developed for domestic purposes by the United States at the National Institute of Standards and Technology. Because of the need for technical studies presented to the ITU to utilize ITU-sanctioned models, P.452 has become the de facto standard for domestic studies that require path loss computations based on actual terrain.

In order to use P.452, it is necessary to purchase a commercial software package such as EDX Signal Pro (favored by the AMT community at the present time), ATOLL (used by cellular carriers), or Visualyse (used by those who need to consider platform motion and the time-dependent effects of this on interference). Such commercial packages typically include most, and sometimes all, of the models listed here.

There is also a non-commercial version of P.452, in the form of macro-enabled Excel spreadsheets, that is available free of charge from the ITU at www.itu.int. It models the effects of terrain using data imported from, readily available terrain databases.

For AMT, the fundamental terrain database is usually the government-provided, freely available USGS 1 arc-second (30 meter) resolution topographic map data. The Shuttle Radar Topography Mission database is sometimes used, although it is comprised of overhead measurements, and its validity for computing point-to-point path loss is sometimes questioned.

It is important to consider how accurate these propagation models are. A comparison study⁶⁹ suggests that error bars of 15 dB in the path loss computation are typical. Perhaps a better approach is to use existing measurement data from NTIA,⁷⁰ which exist in the form of five separate studies that are available from the Defense Technical Information Center. It is straightforward to insert the location, frequency, and antenna height details provided in the studies into any of the commercial models for comparison purposes.

[Figure F-12](#) and [Figure F-13](#) illustrate how data obtained using a commercial package, in this case EDX Signal Pro, are presented for a series of point-to-point links between cellular towers and an AMT receive site at Pax River. The purpose of the simulation is to compute path loss values from each of the cellular sites to the AMT ground station. The assumption that Pax

⁶⁷ International Telecommunication Union. "Method for point-to-area predictions for terrestrial services in the frequency range 30 MHz to 3 000 MHz." ITU-R Recommendation P.1546-5. September 2013. May be superseded by update. Retrieved 30 March 2017. Available at <https://www.itu.int/rec/R-REC-P.1546/en>.

⁶⁸ International Telecommunication Union. "Propagation curves for aeronautical mobile and radionavigation services using the VHF, UHF, and SHF bands." ITU-R Recommendation P.528-3. February 2012. May be superseded by update. Retrieved 30 March 2017. Available at <https://www.itu.int/rec/R-REC-P.528/en>.

⁶⁹ Phillips, C., D. Sicker, and D. Grunwald. "Bounding the Practical Error of Path Loss Models." International Journal of Antennas and Propagation, Volume 2012 (2012). Retrieved 21 March, 2017. Available at <https://www.hindawi.com/journals/ijap/2012/754158/>.

⁷⁰ For example, Hufford, G. A. and F. K. Steele. "Tabulations of Propagation Data over Irregular Terrain in the 75-To 8400-Mhz Frequency Range - Part V: Virginia. NTIA Publication 91-282, December 1991. Retrieved 27 July 2017. Available at <https://www.its.bldrdoc.gov/publications/download/91-282.pdf>.

River is the transmitter site is a feature of the software package's point-to-multipoint analysis routine. Since the purpose of the analysis is to compute a value for the path loss for each link, including the effects of terrain, reversing the roles of transmitter and receiver is of no numerical consequence.

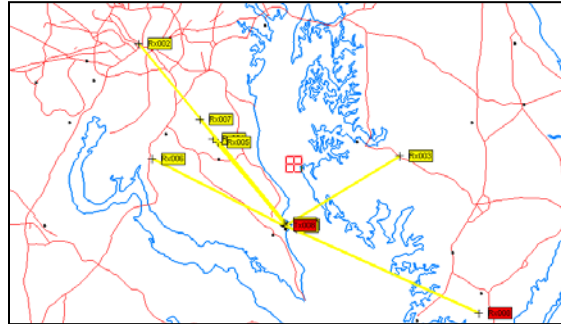


Figure F-12. EDX Signal Pro Map of Hypothetical Transmitters and Receivers in the Pax River Region.

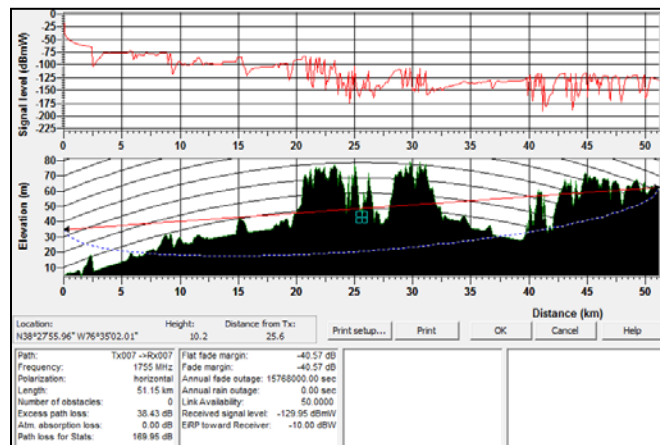


Figure F-13. EDX Signal Pro Path Loss Profile for the TX007 to RX007 Path

The simulation results of [Figure F-12](#) and [Figure F-13](#) are followed in [Figure F-14](#) by experimental data measured by NTIA engineers and reported in Hufford and Steele.

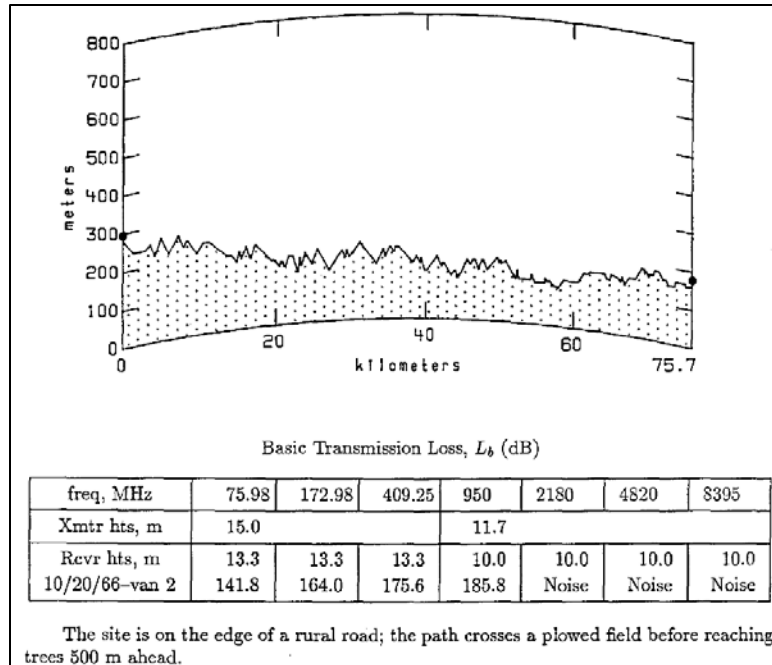


Figure F-14. Actual Measured Path Loss Data from an NTIA Report (cf. footnote 71)

[Figure F-12](#) is a map showing various point-to-point transmitter-to-receiver links, TX001 to RX001, TX002 to RX002, etc. On the map, the same geographic location is used for all the transmitters, with the active transmitter for the example analysis (TX008) displayed on top of the other transmitters. Map data such as this is essential for computing aggregate interference as a function of bearing angle to an AMT site.

[Figure F-13](#) shows the terrain profile, including the effects of the earth's curvature, for the TX007-to-RX007 data link. The path loss, computed in this example using the L-R model, is 169.95 dB. The dashed blue line represents the extent of the Fresnel zone, showing how the terrain blockage impinges the zone, thus creating excess path loss.

For these simulations, it is typically appropriate to use average value settings for parameters related to variability. Although actual values for terrain blockage are used throughout the simulation, it is necessary to make a similar (e.g., average) assumption about whether diffraction due to terrain is modeled as knife-edge versus smooth-edge model.

In any case, it is important to validate model simulations using actual measurements wherever possible. This is the purpose of including [Figure F-14](#), which is an example path profile from the many measurements made by NTIA.

The terrain data in [Figure F-14](#) was obtained from manual inspection of a topographic map by members of the NTIA team, and was hand-entered into the graphing software used for preparing the measurement report. This is an important point. In interference studies, it is often the case that only a few cellular towers or other interference sources cause the aggregate level of interference to exceed Rec M.1459 limits. It is possible to re-create the data used in a commercial package by reference to a local topographic map and enter the data in the ITU-R

P.452 spreadsheet for analysis. The results are as accurate as those produced by the expensive packages, but can be obtained by using Excel spreadsheets.

Given the major effort required to collect experimental data, it is generally not practical to make measurements at all of the frequencies of interest with respect to interference computation. It might well be the case that the path loss at 1500 MHz, rather than the loss at the measured frequency of 2180 MHz, is the value of interest.

Since the wavelength is a component of the path loss value, and since the wavelength depends on the signal frequency, it is necessary to consider how to convert a measurement made at one frequency to an estimate of path loss at a different, but relatively close, value of frequency, such as the 2180-MHz to 1500-MHz example given here.

To a first approximation, path loss is independent of frequency in the 1 – 6 GHz bands, although effects of building attenuation are significant and signal absorption by foliage becomes important at the higher end of this frequency range. At even higher frequencies, such as the 12.6-MHz carrier frequency used for satellite television downlinks, foliage and rain attenuation are both significant. At even higher frequencies atmospheric absorption due to water vapor is extremely important, and care is often taken to operate in windows in the 35-GHz and 90-GHz ranges.

The explicit inclusion of a value for λ in equation F-2 for the path loss is a computational artifact. In the Friis equation, it more properly connects the gain G_{rec} of the receive antenna to its effective area $\lambda^2 G_{rec}/4\pi$. Shifting λ^2 from the effective area to the path loss portion of the equation makes the path loss a dimensionless parameter, which is necessary in order for its value to be specified in dB.

Thus, when a path loss value for 2180 MHz is used as an estimate for the path loss at 1500 MHz, it is necessary to correct the path loss value using equation F-12.

$$path\ loss_{1500} = \left(\lambda_{1500} / \lambda_{2180} \right)^2 \times path\ loss_{2180} \quad (F-12)$$

Example 8. Consideration of the antenna patterns of terrestrial cellular base stations

It is necessary to know specific details of the gain pattern, location, height above ground, and pointing direction of the interfering antenna in order to replicate the computation for the case of a terrestrial interferer. If the terrestrial interferer is a cellular tower that hosts multiple sectorized antennas, this requires specific knowledge about the antennas that are used and how their electronic adjustments, specifically electrical down-tilt, are configured.

This example requires the equation for computing the bearing angle from a cellular tower to an AMT site, and vice versa, when the latitude and longitude of each are specified. This is done using the mathematics of spherical trigonometry for the great circle arc that leads from one site to the other.

Then, using the sector antenna pointing angles relative to true north, the gain of each sectoral antenna on the tower in the direction of the AMT site is derived. The gain of tower-mounted cellular antennas may be specified as two pattern files, one for a 360° horizontal sweep at zero degrees elevation, and one for a 360° vertical sweep at zero degrees of azimuth with respect to the main lobe of the antenna.

To further complicate the problem, the main beam of each sectoral antenna can be pointed downward by varying increments of angle (e.g., 0 – 9 degrees) by remote control using the electrical down-tilt feature of the antenna. For the cellular antennas of interest, each permissible value of down-tilt is accompanied by its own pair of pattern files.

Mechanical down-tilt can also be used. This requires modifying the indexing of entries in the vertical file for the antenna so that, for example, the vertical pattern gain entries are shifted by the amount of the mechanical down-tilt.

The purpose of down-tilt is to permit adjustment of patterns to improve coverage of a typically urban or suburban area as new, additional cellular towers are in-filled, e.g., when a network is expanded to maintain coverage while increasing capacity.

In any case, it is necessary to combine the two-dimensional horizontal and vertical patterns into a single three-dimensional pattern using an interpolation algorithm. Manufacturers of cellular antennas of interest are not the main source of advice on how to do this. Instead, the academic literature summarizes and compares four different algorithms. These are called:

- Arithmetic mean;
- Bi-linear interpolation;
- Weighted bi-linear transformation;
- Horizontal projected interpolation.

With respect to the antenna pattern files, G_{vert} and G_{horiz} , θ represents elevation (with positive θ in the downward direction from $\theta = 0$ at the horizon) and the azimuth ϕ equals 0 in the center of the main lobe (with positive ϕ going counterclockwise as viewed from above).⁷¹

The formula for the arithmetic mean is the simplest, and is given by:

$$G(\theta, \phi) = 1/2 (G_{\text{vert}}(\theta) + G_{\text{horiz}}(\phi)) \quad (\text{F-13})$$

The equations for the second and third algorithms are rather complicated, and are not repeated here.

The final algorithm, horizontal projected interpolation, is used by one of the major commercial software packages. It has also been incorporated into an AFTRCC-developed production-grade interference analysis software package. The algorithm is given by:

$$G(\phi, \theta) = G_h(\phi) - \left[\frac{\pi - |\phi|}{\pi} \cdot (G_h(0) - G_v(\theta)) + \frac{|\phi|}{\pi} \cdot (G_h(\pi) - G_v(\pi - \theta)) \right] \quad (\text{F-14})$$

It is necessary to determine the appropriate values of ϕ and θ to use the interpolation algorithms. These are often generated by the software package that is used to compute the path loss between the AMT site and the individual cellular tower. Typically, the elevation angle θ is close enough to being horizontal that it can be assumed to be zero. Given that the angular resolution of the pattern files is only one degree and that $G_v(0^\circ)$ is approximately equal to $G_v(1^\circ)$, this is a reasonable approximation.

⁷¹ Sign conventions for θ and ϕ should be verified for each case by inspection of the antenna files and cross-checking with the manufacturer's data sheets.

Even when the azimuth angle ϕ is produced by the path loss software, it is helpful to use the formula below to confirm that no data entry errors that would change the value of azimuth have occurred. This is done using the following formula from spherical trigonometry:

$$\sin(\phi) = \frac{\cos(\text{latitude}_{\text{AMT}})}{\sin\left(\frac{\text{Distance}_{\text{cell-AMT}}}{R_{\text{earth}}}\right)} \cdot \sin(\text{longitude}_{\text{cell}} - \text{longitude}_{\text{AMT}}) \quad (\text{F-15})$$

Note that ϕ represents the azimuth angle from the cellular tower to the AMT ground station antenna. For computing the gain of the cellular antenna in the direction of the AMT antenna, the direction that each sectoral antenna mounted on the tower is pointed with respect to north must be added (or subtracted, as appropriate) to compute the sectoral antenna's bearing to the AMT ground station.

As shown in the next example, when computing aggregate interference from an ensemble of cellular towers, it is necessary to compute the bearing of the AMT site to each cellular tower and the angular offset of this bearing from the main lobe of the AMT antenna. This is done by reversing the roles of the AMT site and the cellular tower in the above equation.

Alternatively, the reverse bearing can be computed directly from ϕ for the cellular tower, but certain quadrant conventions are needed in order to resolve ambiguities between the bearing angle ϕ_{amt} and its complement $180 - \phi_{\text{amt}}$. This issue is typically discussed in basic satellite communication textbooks, and is resolved by depicting a simple drawing of the cellular tower and AMT site locations on a chart. When processing hundreds of tower-to-AMT locations at once, the quadrant correction must be programmed carefully.

As always, care must be taken to not inadvertently default to the equations of flat-earth trigonometry. In this limit, the elevation angles to an aircraft from a cellular tower are always overstated, leading to a misapplication of the Rec M.1459 protection criteria.

Example pattern files can be found online.⁷² It is common for the files to give a maximum value of the gain at the center of the main beam of the pattern. The file entries then correspond to the relative attenuation of the pattern relative to this value of G_{max} .

Example 9. Aggregation of interference from a network of cellular base stations to one or more AMT ground stations⁷³

The large-scale simulation of interference from thousands of cellular base stations and their associated handsets will be a major activity for both the civil and DoD AMT communities as government spectrum is auctioned for use by commercial broadband carriers. This example presents a stand-alone, step-by-step procedure for accomplishing this. It can be implemented in a variety of ways, including as a collection of Excel spreadsheets in conjunction with the commercial software packages (e.g., EDX Signal Pro) referenced earlier in this appendix.

The steps for completing a coordination of a large collection of emitters with a single AMT ground station are as follows.

⁷² <http://www.commscope.com/Resources/Calculators/>, accessed 11 July 2017.

⁷³ Analysis of the aggregation of handsets requires the inclusion of statistical parameters that are developed in example 10. The analysis of an aggregation of handsets is provided in example 12.

1. The composite AMT ground station antenna pattern provided by equations 1(a) – 1(f) of Rec M. 1459⁷⁴ is used instead of patterns obtained on a site-specific basis for each of the hundreds of AMT ground stations in the United States. This composite pattern is shown in [Figure F-15](#). Use of this composite antenna pattern addresses several features unique to AMT operations and eliminates the need for detailed, site-specific technical details that are subject to change from one flight-test program to another, or even during individual test flights. The Rec M. 1459 pattern is to be used in lieu of, for example, the Wolfgain and Statgain patterns given in NTIA Report TM-13-489⁷⁵, although the Rec M. 1459 composite patterns are closely related to the Statgain patterns, as shown later in this appendix.

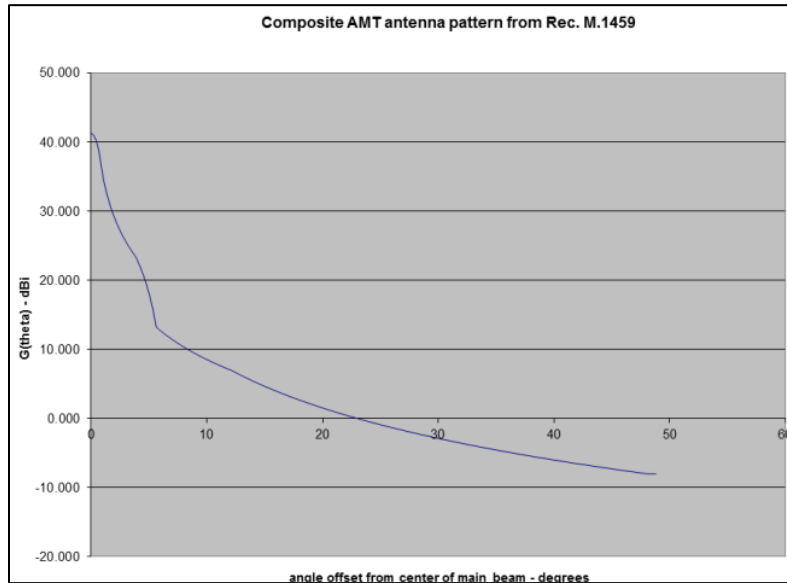


Figure F-15. Composite AMT Pattern from Rec M.1459

2. Instead of traditional interference-to-noise ratio (I/N) criteria, interference received at an AMT ground station is to be computed using the appropriate PFD limit from Rec M.1459. For example, this might be the Rec M. 1459 PFD limit for $0 - 2^\circ$ angles of arrival (with respect to the horizon) for L or S bands, namely -180 or -181 dB W/m² in 4 kHz. These levels represent the total permitted aggregate interference, as computed using the technique given in steps 3 - 5.

3. It is necessary to consider the interference from all directions with respect to the ground station antenna, including interference received through the side lobes and back lobes to compute aggregate interference. Furthermore, this aggregate interference must be recomputed for all possible pointing angles (in azimuth) of the AMT ground station antenna, which can rotate to point in any direction. It would be appropriate, for example, to compute aggregate interference for each of 720 pointing angles, measured in 0.5° increments.

4. To compute aggregate interference from hundreds of base stations, for example, it is necessary to group the eNodeBs into 0.5° -wide azimuth-of-arrival wedges, then to compute the aggregate PFD per wedge for each of these for each of 720 possible pointing angles of the AMT

⁷⁴ The antenna pattern shown in Figure 1 of Rec M.1459 is not the pattern to be used here.

⁷⁵ Wang, C. W. and T. Keech. *Antenna Models For Electromagnetic Compatibility Analyses*, NTIA Report TM-13-489. October 2012. Retrieved 21 March 2017. Available at <https://www.ntia.doc.gov/report/2012/antenna-models-electromagnetic-compatibility-analyses>.

ground station. The aggregate PFD values for each wedge are converted in a received power value using the composite AMT ground station antenna pattern. This pattern, including values for side lobes and back lobes, provides the necessary weighting factors for converting PFD values in W/m^2 to absolute power in watts (cf. equations 1-3).

5. The aggregate power levels for each azimuth-of-arrival wedge are summed for all of the wedges into a single value. This aggregate value is computed for each of the 720 possible pointing angles of the AMT ground station antenna. Each of these 720 values is then converted back into a PFD level and compared with the PFD limit of -180 or $-181 \text{ dBW}/\text{m}^2$ in 4 kHz. This yields a graph and/or table of interference values versus azimuth for the AMT ground station, as shown in notional form in [Figure F-16](#). Note that the scaling of the full bandwidth of the co-channel or adjacent channel interference to the 4-kHz reference bandwidth of the Rec M.1459 protection criteria uses the same linear transformation that is used for a traditional I/N analysis.

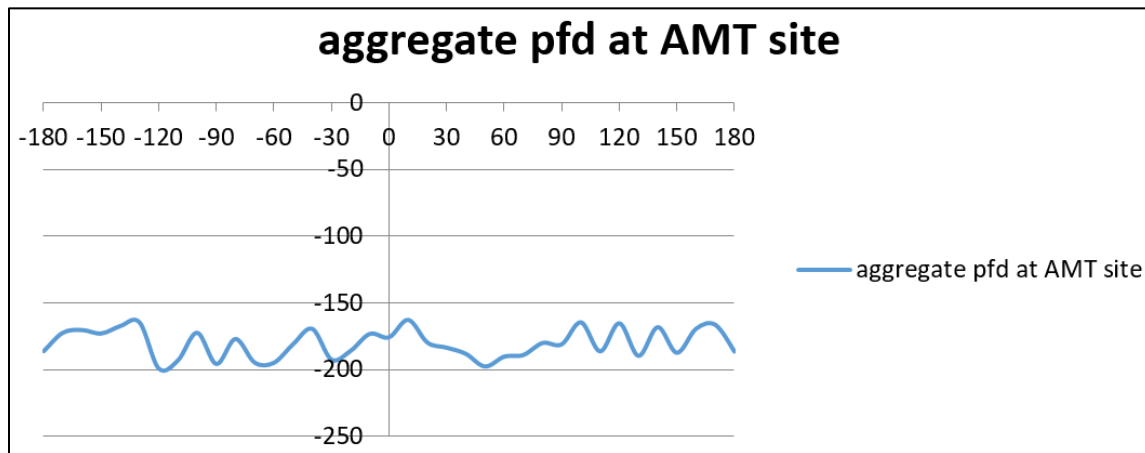


Figure F-16. Aggregate Interference as a Function of AMT Antenna Pointing Angle

6. The above approach is summarized quantitatively in the equations below, which elaborate on those presented earlier, and are re-stated here for the convenience of the reader.

- The value of wavelength that is part of the expression for the effective area of the AMT ground station receive antenna is grouped with the $1/4\pi^2$ spreading term, which is then redefined as path loss. This regrouping then permits the spreading term to be replaced with a single term that includes the effects of spreading, terrain and clutter loss, Fresnel zone impingement, and ground reflection. The numerical computation of values for this composite path loss value is independent of the use of Rec M.1459.
- The conversion of PFD values to received power and vice versa involves the scaling term $4\pi/\lambda^2$. It is important to account for the presence, or absence, of this term in the equations presented below, so as to not inadvertently delete it or count it twice. This is why the equations below err on the side of redundancy; it is easier to ignore an unneeded equation than to re-derive it.

With this as a reference, the following evolution of equations should prove useful.

1. Start with the free-space Friis equation. A_{eff} is the effective area of the AMT ground station receive antenna:

$$P_{rec} = EIRP_{xmt} \times \frac{1}{4\pi r^2} \times A_{eff} \quad (F-16)$$

2. Add antenna gains, the definition of antenna effective area, and the definition of PFD to arrive at:

$$P_{rec} = P_{xmt} G_{xmt} \times \frac{1}{4\pi r^2} \times \frac{\lambda^2 G_{rec}}{4\pi} = pfd_{rec} \times A_{eff} = pfd_{rec} \times \frac{\lambda^2 G_{rec}}{4\pi} \quad (F-17)$$

3. Move $\lambda^2/4\pi$ from effective area term and group with the $\frac{1}{4\pi r^2}$ term per the traditional mathematical definition of path loss. Terrain, ground reflection, clutter, and Fresnel zone effects can now be included in the numerical value used for path loss in subsequent computations:

$$P_{rec} = P_{xmt} G_{xmt} \times \frac{\lambda^2}{4\pi r^2} \times \frac{G_{rec}}{4\pi} = pfd_{rec} \times A_{eff} = pfd_{rec} \times \frac{\lambda^2 G_{rec}}{4\pi} \quad (F-18)$$

$$pfd_{rec} \times \frac{\lambda^2 G_{rec}}{4\pi} = P_{xmt} G_{xmt} \times \frac{\lambda^2}{(4\pi)^2 r^2} \times \frac{G_{rec}}{1} = P_{xmt} G_{xmt} \times (Path_Loss) \times \frac{G_{rec}}{1} \quad (F-19)$$

4. The gain of the AMT ground station receive antenna, G_{rec} , disappears from the equations when computation of the PFD level at the AMT ground station receiver is the desired result:

$$P_{rec} = pfd_{rec} \times \frac{\lambda^2 G_{rec}}{4\pi} = P_{xmt} G_{xmt} \times (Path_Loss) \times \frac{G_{rec}}{1} \quad (F-20)$$

$$pfd_{rec} = P_{xmt} G_{xmt} \times (Path_Loss) \times \frac{4\pi}{\lambda^2} \quad (F-21)$$

5. Use the appropriate eNodeB antenna gains described in step 4 to compute $P_{xmt} G_{xmt}$. Use the speed of light to compute, for this example, the wavelength λ corresponding to a frequency of 1500 MHz. Scale the EIRP values to the 4-kHz reference bandwidth of the Rec M.1459 PFD protection level. This yields the interference from a single handset as a PFD level measured at the location of the AMT ground station antenna. This value can be compared directly with the protection level from Rec M.1459.

$$pfd_{rec\ in\ 4\ kHz} = (Interference\ in\ Watts\ per\ MHz) \times G_{xmt} \times (Path_Loss) \times \frac{4\pi}{\lambda^2} \times \frac{4000\ Hz}{1\ MHz} \quad (F-22)$$

$$\lambda = \frac{3 \times 10^8}{1500 \times 10^6} = 0.20\ meter \quad (F-23)$$

$$= Interference \times G_{xmt} \times (Path_Loss) \times \frac{4\pi}{(0.20)^2} \times \frac{4000\ Hz}{1\ MHz}$$

6. Now that the relationships between interference power, path loss, PFD, and P_{rec} are defined, the aggregation process described earlier can be implemented. The important point is that the PFD values due to each sector of each eNodeB, as measured at an AMT ground station location, are grouped within an angle of arrival wedge, then multiplied by the appropriate value of AMT composite antenna pattern for each angle of arrival value. The total interference from all directions for each possible AMT pointing angle is computed, then changed back into an aggregate value of PFD by the conversion factor $4\pi/\lambda^2$ to arrive at a single value of aggregate

PFD for each of the 720 possible AMT antenna pointing angles. Each entry in this table of values is then compared with the protection limit from Rec M. 1459.

7. Finally, note that interference to an AMT signal is typically averaged over the bandwidth of the affected AMT channel(s), as described previously. This averaging is accomplished in the same manner that would apply to a traditional I/N analysis. The 4-kHz reference bandwidth in Rec M.1459 must be scaled to correspond to AMT channel bandwidths of 1 – 20 MHz, with 5 MHz being a common value for use in analysis.

Example 10. Additional considerations for the modeling of interfering systems

It is important to include effects such as network load factors, transmitters that emit intermittently, and the use of dynamic power control. Note that there are no similar effects related to the performance of AMT operations that need be considered, as these are already captured in Rec M.1459. Annex 2 of Rec M.1459 accounts for signal fades, for the requirement of a minimum value of telemetry link availability, and for the constantly changing location of test aircraft in the sky with respect to both satellite and terrestrial interference sources.

Consider Example 9, coordination of an AMT ground station with emissions from a large network of cellular towers. The cellular industry has noted repeatedly that its networks seldom operate at full load factor. This means that, averaged over several weeks, an individual cellular tower is transmitting only about 60% of the time. Cellular proponents thus advocate a decrease in the computed value of aggregate interference used in analysis by 40%.

The decrease in cellular tower activity at off-peak times corresponds with time slots where flight test activities are also at a minimum (e.g., at night). Furthermore, the time scales over which base station load factors are averaged (weeks) have no correlation with the time duration of interference causing an AMT link to fail (fractions of a second). Short-term interference can cause loss of antenna tracking, which can be difficult to re-establish without the need to re-fly test points.

The point is that when the probability of interference depends on time, it is necessary to use the same time scales for analyzing both the interfering and the victim systems. In the case of AMT operations, this means that all computations need to be performed for the time scale that corresponds to the interval of time that it takes an interfering signal to cause loss of AMT telemetry link bit synchronization. As stated in the previous paragraph, this is not weeks or days, but fractions of a second. In any case, loss of even small amounts of data can make it necessary to re-fly part, or even all, of the maneuvers included in a particular test flight.

Coordination of AMT ground stations with emissions from cellular handsets introduces similar issues. These handsets use dynamic power control, in which a cellular tower measures the received signal from a handset in real time and sends instructions to the handset to adjust its transmit power.

In addition, LTE and WiMAX (i.e., 802.16) systems operate by using orthogonal frequency division multiplexing, in which data are coded among several adjacent frequency subcarriers spread across the 10 – 20 MHz LTE bands.⁷⁶ The power amplitudes of each subcarrier vary with time, yielding variations characterized by what is called the peak-to-average-power-ratio (PAPR). For LTE, the PAPR is about 6 dB, with variations occurring on

⁷⁶ WiMAX will be used for the AeroMACS system at 5091- 5150 MHz, co-channel with AMT.

the order of milliseconds. For WiMAX, the PAPR is as high as 13 dB. The statistical distribution as a function of time for each system is characterized by a complementary cumulative distribution function.

It remains an open question whether PAPR fluctuations, which include reductions as well as surges in transmit power, are a concern.

Example 11. Special considerations regarding AMT antennas

The use of a composite antenna in Rec M. 1459 is referenced multiple times in this appendix. In the recommendation, however, the development of the composite antenna pattern is described in the body of Annex A only for the case of lower L-band, which has a pattern that is based on the NTIA Statgain antenna model of parabolic dish antennas (Wang and Keech, 2012), and is derived numerically for antennas having diameters of 10 meters and 2.44 meters. The composite pattern is derived by comparing the 10-meter and 2.44-meter patterns side-by-side and choosing the value of gain that is higher for a given off-axis pointing angle.

Although not described explicitly in the recommendation, the antenna pattern was modified for the purpose of computing the protection criteria for upper S-band that are also published in the recommendation. The L- and S-band frequencies are sufficiently close in value that the same composite pattern can be used for both bands for purposes of computing aggregate interference. This is a result of certain complex convolution computations described in the methodology provided by the recommendation; however, this simplification does not apply as telemetry systems are deployed at C-band and higher frequencies.

To address the computation of the protection criteria for upper L, lower S, and lower, middle, and upper C-bands, new composite antenna patterns were computed using the NTIA Statgain antenna pattern formulas given below.

Although the antenna patterns are not needed again for purposes of determining the protection criteria, they are needed when computing aggregation from large numbers of terrestrial interferers. For this purpose, the process of computing composite antenna patterns is straightforward, and is described below.

With respect to the computation of composite antenna patterns, the gain of both a 10-meter and 2.44-meter diameter dish were computed for each band using the Statgain formulas with the gain parameter G_{max} for each dish computed using the formula

$$G_{max} = 0.55 \times \left(\pi D / \lambda \right)^2 \quad (\text{F-24})$$

where 0.55 represents the nominal efficiency of the dish antennas.

Then, using the equations below, patterns were computed for both the 10-meter and 2.44-meter antennas for each value of signal wavelength λ . Using a simple spreadsheet, the gains of the two antennas as a function of off-axis angle for each value of λ were compared. The higher gain value of the two antennas was chosen as the value for that angle for the corresponding composite antenna. Although this is a slight simplification of the side-lobe averaging technique used in the recommendation, the impact on the numerical values of the protection criteria was found to be negligible. This means that for computational purposes, the Statgain antenna patterns can be used for C and higher bands without modification.

In addition to the Statgain formulas, which provide an envelope function for the maximum values of the gain pattern, the more general pattern equations are also provided. These are difficult to find in textbooks, but are often useful.

The Statgain radiation patterns, $G(\phi)$, as a function of the angle from the main-beam axis, ϕ , are shown in [Table F-1](#) (Wang and Keech 2012) and the Statgain envelope pattern is presented in [Figure F-17](#) (Wang and Keech 2012). The more general pattern equations, published as part of the Satellite Toolkit software, are provided afterwards.

| Table F-1. Statgain Formulas | | |
|--|---|-----------------------------------|
| Category | Gain(ϕ) (dBi) | Angular Range (deg.) |
| $G_{\max} \geq 48$ dBi | $G_{\max} - 4 \times 10^{-4} (10^{G_{\max}/10}) \phi^2$ | $0 \leq \phi \leq \phi_m$ |
| | $0.75 \times G_{\max} - 7$ | $\phi_m < \phi \leq \phi_{r1}$ |
| | $29 - 25 \times \log(\phi)$ | $\phi_{r1} < \phi \leq \phi_{b1}$ |
| | -13 | $\phi_{b1} < \phi \leq 180^\circ$ |
| $22 \leq G_{\max}(\text{dBi}) < 48$ | $G_{\max} - 4 \times 10^{-4} (10^{G_{\max}/10}) \phi^2$ | $0 \leq \phi \leq \phi_m$ |
| | $0.75 \times G_{\max} - 7$ | $\phi_m < \phi \leq \phi_{r2}$ |
| | $53 - (G_{\max}/2) - 25 \times \log(\phi)$ | $\phi_{r2} < \phi \leq \phi_{b2}$ |
| | $11 - G_{\max}/2$ | $\phi_{b1} < \phi \leq 180^\circ$ |
| $10 \leq G_{\max}(\text{dBi}) < 22$ | $G_{\max} - 4 \times 10^{-4} (10^{G_{\max}/10}) \phi^2$ | $0 \leq \phi \leq \phi_m$ |
| | $0.75 \times G_{\max} - 7$ | $\phi_m < \phi \leq \phi_{r3}$ |
| | $53 - (G_{\max}/2) - 25 \times \log(\phi)$ | $\phi_{r3} < \phi \leq \phi_{b3}$ |
| | 0 | $\phi_{b3} < \phi \leq 180^\circ$ |
| All angles are in degrees. $\phi_m = 50(0.25G_{\max} + 7)^{0.5}/(10^{G_{\max}/20})$ $\phi_{r1} = 27.466 \times 10^{-0.03G_{\max}/10}$ $\phi_{r1} = \phi_{r1} = 250/(10^{G_{\max}/20})$ $\phi_{b1} = \phi_{b2} = 48$ $\phi_{b3} = 131.8257 \times 10^{-G_{\max}/50}$ | | |

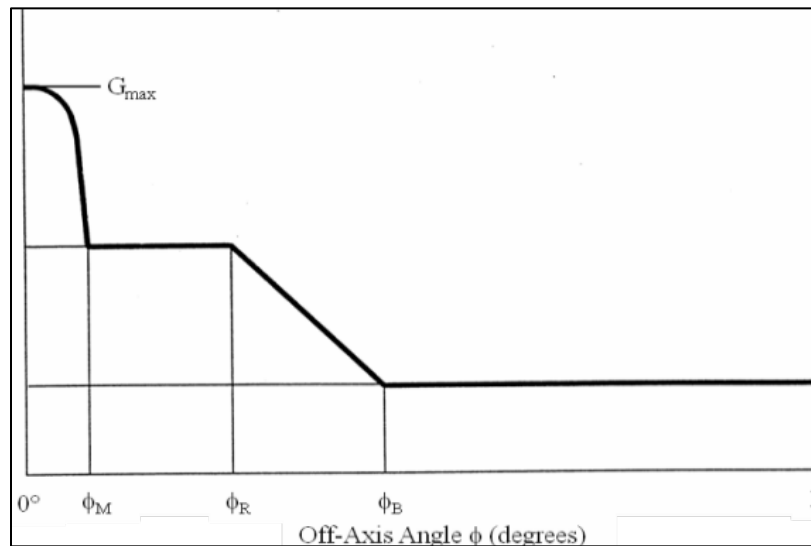


Figure F-17. Statgain Pattern

Note that the Statgain patterns provide an upper envelope of the antenna pattern. The more-generalized parabolic dish equations are available as part of the Analytical Graphics (AGI) Satellite Toolkit software tool.⁷⁷ These equations provide details about the peaks and nulls of the antenna side-lobes as opposed to providing an envelope of the pattern, and are given below.

The parabolic antenna parameters are:

d = diameter of the parabolic dish

λ = wavelength

The gain of a parabolic antenna is modeled by the equations F-25a, F-25b, and F-25c:

$$x = \frac{\pi d}{\lambda} \sin \phi \quad (\text{F-25a})$$

$$G_{Max} = \rho_e \left(\pi \frac{d}{\lambda} \right)^2 \quad (\text{F-25b})$$

$$G(\phi) = G_{Max} \left(\frac{2J_1(x)}{x} \right)^2 \quad (\text{F-25c})$$

where ρ_e = the antenna efficiency, ϕ = angle off boresight, and J_1 = first-order Bessel function. This model is for a uniformly illuminated circular aperture dish.

On a final note, the question has been posed of how to compute protection criteria for antennas whose diameter falls outside the range of 2.44 – 10 meters. The simple and reasonable approach is to recognize that both the gain and beamwidth of a parabolic-dish antenna are related to the parameter D/λ . For the case of an antenna that is 13 meters in diameter but operating at upper L-band (for example), D/λ is about 75. This is comparable to a 10-meter antenna operating at a wavelength of 0.133 meters. Since the protection criteria for upper S-band correspond to a wavelength of 0.128 meters, it seems appropriate to use the protection criteria for upper S-band as the values for a 13-meter diameter antenna operating at upper L-band.

⁷⁷ Maral, G., and M. Bousquet. *Satellite Communications Systems: Systems, Techniques and Technology*. 2nd ed. Chichester: Wiley (1993), sec. 2.1.3; Gagliardi, Robert M. *Satellite Communications*. 2nd ed., New York: Van Nostrand Reinhold (1991), sec. 3.2.

APPENDIX 2-G

Standards for Data Quality Metrics and Data Quality Encapsulation**G.1. Purpose**

This appendix provides a standard for a DQM, determined in the telemetry receiver demodulator, and a standard for DQE allowing for transport of the received telemetry data and associated DQM to a distant best source selector or similar device. The DQE wrapper, commonly referred to as a protocol, will enable telemetry receivers to generate a serial data stream that will include a standardized measurement of the real-time probability of error for a grouping of bits.

G.2. Scope

The DQM standard describes how to map the estimated BEP of the received telemetry data to a 16-bit word. The DQM standard does not define how the telemetry receiver performs BEP estimates. The DQE standard describes how to format the received telemetry data with the associated DQM for transport.

G.3. Data Quality Metric

The general case of DQM is calculated as follows:

$$DQM = \frac{-\log_{10}(LR)}{k} * 2^n$$

where: k is the exponent for lowest estimated BEP
 n is number of bits in the DQM field
 LR is the likelihood ratio

$$LR = \frac{BEP}{(1 - BEP)}$$

For this standard, $k=12$ and $n=16$.

In formula form this calculation can be made with the following equation:

$$DQM = \text{MIN}(\text{ROUND}(-\text{LOG10}(LR)/12 * (2^{16}), 0), 2^{16}-1)$$

- a. The measurement value corresponds to the average quality of the data bits in the payload.
- b. The DQM value is associated with the payload bits in the current block frame. [Table G-1](#) defines LR and DQM for various values of BEP.

| Table G-1. BEP Verses DQM | | |
|----------------------------------|-------------|------------|
| BEP | LR | DQM |
| 0.5 | 1.00 | 0 |
| 1e-01 | 1.11111e-01 | 5211 |
| 1e-02 | 1.01010e-02 | 10899 |

| | | |
|-------|-------------|-------|
| 1e-03 | 1.00100e-03 | 16382 |
| 1e-04 | 1.00010e-04 | 21845 |
| 1e-05 | 1.00001e-05 | 27307 |
| 1e-06 | 1.00000e-06 | 32768 |
| 1e-07 | 1.00000e-07 | 38229 |
| 1e-08 | 1.00000e-08 | 43691 |
| 1e-09 | 1.00000e-09 | 49152 |
| 1e-10 | 1.00000e-10 | 54613 |
| 1e-11 | 1.00000e-11 | 60075 |
| 1e-12 | 1.00000e-12 | 65535 |

NOTE

It is not required that BEP be estimated to the 1e-12 level. Estimates to a lesser level are acceptable; however, the format above shall be followed in all cases. For example, if estimating BEP to the 1e-8 level, the applicable range of DQM values shall be 0 to 43691.

G.4. Data Quality Encapsulation Protocol

The block format is equivalent to a fixed-length PCM frame. Transmission of payload data shall be first in - first out. Transmission of other fields shall be most significant bit first.

| | | | | |
|---------|---------|--------|---------|-------------------|
| 16 Bits | 12 Bits | 4 Bits | 16 Bits | 1024 – 16384 Bits |
| SW | RSV | VER | DQM | PAYLOAD |

- SW = Sync Word. The sync word is a fixed value of 0xFAC4.
- RSV = Reserved. Reserved for future use. These bits shall be set to zero (0) until used.
- VER = IRIG 106 Version number. Version number shall start with Version 0 (0000) for IRIG 106-17.
- DQM = Data Quality Metric. This field will contain the DQM value as defined in Section [G.3](#)
- PAYLOAD = Telemetry data payload to which the DQM value applies. The DQM and the data payload are contained in the same block. The minimum payload size shall be 1024 bits and the maximum size shall be 16,384 bits. Payload size can be any multiple of 32 bits between the minimum size and maximum size.

APPENDIX 2-H

Citations

Code of Federal Regulations, Table of Frequency Allocations, title 47, sec. 2.106.

Consultative Committee for Space Data Systems. *Low Density Parity Check Codes for Use in Near-Earth and Deep Space Applications*. Standard CCSDS 131.1-O-2-S. September 2007. Rescinded. Retrieved 30 June 2015. Available at <http://public.ccsds.org/publications/archive/131x1o2e2s.pdf>.

D.G. Jablonski. "Demonstration Of Closed Loop Steering of Antenna Patterns For Mitigating Antenna-To-Antenna Interference In Two-Antenna Telemetry Installations On Military Aircraft," Instrumentation Test Technical Symposium, New Orleans, LA, 25 August 2004.

Department of Defense. "Requirements for the Control of Electromagnetic Interference Characteristics of Subsystems and Equipment." MIL-STD-461. 11 December 2015. May be superseded by update. Retrieved 23 March 2017. Available at http://quicksearch.dla.mil/qsDocDetails.aspx?ident_number=35789.

E. L. Law. "RF Spectral Characteristics of Random PCM/FM and PSK Signals." International Telemetry Conference Proceedings, pp. 71 80, 1991.

E. Perrins. "FEC Systems for Aeronautical Telemetry". *IEEE Transactions on Aerospace and Electronic Systems*, vol. 49, no. 4, pp. 2340-2352, October 2013.

Eugene Hogenauer. "An Economical Class of Digital Filters for Decimation and Interpolation" in *IEEE Transactions on Acoustics, Speech, and Signal Processing*, 29, No. 2 (1981): 155-162.

Federal Communications Commission. "Amendment of Part 27 of the Commission's Rules to Govern the Operations of Wireless Communications Services in the 2.3 GHz Band." WT Docket No. 07-293. In *Order on Reconsideration*. FCC 12-130. 17 October 2012. Retrieved 27 July 2017. Available at https://apps.fcc.gov/edocs_public/attachmatch/FCC-12-130A1.pdf.

Feher, Kamilo and Shuzo Kato. Correlated signal processor. US Patent 4,567,602. Filed 13 June 1983 and issued 28 January 1986.

Hufford, G. A. and F. K. Steele. "Tabulations of Propagation Data over Irregular Terrain in the 75- To 8400-Mhz Frequency Range - Part V: Virginia. NTIA Publication 91-282, December 1991. Retrieved 27 July 2017. Available at <https://www.its.bldrdoc.gov/publications/download/91-282.pdf>.

I. Korn. *Digital Communications*. New York; Van Nostrand, 1985.

- International Telecommunications Union. “Compatibility between the Earth exploration-satellite service (passive) and relevant active services” *Final Acts WRC-15 – World Radiocommunication Conference*. Geneva, 2015. pp. 399-403.
- . “Method for point-to-area predictions for terrestrial services in the frequency range 30 MHz to 3 000 MHz.” ITU-R Recommendation P.1546-5. September 2013. May be superseded by update. Retrieved 30 March 2017. Available at <https://www.itu.int/rec/R-REC-P.1546/en>.
- . “Prediction procedure for the evaluation of interference between stations on the surface of the Earth at frequencies above about 0.1 GHz.” ITU-R Recommendation P.452-16. July 2015. May be superseded by update. Retrieved 30 March 2017. Available at <https://www.itu.int/rec/R-REC-P.452/en>.
- . “Propagation curves for aeronautical mobile and radionavigation services using the VHF, UHF, and SHF bands.” ITU-R Recommendation P.528-3. February 2012. May be superseded by update. Retrieved 30 March 2017. Available at <https://www.itu.int/rec/R-REC-P.528/en>.
- . “Protection criteria for telemetry systems in the aeronautical mobile service...” ITU-R Recommendation M.1459. May 2000. May be superseded by update. Available at <https://www.itu.int/rec/R-REC-M.1459-0-200005-I/en>.
- . “Radio Regulations: Articles.” 2012. May be superseded by update. Available at <http://search.itu.int/history/HistoryDigitalCollectionDocLibrary/1.41.48.en.101.pdf>.
- Jensen, M., M. Rice, and A. Anderson. “Aeronautical Telemetry Using Multiple-Antenna Transmitters.” *IEEE Transactions on Aerospace and Electronic Systems*, vol. 43, no. 1, pp. 262-272, January 2007.
- K. Temple. “Performance Evaluation of Space-Time coding on an Airborne Test Platform.” Paper presented at the 50th International Telemetry Conference, San Diego, CA, October 2014
- Kamilo Feher. *Digital Communications: Satellite/Earth Station Engineering*. Englewood Cliffs: Prentice-Hall, 1983, pp. 168-170.
- M. G. Pelchat. “The Autocorrelation Function and Power Spectrum of PCM/FM with Random Binary Modulating Waveforms.” *IEEE Transactions*, Vol. SET 10, No. 1, pp. 39 44, March 1964.
- M. Richharia. *Satellite Communications Systems, Second Edition*. New York; London: McGraw-Hill, 1999, page 37.
- Maral, G., and M. Bousquet. *Satellite Communications Systems: Systems, Techniques and Technology*. 2nd ed. Chichester: Wiley (1993), sec. 2.1.3; Gagliardi, Robert M. *Satellite Communications*. 2nd ed., New York: Van Nostrand Reinhold (1991), sec. 3.2.

- Mark Geoghegan. "Description and Performance Results for the Multi-h CPM Tier II Waveform." Paper presented at the 36th International Telemetry Conference, San Diego, CA, October 2000.
- . "Implementation and Performance Results for Trellis Detection of SOQPSK." Paper presented at the 37th Annual International Telemetry Conference, Las Vegas, NV, October 2001.
- . "Improving the Detection Efficiency of Conventional PCM/FM Telemetry by using a Multi-Symbol Demodulator", Proceedings of the 2000 International Telemetry Conference, Volume XXXVI, 675-682, San Diego CA, October 2000.
- Marvin Simon. "Bandwidth-Efficient Digital Modulation with Application to Deep Space Communications." JPL Publication 00-17. June 2001. Retrieved 3 June 2015. Available at <http://descanso.jpl.nasa.gov/monograph/series3/complete1.pdf>.
- . "Multiple-Bit Differential Detection of Offset Quadriphase Modulations." IPN Progress Report 42-151. 15 November, 2002. Jet Propulsion Laboratory, Pasadena, CA. Retrieved 4 June 2015. Available at http://ipnpr.jpl.nasa.gov/progress_report/42-151/151A.pdf.
- Michael Rice. *Digital Communications: A Discrete-Time Approach*. Pearson/Prentice-Hall. Upper Saddle River, NJ, 2009.
- . "Space-Time Coding for Aeronautical Telemetry: Part 1 – System Description," in *Proceedings of the International Telemetry Conference*, Las Vegas, NV, October 2011.
- National Telecommunications and Information Administration. "Manual of Regulations and Procedures for Federal Radio Frequency Management." September 2015. May be superseded by update. Retrieved 23 March 2017. Available at https://www.ntia.doc.gov/files/ntia/publications/manual_sep_2015.pdf.
- Osborne, W. P. and M. B. Luntz. "Coherent and Noncoherent Detection of CPFSK," IEEE Transactions on Communications, August 1974.
- Phillips, C., D. Sicker, and D. Grunwald. "Bounding the Practical Error of Path Loss Models." International Journal of Antennas and Propagation, Volume 2012 (2012). Retrieved 21 March, 2017. Available at <https://www.hindawi.com/journals/ijap/2012/754158/>.
- Proakis, J. G. and M. Salehi. *Digital Communications*. 5th Edition. Boston: McGraw-Hill, 2008.
- R. Clewer. "Report on the Status of Development of the High Speed Digital Satellite modem", RML-009-79-24, Spar Aerospace Limited, St. Anne de Bellevue, P.Q., Canada, November 1979. Quoted in Kamilo Feher. *Digital Communications: Satellite/Earth Station Engineering*. Englewood Cliffs: Prentice-Hall, 1983.

- Range Commanders Council. *Test Methods for Telemetry Systems and Subsystems Volume 2*. RCC 118-12. May be superseded by update. Retrieved 4 June 2015. Available at http://www.wsmr.army.mil/RCCsite/Documents/118-12_Vol_2-Test_Methods_for_Telemetry_RF_Subsystems/.
- Rice, M. and K. Temple, "Space-Time Coding for Aeronautical Telemetry: part II – Experimental Results," in *Proceedings of the International Telemetry Conference*, Las Vegas, NV, October 2011.
- S. Alamouti. "A Simple Transmit Diversity Technique for Wireless Communications." *IEEE Journal on Selected Areas in Communications*, vol. 16, no. 8, pp. 1451-1458, October 1998.
- T. J. Hill. "An Enhanced, Constant Envelope, Interoperable Shaped Offset QPSK (SOQPSK) Waveform for Improved Spectral Efficiency." Paper presented during 36th Annual International Telemetry Conference, San Diego, CA. October 23-26, 2000.
- Tey, W. M. and T. Tjhung. "Characteristics of Manchester Coded FSK." *IEEE Transactions on Communications*, Vol. COM 27, pp. 209 216, January 1979.
- Thomas Schwengler. "Wireless & Cellular Communications. Class notes for TLEN-5510 - Fall 2016. Accessed 27 July 2017. Available at <http://morse.colorado.edu/~tlen5510/text/classwebch3.html>.
- W. J. Weber III. "Differential Encoding for Multiple Amplitude and Phase Shift Keying Systems." In *IEEE Transactions on Communications*, Vol. COM-26, No. 3, March 1978.
- Wang, C. W. and T. Keech. *Antenna Models For Electromagnetic Compatibility Analyses*, NTIA Report TM-13-489. October 2012. Retrieved 21 March 2017. Available at <https://www.ntia.doc.gov/report/2012/antenna-models-electromagnetic-compatibility-analyses>.
- Watt, A. D., V. J. Zurick, and R. M. Coon. "Reduction of Adjacent Channel Interference Components from Frequency Shift Keyed Carriers." *IRE Transactions on Communication Systems*, Vol. CS 6, pp. 39 47, December 1958.
- Wikipedia. "Rayleigh fading." Retrieved 27 July 2017. Available at https://en.wikipedia.org/wiki/Rayleigh_fading
- Wireless Communications Association, "4G Device Out of Band Emissions and Larger Channel Bandwidths," October 2011. Accessed 21 March 2017. Available at <https://ecfsapi.fcc.gov/file/7021715550.pdf>.
- Younes, B., J. Brase, C. Patel, and J. Wesdock. "An Assessment of Shaped Offset QPSK for Use in NASA Space Network and Ground Network Systems" in *Proceedings of the CCSDS RF and Modulation Subpanel 1E Meeting of May 2001 Concerning Bandwidth-Efficient Modulation*. CCSDS B20.0-Y-2. June 2001. Retrieved 4 June 2015. Available at <http://public.ccsds.org/publications/archive/B20x0y2.pdf>.

****** END OF CHAPTER 2 ******